

**Fluoro-Complexes of
Iridium and Platinum**

A thesis presented for the degree of
Doctor of Philosophy

in the

Department of Chemistry

of the

Faculty of Science

at the

University of Leicester

by

Lee Anthony Peck

1995

UMI Number: U075065

All rights reserved

INFORMATION TO ALL USERS

The quality of this reproduction is dependent upon the quality of the copy submitted.

In the unlikely event that the author did not send a complete manuscript and there are missing pages, these will be noted. Also, if material had to be removed, a note will indicate the deletion.



UMI U075065

Published by ProQuest LLC 2015. Copyright in the Dissertation held by the Author.
Microform Edition © ProQuest LLC.

All rights reserved. This work is protected against
unauthorized copying under Title 17, United States Code.



ProQuest LLC
789 East Eisenhower Parkway
P.O. Box 1346
Ann Arbor, MI 48106-1346



To My Mother,

Thanks for everything.

Statement

The experimental work described in this thesis has been carried out by the author in the Department of Chemistry at the University of Leicester between October 1992 and September 1995. The work has not been submitted, and is not presently being submitted, for any other degree at this time or any other university:

Signed:



Date: 26/1/96

Department of Chemistry,
University of Leicester,
University Road,
Leicester,
U. K.
LE1 7RH.

Abstract

A range of low-valent iridium and platinum fluoro-complexes have been prepared and characterized by a combination of mass spectrometry, ^{19}F , $^{31}\text{P}\{^1\text{H}\}$, $^{195}\text{Pt}\{^1\text{H}\}$ and infrared spectroscopies and EXAFS where possible.

[Dichlorobis(amine)platinum(II)] complexes of the type $[\text{PtCl}_2(\text{L})_2]$ ($\text{L} = \text{NMe}_3, \text{NH}_3, \text{py}$; $\text{L}_2 = \text{en}, \text{bipy}$) have been reacted with $[\text{XeF}_2]$, undergoing oxidative fluorination, to afford various isomers of platinum(IV) amine-fluoride species. The presence of anhydrous hydrofluoric acid (AHF) was observed to influence the nature of the products formed whilst the *cis*- or *trans*- stereochemistry of the starting materials was found to determine the number of isomers formed.

The first unambiguously characterized difluorobis(phosphine)-platinum(II) complex, *cis*- $[\text{PtF}_2(\text{PEt}_3)_2]$ was formed from the reaction of *cis*- $[\text{PtMe}_2(\text{PEt}_3)_2]$ and AHF with the elimination of methane gas being the driving force for the reaction. The difluoro-complex, is stable only in AHF or under vacuum, it was characterized by low-temperature $^{195}\text{Pt}\{^1\text{H}\}$ NMR spectroscopy.

Analogues of Vaska's complex of the type, *trans*- $[\text{IrCl}(\text{CO})(\text{PR}_3)_2]$ ($\text{PR}_3 = \text{PPh}_3, \text{Pcy}_3$) have been shown to undergo oxidative fluorination reactions with $[\text{XeF}_2]$ resulting in the formation of *cis*-, *trans*- $[\text{IrF}_2\text{Cl}(\text{CO})(\text{PR}_3)_2]$. Furthermore, the reaction between fluoro-Vaska's *trans*- $[\text{IrF}(\text{CO})(\text{PPh}_3)_2]$ and $[\text{XeF}_2]$ has been found to afford the novel trifluoro-complex *mer*-, *trans*- $[\text{IrF}_3(\text{CO})(\text{PPh}_3)_2]$.

A series of complexes of the type *mer*-, *trans*- $[\text{IrF}_3(\text{CO})(\text{L})_2]$ ($\text{L} =$ tertiary phosphine, amine or arsine) have been prepared from the reaction of *fac*- $[\text{IrF}_3(\text{CO})_3]$ and the appropriate Lewis base. The amine and arsine derivatives represent the first examples of fluoroiridium(III) amine or arsine complexes.

X-ray crystal structure determinations for the complexes *trans*- $[\text{PtCl}_2(\text{NMe}_3)_2]$, $[\text{Pt}(\text{C}_6\text{H}_4\text{PPh}_2)(\text{PPh}_3)_2][\text{SbF}_6]$, *trans*- $[\text{Ir}(\text{C}_6\text{F}_5)(\text{CO})\{\text{PPh}_2(\text{C}_6\text{F}_5)_2\}_2]$ and $[\text{HNEt}_3][\text{PtCl}_3(\text{NEt}_3)]$ are described.

Contents

Statement	i
Abstract	ii
Contents	iii
Acknowledgements	ix
Abbreviations	x

Chapter One: Introduction

1.1 Introduction	2
References for Chapter One	9

Chapter Two: Preparation of Platinum Fluoride Amine Complexes

2.1 An Introduction to the Area of Platinum Amine Complexes	12
2.1.2 Platinum(II) Amine Complexes	12
2.1.3 Platinum(IV) Amine Complexes	13
2.2.1 Amine-Fluoride Complexes of the Transition Metals	14
2.2.2 Complexes of Titanium and Zirconium	15
2.2.3 Complexes of Vanadium, Niobium and Tantalum	17
2.2.4 Complexes of Chromium	19
2.2.5 Complexes of Molybdenum and Tungsten	21
2.2.6 Complexes of Manganese and Rhenium	25
2.2.7 Complexes of Iron, Ruthenium and Osmium	27
2.2.8 Complexes of Cobalt, Rhodium and Iridium	28
2.2.9 Complexes of Nickel, Palladium and Platinum	29
2.2.10 Complexes of Copper, Silver and Gold	32
2.3 Summary	33
2.4 Introduction to Results and Discussion	34

2.5	Metathetical Reactions of Various Dichloroplatinum(II) Complexes Containing N-Donor Ligands with AHF	35
2.5.1	The Metathesis Reaction of <i>trans</i> -[PtCl ₂ (NMe ₃) ₂] with Silver Fluoride	39
2.6	Reaction of <i>trans</i> -[PtCl ₂ (NMe ₃) ₂] and [XeF ₂] in AHF	41
2.6.1	Mechanism of Oxidative Fluorination of <i>trans</i> -[PtCl ₂ (NMe ₃) ₂] by [XeF ₂]	47
2.6.2	Reaction of <i>trans</i> -[PtCl ₂ (NMe ₃) ₂] and [XeF ₂] in CH ₃ CN	49
2.6.3	X-Ray Crystal Analysis of <i>trans</i> -[PtCl ₂ (NMe ₃) ₂]	50
2.6.4	EXAFS Analysis of <i>trans</i> -[PtF ₂ Cl ₂ (NMe ₃) ₂]	52
2.7	Reaction of <i>cis</i> -[PtCl ₂ (NH ₃) ₂] and [XeF ₂] in AHF	56
2.7.1	Reaction of <i>cis</i> -[PtCl ₂ (NH ₃) ₂] and [XeF ₂] in CH ₃ CN	62
2.8	Reaction of <i>trans</i> -[PtCl ₂ (NH ₃) ₂] and [XeF ₂] in AHF	63
2.8.1	Reaction of <i>trans</i> -[PtCl ₂ (NH ₃) ₂] and [XeF ₂] in CH ₃ CN	67
2.9	Discussion of the Reactions of <i>cis</i> - and <i>trans</i> -[PtCl ₂ (NH ₃) ₂] with [XeF ₂]	68
2.10	Reaction of <i>cis</i> -[PtCl ₂ (en)] and [XeF ₂] in AHF	69
2.10.1	Reaction of <i>cis</i> -[PtCl ₂ (en)] and [XeF ₂] in CH ₃ CN	74
2.11	Reaction of <i>cis</i> -[PtCl ₂ (bipy)] and [XeF ₂] in AHF	77
2.11.1	Reaction of <i>cis</i> -[PtCl ₂ (bipy)] and [XeF ₂] in CH ₃ CN	80
2.12	Reaction of <i>cis</i> -[PtCl ₂ (py) ₂] and [XeF ₂] in AHF	81
2.12.1	Reaction of <i>cis</i> -[PtCl ₂ (py) ₂] and [XeF ₂] in CH ₃ CN	82
2.13	Reaction of [Pt(en) ₂]Cl ₂ and [XeF ₂]	84
2.14	Discussion of the Oxidative Fluorinations	87
	References for Chapter Two	91

Chapter Three: Preparation of Platinum Fluoride-Phosphine Complexes

3.1	An Introduction to the Chemistry of Platinum Phosphine Complexes	98
-----	---	----

3.1.2	Platinum(0) Phosphine Complexes	98
3.1.3	The Reactions of Zerovalent Platinum Phosphine Complexes with Oxidative Fluorinating Agents	100
3.1.4	Platinum(II) Phosphine Complexes	106
3.1.5	Platinum(II) Fluoride Phosphine Complexes	110
3.1.6	Platinum(IV) Phosphine Complexes	112
3.1.7	Platinum(IV) Fluoride Phosphine Complexes	112
3.1.8	Summary	113
3.2	Reaction of <i>cis</i> -[PtMe ₂ (PEt ₃) ₂] with AHF	114
3.2.1	The Mechanism for the Reaction of AHF with <i>cis</i> -[PtMe ₂ (PEt ₃) ₂]	126
3.3	Reaction of <i>cis</i> -[PtCl ₂ (PEt ₃) ₂] with AHF	129
3.4	Reaction of <i>cis</i> -[PtX ₂ (PEt ₃) ₂] with AHF in CD ₂ Cl ₂ [X = Cl, Me]	131
3.5	Reactions of <i>cis</i> -[PtCl ₂ (PR ₃) ₂] {PR ₃ = PMe ₃ , PMe ₂ Ph, PEtPh ₂ and (PR ₃) ₂ = dppe} with AHF	134
3.6	Reactions of <i>cis</i> -[PtMe ₂ (PR ₃) ₂] (PR ₃ = PMe ₃ , PMe ₂ Ph, Pcy ₃ and PEtPh ₂) with AHF	135
3.6.1	<i>cis</i> -[PtMe ₂ (PMe ₃) ₂]	136
3.6.2	<i>cis</i> -[PtMe ₂ (Pcy ₃) ₂]	138
3.6.3	<i>cis</i> -[PtMe ₂ (PMe ₂ Ph) ₂]	138
3.6.4	<i>cis</i> -[PtMe ₂ (PEtPh ₂) ₂]	139
3.7	Reactions of <i>cis</i> -[PtX ₂ (PPh ₃) ₂] (X = Cl, Me) with AHF	147
3.8	Discussion of the Reactions of <i>cis</i> -[PtX ₂ (PR ₃) ₂] with AHF	150
3.9	Preparation of [PtF(PR ₃) ₃][BF ₄] (PR ₃ = PEt ₃ and PPh ₃)	150
3.10	EXAFS Analysis of [PtF(PPh ₃) ₃][SbF ₆]	155
3.11	Reaction of [PtF(PPh ₃) ₃][X] (X = HF ₂ ⁺ and SbF ₆ ⁻) with CD ₂ Cl ₂	158

3.12	Crystal Structure Analysis of $[\text{Pt}(\text{C}_6\text{H}_4\text{PPh}_2)(\text{PPh}_3)_2]$	166
3.13	Discussion of the Decomposition of $[\text{PtF}(\text{PPh}_3)_3]^+$ in CD_2Cl_2	167
3.14	Reaction of $[\text{XeF}_2]$ with $[\text{Pt}(\text{PEt}_3)_4][\text{PF}_6]_2$	170
3.15	Summary	171
	References for Chapter Three	172

Chapter Four: The Reactions of Iridium(I) Carbonyl-Phosphine

Complexes with Xenon Difluoride

4.1	A Brief History of Vaska's Complex and its Analogues	178
4.2	Fluoride-Containing Vaska's Complexes	180
4.3	Iridium(III) Fluoro-Carbonyl-Phosphine Complexes	183
4.3.1	Oxidative Fluorination Reactions of Vaska's Complex and its Derivatives	183
4.3.2	Oxidative Addition Reactions of Fluoro-Vaska's Complexes	188
4.4	Summary	190
4.5	Preparation of <i>trans</i> - $[\text{IrF}(\text{CO})(\text{PPh}_3)_2]$	191
4.6	Preparation of <i>trans</i> - $[\text{IrCl}(\text{CO})(\text{Pcy}_3)_2]$	192
4.6.1	Reaction of <i>trans</i> - $[\text{IrCl}(\text{CO})(\text{Pcy}_3)_2]$ and $[\text{NH}_4\text{F}]/[\text{Ag}_2\text{CO}_3]$ in methanol	193
4.7	EXAFS Analysis of <i>trans</i> - $[\text{IrCl}(\text{CO})(\text{Pcy}_3)_2]$	194
4.8	EXAFS Analysis of <i>trans</i> - $[\text{IrF}(\text{CO})(\text{PPh}_3)_2]$	196
4.9	Reaction of <i>trans</i> - $[\text{IrCl}(\text{CO})(\text{PR}_3)_2]$ ($\text{PR}_3 = \text{PPh}_3$ and Pcy_3) with $[\text{XeF}_2]$	198
4.10	EXAFS Analysis of <i>cis</i> -, <i>trans</i> - $[\text{IrF}_2\text{Cl}(\text{CO})(\text{Pcy}_3)_2]$	208
4.11	Reaction of <i>trans</i> - $[\text{IrF}(\text{CO})(\text{PPh}_3)_2]$ with $[\text{XeF}_2]$	210
	References for Chapter Four	214

Chapter Five: The Syntheses and Characterization of Iridium(III)

Fluoride-Carbonyl-Phosphine Complexes

5.1	Introduction	218
5.2	Reactions of $[\text{XeF}_2]$ with the Cationic Species $[\text{Ir}(\text{CO})_3\text{L}_2]^+$	218
5.3	The Reaction between <i>fac</i> - $[\text{IrF}_3(\text{CO})_3]$ and a Lewis base	222
5.4	Summary	224
5.5	Reactions of <i>fac</i> - $[\text{IrF}_3(\text{CO})_3]$ with Monodentate Phosphine ligands	225
5.5.1	^{19}F and $^{31}\text{P}\{^1\text{H}\}$ NMR Spectroscopy	226
5.5.2	Infrared and Mass Spectrometry	237
5.6	EXAFS Analysis of $[\text{IrF}_3(\text{CO})(\text{PEt}_3)_2]$	241
5.7	The Reactions of <i>fac</i> - $[\text{IrF}_3(\text{CO})_3]$ with Trimethylamine and Triphenylarsine	245
5.8	The Reaction of <i>fac</i> - $[\text{IrF}_3(\text{CO})_3]$ with Multidentate Phosphine Ligands	248
5.8.1	The Reaction of <i>fac</i> - $[\text{IrF}_3(\text{CO})_3]$ with dppe	251
5.8.2	The Reaction of <i>fac</i> - $[\text{IrF}_3(\text{CO})_3]$ with Triphos (P_3)	255
5.8.3	The Reaction of <i>fac</i> - $[\text{IrF}_3(\text{CO})_3]$ with Tetraphos (PP_3)	256
5.9	Introduction to the Stability of the Complexes of the Type, <i>mer</i> -, <i>trans</i> - $[\text{IrF}_3(\text{CO})(\text{PR}_3)_2]$	259
5.10	Stability of the Complexes <i>mer</i> -, <i>trans</i> - $[\text{IrF}_3(\text{CO})(\text{PR}_3)_2]$ 5a - 5j	260
5.10.1	Decomposition to Iridium(I) Complexes	261
5.10.2	Crystal Structure of <i>trans</i> - $[\text{Ir}(\text{C}_6\text{F}_5)(\text{CO})\{\text{PPh}_2(\text{C}_6\text{F}_5)\}_2]$	274
5.10.3	Decomposition to Mixed-Halo-Iridium(III) Species	275
5.11	Summary	276
	References for Chapter Five	277

Chapter Six: Experimental

6.1	Metal Vacuum Line	281
6.2	Inert Atmosphere Dry Box	284
6.3	Reaction Vessels	284
6.4	Analytical Techniques	285
6.4.1	Nuclear Magnetic Resonance Spectroscopy	285
6.4.2	Infrared Spectroscopy	288
6.4.3	Mass Spectrometry	288
6.4.4	EXAFS Spectroscopy	288
6.4.5	Preparation of EXAFS Samples	289
6.4.6	X-Ray Crystal Structure Analysis	289
6.5	Sources of Chemicals and Methods of Purification	292
6.6	Solvents	297
6.7	Preparation of Xenon Difluoride	298
6.8	Preparation of <i>fac</i> -[IrF ₃ (CO) ₃]	298
6.9	Reactions of <i>fac</i> -[IrF ₃ (CO) ₃] with Lewis Bases on the Metal Vacuum Line	299
6.10	Reactions of <i>fac</i> -[IrF ₃ (CO) ₃] with Lewis Bases on the Schlenk Line	300
6.11	Preparation of <i>trans</i> -[IrF(CO)(PPh ₃) ₂]	302
6.12.1	Preparation of <i>trans</i> -[IrCl(CO)(PR ₃) ₂], for PR ₃ = Pcy ₃ and PPh(C ₆ F ₅) ₂	302
6.12.2	Preparation of <i>trans</i> -[IrCl(CO){P(C ₆ F ₅) ₃ } ₂]	303
6.13	Reactions of <i>trans</i> -[IrCl(CO)(PR ₃) ₂] {PR ₃ = PPh ₃ , Pcy ₃ , P(C ₆ F ₅) ₃ and PPh(C ₆ F ₅) ₂ } with [XeF ₂]	303
6.14	Reactions of <i>cis</i> -[PtCl ₂ (PR ₃) ₂] (PR ₃ = PPh ₃ , PMe ₃ , PEt ₃ , PMe ₂ Ph, PEtPh ₂ and (PR ₃) ₂ = dppe) with AHF	303
6.15	Reactions of <i>cis</i> -[PtMe ₂ (PR ₃) ₂] (PR ₃ = PPh ₃ , PMe ₃ , PEt ₃ , PMe ₂ Ph, PEtPh ₂ and Pcy ₃) with AHF	304

6.16	Preparation of $[\text{PtF}(\text{PPh}_3)_3][\text{X}]$ ($\text{X} = \text{SbF}_6^-, \text{BF}_4^-$)	304
6.17	Preparation of Fluoro(triethylphosphine)platinum(II)- hexafluorophosphate	305
6.18	The Reaction of $[\text{Pt}(\text{PEt}_3)_4][\text{PF}_6]_2$ with $[\text{XeF}_2]$	305
6.19	Reactions of $[\text{PtCl}_2(\text{L})_2]$ ($\text{L} = \text{NH}_3, \text{NMe}_3, \text{Py}$ and $\text{L}_2 = \text{bipy}, \text{en}$) Complexes with AHF	306
6.20	Reactions of $[\text{PtCl}_2(\text{L})_2]$ ($\text{L} = \text{NH}_3, \text{NMe}_3, \text{Py}$ and $\text{L}_2 = \text{bipy}, \text{en}$) Complexes with $[\text{XeF}_2]$ in CH_3CN	306
6.21	Reactions of $[\text{PtCl}_2(\text{L})_2]$ ($\text{L} = \text{NH}_3, \text{NMe}_3, \text{Py}$ and $\text{L}_2 = \text{bipy}, \text{en}$) Complexes with $[\text{XeF}_2]$ in AHF	307
6.22	The Reaction of <i>trans</i> - $[\text{PtCl}_2(\text{NMe}_3)_2]$ with AgF	307
6.23	Preparation of <i>trans</i> - $[\text{PtCl}_2(\text{NEt}_3)_2]$	307
	References for Chapter Six	309

Appendix

	Discussion of the Crystal Structure for $[\text{HNEt}_3][\text{PtCl}_3(\text{NEt}_3)]$	310
	References for Appendix	313

Acknowledgements

I would like to take this opportunity to thank my supervisor Dr Eric Hope and Professor Holloway for their continued help and guidance throughout my time in the Fluorine Research Group.

I must also acknowledge Dr's J. Fawcett, G. Griffith and G. Eaton for their help in solving crystal structures (although, not always what was anticipated !) recording NMR and mass spectra respectively.

To the members of the fluorine group past and present, and to the rest of Chemistry Department in general, thanks for making my time at Leicester excellent and for putting up with my awful jokes. A special thankyou goes to three people; my good friend Lee (Wootton) for lending me his computer and for countless evenings enjoying a quiet drink or too!!!!, my girlfriend Rhian for being there and finally, my brother who has always encouraged me and helped me out when I've needed it.

For financial support I am very grateful to the E. P. S. R. C. (formally S. E. R. C.) and to the Univeristy for extra pocket money!!

Abbreviations

AHF : anhydrous hydrofluoric acid

bipy : 2,2'-bipyridine

cy : cyclohexyl

δ : NMR chemical shift

DMSO : dimethyl sulphoxide

dppe : 1,2-bis(diphenylphosphino)ethane

en : ethylenediamine

E. I. : electron impact

Et : ethyl

EXAFS : Extended X-ray Absorption Fine Structure

FEP : tetrafluoroethane / perfluoropropane copolymer

Hz : Hertz

i. d. : internal diameter

o. d. : outside diameter

Kel - F : poly(chlorotrifluoroethylene)

Me : methyl

NMR : nuclear magnetic resonance

ppm : parts per million

Ph : phenyl

pn : propylenediamine

py : pyridine

tmeda : tetramethylethylenediamine

ν : stretching frequency

CHAPTER

ONE

Introduction

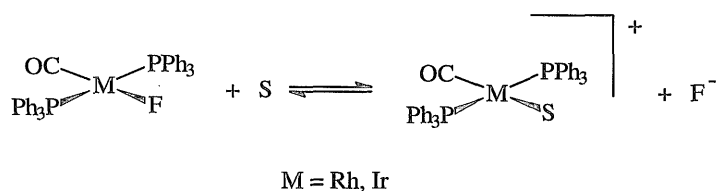
1.1 An Introduction to Low-Valent Metal Fluoro-Complexes

The coordination of chloride, bromide and iodide ligands to organo-transition-metal complexes is well documented. The nature of the metal, the halide and the subsidiary ligands bound to the metal all contribute to the reactivity of the species. However, there have only been a limited number of reports of species in which a fluoride ligand is coordinated to metals in low oxidation states. A recent review article by Doherty and Hoffman,¹ has highlighted the scarcity of these species compared to those of the heavier halogens. There are many instances where a particular type of halo-complex has been established for all of the halogens except fluoride, *e.g.* the formation of all of the species *cis*-[PtX₂(PMe₂Ph)₂], where X is chloride, bromide and iodide but not where X = fluoride.²

Several factors have contributed to this lack of study. The principle one appears to be the labelling of a low-valent metal centre and a fluoride ion as unstable on the basis of the Pearson hard/soft acid/base rules.³ Many organotransition-metal systems contain low-valent metal centres with loosely-held electron density, so these, according to the Pearson system, are considered soft acids. In contrast, fluorine is known to be the most electronegative element in the periodic table, it is small and weakly polarizable and is, therefore, considered a hard base in the Pearson system. In solution, the Pearson rules predict that a soft acid will form more stable complexes with soft bases than with hard bases. Therefore, in terms of their electronic properties, the preference of halides in solution for low-valent organometallic centres should follow the trend $F^- < Cl^- < Br^- < I^-$. This trend is, indeed, observed in the synthesis of Rh and Ir Vaska's derivatives where the fluoride ligand in [MF(CO)(PPh₃)₂] is very labile in methanol and easily replaced by X⁻ (X = is an electron pair donor).⁴ However, the situation is not as straightforward as the Pearson rules predict since solvent-anionic

interactions are also important. Both *trans*-[RhF(CO)(PPh₃)₂] and *trans*-[IrF(CO)(PPh₃)₂] have been shown to behave as weak electrolytes in methanol^{5,6} or tetrahydrofuran,⁷ but not in acetone or nitrobenzene.^{5,6} This suggests that the solvolytic equilibrium in Scheme 1.1 is important in some media.

Scheme 1.1



Thus, in protic media, such as water and methanol, the high affinity of the uncomplexed fluoride ion for these solvent molecules due to strong hydrogen bonding to their hydroxyl groups,⁸ is, most probably, the driving force for this solvation reaction (Scheme 1.1).

Hence, in the rhodium system *trans*-[RhX(CO)(PPh₃)₂] anionic preference in dichloromethane solution has been shown to follow the trend X⁻ = F⁻ > Cl⁻ > Br⁻ > I⁻ (the equilibrium in Scheme 1.2 lie predominantly to the left)⁸ which is opposite to that predicted by the Pearson rules.³

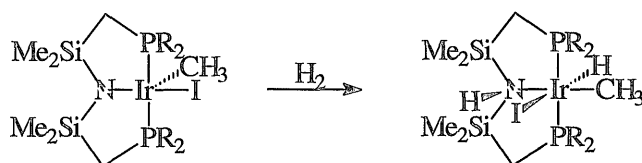
Scheme 1.2



However, the presence of small amounts of compounds such as water and methanol will shift the equilibrium to the right, presumably as a result of the high affinity of uncomplexed fluoride for these species.

Consequently, to date there are insufficient numbers of low-valent metal fluoride complexes to conclude whether the hard/soft acid/base rules are valid for fluoro-species. Nevertheless, for other ligands, it has been shown that soft metal/hard ligand combinations can lead to interesting chemistry. The electron rich Rh(I) compound, $[\text{Rh}(\text{OR})(\text{PMe}_3)_3]$, will react with ROH to yield $[\text{Rh}(\text{PMe}_3)_3\text{O}(\text{R})\cdots\text{H}-\text{OR}]$. This complex contains an unusually strong hydrogen bond, its enthalpy of formation being comparable to those of proton donors and anionic species (e.g. HF_2^-) rather than neutral electron-pair donors.⁹ Another reported example of such a combination leading to interesting chemistry is the oxidative addition of dihydrogen to the Ir(III) complex (Scheme 1.3).¹⁰

Scheme 1.3



The possibilities for synthetic chemistry involving metal-fluoride species containing low-valent metals have not been explored.

The second reason for this lack of study is, probably, the commonly held belief that complications will arise if attempts are made to introduce fluorine or fluoride into organometallic systems. From a thermodynamic viewpoint, the bond dissociation energy of F_2 gas

(153 kJ mol⁻¹) is small whereas, the heat of formation of bonds to fluorine is large *e.g.* H-F 570 kJ mol⁻¹ which is the strongest single bond known. Consequently, fluorine is highly reactive and tends to 'fire' with most compounds unless reaction conditions are rigorously controlled.

From a practical viewpoint, until recently, synthetic schemes for low-valent metal fluorides were limited to fluoride exchange reactions (metathesis reactions) with AHF and AgF and oxidative fluorinations with F₂ gas or [XeF₂]. Thus, if AHF or F₂ are considered as reagents for the introduction of fluorine or fluoride into transition-metal species, the need for specialized equipment and expertise has contributed to this lack of study. The suitability of F₂ and AHF as reagents has also been questioned from the view-point of the difficulties in controlling the aggressive nature of these reagents.

An additional, practical, problem associated with introducing fluoride *via* metathesis reactions is solubility. Although AgF is an obvious choice for F⁻/X⁻ exchange, since AgX can be precipitated from the reaction solution, AgF is light sensitive and is also fairly insoluble in non-polar solvents such as CH₂Cl₂. These difficulties have been conveniently overcome by the *in situ* formation of AgF, by the reaction of [Ag₂CO₃] with [NH₄F]. Successful examples employing this method include the preparation of [MF(CO)(PPh₃)₂] (M = Rh or Ir) from their chloro-analogues first reported by Vaska *et al.*¹¹

However, with the recent application of the less reactive and easier to manipulate fluorine containing reagents such as Olah's reagent (a solution of pyridine and AHF),¹² [AsF₃],¹³ [TAS-F] [tris(dimethylamino)sulphur-(trimethylsilyl)-difluoride],¹⁴ [SF₄]¹⁵ and [HBF₄·OEt₂]¹⁶ to transition-metal systems, convenient routes to fluoro-organotransition-metal complexes have started to appear in the literature (Table 1.1).

Previous literature surveys^{1,17} have adequately summarised the information available on low-valent metal fluoride complexes containing

carbonyl, phosphine and arsine ligands. In summary, despite the early successes in the formation of derivatives of fluoro-Vaska's complex and the more recent developments of new fluorine containing reagents there have been only an approximate total of 200 claims for low-valent metal fluoro-complexes, many of which have subsequently been shown to be incorrect. Earlier work from Leicester scientists has included investigations of the rhenium carbonyl fluoride,¹⁸ osmium carbonyl fluoride^{19,20} and ruthenium carbonyl fluoride²⁰ species.

In this thesis, the systematic extension of the synthesis and characterization of low-valent metal fluoride complexes to four areas, d⁸ iridium(I) and platinum(II) complexes and d⁶ iridium(III) and platinum(IV) complexes, will be described. The classification of Pt(IV) as a low-valent metal centre is made by comparison with complexes of fluoride with metals in very high oxidation states *e.g.* Pt(VI), Os(VIII).

Firstly, chapter two describes the preparation of some platinum amine fluoro-complexes by 2 routes:-

(i) The metathetical reactions of AgF and AHF with some platinum(II) amine dichloro-species yielding mono- or di-fluoro substituted complexes.

(ii) The oxidative fluorination, employing [XeF₂], of some platinum(II) amine dichloro-species in both AHF and CH₃CN affording various Pt(IV) fluoro-species.

These species have been characterized by ¹⁹F NMR spectroscopy and in some cases infrared and mass spectrometry. The first structural characterization, employing EXAFS spectroscopy, of a platinum(IV) amine fluoro-complex is reported in chapter two. The area of metal-amine-fluoride chemistry has not been considered elsewhere, and chapter two is introduced by a general discussion of this class of complex.

Table 1.1 Examples of Routes to Fluoro-organotransition-metal Complexes

Product	Reagents	Refs.
$[\text{Mo}_2\text{F}_4(\text{PR}_3)_4]$	$[\text{Mo}_2\text{Me}_4(\text{PR}_3)_4] + [\text{py} \cdot x\text{HF}]$	12
$[\text{FRh}(\text{C}_2\text{H}_4)(\text{C}_2\text{F}_4)]_4$	$[\text{ClRh}(\text{C}_2\text{H}_4)(\text{C}_2\text{F}_4)]_4 +$ $[\text{AgBF}_4]/[\text{TAS-F}]$	14
$[\text{Ta}(\eta^5\text{-C}_5\text{Me}_5)\text{F}_4]$	$[\text{Ta}(\eta^5\text{-C}_5\text{Me}_5)\text{Cl}_4] +$ $[\text{AsF}_3]$	13
$[\text{IrFX}(\text{CO})(\text{PEt}_3)_2(\text{SF}_3)]$ (X = Cl ⁻ , Br ⁻ and I ⁻)	<i>trans</i> - $[\text{IrX}(\text{CO})(\text{PEt}_3)_2] +$ $[\text{SF}_4]$	15
$[\{\text{W}(\text{CO})_2(\text{PMe}_2\text{Ph})_2\}_2(\mu\text{-F})_3]$	$[\text{WH}_6(\text{PMe}_2\text{Ph})_3] +$ $[\text{HBF}_4 \cdot \text{OEt}_2]$	16

Chapter three describes the preparation of some platinum(II) fluoride-phosphine complexes and also investigates the validity and stability of previously reported complexes of this type. Combinations of multinuclear NMR, infrared and mass spectrometry were employed to characterize the products, with EXAFS providing structural information in some cases. In chapter three, the first unambiguously characterized difluoride(bisphosphine)-platinum(II) complex is reported.

In chapter four an alternative route to the formation of the one of the trifluoro-complexes *mer*-, *trans*- $[\text{IrF}_3(\text{CO})(\text{PR}_3)_2]$, presented in chapter five is described. The related oxidation reactions of $[\text{XeF}_2]$ with Vaska's complex and its analogues are also explored. Characterization of these species relies upon NMR, infrared and mass spectrometry. Structural data of an iridium(III) difluoro-complex obtained by EXAFS spectroscopy is also described.

Finally, in chapter five, the reactions of the highly reactive *fac*-[IrF₃(CO)₃] with various Lewis bases are reported affording a novel group of air-stable Ir(III) carbonyl-phosphine-fluoride complexes of the type *mer*-, *trans*-[IrF₃(CO)(PR₃)₂] (where PR₃ is a tertiary phosphine). All complexes have been characterized by ¹⁹F NMR, ³¹P{¹H} NMR, infrared, mass spectrometry and where possible structural data has been obtained by EXAFS spectroscopy. The related NMe₃ and AsPh₃ derivatives represent the first examples of iridium(III) fluoride amine or arsine complexes. Furthermore, investigations of the stabilities and reactivity, towards chlorinated solvents, of the complexes described in this chapter are outlined. ¹⁹F and ³¹P{¹H} NMR studies and in some cases infrared, mass spectrometry and X-ray single crystal analysis led to either full or partial characterization of some novel fluoro-complexes of Ir(I) and Ir(III).

Throughout, each topic will be introduced separately by brief summaries of the related halo-metal and earlier fluoro-metal chemistry.

References for Chapter One

1. N. M. Doherty and N. W. Hoffman, *Chem. Rev.*, 1991, **91**, 553.
2. J. D. Kennedy, W. McFarland and R. J. Puddephatt, P. J. Thompson, *J. Chem. Soc., Dalton Trans.*, 1976, 874.
3. R. G. Pearson, *J. Am. Chem. Soc.*, 1963, **85**, 3533.
4. J. Peone Jr. and L. Vaska, *J. Chem. Soc., Chem. Commun.*, 1971, 418.
5. J. Peone Jr. and L. Vaska, *Inorg. Synth.*, 1974, **15**, 64.
6. C. M. Jones, D. M. T. Chan, N. M. Doherty and J. C. Calabrese, unpublished work reported in reference (1).
7. D. M. Branan, N. W. Hoffman, E. A. McElroy, N. C. Miller, D. L. Ramage, A. F. Schott and S. H. Young, *Inorg. Chem.*, 1987, **26**, 2915.
8. F. Aaghizadeh, D. L. Branan, N. W. Hoffman, J. H. Jones, E. A. McElroy, N. C. Miller, D. L. Ramage, D. L. Salazar and S. H. Young, *Inorg. Chem.*, 1988, **27**, 3752.
9. S. E. Kegley, C. J. Schaverien, J. H. Freudenberger, R. G. Bergmann, S. P. Nolan and C. D. Hoffman, *J. Am. Chem. Soc.*, 1987, **109**, 6563.
10. M. D. Fryzuk, P. A. MacNeil and S. J. Rettig, *Organometallics*, 1985, **4**, 1145.
11. L. Vaska and J. Peone, *Inorg. Synth.*, 1971, **13**, 126.
12. G. A. Olah, J. T. Welch, Y. D. Vankar, M. Nojima, J. Kerekes and J. A. Olah, *J. Org. Met. Chem.*, 1979, **44**, 22; F. A. Cotton and K. J. Wiesinger, *Inorg. Chem.*, 1992, **31**, 1920.
13. H. W. Roesky, F. Schruppf and M. Noltermeyer, *J. Chem. Soc., Dalton Trans.*, 1990, 713.
14. In ref. 1, ref. 22: C.M. Jones, D. M. T. Chan, N. M. Doherty and J. C. Calabrese, manuscript in preparation; ref. 129: A. Rai-Chaudhuri, M. J. Seidel and D. L. Lichtenberger, manuscript in preparation.

15. R. W. Cockman, E. A. V. Ebsworth and J. H. Holloway, *J. Am. Chem. Soc.*, 1987, **109**, 2194.
16. R. H. Crabtree, G. G. Hlatky and E. M. Holt, *J. Am. Chem. Soc.*, 1983, **105**, 7302; D. M. Dawson, R. A. Henderson, A. Hills and D. L. Hughes, *J. Chem. Soc., Dalton Trans.*, 1992, 973
17. S. A. Brewer, PhD Thesis, 1993.
18. D. M. Bruce, J. H. Holloway and D. R. Russell, *J. Chem. Soc., Dalton Trans.*, 1978, 64.
19. S. A. Brewer, J. H. Holloway and E. G. Hope, *J. Chem. Soc., Dalton Trans.*, 1994, 1067.
20. S. A. Brewer, K. S. Coleman, J. Fawcett, J. H. Holloway, E. G. Hope, D. R. Russell and P. G. Watson, *J. Chem. Soc., Dalton Trans.*, 1995, 1073.

CHAPTER

TWO

Preparation of Platinum Fluoride

Amine Complexes

2.1 An Introduction to the Area of Platinum Amine Complexes

Amines complex to platinum by donation of an electron pair from an sp^3 orbital on nitrogen to an empty orbital of correct symmetry on platinum. Since there are no low-energy empty orbitals on nitrogen suitable for π back-donation, the Pt-N bond can be considered to be a pure σ -bond. Thus platinum amine complexes are stable for the metal in the +II or the +IV oxidation states.

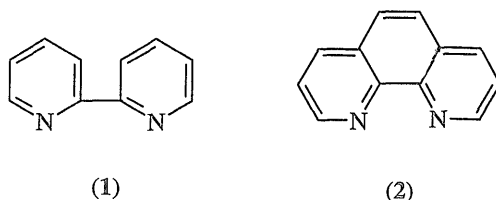
The heterocycles pyridine and 2, 2'-bipyridine are considered throughout this chapter to be amines.

2.1.2 Platinum(II) Amine Complexes

Platinum complexes with ammonia and amines, especially those of the types $[PtL_4]^{2+}$ and $[PtX_2L_2]$ (L = amine or ammonia; X= Cl, Br, I) have been extensively studied and, consequently, there is a vast area of literature available on such species. Many of them were amongst the first complexes of platinum to be prepared. For example, in 1828, G. Magnus prepared the first platinum amine complex $[Pt(NH_3)_4]Cl_2$ from $[PtCl_2]$ and NH_3 . Platinum(II) amine complexes were also very important in Werner's early studies in coordination chemistry (see **Coordination Chemistry: History**).¹ More recent review articles, on platinum amine complexes, can be found in; 'The Chemistry of Platinum and Palladium',² 'Comprehensive Coordination Chemistry'³ and 'Encyclopedia of Inorganic Chemistry'.⁴ Outlined in the next sections is an overview of the chemistry of platinum amine complexes which has a direct relevance to the work presented in this thesis.

The bis-amine complexes, $[PtX_2L_2]$ (X = Cl, Br, I), which can exist as *cis*- and *trans*- isomers, are prepared in accordance with the *trans*-effect series.^{5,6} Thus, *trans*- $[PtCl_2(NH_3)_2]$ ⁷ is formed from chloride attack on $[Pt(NH_3)_4]^{2+}$, while the *cis* complex⁸ is formed from NH_3 attack on $[PtCl_4]^{2-}$.

The *cis*- and *trans*-isomers of $[\text{PtCl}_2(\text{py})_2]$ have also been synthesized by making use of the *trans* effect method. Alternatively, the halide compounds $[\text{PtX}_2]$ can be used as precursor synthons. For example, in pyridine solvent $[\text{PtI}_2]$ gives a series of adducts $[\text{PtI}_2(\text{py})_n]$ ($n = 2, 4, 6$).⁹ The compound $[\text{PtI}_2(\text{py})_2]$ has *trans* stereochemistry.⁹ Bipyridyl (1, bipy) and 1,10-phenanthroline (2, phen) are common aromatic nitrogen ligands which form chelate complexes with platinum, $[\text{PtX}_2\text{L}]$ (L = bipy or phen; X = halides, alkyls, aryls).



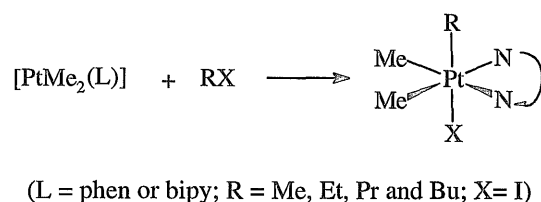
The aromatic heterocyclic nitrogen ligands, pyridine, bipy and phen have π -electron systems and therefore, in addition to the σ -component, there is the possibility of a π -component in the metal-nitrogen bond. Thus, these ligands show some properties reminiscent of tertiary phosphines and as such are able to stabilize platinum-carbon σ -bonds since the additional electron density on the metal centre, as a result of the inductive effect of the alkyl and aryl species, can be distributed into the π -component in the metal-nitrogen bond.^{10,11}

2.1.3 Platinum(IV) Amine Complexes

Amine complexes of platinum(IV) can be prepared; (A) by oxidative addition of a halogen or an alkyl halide to the corresponding platinum(II) complex or (B) by amine coordination to platinum(IV) halides. The

chlorination of the complexes *cis*-[PtCl₂(NH₃)₂], *cis*-[PtCl₂(bipy)] and *cis*-[PtCl₂(en)] (en = ethylenediamine) have been reported to yield the platinum(IV) compounds, *cis*-[PtCl₄(NH₃)₂]¹², *cis*-[PtCl₄(bipy)]¹³ and *cis*-[PtCl₄(en)].¹⁴ The complexes *cis*-[PtMe₂(L)] (L = bipy or phen) have been shown to undergo oxidative addition with a variety of alkyl halides (Scheme 2.1).¹⁵

Scheme 2.1



The reaction of [PtX₆]²⁻ and liquid ammonia gives mixtures of haloamine complexes [PtX_n(NH₃)_{6-n}]⁺X_{4-n} (X = Cl, Br, I; n = 3, 2, 1, 0).¹⁶

2.2.1 Amine-Fluoride Complexes of the Transition Metals

As may be seen from the literature the chemistry of amine complexes of the type [PtX₂L₂], where X is Cl, Br, and I, is well established. In marked contrast, the chemistry of the analogous fluoride complexes of platinum (see section 2.2.9) and, indeed, the other transition metals is an area that is relatively unexplored. Here, the term metal amine-fluoride complex is defined as a species containing direct metal-nitrogen and metal-fluorine bonds. This does not include the ionic [M(L)_x]ⁿ⁺(F⁻)_n complexes *e.g.* [Cr(NH₃)₆][F]₃.¹⁷ The earliest attempt to form a transition-metal fluoride complex with a N-donor ligand was in 1905 when Eisner and Ruff¹⁸ treated

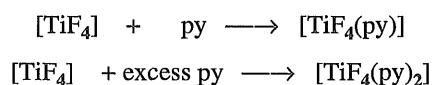
tungsten hexafluoride (WF_6) with gaseous and liquid ammonia. They isolated a white solid and an orange-brown solid, which were not fully identified. Despite this early attempt, it is evident from the literature that there have been very few concerted efforts to synthesize transition-metal amine-fluoride complexes. The majority of the work in the area of transition-metal amine-fluoride complexes was carried out in the late sixties and early seventies. Thus, analytical techniques were limited to mainly elemental analysis and infrared spectroscopy. A consequence of this is that characterizations, in retrospect, were probably not definitive and, thus, a re-investigation into this early work, employing modern spectroscopic and analytical techniques, might elucidate the reaction products and confirm, or otherwise, the original formulations. Furthermore, single crystal X-ray diffraction has only recently provided the first structural information on transition-metal amine-fluoride complexes (see sections 2.2.5 and 2.2.6). Outlined in the following sections are the reported examples of transition-metal amine-fluoride complexes. There are two established routes for the preparation of transition-metal amine-fluoride complexes:-

- (A) Reaction of a transition-metal fluoride (MF_n) or a metal-oxyfluoride (MOF_n) with an appropriate N-donor ligand.
- (B) Reaction of a transition-metal amine complex with a fluorine containing reagent.

2.2.2 Complexes of Titanium and Zirconium

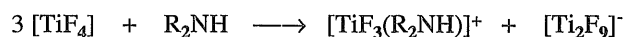
Titanium tetrafluoride reportedly reacts with diisopropylamine, diethylamine, pyridine (Scheme 2.2) or triethylamine to afford either 1:1 or 1:2 addition adducts.¹⁹ All compounds were characterized on the basis of infrared spectroscopy and elemental analysis with conductance measurements confirming their non-electrolytic nature.

Scheme 2.2



The secondary amine systems were shown to be quite complicated by Drago and coworkers.¹⁹ For example, in $[\text{TiF}_4]$ rich solutions in acetone, high conductance has been explained by the reaction depicted in Scheme 2.3.

Scheme 2.3



Clark *et al.*²⁰ reported that $[\text{TiF}_4]$ reacts with bipy, phen and o-phenylenebisdimethylamine to afford the complexes $[\text{TiF}_4\text{bipy}]$, $[\text{TiF}_4\text{phen}]$ and $[\text{TiF}_4\text{diamine}]$ (Table 2.1).

Analysis by conductance measurements, infrared spectroscopy (Table 2.1) and elemental analysis led to the formulations of these as $[\text{TiF}_4]$ adducts.

In comparison, octahedral 1:2 adducts $[\text{ZrF}_4\text{L}_2]$ are the usual products from the reactions of $[\text{ZrF}_4]$ with monodentate amines (Table 2.1). Whereas the reaction of the bidentate amine, bipy, with $[\text{ZrF}_4]$ affords the eight coordinate $[\text{ZrF}_4(\text{bipy})_2]$ (Table 2.1). The monodentate amine, [4-MeC₅H₄N], adduct of zirconium was characterized on the basis of elemental analysis and thus there is little evidence to support its formulation. The complex $[\text{ZrF}_4(\text{bipy})_2]$ was assigned an eight coordinate structure on the basis of infrared spectroscopy and conductance measurements. This compound exhibits two $\nu(\text{Zr-F})$ bands which is consistent with a dodecahedral structure of symmetry D_{2d}.²⁰

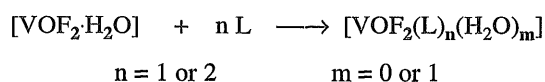
Table 2.1 Amine Adducts of Titanium and Zirconium Tetrafluorides

Product	Reagents	$\nu(\text{M-F}) \text{ cm}^{-1}$	Refs.
$[\text{TiF}_4\cdot\text{phen}]$	phen	645, 570, 562	20
$[\text{TiF}_4\cdot\text{bipy}]$	bipy	634, 562, 450	20
$[\text{TiF}_4\cdot(2\text{C}_5\text{H}_5\text{N})]$	$2\text{C}_5\text{H}_5\text{N}$	650, 600, 510	20
$[\text{ZrF}_4(4\text{-MeC}_5\text{H}_4\text{N})_2]$	$4\text{-MeC}_5\text{H}_4\text{N}$	-	21
$[\text{ZrF}_4(\text{bipy})_2]$	bipy	504, 483	20

2.2.3 Complexes of Vanadium, Niobium and Tantalum

The tetrafluoride of vanadium is reported to react with ammonia and pyridine to yield the 1:1 complexes $[\text{VF}_4\cdot\text{NH}_3]$ and $[\text{VF}_4\cdot\text{py}]$,²² with the former probably being polymeric. No adducts for VF_5 have been described. Adducts of $[\text{VOF}_2]$ (Table 2.2) can be easily prepared by the reaction shown in Scheme 2.4.²³

Scheme 2.4



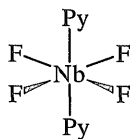
All of the vanadium adducts have been characterized by elemental analysis, with conductance measurements establishing that they are non-electrolytes in solution.

Table 2.2 Heterocyclic Amine Adducts of [VOF₂]

Product	Reagent	Refs.
[VOF ₂ ·py ₂]	2 py	23, 24
[VOF ₂ ·(phen)]	phen	23, 24
[VOF ₂ ·(4-MeC ₅ H ₄ N) ₂]	2 (4-MeC ₅ H ₄ N)	23

Niobium and tantalum pentafluorides form adducts with various Lewis bases including aliphatic and aromatic amines (Table 2.3). Analysis by infrared spectroscopy and elemental analysis led to the formulation of all the niobium complexes. The tantalum adduct is only mentioned in a review article²⁶ as unpublished observations and consequently no data have been reported.

In comparison, the only reported MF₄ adduct is the dipyridinetetrafluoro-niobium, [NbF₄(py)₂],³¹ which exists as the *trans*-isomer as determined by infrared and Raman spectroscopies.



D_{4h}

Table 2.3 Amine Adducts of $[\text{MF}_5]$ ($\text{M} = \text{Nb}$ or Ta)

Products	Reagent (L = amine)	Refs.
$[\text{NbF}_5\text{L}_2]$	NH_2R ($\text{R} = \text{H}, \text{Et}$)	25, 26, 27
$[\text{NbF}_5(\text{NHEt}_2)]$	NHEt_2	26, 27, 28
$[\text{NbF}_5\text{L}]$	NR_3 ($\text{R} = \text{Me}, \text{Et}$)	26, 27
$[\text{NbF}_5(\text{py})_2]$	py	25, 29
$[\text{NbF}_5(\text{bipy})]$	bipy	30
$[\text{TaF}_5(\text{py})_2]$	py	26

2.2.4 Complexes of Chromium

In contrast to the other transition-metals, amine-fluoride complexes of chromium(III) have been extensively studied.³²⁻³⁴ The small highly basic fluoride ligand forms a strong bond to the Cr(III) centre which remains intact in the absence of acid. Thus, the Cr-F bond can be carried through various syntheses and removed when necessary affording numerous Cr(III) amine-fluoride species of the general type; $[\text{CrF}(\text{N})_5]^{2+}$ *e.g.* $[\text{CrF}(\text{NH}_3)_5]^{2+}$ ³⁵, $[\text{CrF}_2(\text{N})_4]^+$ *e.g.* $[\text{CrF}_2(\text{en})_2]^+$ ³⁶, $[\text{CrF}_3(\text{N})_3]$ *e.g.* $[\text{CrF}_3(\text{py})_3]$ ³⁷ and $[\text{CrF}_4(\text{N})_2]^-$ *e.g.* $[\text{CrF}_4(\text{en})]^-$ ($\text{N} = \text{N-donor ligand}$).³³

Diamine-fluoride complexes of the type, $[\text{CrF}_2(\text{L})_2]^+$ ($\text{L} = \text{bidentate amines}$) have been reported to be prepared by numerous routes however, the most convenient are:-

- (i) reaction of $[\text{CrF}_3] \cdot 3.5\text{H}_2\text{O}$ with the appropriate diamine (Scheme 2.5).
- (ii) treatment of a dilute aqueous HF solution of $[\text{CrCl}_3] \cdot 6\text{H}_2\text{O}$ with the required diamine.

(iii) reaction of $trans-[CrF_2(py)_4]^+$ with the diamine in boiling 2-methoxyethanol (Scheme 2.6).

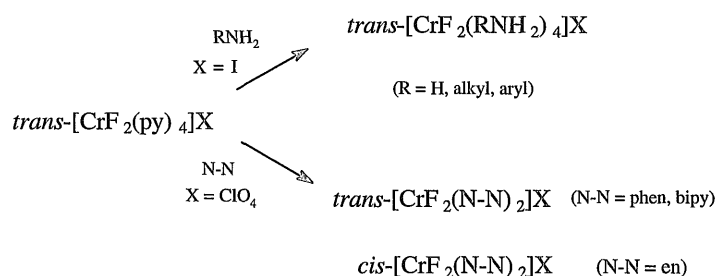
Scheme 2.5



(L = en, pn, tmd or dach)

$Trans-[CrF_2(py)_4]^+$, formed by the addition of pyridine to a solution containing a high concentration of Cr^{3+} and F^- ,³⁸ is a convenient starting material for a variety of $[CrF_2N_4]^+$ complexes (Scheme 2.6). These reactions are usually carried out in boiling 2-methoxyethanol. Under acid conditions, the F^- ligands can be substituted to give complexes of the type $[CrF(Y)N_4]^+$ (Y = Cl, Br, I, OH, NCS *etc.*).³²

Scheme 2.6



The majority of the Cr(III) amine-fluoride complexes have been characterized by infrared spectroscopy since $\nu(Cr-F)$ bands are strong and appear in a characteristic region between $355-370\text{ cm}^{-1}$.

In marked contrast to the earlier transition-metals there are no reported N-donor adducts of $[\text{CrF}_4]$, $[\text{CrOF}_3]$ and $[\text{CrF}_5]$. This is a consequence of the increasing fluorinating ability, as we traverse the transition-metals from left to right, and therefore reducing the complexing ability.

2.2.5 Complexes of Molybdenum and Tungsten

In common with the previously discussed metal tetrafluorides, $[\text{TiF}_4]$, $[\text{ZrF}_4]$, $[\text{VF}_4]$ and $[\text{NbF}_4]$, Muetterties²¹ reported that $[\text{MoF}_4]$ also reacted with the amines, $\text{C}_6\text{H}_5\text{N}(\text{CH}_3)_2$, pyridine and trimethylamine to afford 1:1 adducts. Analysis by partial elemental analysis led to the formulation of these complexes. More recently Chakravorti *et al.*,³⁹ reported the dimeric molybdenum species, $[\text{Mo}_2\text{O}_3\text{F}_4(\text{L})_2]$ and $[\text{Mo}_2\text{O}_4\text{F}_2(\text{L})_2]$ (L = bipy or phen), containing bridging oxygen ligands.

Ever since Eisner and Ruff¹⁸ first treated $[\text{WF}_6]$ with ammonia, reactions of this type have been investigated in an attempt to elucidate the products. Clark and Emeleus⁴⁰ repeated the reaction with ammonia and also carried out subsequent reactions with pyridine and methylamine to afford $[\text{WF}_6 \cdot 4\text{NH}_3]$, $[\text{WF}_6 \cdot 3\text{py}]$ and $[\text{WF}_6 \cdot (\text{MeNH}_2)_3]$, respectively. However, work employing ^{19}F NMR spectroscopy, by Winfield *et al.*,^{41,42} showed that the reaction of $[\text{WF}_6]$ with amines proceeds *via* iminolysis {complex containing a metal to nitrogen double (imido) bond ($\text{M}=\text{N}$)}. A ^{19}F NMR study of the reaction between $[\text{WF}_6]$ and NH_3 ⁴³ also showed iminolysis to occur. Furthermore, the reaction of $[\text{MoF}_6]$ with NH_3 has been reported to yield a mixture of ammonium fluoride and $[\text{MoF}_5 \cdot 4\text{NH}_3]$,⁴⁴ again it seems likely that, in this case too, iminolysis has occurred.

More recently, Bougon *et al.*, have investigated the interactions of tungsten hexafluoride (WF_6) and tungsten oxide tetrafluoride (WOF_4) with various nitrogen-donor ligands their results are reported in Table 2.4. All of

the complexes (1) - (13) have been characterized by elemental analysis, infrared spectroscopy and X-ray powder diffraction. Structural information has been obtained, from single crystal X-ray diffraction, for the majority of complexes with the exception of (1), (5), (8), (9) and (10). For example, the X-ray crystal structure determination of complex (2) revealed the tungsten atom surrounded by an undecahedron of ligands derived from a trigonal prism by the capping of two square faces (2:2:4 ligand arrangement; Figure 2.1).

Figure 2.1 X-Ray Crystal Structure of Complex (2)

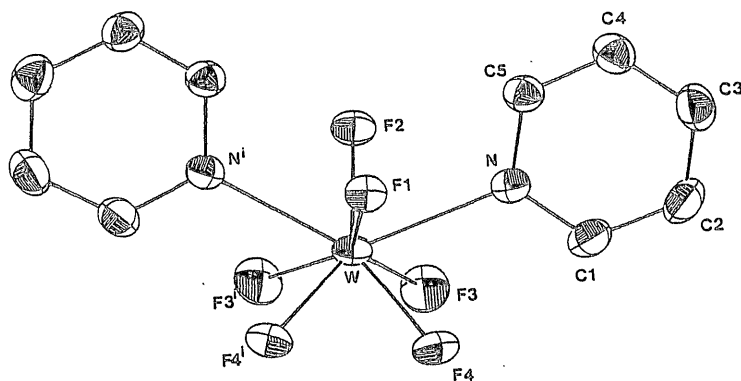


Table 2.4 Amine Adducts of WF_6 and WOF_4

Product	Reactants	Refs.
$[\text{WF}_6\text{py}]$ (1)	$[\text{WF}_6] + \text{py}$	45
$[\text{WF}_6\cdot 2\text{py}]$ (2)	$[\text{WF}_6] + \text{excess py}$	45
$[\text{WOF}_4(\text{F-py})]$ (3)	$[\text{WOF}_4] + \text{F-py}$	46
$[\text{WF}_6(\text{F-py})]$ (4)	$[\text{WF}_6] + \text{F-py}$	46
$[\text{WF}_6(\text{bipy})]$ (5)	$[\text{WF}_6] + \text{bipy}$	47
$[\text{WF}_4(\text{bipy})_2][\text{WF}_7]_2$ (6)	$[\text{WF}_6(\text{bipy})] + \text{bipy} + [\text{WF}_6]^{\text{a}}$	47
$[\text{WF}_4(\text{bipy})_2][\text{W}_2\text{O}_2\text{F}_9]_2$ (7)	$[\text{WF}_6(\text{bipy})] + \text{bipy} + [\text{WF}_6]^{\text{b}}$	48
$[\text{WOF}_4(\text{napy})]$ (8)	$[\text{WOF}_4] + \text{napy}$	49
$[\text{WOF}_4(\text{dmnapy})]$ (9)	$[\text{WOF}_4] + \text{dmnapy}$	49
$[\text{WOF}_4(\text{bipy})]$ (10)	$[\text{WOF}_4] + \text{bipy}$	50
$[\text{WO}_2\text{F}_2(\text{bipy})]$ (11)	$[\text{WOF}_4(\text{bipy})]$ in CH_2Cl_2	50
$[\text{WOF}_4(\text{py})_2]$ (12)	$[\text{WOF}_4] + 2 \text{ py}$	51
$[\text{WOF}_4(\text{py})]$ (13)	$[\text{WOF}_4] + \text{py}$	51

(a) anhydrous conditions

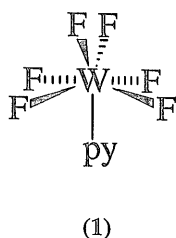
(b) hydrous conditions

(napy = 1,8-naphthyridine and dmnapy = 2,7-dimethyl-1,8-naphthyridine)

The ^{19}F NMR spectrum, at 193 K, for complex (2) shows an A_4X_2 pattern with the triplet resonance being observed at δ 124 and the corresponding quintet at δ 75 with $^2J_{\text{FF}} = 88$ Hz. The triplet corresponds to the four equivalent fluorine atoms of the square face and the quintet to the two equivalent fluorine atoms of the edge opposite this face which is

consistent with the solid-state structure being retained in solution (see Figure 2.1). The ^{19}F NMR spectrum of complex (1) recorded at 140 K was also found to be of the A_4X_2 type with a triplet at δ 145.5 and a quintet at δ 207 with $^2J_{\text{FF}} = 48$ Hz. However, in comparison with $[\text{WF}_6]$ (δ 167) the signal for the four equivalent fluorine atoms has shifted to a lower frequency, whereas that due to the other fluorine atoms has shifted to a higher frequency. This shows that in $[\text{WF}_6(\text{py})]$ (1), in particular, the two fluorine atoms opposite to the py ligand are deshielded with respect to the four others and molecular $[\text{WF}_6]$, an effect described as the "NMR *trans*-influence" *i.e.* the ^{19}F resonances are dependent upon the *trans*- or pseudo-*trans*-ligands. Although, the geometry around the tungsten centre could not be determined by X-ray diffraction methods, the 1:2:4 arrangement of the ligands indicated by the ^{19}F NMR data corresponds to a monocapped trigonal prism (Figure 2.2).

Figure 2.2 Monocapped Trigonal Prism of Complex (1)



Where reported, the ^{19}F NMR spectra of the complexes containing the moiety $[\text{WOF}_4]$ show singlet resonances, due to the chemical equivalence of the four fluorine atoms, with ^{183}W satellites, $^1J_{\text{WF}} \approx 65$ Hz, at $\delta \approx 70$.

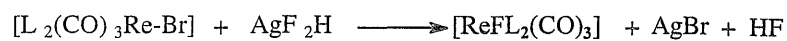
An alternative route to a transition-metal amine-fluoride complex has been reported in the reaction of $[\text{W}(\text{CO})_2(\text{bipy})_2][\text{BF}_4]_2$ with the appropriate ligand L-L (L-L = dppe or dppm) which affords the seven coordinate $[\text{WF}(\text{CO})_2(\text{bipy})(\text{L-L})][\text{BF}_4]$.⁵² Metal-centre abstraction of a fluoride ion from $[\text{BF}_4]^-$ or $[\text{PF}_6]^-$ counterions is a common, if not deliberate, route to metal-fluoride coordination compounds. The structures of these complexes were established by NMR spectroscopy. The $^{31}\text{P}\{^1\text{H}\}$ NMR spectrum of the dppe complex consists of a doublet at δ 50.4 with ^{183}W satellites, exhibiting coupling to fluorine ($^2J_{\text{PF}} = 33.2$ Hz). Corresponding results were obtained for the dppm complex ($^{31}\text{P}\{^1\text{H}\}$ δ -8.84, $^2J_{\text{PF}} = 33.2$ Hz). The ^{19}F NMR spectrum of the dppe complex shows a singlet, δ -151.7, assigned to the $[\text{BF}_4]^-$, and a triplet at δ -169.3 ($^1J_{\text{WF}} = 61.6$ Hz), assigned to the tungsten-bonded fluorine. It is more likely that the triplet is due to the fluorine coupling to the two equivalent phosphorus atoms since the reported $^1J_{\text{WF}}$ coupling constant is approximately double the value quoted for the $^2J_{\text{PF}}$, 62 and 33 Hz respectively. Low frequency ^{19}F NMR signals are diagnostic for fluoride ligands coordinated to low-valent metal centres.

To date there have been no reported Mo(III) or W(III) amine-fluoride complexes.

2.2.6 Complexes of Manganese and Rhenium

To date there has been only one reported example of a manganese amine-fluoride complex, $[\text{MnF}_3(\text{phen})(\text{H}_2\text{O})]$,⁵³ formed by the reaction of $[\text{Mn}_2\text{O}_3]$ and phen in 40% HF, which was characterized on the basis of elemental analysis. Amine-fluoride complexes of the type $[\text{ReF}(\text{CO})_3\text{L}_2]$ ($\text{L}_2 = \text{bipy}$ or tmeda) have been obtained in good yield by bromide abstraction from the corresponding bromo-analogue with silver bifluoride (Scheme 2.7).⁵⁴

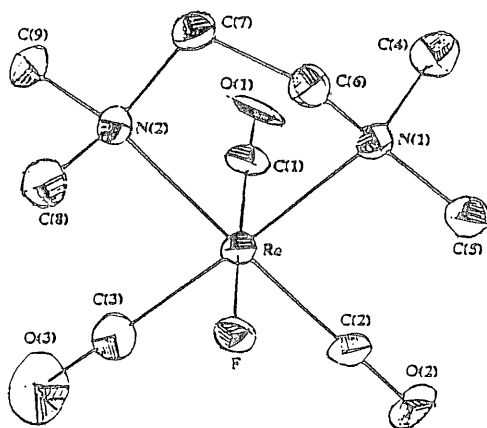
Scheme 2.7



L_2 = tmeda or bipy

The crystal structure of $[ReF(CO)_3(tmeda)]$ has been determined, and confirmed an octahedral geometry around the central rhenium atom with *facial* carbonyl ligands (Figure 2.3). No ^{19}F NMR data have been reported for these derivatives.

Figure 2.3 X-Ray Crystal Structure of $[Re(CO)_3(tmeda)F]$



2.2.7 Complexes of Iron, Ruthenium and Osmium

The amine-fluoride chemistry of iron, ruthenium and osmium has received significantly less attention than that of the early transition metals. Thus, the literature contains only a few examples of iron, ruthenium and osmium amine-fluoride complexes (Table 2.5).

Table 2.5 Amine-Fluoride Complexes of Iron, Ruthenium and Osmium

Products	Reagents	Refs.
$[(\text{OEP})\text{Fe}-\text{F}-\text{Cu}(\text{bnpy}_2)(\text{OCIO}_3)][\text{PF}_6]^{\text{a}}$ (1)	$[\text{Cu}_2\text{F}_2(\text{bnpy}_2)_2][\text{PF}_6] +$ $[\text{Fe}(\text{OEP})(\text{OCIO}_3)]$	55
$[\text{M}(\text{F}(\text{NH}_3)_4\text{NO})\text{SiF}_6]$ (2) M = Ru, Os	$[\text{MCl}_5\text{NO}][\text{SiF}_6] +$ $[\text{NH}_4\cdot\text{HF}_2]$	56
$[\text{Ru}(\text{bipy})_2\text{F}_2]$ (3)	$[\text{Ru}(\text{bipy})_3]\text{F}_2 + \text{DMF}$	57
$[\text{RuHF}(\text{CO})(\text{py})(\text{P}^t\text{Bu}_2\text{Me})_2]$ (4)	$[\text{RuHF}(\text{CO})(\text{P}^t\text{Bu}_2\text{Me})_2]$ + excess py	58
$[\text{OsO}_2\text{F}_2(\text{py})_2]$ (5)	$[\text{OsO}_2(\text{py})_2(\text{OCF}_2\text{CF}_2\text{O})]$ + Δ	59

(a) see section 2.2.10 (OEP = porphyrin ring and bnpy₂ = bis[2-(2-pyridyl)ethyl]amine)

The mixed metal fluorine-bridged (1) complex and the fluorotetra-aminenitrosyl-osmium and ruthenium (2) species are air-stable and have been unambiguously characterized by single crystal X-ray diffraction. Analysis by UV visible spectroscopy led to the formulation of the complex $[\text{Ru}(\text{bipy})_2\text{F}_2]$ (3), thus there is no direct evidence for the existence of a ruthenium-fluoride bond in this complex. However, ¹⁹F NMR studies were performed on the complexes $[\text{RuHF}(\text{CO})(\text{py})(\text{P}^t\text{Bu}_2\text{Me})_2]$ (4) and $[\text{OsO}_2\text{F}_2(\text{py})_2]$ (5) and both

gave rise to resonances indicative of metal-bound fluoride ligands.

Resonances at δ -389 (triplet, $^2J_{\text{FP}} = 24$ Hz) and -109 were observed for the ruthenium and osmium complexes respectively, with the former showing coupling to the phosphorus and hydrogen nuclei.

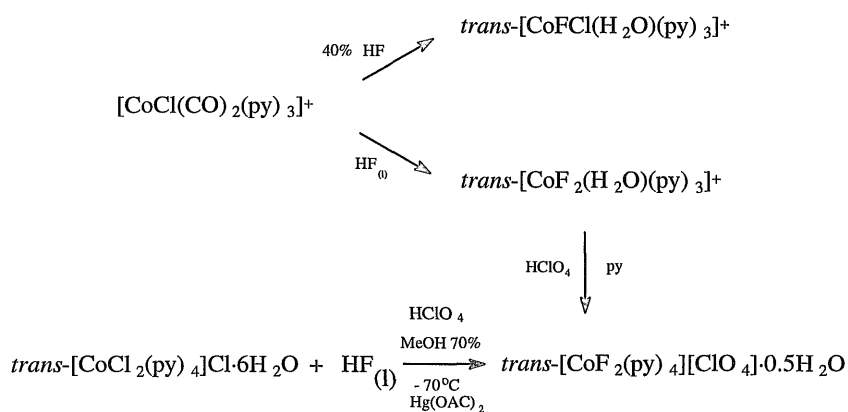
Recently Coleman *et al.*,⁶⁰ described complexes of the type *cis*, *cis*- $[\text{OsF}_2(\text{CO})_2\text{L}_2]$ (L = py and NEt_3) formed from the reaction of the novel, highly reactive $[\text{OsF}_2(\text{CO})_3]_4$ with the appropriate ligand, L, in CH_2Cl_2 . A combination of mass spectrometry, ^{19}F NMR and infrared spectroscopy led to the formulation of these complexes.

2.2.8 Complexes of Cobalt, Rhodium and Iridium

Cobalt(II)-fluoride has been reported to react with 3-hydroxypyridine (py3OH) to afford the octahedral complex $[\text{CoF}_2(\text{py3OH})_4]$.⁶¹ Amine-fluoride complexes of Co(III) have received more attention than those of Co(II) with species of the type, $[\text{CoF}(\text{NH}_3)_5][\text{X}]_2$ (X = NO_3^- , F^- , Cl^- , Br^- and ClO_4^-)⁶² and $[\text{CoF}(\text{Y})(\text{en})_2][\text{X}]$ (Y = F, Cl, NO_2 ; X = NO_3^- , F^- , HF_2^-)⁶³ being reported in the literature. Furthermore, the Co(III) complexes, $[\text{CoCl}(\text{CO})_2(\text{py})_3]^+$ and $[\text{CoCl}_2(\text{py})_4]\text{Cl}$ have been shown to undergo halide metathesis with HF affording Co(III) amine-fluoride compounds (Scheme 2.8).^{64,65} Elemental analysis and visible absorption spectroscopy led to the characterization of the Co(III) amine-fluoride complexes.

To date there have been no reported iridium amine-fluoride complexes. For rhodium, literature reports are limited to the poorly characterized *trans*- $[\text{RhF}(\text{en})_2(\text{H}_2\text{O})][\text{ClO}_4]_2$,⁶⁶ reputedly formed by the reaction of *trans*- $[\text{Rh}(\text{en})_2\text{Cl}_2]\text{ClO}_4$ and AgF in water.

Scheme 2.8



2.2.9. Complexes of Nickel, Palladium and Platinum

In contrast to palladium and platinum there are several literature reports of nickel(II) amine-fluoride complexes. The complex $[\text{NiF}_2(\text{py})_4]$ was reported by Knyazeva *et al.*⁶⁷ in 1967 and is characterized by partial elemental analysis. Further investigation by Smit and coworkers⁶¹ reported the complex $[\text{NiF}_2(\text{py}3\text{OH})_4]$ ($\text{py}3\text{OH}$ = 3-hydroxypyridine) formed by the reaction of $[\text{NiF}_2]$, slightly acidified with HF, and excess 3-hydroxypyridine. Analysis by elemental analysis and infrared spectroscopy, with a band at 435 cm^{-1} being assigned to the $\nu(\text{Ni-F})$, led to the formulation of this complex.

The reaction of nickel(II) fluoride hydrate, $[\text{NiF}_2]\cdot 4\text{H}_2\text{O}$, with various amines in methanol has been reported to afford complexes of the type $[\text{NiL}_3]\text{F}_2$ ⁶⁸ (L = en, bipy and phen). Further reaction of $[\text{NiL}_3]\text{F}_2$ with $[\text{NiF}_2]\cdot 4\text{H}_2\text{O}$ in methanol led to the formation of the dimeric $[\text{L}_2\text{Ni}(\mu\text{-F})_2\text{NiL}_2]\text{F}_2$ complex (Table 2.6). However, the more sterically demanding $\text{Me}_2\text{NCH}_2\text{CH}_2\text{NMe}_2$ is reported to yield $[\text{Ni}(\text{Me}_2\text{NCH}_2\text{CH}_2\text{NMe}_2)\text{F}_2]$ when heated with $[\text{NiF}_2]\cdot 4\text{H}_2\text{O}$ in 2-propanol. The dimeric nickel complexes were

characterized by elemental analysis and infrared spectroscopy (Table 2.6) with conductance studies confirming the presence of electrolytes in solution.

Table 2.6 Infrared Data for the $\nu(\text{Ni-F}_{\text{Bridge}})$ of the Dimeric Nickel Complexes

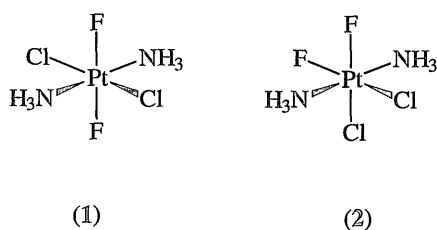
Compound	$\nu(\text{Ni-F}_{\text{Bridge}}) / \text{cm}^{-1}$
$[(\text{en})_2\text{Ni}(\mu\text{-F})_2\text{Ni}(\text{en})_2]\text{F}_2$	~ 378
$[(\text{bipy})_2\text{Ni}(\mu\text{-F})_2\text{Ni}(\text{bipy})_2]\text{F}_2$	~ 360
$[(\text{phen})_2\text{Ni}(\mu\text{-F})_2\text{Ni}(\text{phen})_2]\text{F}_2$	~ 358

More recently Emsley *et al.*⁶⁹ found that prolonged refluxing, in methanol, of $[\text{NiF}_2] \cdot 4\text{H}_2\text{O}$ and bipy followed by dissolution in ethanol afforded $[(\text{bipy})_2\text{F}(\mu\text{-F})\text{NiF}(\text{bipy})_2]^+ [\text{F}(\text{EtOH})_2(\text{H}_2\text{O})_2]^- \cdot \text{H}_2\text{O}$ and not the previously described $[\text{Ni}(\text{bipy})_3]\text{F}_2$.⁶⁸ This complex has been characterized by single crystal X-ray diffraction.

To date there has been only one reported example of a palladium amine-fluoride complex $[\text{PdF}(\text{Me})_2(\text{CH}_2\text{Ph})(\text{bipy})]$ ⁷⁰ formed by fluoride metathesis of the corresponding bromo-analogue. Characterization was by ^1H NMR spectroscopy and thus there is little evidence to support the formation of a palladium-fluoride bond.

As stated in section 2.1 complexes of the type $[\text{PtX}_2\text{L}_2]$ and $[\text{PtX}_4\text{L}_2]$ ($\text{X} = \text{Cl}, \text{Br}, \text{I}$; $\text{L} = \text{ammonia or amine}$) are well established. In marked contrast the analogous fluoro-complexes have received significantly less attention and thus are limited to four reports in the literature, $[\text{Pt}(\text{N-N})\text{FCl}_2]$ ⁷¹ ($\text{N-N} = \text{protonated N-aminopiperidine}$), $[\text{PtF}_2\text{Cl}_2(\text{NH}_3)_2]$ ⁷² $[\text{PtF}(\text{Me})_2(\text{Me}_2\text{NCH}_2\text{CH}_2\text{N}=\text{CHC}_6\text{F}_4)]$ (3)⁷³ and $[\text{PtF}(\text{Me})_2\{\text{Me}_2\text{NCH}_2\text{CH}_2\text{NHCH}(\text{CH}_2\text{COMe})\text{C}_6\text{F}_4\}]$ (4).⁷⁴ Halide metathesis

of $[\text{Pt}(\text{N-N})\text{Cl}_3]$ with AgF , in water, led to the formation of $[\text{Pt}(\text{N-N})\text{FCl}_2]$, which was characterized by partial elemental analysis. The platinum(IV) complex $[\text{PtF}_2\text{Cl}_2(\text{NH}_3)_2]$ was formed by the reaction of *trans*- $[\text{PtCl}_2(\text{NH}_3)_2]$ and $[\text{XeF}_2]$ in AHF .⁷² This complex, which represents the first example of oxidative fluorination of a platinum(II) compound, was characterized by elemental analysis and ^{19}F NMR spectroscopy. The ^{19}F NMR spectrum of $[\text{PtF}_2\text{Cl}_2(\text{NH}_3)_2]$ showed a singlet resonance at δ -387 with the associated platinum satellites ($^1J_{\text{PtF}} = 1790$ Hz). However, on the basis of a singlet being observed 2 structural isomers are possible, one with F *trans* F (1) and the other with F *trans* Cl (2) with, in both cases, retention of the *trans*-arrangement of the amines.



Although there is the possibility of two isomers the authors do not suggest which of the two is formed in their reaction.

The reaction between the ligand $\text{Me}_2\text{NCH}_2\text{CH}_2\text{N}=\text{CHC}_6\text{F}_5$ and $[\text{Pt}_2\text{Me}_4(\mu\text{-SMe}_2)_2]$ in acetone solution was reported to afford sequentially $[\text{PtMe}_2(\text{Me}_2\text{NCH}_2\text{CH}_2\text{N}=\text{CHC}_6\text{F}_5)]$, then (3) and (4). There is no doubt as to the existence of a platinum-fluoride bond in complex (4) since it was structurally characterized by single crystal X-ray diffraction (see section 2.6.4). However, the existence of a Pt-F bond, in complex (3), was confirmed by the observation of a resonance at $\delta(^{19}\text{F})$ -241 with a $^1J_{\text{PtF}} = 145$ Hz.

2.2.10 Complexes of Copper, Silver and Gold

To date there are no reported examples of amine-fluoride complexes of silver or gold however, there are several reports of such compounds of copper (Table 2.7).

All of the complexes presented in Table 2.7 have been unambiguously characterized by single crystal X-ray diffraction.

Table 2.7 Amine-Fluoride Complexes of Copper

Product	Reactant	Refs.
$[\text{Cu}_2\text{F}_2(\text{bnpy})_2][\text{PF}_6]_2$ (1)	$[\text{Cu}(\text{MeCN})_4][\text{PF}_6] + \text{bnpy} + \text{O}_2$	55
$[(\text{OEP})\text{Fe}-\text{F}-\text{Cu}(\text{bnpy})_2(\text{OCIO}_3)][\text{PF}_6]$ (2)	$[\text{Cu}_2\text{F}_2(\text{bnpy})_2][\text{PF}_6]_2 + [\text{Fe}(\text{OEP})(\text{OCIO}_3)]$	55
$[\text{CuF}_2(\text{TMPA})]_2[\text{PF}_6]_2$ (3)	$[\text{Cu}(\text{TMPA})\text{CH}_3\text{CN}][\text{PF}_6] + \text{O}_2$	75
$[\text{CuF}(\text{TMPA})][\text{PF}_6]$ (4)	$[\text{Cu}(\text{TMPA})\text{CH}_3\text{CN}][\text{PF}_6] + \text{O}_2$	75

bnpy = bis[2-(2-pyridyl)ethyl]amine, OEP = porphyrin ring and TMPA = tris[(2-pyridyl)methyl]amine

2.3 Summary

It may be seen from the literature that the preparation and chemistry of transition metal amine-fluoride complexes, with the exception of chromium, is an area that has received little attention. Furthermore, the earlier examples were characterized on the basis of elemental analysis and infrared spectroscopy thus, there is little evidence to support their formulations. However, more recently the majority of the reported complexes have been characterized by single crystal X-ray diffraction and, therefore, no doubt can be cast as to their existence.

It has been shown that the Pt(II) amine complexes will undergo oxidative addition reactions with halogens to afford stable platinum(IV) species. Thus, the reactions of $[\text{XeF}_2]$, which is well established as a convenient route for the introduction of fluorine into low-valent metal centres, with a variety of dichloro(bisamino)platinum(II) complexes are discussed in this chapter. The metathetical reactions with AHF and, in some cases, AgF are also reported in this chapter. Combinations of ^{19}F NMR, infrared and mass spectrometry were employed to characterize the products. To date, structural data on transition metal amine-fluoride complexes are limited to only a few reports in the literature. The structural characterization, employing EXAFS spectroscopy, of a platinum(IV) amine-fluoride complex is reported in this chapter.

2.4 Introduction to Results and Discussion

In the following sections the reactions of $[\text{XeF}_2]$, which has been proven to be a good oxidative fluorinator (see Chapter 4), with complexes of the type $[\text{PtCl}_2(\text{L})_2]$ ($\text{L} = \text{NH}_3, \text{NMe}_3, \text{py}$; $\text{L}_2 = \text{en}, \text{bipy}$) are described. The oxidative fluorination reactions were performed in two solvents, AHF and CH_3CN , to ascertain if the nature of the solvent influenced the reaction and, thus, the products formed. In AHF solution $[\text{XeF}_2]$ is reported to form an $\text{F-Xe}^{\delta+}\cdots\text{F}\cdots\text{H-F}^{\delta-}$ adduct which is an aggressive fluorinating agent.⁷⁶ In contrast, $[\text{XeF}_2]$ in CH_3CN solution is a mild fluorinating agent. Thus, the influence of the solvent, by comparison of the products, can be clearly seen. Furthermore, CH_3CN was employed rather than a chlorinated solvent to avoid the possibility of fluorine/chlorine exchange. Where possible the corresponding *cis*- and *trans*-isomers were studied to ascertain whether, or not, the configuration of the N-donor ligands were retained during the reaction. Unfortunately, the *cis*-isomer of $[\text{PtCl}_2(\text{NMe}_3)_2]$ was not studied since, it is not reported in the literature and all attempts to prepare this complex were unsuccessful. Furthermore, the species of the type $[\text{PtCl}_4]^{2-}$, $[\text{PtCl}_3\text{N}]^-$, $[\text{PtClN}_3]^+$ and $[\text{PtN}_4]^{2+}$ ($\text{N} = \text{N-donor ligand}$) were, with the exception of $[\text{PtCl}_4]^{2-}$ and $[\text{PtN}_4]^{2+}$, not included in the studies owing to the time available. However, $[\text{PtCl}_4]^{2-}$ was found to afford no fluoro-species when reacted with $[\text{XeF}_2]$ whereas, the analogous reaction with $[\text{PtN}_4]^{2+}$ ($\text{N}_4 = (\text{en})_2$) did yield an amine-fluoride complex and is discussed in section 2.13.

It is important to note that the majority of the oxidative fluorination reactions, with $[\text{XeF}_2]$, afforded several structural isomers. Unfortunately, all attempts to separate the isomers were unsuccessful thus, in most cases, infrared spectroscopy, mass spectrometry and elemental analysis were not informative and consequently, all characterizations were reliant on ^{19}F NMR spectroscopy.

Owing to the dearth of reported platinum amine-fluoride complexes there is only one report of ^{19}F NMR data, in the literature, in which comparisons with this work can be made. The reported data are for the complex $[\text{PtF}_2\text{Cl}_2(\text{NH}_3)_2]$ (see section 2.2.9) which exhibits a singlet at δ -387 with a $^1J_{\text{PtF}} = 1790$ Hz.⁷² However, a recent ^{19}F NMR spectroscopy study, by Preetz *et al.*,⁷⁷ of the anions $[\text{PtF}_n\text{Cl}_{6-n}]^{2-}$ ($n = 0-6$) enabled comparisons with this work to be made. Preetz and co-workers reported two distinct ^{19}F chemical shift regions: one which falls in the region δ -357 to -382 and is assigned to F *trans* F, the other falls in the range δ -268 to -287 and is attributed to F *trans* Cl. Furthermore, the corresponding $^1J_{\text{PtF}}$ coupling is significantly different with the magnitude being ≈ 1900 and 1300 Hz for F *trans* F and F *trans* Cl respectively. It is evident, from the data reported by Preetz, that the $\delta(^{19}\text{F})$ for the F *trans* F environment is found at a lower frequency (≈ 100 ppm) than that observed for the F *trans* Cl environment. The magnitude of the $^1J_{\text{PtF}}$ coupling has also been proven to be indicative of the environment with the $^1J_{\text{PtF}}$ coupling for F *trans* F being larger (≈ 600 Hz) than the corresponding value for F *trans* Cl.

By comparison of the ^{19}F NMR data reported for the complex $[\text{PtF}_2\text{Cl}_2(\text{NH}_3)_2]$ ⁷² with that documented by Preetz, it can be concluded that this species is the isomer with both the ammonia groups and fluorine ligands *trans* to each other since both the $\delta(^{19}\text{F})$ and magnitude of the $^1J_{\text{PtF}}$ coupling are characteristic of F *trans* F.

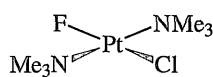
2.5 Metathetical Reactions of Various Dichloroplatinum(II) Complexes Containing N-Donor Ligands with AHF

A sample of the complex $[\text{PtCl}_2(\text{L})_2]$ ($\text{L} = \text{NH}_3$, py, NMe_3 , NEt_3 ; $\text{L}_2 = \text{bipy}$, en) was treated with AHF as described in section 6.19. After 2-24 hours

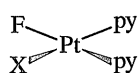
the solvent was removed affording, in most cases, an apparently unchanged yellow solid which was subsequently dissolved in d_6 -DMSO and analysed by ^{19}F NMR spectroscopy. All the ^{19}F NMR data are presented in Table 2.8.

Table 2.8 ^{19}F NMR Data for the Products Formed from the Metathetical Reactions of Various Platinum(II) complexes with AHF

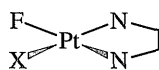
Product	Starting Material	$\delta(^{19}\text{F})/\text{ppm}$	$^1J(\text{PtF})/\text{Hz}$
(1)	<i>trans</i> -[PtCl ₂ (NMe ₃) ₂]	-304	1223
(2)	<i>trans</i> -[PtCl ₂ (NEt ₃) ₂] ^a	-250	453
(3)	<i>cis</i> -[PtCl ₂ (py) ₂]	-342	1001
(4)	<i>cis</i> -[PtCl ₂ (en)]	-351	617
(5)	<i>cis</i> -[PtCl ₂ (bipy)]	-331	834
(6)	<i>cis</i> -[PtCl ₂ (NH ₃) ₂]	-	-
(7)	<i>trans</i> -[PtCl ₂ (NH ₃) ₂]	-	-



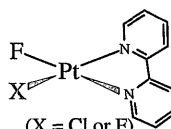
(1)



(X = Cl or F)
(3)



(X = Cl or F)
(4)



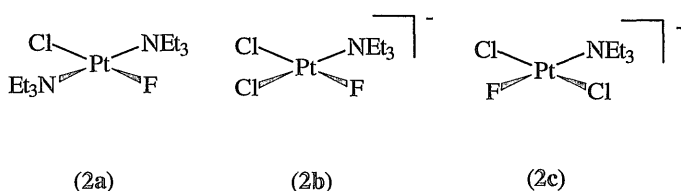
(X = Cl or F)
(5)

(a) The evidence for this starting material is inconclusive and thus assignment of complex (2) is only tentative

All complexes, except (6) and (7) which were not identified, exhibited a singlet with the associated ^{195}Pt satellites in their respective ^{19}F NMR spectra. In all cases evidence for unreacted starting material was found in the mass spectra thus indicating that these reactions were not quantitative.

Halide metathesis reactions of AHF and *cis*- $[\text{PtX}_2(\text{PPh}_3)_2]$ ($\text{X} = \text{Cl}, \text{Br}$), affording *cis*- $[\text{PtFX}(\text{PPh}_3)_2]$ have been reported previously.⁷⁸ Thus, complex (1) has been assigned to *trans*- $[\text{PtFCl}(\text{NMe}_3)_2]$ with a $^1J_{\text{PtF}}$ coupling of 1223 Hz. Further evidence to substantiate the formulation of (1) is the observation of a peak centred at m/z 368, in the E. I. mass spectrum, which corresponds to *trans*- $[\text{PtFCl}(\text{NMe}_3)_2]$. The formation of the monofluoro-complex and not the difluoro-species is justified by taking into account the "trans directing influence",⁷⁹ which is the role played by the *trans* ligand (Y) in deciding which ligand, X or Y, is substituted by the incoming ligand. The "trans directing influence" exhibited by fluorine is not as great as that by chlorine and thus replacement of the second chloride will not occur.

In the reaction which affords complex (2) there is doubt cast as to the exact nature of the starting material. Initially, the starting material was presumed to be the novel complex *trans*- $[\text{PtCl}_2(\text{NEt}_3)_2]$, which was prepared as described in section 6.23, characterized by a combination of ^1H NMR spectroscopy and E. I. mass spectrometry. However, an attempt to grow crystals of *trans*- $[\text{PtCl}_2(\text{NEt}_3)_2]$ led to the isolation and structural characterization of the novel anionic complex $[\text{HNEt}_3][\text{PtCl}_3(\text{NEt}_3)]$ (see Appendix A). Therefore, the nature of complex (2) could be a result of the metathesis reaction of either *trans*- $[\text{PtCl}_2(\text{NEt}_3)_2]$ or $[\text{HNEt}_3][\text{PtCl}_3(\text{NEt}_3)]$ with AHF. The former would yield, by analogy with the NMe_3 derivative, the monofluoro-complex *trans*- $[\text{PtFCl}(\text{NEt}_3)_2]$ (2a) and the latter would afford either of the two structural isomers of $[\text{HNEt}_3][\text{PtFCl}_2(\text{NEt}_3)]$ (2b) and (2c).



Complex (2a) would exhibit a $^1J_{\text{PtF}}$ coupling in the order of magnitude similar to that reported for (1) and furthermore, the chemical shift would probably be in the same region *ca.* δ -304 as the NMe_3 derivative. However, both the chemical shift and coupling constant deviate significantly from those reported for *trans*- $[\text{PtFCl}(\text{NMe}_3)_2]$. Therefore, it is plausible to suggest that the resonance observed at δ -250 is due to either complex (2b) or (2c). The ^{19}F chemical shift, although still within the expected region for F *trans* Cl or F *trans* N are observed at higher frequency than those presented in Table 2.8. This is somewhat surprising as increasing negative ionic charge is usually associated with increase in the shielding of the NMR nucleus. However, this phenomenon has been observed previously, by Brewer *et al.*,⁸⁰ for the complex $[\text{IrF}_4(\text{CO})(\text{PMe}_3)]^-$ which exhibits ^{19}F resonances at higher frequencies than those of the analogous neutral species *fac*- $[\text{IrF}_3(\text{CO})_3]$ and $[\text{IrF}_3(\text{CO})(\text{PR}_3)_2]$ (see Chapter 5). Therefore, the resonance at δ -250 is plausible for fluoride in either (2b) or (2c) however, further characterization was not possible with the limited data.

Complexes (3), (4) and (5) all exhibit singlets in the chemical shift region which, by analogy with *trans*- $[\text{PtFCl}(\text{NMe}_3)_2]$, are diagnostic of fluoride bound to platinum(II). It is plausible to suggest that the metathetical reactions all proceed with retention of the *cis* arrangement of the amine ligands therefore, since the starting compounds are all *cis* isomers the resonances observed are all attributed to F *trans* N. It is plausible that complexes (3), (4) and (5) could be either the difluoro- or the monofluoro-

species and without further information a definitive characterization cannot be made. All attempts to obtain further spectroscopic data were, as a result of the presence of unreacted starting material, unsuccessful and, thus, assignments remain tentative.

2.5.1 The Metathesis Reaction of *trans*-[PtCl₂(NMe₃)₂] with Silver Fluoride

Yellow *trans*-[PtCl₂(NMe₃)₂] and AgF were reacted in acetone, as described in section 6.22, for a period of 24 hours. Removal of the solvent afforded an air-stable brown solid which was dissolved in d₆-acetone and subsequently analysed by ¹⁹F NMR spectroscopy.

The ¹⁹F NMR spectrum (Figure 2.4) showed one singlet resonance at δ -304 with the associated ¹⁹⁵Pt satellites with a ¹J_{PtF} = 1224 Hz. The resonance was therefore, by analogy with the reaction with AHF, attributed to *trans*-[PtFCl(NMe₃)₂]. E. I. mass spectrometry confirmed the presence of the complex *trans*-[PtFCl(NMe₃)₂], *m/z* 368, and *trans*-[PtCl₂(NMe₃)₂], *m/z* 384, (Figure 2.5).

Figure 2.4 The ^{19}F NMR spectrum of *trans*-[PtFCl(NMe₃)₂]

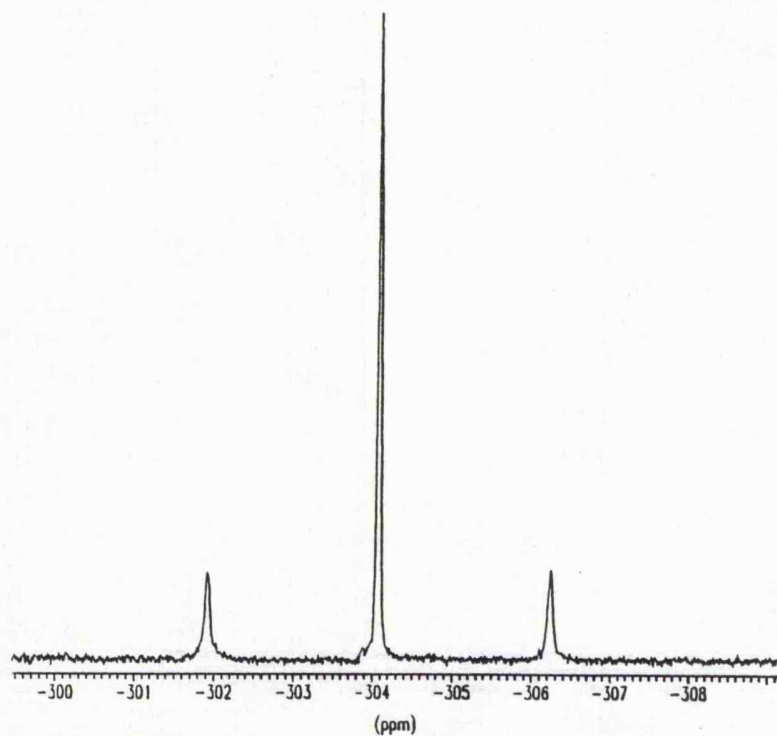
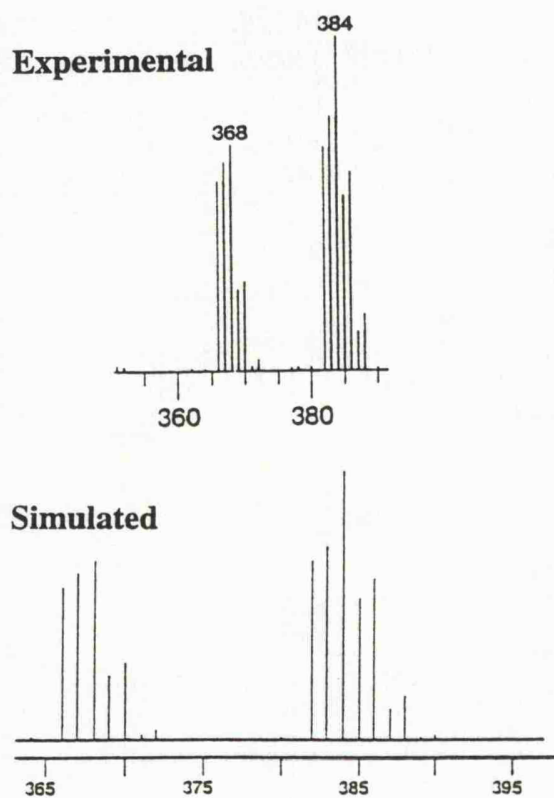


Figure 2.5 Experimental and Theoretical Mass Spectra of *trans*-[PtCl₂(NMe₃)₂] and *trans*-[PtFCl(NMe₃)₂]



The complex *trans*-[PtFCl(NMe₃)₂] formed by the reaction of the dichloro-species with a 2 molar equivalent of AgF is further evidence to help substantiate that the "*trans* directing influence" predicts that the second chloride will not be substituted by another entering fluoride. However, one could argue that the silver fluoride is decomposing before it has time to substitute the second chloride but, this cannot be the case in the analogous AHF reaction. Furthermore, AHF has been shown to act as a halide metathesis reagent under the right conditions.

2.6 Reaction of *trans*-[PtCl₂(NMe₃)₂] and [XeF₂] in AHF

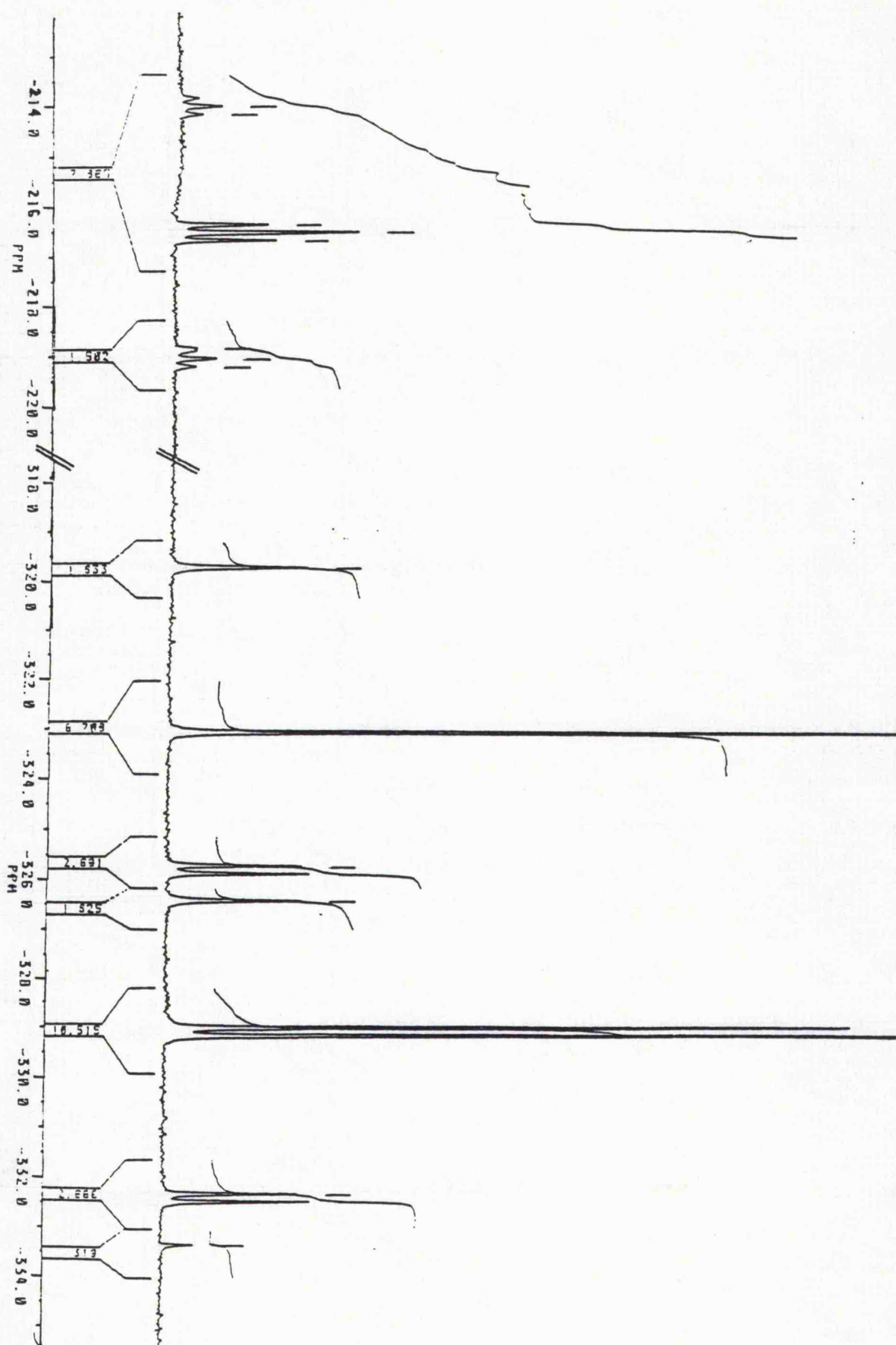
In light of the successful characterization of *trans*-[PtFCl(NMe₃)₂] (1) (sections 2.5 and 2.6) it was thought to be of interest to investigate the reaction of *trans*-[PtCl₂(NMe₃)₂] and [XeF₂] in AHF.

Yellow *trans*-[PtCl₂(NMe₃)₂] was allowed to react with [XeF₂] in AHF, as described in section 6.21, affording an orange solution. Removal of the solvent yielded an air-stable orange solid which was subsequently dissolved in d₆-DMSO and analysed by ¹H and ¹⁹F NMR spectroscopy.

The ¹H NMR spectrum revealed several resonances, at $\approx \delta$ 2.6, in a region characteristic of the NMe₃ group *cf.* *trans*-[PtCl₂(NMe₃)₂] δ 2.7, ³J_{PtH} = 26 Hz.

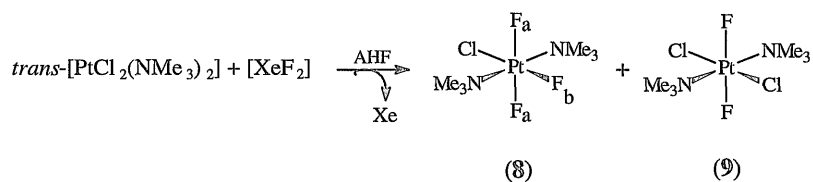
The ¹⁹F NMR spectrum (Figure 2.6) showed two mutually coupled resonances: a doublet at δ -329, ²J_{FF} = 44 Hz, and a triplet at δ -217, ²J_{FF} = 44 Hz. Both resonances exhibit the associated ¹⁹⁵Pt satellites, ¹J_{PtF} = 1870 Hz and ¹J_{PtF} = 1434 Hz for the doublet and triplet respectively. An additional singlet resonance was also observed at δ -323 with a ¹J_{PtF} = 1894 Hz.

Figure 2.6 ^{19}F NMR Spectrum of Complexes (8) and (9)



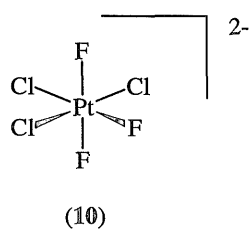
It is evident from the ^{19}F NMR data that the reaction, between *trans*- $[\text{PtCl}_2(\text{NMe}_3)_2]$ and $[\text{XeF}_2]$ in AHF, proceeds *via* Scheme 2.9 to afford two products.

Scheme 2.9



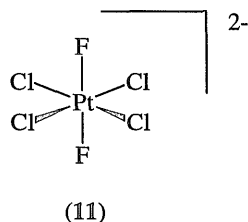
Assignment of complexes (8) and (9) are made by analogy with the ^{19}F NMR data, reported by Preetz *et al.*,⁷² for anions of the type $[\text{PtF}_n\text{Cl}_{6-n}]^{2-}$ ($n = 0-6$), and assuming that the reaction proceeds with retention of configuration of the NMe_3 groups.

The anion *mer*- $[\text{PtF}_3\text{Cl}_3]^{2-}$ (10) is reported to exhibit two mutually coupled resonances: a doublet at $\delta -372$, $^2J_{\text{FF}} = 44$ Hz, and a triplet at $\delta -273$, $^2J_{\text{FF}} = 44$ Hz with ^{195}Pt satellites, $^1J_{\text{PtF}} = 1860$ and 1285 Hz respectively.⁷⁷ Thus, the doublet, attributed to F_a , and the corresponding triplet, assigned to F_b in complex (8) are, by comparison with those reported by Preetz and co-workers, typical *cis* $^2J_{\text{FF}}$ coupling.



Furthermore, the chemical shifts for the resonances assigned to F_a and F_b are, by comparison with those reported for complex (10), in a region characteristic of fluorine *trans* to fluorine and fluorine *trans* to chlorine respectively, since the latter is observed at a higher frequency (≈ 100 ppm, see section 2.4). It is worth noting that the shift to a higher frequency for the platinum(IV) complex in relation to the platinum(II) species (see section 2.5), *ca.* δ -304, can be explained by considering the extent of shielding of the appropriate fluorine nuclei. In the platinum(II) complex the fluorine nucleus is shielded more, as a result of the increase in electron density on the metal centre, than in the related Pt(IV) species and thus, is observed at a lower frequency. It is also evident from the NMR data that the magnitude of the $^1J_{PtF}$ coupling is dependent on the *trans* ligand as observed by Preetz and co-workers. This apparent difference in the $^1J_{PtF}$ coupling, for F *trans* F and F *trans* Cl, can be understood by considering the "NMR *trans* influence", which relates the magnitude of the one-bond metal-ligand coupling constant to the *trans* influence of the *trans* ligand. Thus, the higher the *trans* influence of a ligand, the lower will be the one-bond coupling constant between the metal and the *trans* ligand. Therefore, the smaller $^1J_{PtF}$ coupling for F *trans* Cl is as expected since chloride has a higher *trans* influence than fluoride.

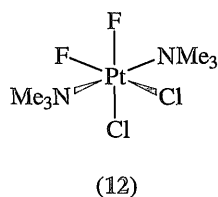
The ^{19}F NMR spectrum of the anion $[PtF_2Cl_4]^{2-}$ (11) was reported to show a singlet at δ -382 with a $^1J_{PtF}$ coupling of 1850 Hz.



Both the chemical shift, which is characteristic of F *trans* F, and the $^1J_{\text{PtF}}$ coupling constant, which is indicative of F *trans* F, for complex (9) compare well with those reported for (11).

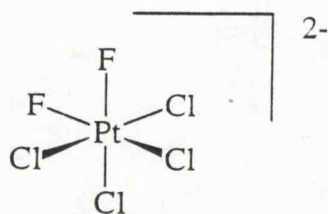
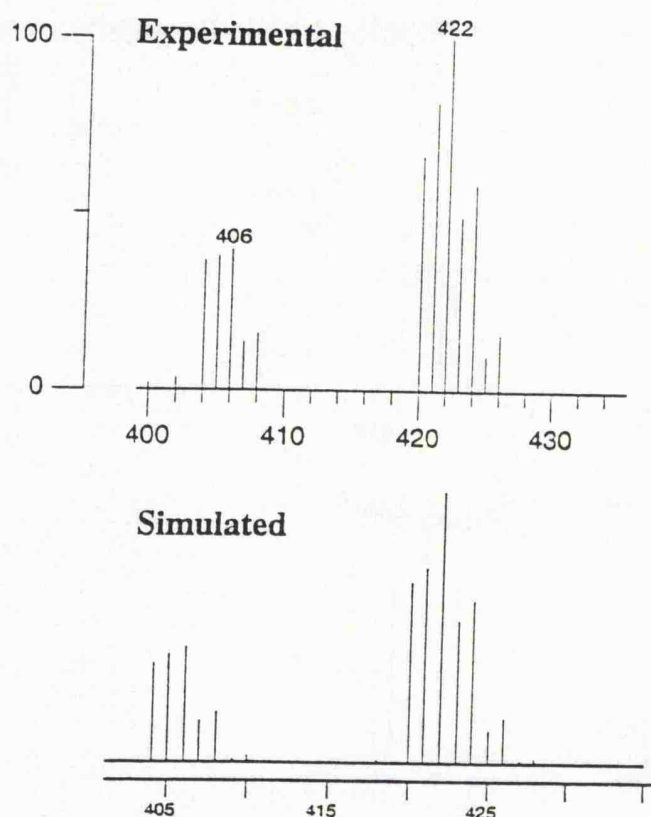
Further evidence to confirm the formulations of complexes (8) and (9) was the observation of the parent ions, $[M]^+$, in the E. I. mass spectrum centred at m/z 406 and 422 respectively (Figure 2.7)

During the studies, of the reactions between *trans*- $[\text{PtCl}_2(\text{NMe}_3)_2]$ and $[\text{XeF}_2]$ in AHF, evidence of a third species was observed in the ^{19}F NMR spectra. Although only a minor component of the reaction mixture, this additional species exhibited a singlet at δ -219 with a $^1J_{\text{PtF}}$ coupling of 1402 Hz. By analogy with the previously reported ^{19}F NMR data the singlet resonance was assigned to the complex *cis, cis, trans*- $[\text{PtF}_2\text{Cl}_2(\text{NMe}_3)_2]$ (12).



The chemical shift and $^1J_{\text{PtF}}$ coupling are both typical of a fluorine *trans* chlorine environment. The ion $[\text{PtF}_2\text{Cl}_4]^{2-}$ (13) ⁷⁷ is reported to show a singlet at δ -276 with a $^1J_{\text{PtF}}$ = 1280 Hz which compares well, in that the $^1J_{\text{PtF}}$ coupling is significantly smaller. Furthermore, the $\delta(^{19}\text{F})$ is observed at a higher frequency than that found for F *trans* F and is consistent with that observed for (12).

Figure 2.7 Experimental and Theoretical Mass Spectra for Complexes (8) and (9)



(13)

All attempts to substantiate the formulations further by obtaining the corresponding ^{195}Pt NMR spectra were unsuccessful. However, no resonances exhibiting platinum-fluorine couplings were resolved but four singlets at δ -2948, -3039, -3111 and -3441 were observed which did not correspond to *trans*- $[\text{PtCl}_2(\text{NMe}_3)_2]$ cf. δ -1894.

A change in the oxidation state of platinum from (II) to (IV) is usually accompanied by a shift to higher frequency *ca.* $[\text{PtBr}_4]^{2-}$ δ -2690 and $[\text{PtBr}_6]^{2-}$ δ -1860.⁸¹ Therefore, the shift to lower frequency, of the four resonances, compared to that of *trans*- $[\text{PtCl}_2(\text{NMe}_3)_2]$ does not indicate a change in the oxidation state of platinum from (II) to (IV). However, no other resonances, in a chemical shift region diagnostic of a platinum(IV) species, were observed. In a review article, by Pregosin,⁸² it was reported that generally the coordination of nitrogen ligands to platinum caused complications in recording ^{195}Pt NMR spectra since, once the lone-pair coordinates, the ^{14}N relaxation is slower and often affects the ^{195}Pt NMR spectrum adversely. Thus, the reported difficulties in obtaining ^{195}Pt NMR spectra on *cis*- $[\text{PtCl}_2(\text{NH}_3)_2]$ ⁸³ and its derivatives have been justified. Therefore, a plausible explanation exists for the absence of the corresponding ^{195}Pt resonances for complexes (8) and (9).

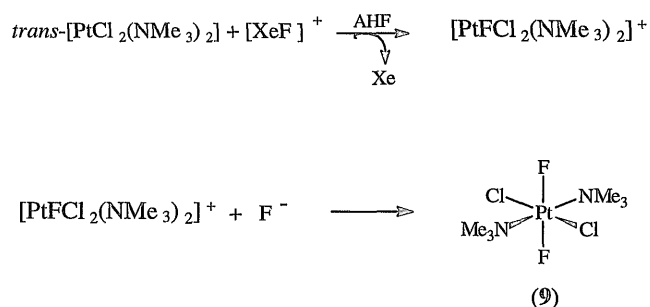
2.6.1 Mechanism of Oxidative Fluorination of *trans*- $[\text{PtCl}_2(\text{NMe}_3)_2]$ by $[\text{XeF}_2]$

Although there is no direct evidence as to the mechanism of oxidative fluorination, the formation of (9) suggests that addition may not be concerted. In AHF solution $[\text{XeF}_2]$ is reported to form an $\text{F-Xe}^{\delta+}\cdots\text{F}\cdots\text{H-F}^{\delta-}$ adduct which is an aggressive fluorinating agent.⁷⁶ Thus, it is feasible that oxidative fluorination proceeds according to Scheme 2.10.

This mechanism for oxidative fluorination, by $[\text{XeF}_2]$, has been suggested previously, by Ebsworth *et al.*,⁸⁴ for *trans*- $[\text{IrF}_2(\text{dppe})_2]^+$ formed by the reaction of *trans*- $[\text{Ir}(\text{dppe})_2]^+$ and $[\text{XeF}_2]$ (see section 5.8). Furthermore, the reactions of $[\text{XeF}_2]$ with the cationic complexes $[\text{Ir}(\text{CO})_3(\text{PR}_3)_2]^+$ ($\text{PR}_3 = \text{PEt}_3, \text{PMe}_3, \text{PMe}_2\text{Ph}, \text{PEt}_2\text{Ph}$ and PEtPh_2)⁸⁵ and the neutral species $[\text{M}(\text{CO})_3(\text{PPh}_3)_2]$ ($\text{M} = \text{Os}, \text{Ru}$)⁸⁶ were reported to proceed

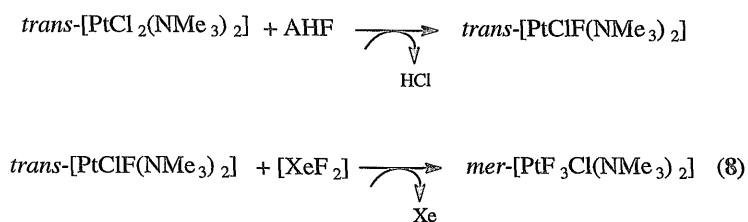
via a two step mechanism, involving initial reaction of the $[\text{XeF}]^+$ fragment and then nucleophilic attack by F^- at coordinated CO.

Scheme 2.10



In section 2.5 the complex $\text{trans-}[\text{PtClF}(\text{NMe}_3)_2]$ (**1**) formed by the reaction of $\text{trans-}[\text{PtCl}_2(\text{NMe}_3)_2]$ and AHF was described. Thus, it is feasible that complex (**8**), $\text{mer-}[\text{PtF}_3\text{Cl}(\text{NMe}_3)_2]$, was formed from the halide metathetical reaction of $\text{trans-}[\text{PtCl}_2(\text{NMe}_3)_2]$ and then subsequent oxidative fluorination by $[\text{XeF}_2]$ (Scheme 2.11).

Scheme 2.11



2.6.2 Reaction of *trans*-[PtCl₂(NMe₃)₂] and [XeF₂] in CH₃CN

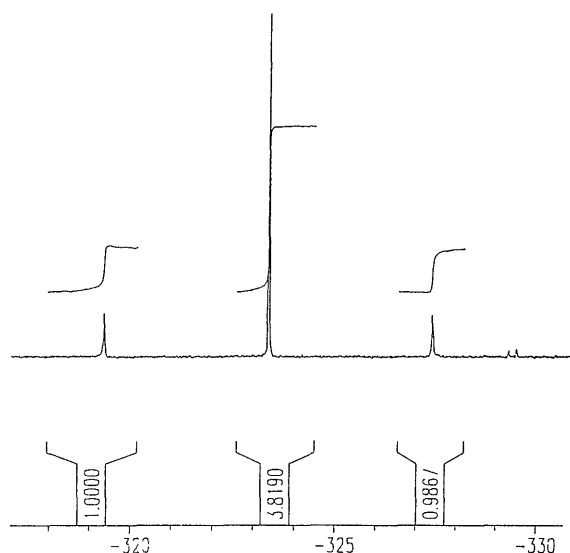
In an attempt to isolate one product, from the reaction of *trans*-[PtCl₂(NMe₃)₂] and [XeF₂], CH₃CN was employed as the solvent and thus, prevented the formation of *mer*-[PtF₃Cl(NMe₃)₂] (**8**).

Yellow *trans*-[PtCl₂(NMe₃)₂] was allowed to react with [XeF₂] in CH₃CN, as described in section 6.20, affording a partially soluble orange solid. Removal of the solvent yielded an air-stable orange solid which was subsequently dissolved in d₆-DMSO and analysed by ¹⁹F NMR spectroscopy.

The ¹⁹F NMR spectrum revealed resonances consistent with *trans*-[PtF₂Cl₂(NMe₃)₂] (**9**) and *cis, cis, trans*-[PtF₂Cl₂(NMe₃)₂] (**12**). However, minor resonances associated with complex (**8**) were also observed. Any HF produced *in situ*, from the reaction of [XeF₂] with moisture in CH₃CN (acetonitrile is notoriously difficult to free completely of water), would react with *trans*-[PtCl₂(NMe₃)₂] yielding *trans*-[PtClF(NMe₃)₂] and consequently, complex (**8**).

Note: It became evident that during the studies of the reactions of *trans*-[PtCl₂(NMe₃)₂] and [XeF₂] in both AHF and CH₃CN, no control could be exercised over the ratio of the products formed. Generally, (**9**) and (**12**) would be the major products formed with (**8**) being only a minor component ($\approx 20\%$). However, in some instances complex (**9**) would represent almost 100% of the reaction mixture (Figure 2.8), and consequently, EXAFS studies, where purity is essential, could be used to obtain structural information in the absence of crystals suitable for X-ray analysis (see section 2.6.4).

Figure 2.8 ^{19}F NMR Spectrum of Complex (9)



2.6.3 X-Ray Crystal Analysis of *trans*-[PtCl₂(NMe₃)₂]

Crystals of *trans*-[PtCl₂(NMe₃)₂], suitable for single crystal X-ray structure determination, were obtained from an CH₃CN solution of "[PtF₂Cl₂(NMe₃)₂]" by slow evaporation of the solvent. Evidence for *trans*-[PtCl₂(NMe₃)₂] was found in both the E. I. mass and ^1H NMR spectra thus, there is a precedent for unreacted starting material crystallizing rather than decomposition, during the crystal growing process, of the fluoro-species and subsequent growth of crystals. The molecular structure (Figure 2.9) of *trans*-[PtCl₂(NMe₃)₂] confirms the *trans* geometry around the metal centre. Selected bond lengths and angles are presented in Table 2.9.

Figure 2.9 Crystal Structure of *trans*-[PtCl₂(NMe₃)₂]

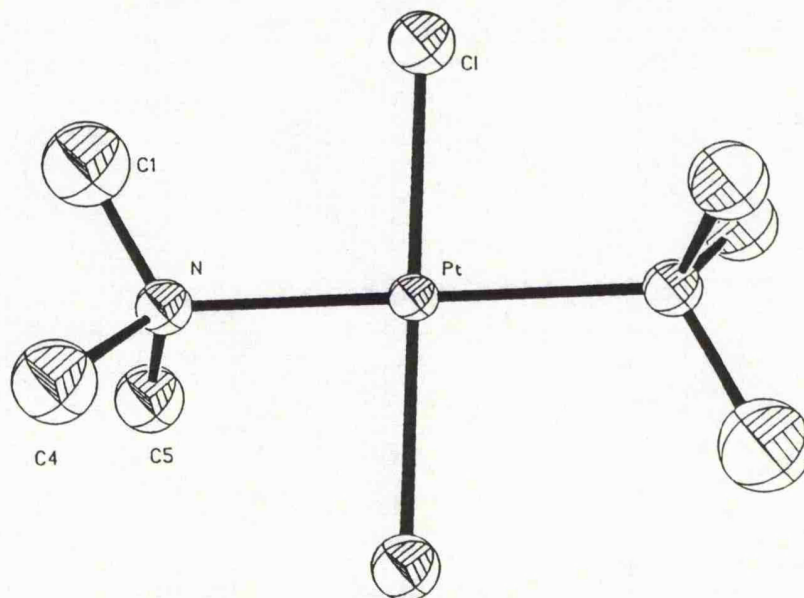


Table 2.9 Selected Bond Lengths (Å) and Angles(°)

Bond Lengths	Pt-Cl 2.301 (4) Pt-N 2.130 (11) mean N-C 1.437 (21)
Bond Angles	N-Pt-N 180.0 (1) Cl-Pt-Cl 180.0 (1)

Both the Pt-N and Pt-Cl bond lengths are reasonable when compared to those of related platinum(II) complexes. In the complexes *trans*-[PtCl₂(NH₃)₂] and *cis*-[PtCl₂(bipy)] the Pt-Cl bond lengths are reported to be 2.32(5)⁸⁷ and 2.306(4)⁸⁸ Å respectively. Although, in *cis*-[PtCl₂(bipy)] the Pt-N bond length is 2.001(11) Å the corresponding distance in *trans*-[PtCl₂(NH₃)₂] is 2.05(8) Å which is comparable to that observed for *trans*-[PtCl₂(NMe₃)₂] ((Table 2.9).

2.6.4 EXAFS Analysis of *trans*-[PtF₂Cl₂(NMe₃)₂]

An inability to obtain suitable single crystals for X-ray crystallographic studies meant that structural information had to be obtained by an alternative technique. The recent structural characterization of *fac*-[IrF₃(CO)₃]⁸⁹ and complexes of the type [RhCl(CO){PPh_x(C₆F₅)_{3-x}]₂]⁹⁰ by EXAFS has shown this technique to be a valuable tool for obtaining bond length data on compounds when other methods have failed. In the absence of structurally characterized Pt(IV) amine-fluoride complexes as model compounds, the reliability of the data collection and treatment was confirmed by the analysis of the platinum L_{III}-edge EXAFS data on *trans*-[PtCl₂(NMe₃)₂]. All the fits discussed below are compared with the average raw (background-subtracted) EXAFS data.

Initially, for *trans*-[PtCl₂(NMe₃)₂], the data were modelled, utilising EXCURV92,⁹¹ to 2 shells of 2 chlorine atoms at *ca.* $r = 2.28(2)$ Å and 2 nitrogen atoms at *ca.* $r = 2.15(2)$ Å (Figure 2.10.1). An additional weak broad feature around 3.0 Å was observed upon examination of the Fourier transforms. This feature was attributed to the 6 carbon atoms on the NMe₃ groups. So, further modelling of the EXAFS data using 3 shells resulted in significant reductions in the R-factor and fit index (Figure 2.10.2). The Pt-C non-bonded distance was calculated to be 3.03 Å from the X-ray data. Thus, the results are in satisfactory agreement with the data from the single crystal X-ray analysis (see section 2.6.3).

For *trans*-[PtF₂Cl₂(NMe₃)₂] (**9**) the data were modelled, utilising EXCURV92,⁹¹ to 4 shells of 2 chlorine atoms at *ca.* $r = 2.25(2)$ Å, 2 nitrogen atoms at *ca.* $r = 2.21(2)$ Å, 2 fluorine atoms at *ca.* $r = 1.93(2)$ Å and 6 carbon atoms at a non-bonded distance of *ca.* 2.98(2) Å (Figure 2.11). All shells were tested for statistical significance.⁹²

Figure 2.10.1 The Background-Subtracted EXAFS (K^3 weighted) and the Fourier Transform EXAFS of *trans*-[PtCl₂(NMe₃)₂] (modelled to 2 shells)

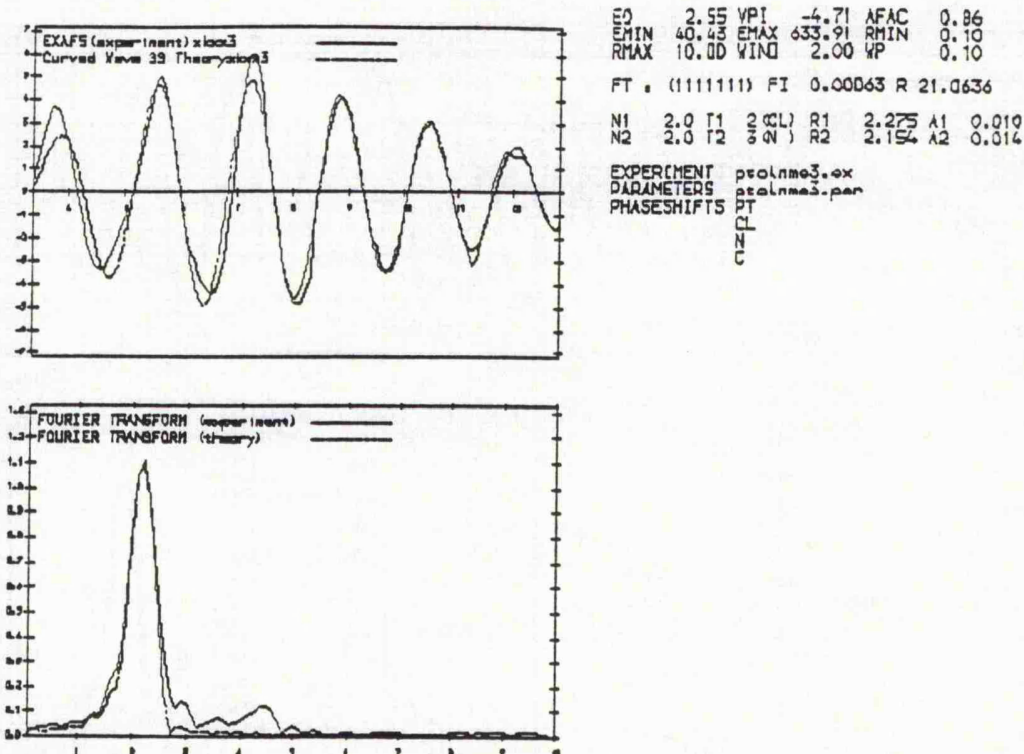


Figure 2.10.2 The Background-Subtracted EXAFS (K^3 weighted) and the Fourier Transform EXAFS of *trans*-[PtCl₂(NMe₃)₂] (modelled to 3 shells)

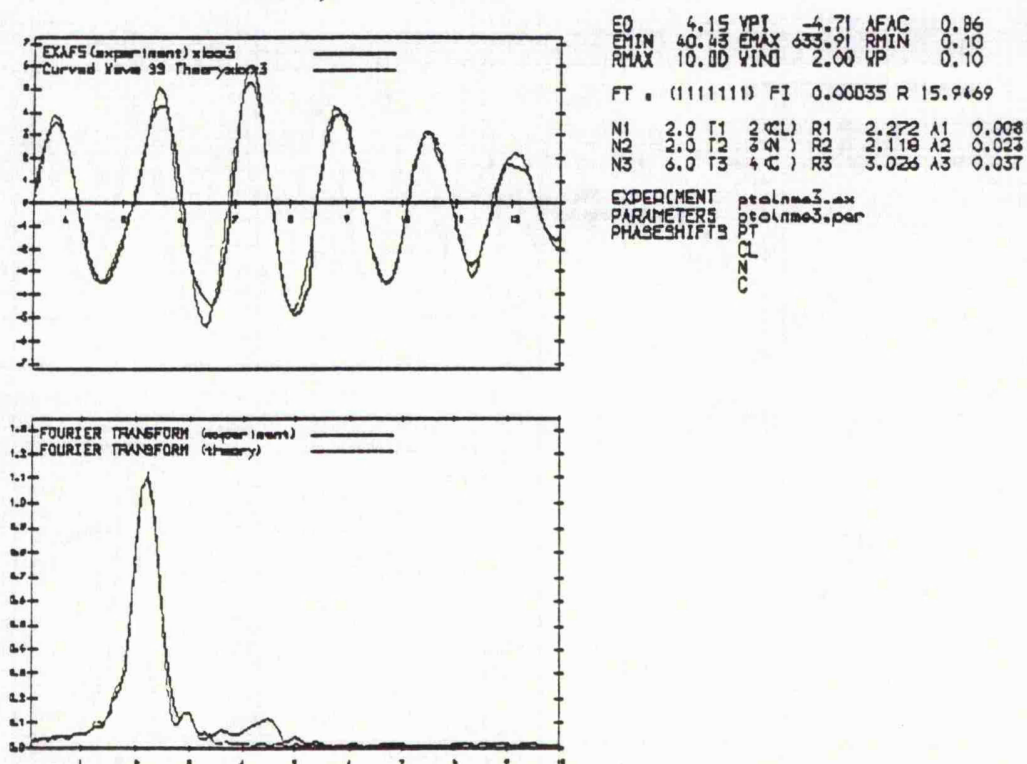
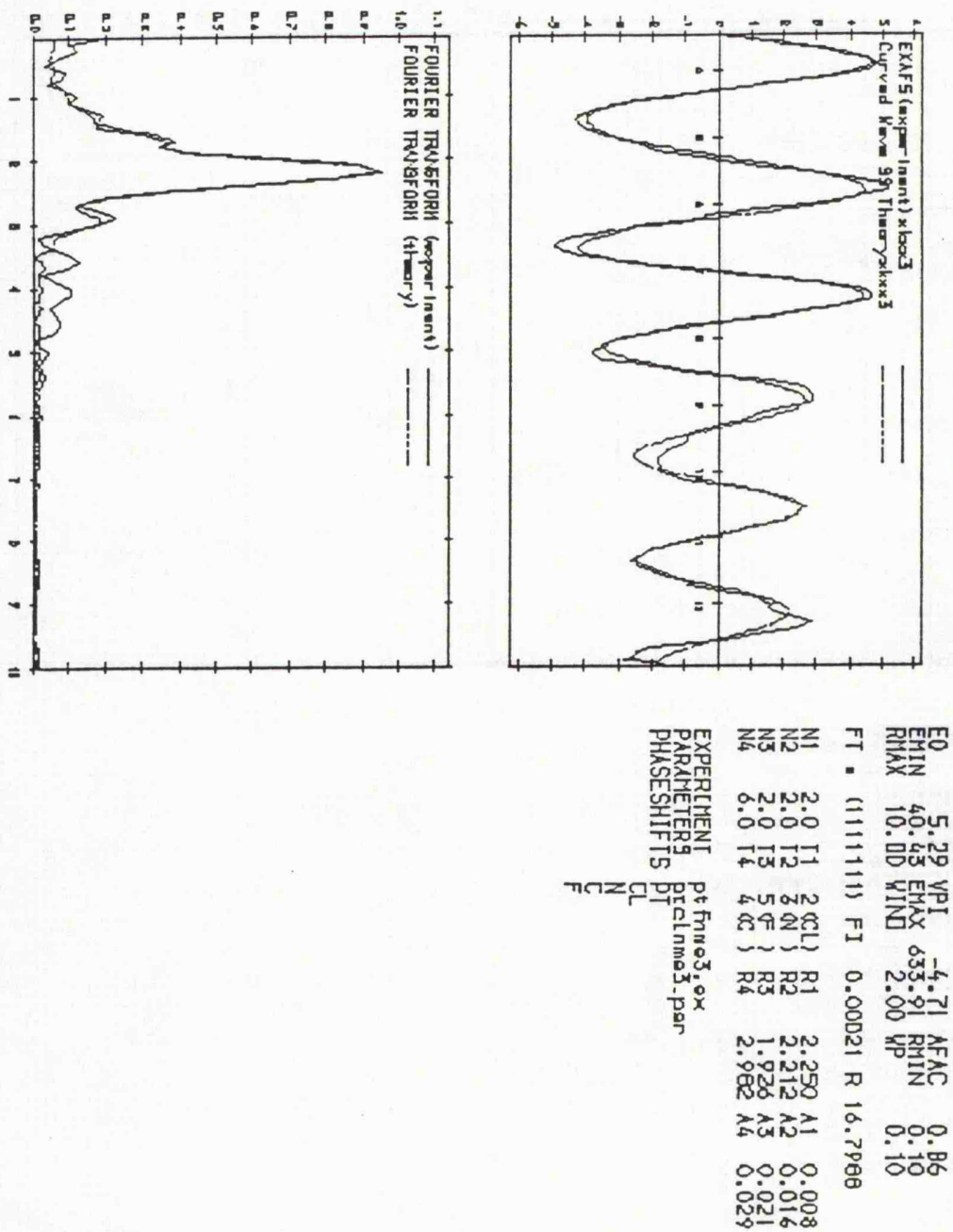


Figure 2.11 The Background-Subtracted EXAFS (K^3 weighted) and the Fourier Transform EXAFS of *trans*-[PtF₂Cl₂(NMe₃)₂]



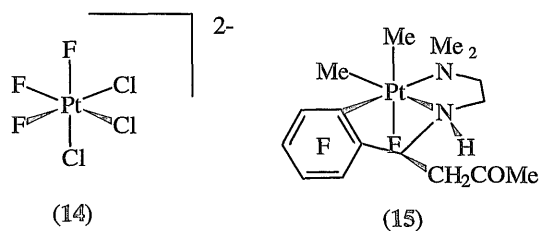
The bond length data obtained by EXAFS for *trans*-[PtF₂Cl₂(NMe₃)₂] are reasonable when compared with those of other platinum(IV) fluoride complexes (Table 2.10).

Table 2.10 Comparison of the Bond Length Data of some Platinum(IV) Fluoride Species

Complex	M-F (<i>trans</i> F)	M-F (<i>trans</i> Cl)	M-Cl (<i>trans</i> F)	M-Cl (<i>trans</i> Cl)	M-N	Refs.
(9)	1.93(2)	-	2.26(2)	-	2.21(2)	-
(10)	1.936(3)	1.972(3)	2.282(2)	2.303(1)	-	93
(14)	-	1.977(3) ^a	-	2.272(1) ^a	-	93
(15)	-	2.070(5) ^b	-	-	2.242(10)	73

(a) mean distances

(b) F *trans* Me



It is evident, from the data reported in Table 2.10, that the Pt-F bond is significantly shortened when *trans* to fluorine.

2.7 Reaction of *cis*-[PtCl₂(NH₃)₂] and [XeF₂] in AHF

The reaction of *trans*-[PtCl₂(NH₃)₂] with [XeF₂], in AHF, has been reported to afford the corresponding platinum(IV) complex [PtF₂Cl₂(NH₃)₂] (see sections 2.2.9, 2.4 and 2.8).⁷² Whereas, the analogous reaction of *cis*-[PtCl₂(NH₃)₂] has been reported to yield a compound whose chemical composition resembled that of the polymeric species [PtCl₂(NH₃)₂(OH)]_n.⁹⁴ Therefore, it was thought to be of interest, owing to the dearth of conclusive evidence as to the products formed by the reactions of *cis*- and *trans*-[PtCl₂(NH₃)₂] and [XeF₂] in AHF, to repeat this work.

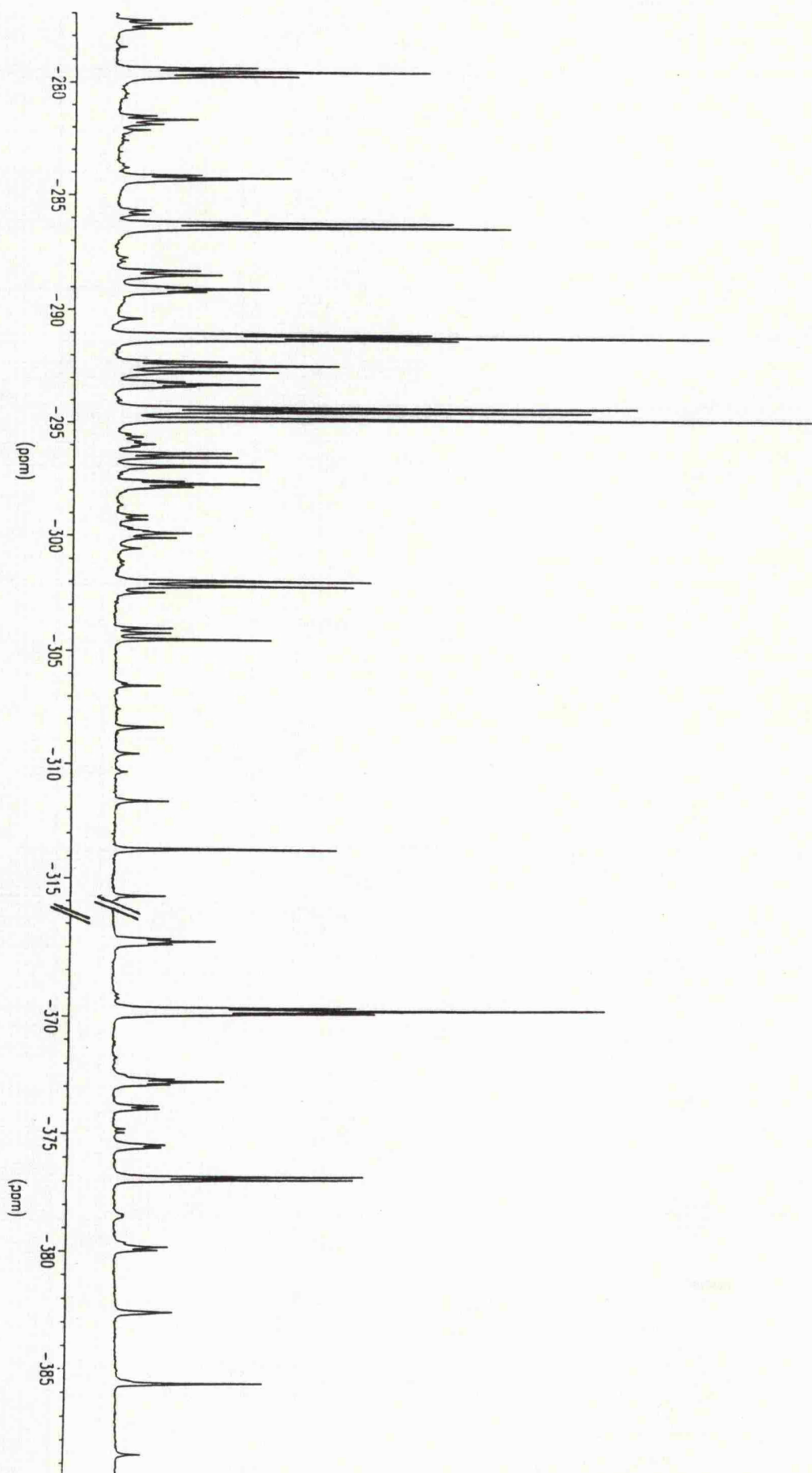
Yellow *cis*-[PtCl₂(NH₃)₂] was allowed to react with [XeF₂] in AHF, as described in section 6.21, affording a sparingly soluble orange solid. Removal of the solvent yielded an air-stable orange solid which was subsequently dissolved in d₆-DMSO and analysed by ¹H and ¹⁹F NMR spectroscopy.

The ¹H NMR spectrum showed broad resonances at $\approx \delta$ 3.0, characteristic of the NH₃ and, thus, was uninformative.

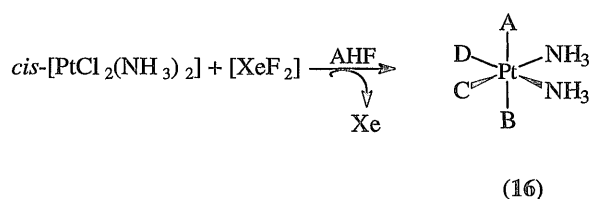
The ¹⁹F NMR spectrum revealed some surprising results, Figure 2.12. The ¹⁹F NMR data are presented in Table 2.11.

It is evident from the ¹⁹F NMR spectrum (Figure 2.12) that [XeF₂] reacts with *cis*-[PtCl₂(NH₃)₂] to afford several species. However, by comparison of the ¹⁹F NMR data reported in Table 2.11 with those previously discussed in sections 2.5 and 2.6, the majority of the products can be elucidated. Assuming that the reaction proceeds with retention of the *cis* arrangement of the ammonia groups, this would leave four coordination sites that could accommodate either chlorine or fluorine (Scheme 2.12).

Figure 2.12 ^{19}F NMR Spectrum of the Structural Isomers of Complex (16)



Scheme 2.12



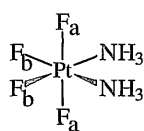
It is also evident from the reported ^{19}F NMR data that two distinct chemical shift regions are observed, one which is characteristic of fluorine *trans* to fluorine (δ -370 to -385) and the other, by comparison with the data reported in section 2.6, is typical of fluorine *trans* to chlorine (δ -286 to -294). However, assuming that the products retain the *cis* arrangement of the ammonia groups then a fluorine *trans* to nitrogen environment could also be present. Although there have been no reports in the literature of the chemical shift region associated with F *trans* N it is possible, by analogy with the ^{19}F NMR data presented in this chapter, to distinguish between the resonances associated with F *trans* N and those with F *trans* Cl. In general, the chemical shift for F *trans* N is found at a lower frequency than that for F *trans* Cl. The ^{19}F resonances for F *trans* Cl are, therefore, being deshielded relative to the resonances observed for F *trans* N. This is as expected since chlorine is a good π -acceptor whereas the NH_3 ligand cannot π -accept.

Considering the apparent complexity of the ^{19}F NMR spectrum and that the coordination sites A, B, C and D could be occupied by any combination of fluorine and chlorine, 8 products (Table 2.11) are possible:

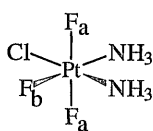
Table 2.11 ^{19}F NMR Data for the Products (16) formed from the Reaction of *cis*- $[\text{PtCl}_2(\text{NH}_3)_2]$ and $[\text{XeF}_2]$ in AHF

Structural Isomer (F or Cl)				F <i>trans</i> F (δ -370 to -385)			F <i>trans</i> N (δ -291 to -313)			F <i>trans</i> Cl (δ -286 to -294)		
A	B	C	D	$\delta(^{19}\text{F})$ / ppm	$^2J(\text{FF})$ / Hz	$^1J(\text{PtF})$ / /Hz	$\delta(^{19}\text{F})$ / ppm	$^2J(\text{FF})$ / Hz	$^1J(\text{PtF})$ / /Hz	$\delta(^{19}\text{F})$ / ppm	$^2J(\text{FF})$ / Hz	$^1J(\text{PtF})$ / /Hz
(17)	F	F	F	t-370	35	1701	t-291	35	1171	-	-	-
(18)	F	F	F	d-377	40	1689	t-297	40	1165	-	-	-
(19)	F	F	Cl	s-385	-	1712	-	-	-	-	-	-
(20)	F	Cl	F	-	-	-	d-294	54	1157	t-279	54	1185
(21)	F	Cl	Cl	-	-	-	d-302	60	1164	d-286	60	1177
(22)	F	Cl	Cl	-	-	-	-	-	-	s-295	-	1184
(23)	Cl	Cl	F	-	-	-	s-304	-	1157	-	-	-
(24)	Cl	Cl	F	-	-	-	s-313	-	1175	-	-	-

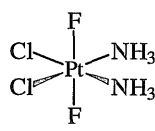
multiplicity: t = triplet, d = doublet and s = singlet



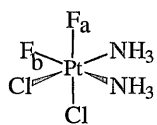
(17)



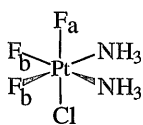
(18)



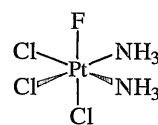
(19)



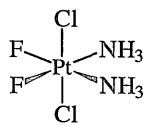
(20)



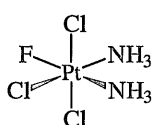
(21)



(22)

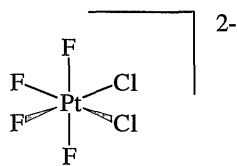


(23)



(24)

The two mutually coupled triplets observed at δ -370, which is characteristic of F *trans* F, and δ -291 are assigned to F_a and F_b, respectively in complex (17). The triplet couplings of 35 Hz, typical of *cis*- $^2J_{\text{FF}}$, compare well with that reported for the complex, [PtF₄Cl₂]²⁻ (25).⁷²



(25)

The ^{19}F NMR spectrum for complex (25) is reported to exhibit two mutually coupled triplets at δ -364 and -267 with a $^2J_{\text{FF}}$ = 39 Hz. By the same reasoning the mutually coupled doublet and triplet resonances, at δ -377 and

-297, are assigned to F_a and F_b , in complex (18), respectively. The chemical shifts, when considering the relative $\delta(^{19}\text{F})$ for $F \text{ trans } F$ and $F \text{ trans } X$ ($X = \text{Cl, N}$) environments, and coupling are comparable with those reported for the anionic complex $\text{mer-}[\text{PtF}_3\text{Cl}_3]^{2-}$ (10) in section 2.6.

The singlet observed at δ -385, with a $^1J_{\text{PtF}} = 1712$ Hz, is consistent with the structure of (19).

The two mutually coupled doublets at δ -302 and -286, with a $^2J_{\text{FF}} = 60$ Hz, are assigned to F_b and F_a , in complex (20), respectively.

By analogy with the assignments for complex (20) the mutually coupled doublet and triplet at δ -294 and -279, with a $^2J_{\text{FF}} = 54$ Hz, are attributed to F_b and F_a , in complex (21), respectively.

It is apparent that, by examining the data presented in Table 2.11, there is an additive relationship between the number of fluorine atoms on the isomer and the $\delta(^{19}\text{F})$ shift. The ^{19}F chemical shifts; for $F \text{ trans } F$, $F \text{ trans } N$ and $F \text{ trans } Cl$ resonances, are observed at lower frequencies as the number of fluorine atoms on the complexes are sequentially decreased. The observed shift is of the order of 6-10 ppm to lower frequency with a sequential decrease in the number of fluorine atoms on the isomers. Thus, the singlets observed at δ -295, -304 and -313 are tentatively assigned to (22), (23) and (24). In order to ascertain the definitive structures of (22), (23) and (24) additional spectroscopic studies, such as ^{195}Pt NMR spectroscopy, would have to be undertaken. However, with ^{195}Pt NMR studies being unsuccessful in a relatively simple system, as discussed in section 2.6, an alternative approach was pursued. In light of the aggressive nature of $[\text{XeF}_2]$ in AHF (see section 2.6) the analogous reaction of $\text{cis-}[\text{PtCl}_2(\text{NH}_3)_2]$ with $[\text{XeF}_2]$ in CH_3CN was investigated in an attempt to isolate fewer products, thereby facilitating a comprehensive analysis.

2.7.1 Reaction of *cis*-[PtCl₂(NH₃)₂] and [XeF₂] in CH₃CN

A sample of yellow *cis*-[PtCl₂(NH₃)₂] and [XeF₂] in CH₃CN were allowed to react, as described in section 6.20, yielding a green precipitate.

The lack of solubility of the green solid, in acetonitrile and the majority of other solvents, indicate that the compound is possibly polymeric in nature. A green solid has been reported previously⁷² to be the hydroxy-bridged complex [PtCl₂(NH₃)₂(OH)]_n yielded from the reaction of *cis*-[PtCl₂(NH₃)₂] and [XeF₂] in HF. All attempts to obtain spectroscopic data, that would help substantiate the formulation of the green solid as the polymeric [PtCl₂(NH₃)₂(OH)]_n, were unsuccessful. However, dissolution, in d₆-DMSO, of the compound allowed analysis by ¹⁹F NMR spectroscopy which subsequently, revealed no resonances indicative of fluorine bound to platinum. Furthermore, the E. I. mass spectrum shows the most intense peak centred at *m/z* 300 which corresponds to *cis*-[PtCl₂(NH₃)₂] and is plausibly the result of cleavage of the dimer, [PtCl₂(NH₃)₂(OH)]₂.

Discussion

The reaction of *cis*-[PtCl₂(NH₃)₂] and [XeF₂] has been shown to be influenced by the solvent. The reaction in AHF affords 8 platinum-fluoride complexes whereas, in CH₃CN only the tentatively assigned polymer [PtCl₂(NH₃)₂(OH)]_n is formed. The hydrous conditions, in the CH₃CN system, is a plausible explanation for the formation of a hydroxy-bridged polymer. It is therefore, a possibility that the previously reported reaction of *cis*-[PtCl₂(NH₃)₂] and [XeF₂] was performed in aqueous HF thus, accounting for the formation of the polymeric species.

The complexes (17)-(24) were all assigned on the assumption that the reaction proceeded with retention of the *cis* arrangement of the N-donor ligands. In the next section the analogous reaction of *trans*-[PtCl₂(NH₃)₂]

will be described which will, by comparison of ^{19}F NMR data, ascertain if the above assumption is valid.

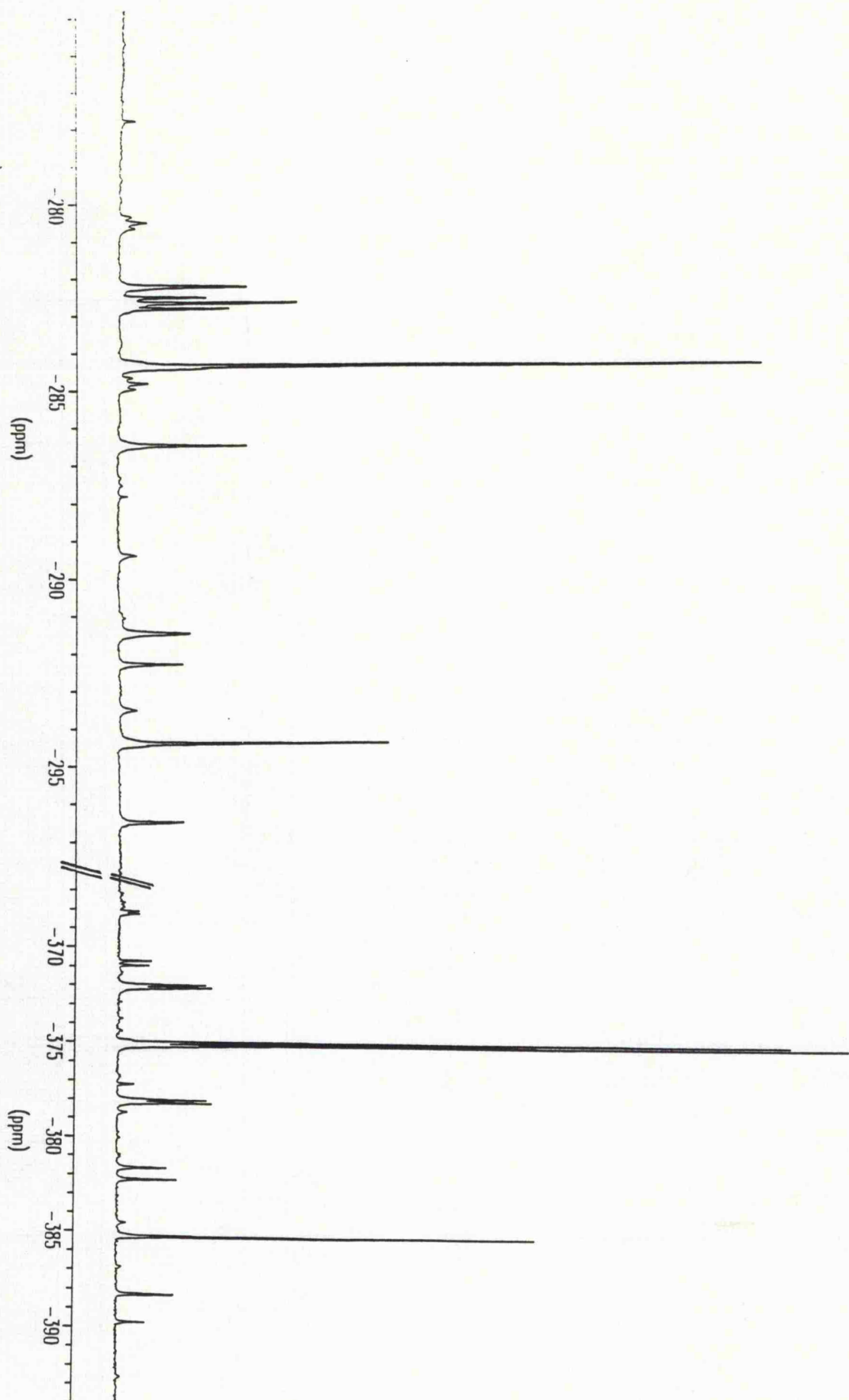
2.8 Reaction of *trans*-[PtCl₂(NH₃)₂] and [XeF₂] in AHF

Yellow *trans*-[PtCl₂(NH₃)₂] was allowed to react with [XeF₂] in AHF, as described in section 6.21, affording an orange solution. Removal of the solvent yielded an air-stable orange solid which was subsequently dissolved in d₆-DMSO and analysed by ^1H and ^{19}F NMR spectroscopy.

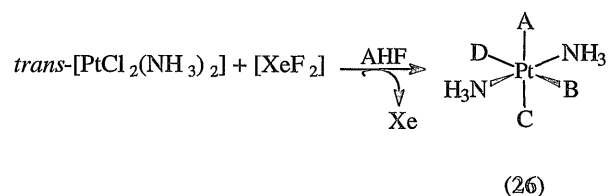
The ^1H NMR revealed broad resonances in a region assignable to the NH₃ groups but was not interpretable.

The ^{19}F NMR spectrum (Figure 2.13) showed a mutually coupled doublet and triplet at δ -375 and -282 respectively which are consistent with *mer, trans*-[PtF₃Cl(NH₃)₂]. Additional singlet resonances were observed at δ -385, -294 and -284. All resonances exhibited the associated ^{195}Pt satellites. The ^{19}F NMR data is presented in Table 2.12 for the reaction depicted in Scheme 2.13.

Figure 2.13 ^{19}F NMR Spectrum of the Structural Isomers of Complex (26)



Scheme 2.13



Although, a mutually coupled doublet and triplet could be attributed to either *mer, trans*-[PtF₃Cl(NH₃)₂] (**27**) or *mer, cis*-[PtF₃Cl(NH₃)₂] (**18**) the structural isomers are distinguishable by comparison of their respective triplet resonances. In complex (**18**) the triplet resonance is observed at a higher frequency which is characteristic of F *trans* N with the corresponding triplet in (**27**) appearing at a lower frequency. Thus, it is plausible to suggest that both reactions proceed with retention of the arrangement of the NH₃ ligands. Further evidence to substantiate this is the absence of the two mutually coupled triplets, discussed previously in section 2.7, assigned to the tetrafluoro-complex *cis*-[PtF₄(NH₃)₂] (**17**).

The analogous tetrafluoro-complex *trans*-[PtF₄(NH₃)₂] (**28**) would exhibit a singlet, in a chemical shift region characteristic of F *trans* F, by virtue of the four equivalent fluorine nuclei.

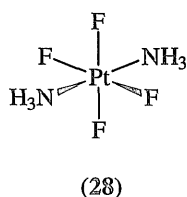
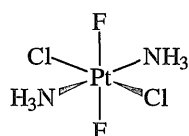


Table 2.12 ^{19}F NMR Data for the Structural Isomers of Complex (26)

Structural Isomer					F <i>trans</i> F			F <i>trans</i> Cl		
	A	B	C	D	$\delta(^{19}\text{F})/\text{ppm}$	$^2J(\text{FF})/\text{Hz}$	$^1J(\text{PtF})/\text{Hz}$	$\delta(^{19}\text{F})/\text{ppm}$	$^2J(\text{FF})/\text{Hz}$	$^2J(\text{FF})/\text{Hz}$
(27)	F	F	F	Cl	d -375	42	1714	t -282	42	1220
(29)	F	Cl	F	Cl	s -385	-	1704	-	-	-
(30)	F	F	Cl	Cl	-	-	-	s -284	-	1203
(31)	F	Cl	Cl	Cl	-	-	-	s -294	-	1189

Multiplicity: t = triplet, d = doublet and s = singlet

Although, we do report a singlet at δ -385, $^1J_{\text{PtF}} = 1704$ Hz, it is not attributed to (28) but to the difluoro-dichloro-species (29).

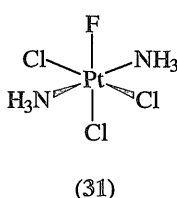
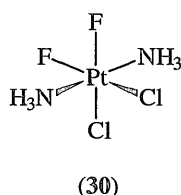


(29)

The complex $[\text{PtF}_2\text{Cl}_2(\text{NH}_3)_2]$ (see section 2.2.9), the only product formed from the analogous reaction of *trans*- $[\text{PtCl}_2(\text{NH}_3)_2]$ and $[\text{XeF}_2]$, was reported to exhibit a singlet resonance at δ -387 with a $^1J_{\text{PtF}} = 1790$ Hz.⁷² Although, the magnitude of the reported $^1J_{\text{PtF}}$ coupling is significantly higher than that for (29) it is plausible to suggest that, by comparison of the ^{19}F NMR data, they have formed the *trans* isomer, in which fluorine is *trans* to

fluorine, and not the isomer where the fluorines are *cis* to each other and *trans* to chlorine.

The trend relating the $\delta(^{19}\text{F})$ with the number of fluorine atoms on the isomer, as discussed in section 2.7, is also evident from the data presented in Table 2.12. Thus, the remaining two singlets observed at δ -284 and -294 are attributed to *cis*, *cis*, *trans*-[PtF₂Cl₂(NH₃)₂] (30) and *mer*-[PtCl₃F(NH₃)₂] (31) respectively since, the isomer with the fewer fluorine atoms is observed at a lower frequency.



2.8.1 Reaction of *trans*-[PtCl₂(NH₃)₂] and [XeF₂] in CH₃CN

The reaction of *trans*-[PtCl₂(NH₃)₂] and [XeF₂] in hydrous HF was reported⁷² to afford no fluoride containing species, but, as in the reaction of the *cis*-complex, the hydroxy-bridged polymer [PtCl₂(NH₃)₂(OH)]_n. Thus, since it is possible that this polymer was formed in the analogous reaction of *cis*-[PtCl₂(NH₃)₂] and [XeF₂] in CH₃CN it was of interest to study the effect of the solvent on this reaction.

A sample of yellow *trans*-[PtCl₂(NH₃)₂] and [XeF₂] in CH₃CN were allowed to react, as described in section 6.20, yielding a green precipitate.

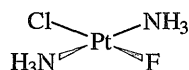
Although, the colouration was indicative of the hydroxy polymer the subsequent ¹⁹F NMR spectrum did reveal resonances characteristic of fluorine bound to platinum. Two singlet resonances were observed at δ -284, $^1J_{\text{PtF}} = 1205$ Hz, and δ -294, $^1J_{\text{PtF}} = 1192$, which were assigned by analogy

with the previous ^{19}F NMR data, to *cis*, *cis*, *trans*- $[\text{PtF}_2\text{Cl}_2(\text{NH}_3)_2]$ (**30**) and *mer*- $[\text{PtCl}_3\text{F}(\text{NH}_3)_2]$ (**31**) respectively.

2.9 Discussion of the Reactions of *cis*- and *trans*- $[\text{PtCl}_2(\text{NH}_3)_2]$ with $[\text{XeF}_2]$

The results of these reactions are undoubtedly oxidative fluorinations of the metal centre with retention of the arrangement of the NH_3 ligands. In the *cis*- system 8 products are formed whereas, in the *trans*- system only 4 are formed with the *cis* and *trans* arrangement of the NH_3 ligands determining the number of products that are possible. Furthermore, in the *cis*- system the tetrafluoro-complex (**17**) is formed but, in the *trans*- system only the trifluoro-species (**27**) is observed. A plausible explanation for the absence of the tetrafluoro-complex in the *trans*- system can be determined by considering the *trans* effect of the ligands.

In the complex *trans*- $[\text{PtCl}_2(\text{NH}_3)_2]$ substitution of chloride for fluoride would hypothetically afford the monofluoro-species *trans*- $[\text{PtFCl}(\text{NH}_3)_2]$ (**32**).



(32)

The "*trans* directing influence"⁸⁵, predicts that the monofluoro-complex and not the difluoro-species will be formed since, the second chloride will not be replaced by another entering fluorine ligand *cf.*

trans-[PtCl₂(NMe₃)₂] and AHF (see section 2.6). Subsequent oxidation of (32) by [XeF₂] will afford the complex *mer*-[PtF₃Cl(NMe₃)₂] (27).

However, in the reactions of *trans*- and *cis*-[PtCl₂(NH₃)₂] with AHF (section 2.5) no resonances characteristic of fluorine bound to platinum were observed and therefore, in the analogous reactions with [XeF₂] there is no evidence to suggest an initial metathetical reaction. Thus, intermolecular halogen exchange is suggested as the reason for the formation of the products which cannot be justified by direct oxidation alone. It is plausible that the initially formed platinum(IV) fluoride amine complex, [PtF₂Cl₂(NH₃)₂], could undergo fluoride metathesis with the AHF solvent however, this would only account for the products containing more fluorine atoms than two and not those products with more than two chlorine atoms.

Therefore, in the next sections the analogous reactions of *cis*-[PtCl₂(en)] and *cis*-[PtCl₂(bipy)] will be described to further investigate the reactions of complexes of this type with [XeF₂]. Furthermore, the chelating nature of the N-donor ligands will help to substantiate the speculation that these reactions proceed with retention of the arrangement of these ligands.

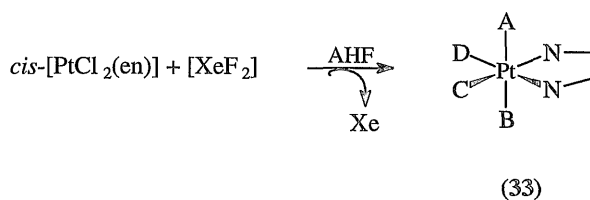
2.10 Reaction of *cis*-[PtCl₂(en)] and [XeF₂] in AHF

Yellow *cis*-[PtCl₂(en)] was allowed to react with [XeF₂] in AHF, as described in section 6.21, affording an orange solution. Once the reaction was adjudged to be complete removal of the AHF resulted in the formation of an air-stable orange solid. The compound was analysed by ¹H and ¹⁹F NMR spectroscopy.

The ^1H NMR spectrum showed broad resonances in regions indicative of NH_2 and CH_2 protons however, no definitive information could be obtained.

The ^{19}F NMR spectrum (Figure 2.14), which is analogous to Figure 2.12, revealed resonances in chemical shift regions characteristic of F *trans* F, F *trans* Cl and F *trans* N. The ^{19}F NMR data is presented in Table 2.13. Thus, the reaction between *cis*-[PtCl₂(en)] and [XeF₂] in AHF proceeds according to Scheme 2.14 in which the coordination sites A, B, C or D are occupied by any combination of fluorine or chlorine ligands.

Scheme 2.14



It is evident from the data presented in Table 2.13 that the structural isomers from the reaction of *cis*-[PtCl₂(en)] and [XeF₂] correspond to those reported for the analogous reaction of *cis*-[PtCl₂(NH₃)₂] and [XeF₂] in section 2.7. Thus, the similarity in results is further evidence that these reactions occur with retention of the *cis*- arrangement of the N-donor ligands.

In marked contrast to the failure to observe reaction between either *cis*- or *trans*-[PtCl₂(NH₃)₂] with AHF evidence for a platinum-fluoride species, from the reaction of *cis*-[PtCl₂(en)] and AHF, was reported in section 2.5. Therefore, there is a precedent for halide metathesis in the Pt(II) complex, rather than intermolecular halogen exchange or halide-metathesis in the Pt(IV) complex, for the formation of those products which cannot be

justified solely by direct oxidative fluorination. Due to the complexity of the reaction products all attempts to obtain mass spectral and infrared data were unsuccessful.

Figure 2.14 ^{19}F NMR Spectrum of the Structural Isomers of Complex (33)

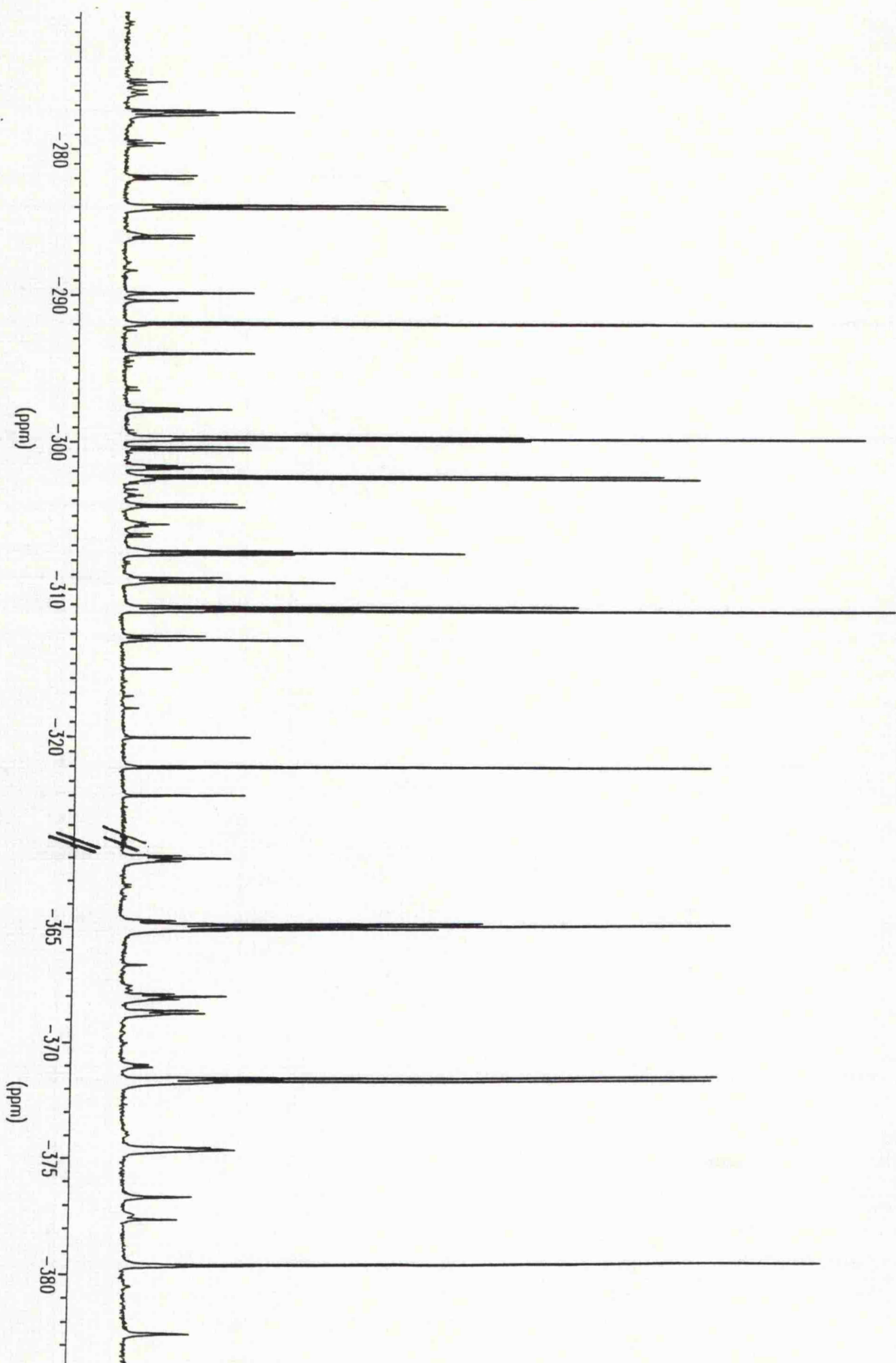


Table 2.13 ^{19}F NMR Data for the Products (33) formed from the Reaction of *cis*-[PtCl₂(en)] and [XeF₂] in AHF

Structural Isomer (F or Cl)				F <i>trans</i> F (δ -365 to -379)			F <i>trans</i> N (δ -299 to -322)			F <i>trans</i> Cl (δ -277 to -292)		
A	B	C	D	$\delta(^{19}\text{F})$ / ppm	$^2J(\text{FF})$ / Hz	$^1J(\text{PtF})$ / Hz	$\delta(^{19}\text{F})$ / ppm	$^2J(\text{FF})$ / Hz	$^1J(\text{PtF})$ / Hz	$\delta(^{19}\text{F})$ / ppm	$^2J(\text{FF})$ / Hz	$^1J(\text{PtF})$ / Hz
F	F	F	F	t -365	35	1687	t -299	35	1102	-	-	-
F	F	F	Cl	d -371	40	1670	t -307	40	1098	-	-	-
F	F	Cl	Cl	s -379	-	1670	-	-	-	-	-	-
F	Cl	F	F	-	-	-	d -302	54	1094	t -277	54	1176
F	Cl	Cl	F	-	-	-	d -311	60	1040	d -283	60	1100
F	Cl	Cl	Cl	-	-	-	-	-	-	s -292	-	1160
Cl	Cl	F	F	-	-	-	s -312	-	1118	-	-	-
Cl	Cl	F	Cl	-	-	-	s -322	-	1114	-	-	-

multiplicity: t = triplet, d = doublet and s = singlet

2.10.1 Reaction of *cis*-[PtCl₂(en)] and [XeF₂] in CH₃CN

The influence of the solvent was investigated by performing the analogous reaction, as described in section 6.20, in CH₃CN.

A sample of *cis*-[PtCl₂(en)] and [XeF₂] in CH₃CN were allowed to react affording a partially soluble orange solid. The solvent was removed and the solid was subsequently dissolved, in d₆-DMSO, and analysed by ¹⁹F NMR spectroscopy.

The ¹⁹F NMR spectrum (Figure 2.15) revealed four singlet resonances with the associated ¹⁹⁵Pt satellites, their NMR data is presented in Table 2.14.

The resonances at δ -292, -322 and -379 were observed in the analogous reaction in AHF and are assigned to complexes (34), (36) and (37). The only explanation for the formation of (34) and (36) is intermolecular halogen exchange which was proposed in section 2.7.

The resonance observed at δ -304 exhibits an unusually small ¹J_{PtF} coupling of 912 Hz which is tending towards the magnitude reported for Pt(II) species (see section 2.5).

Figure 2.15 ^{19}F NMR Spectrum of the Products from the Reaction of *cis*- $[\text{PtCl}_2(\text{en})]$ and $[\text{XeF}_2]$ in CH_3CN

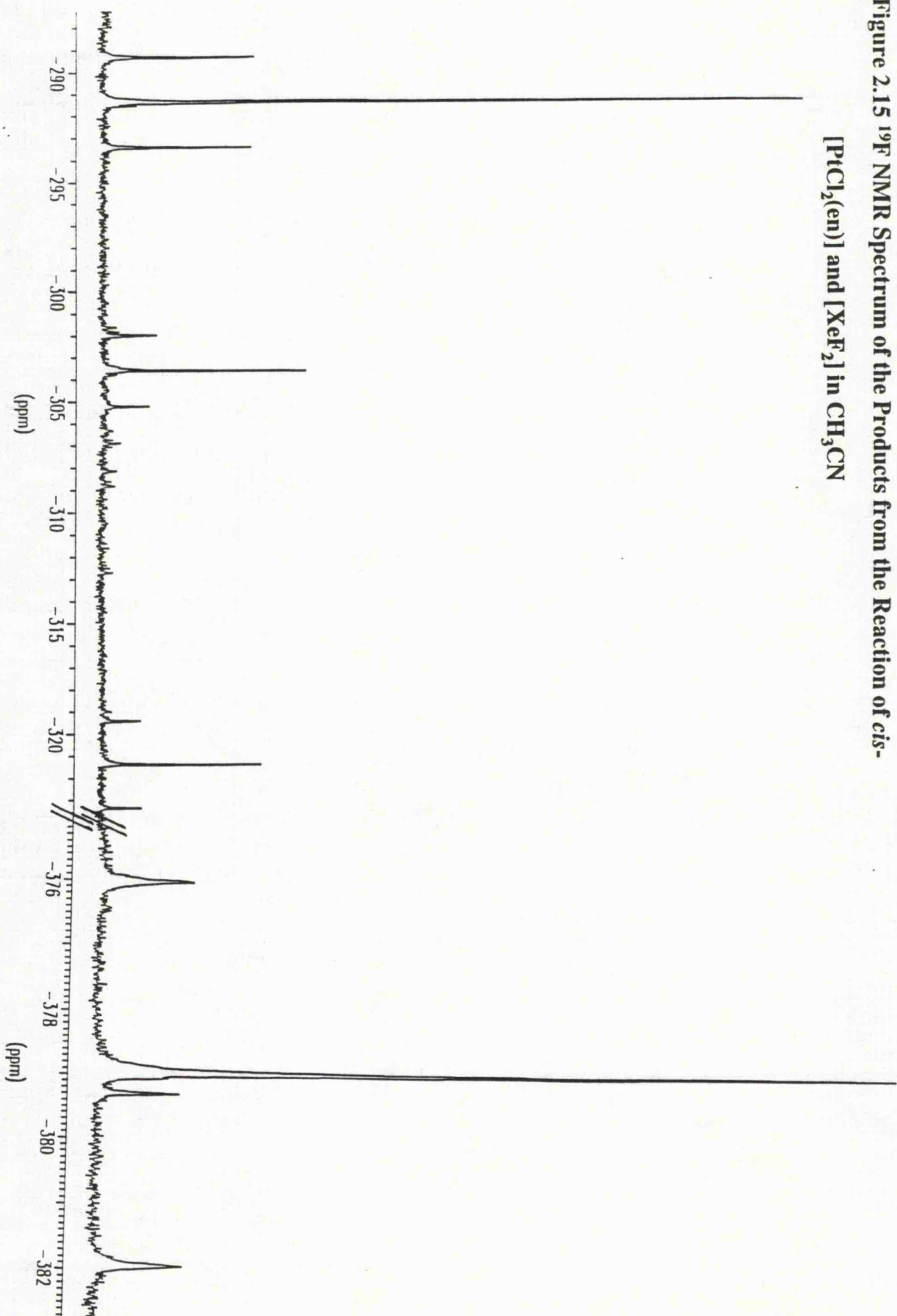
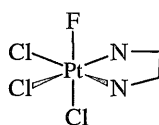
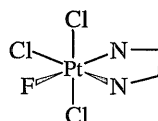


Table 2.14 ^{19}F NMR Data for the Products of the Reaction between *cis*- $[\text{PtCl}_2(\text{en})]$ and $[\text{XeF}_2]$ in CH_3CN

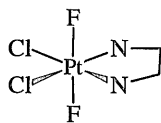
Complex	$\delta(^{19}\text{F})/\text{ppm}$	$^1J(\text{PtF})/\text{Hz}$
(34)	-292	1160
(35)	-304	912
(36)	-322	1115
(37)	-379	1669



(34)



(36)



(37)

Thus, with the chemical shift being characteristic of F *trans* N the resonance is tentatively assigned to either the difluoro-species *cis*- $[\text{PtF}_2(\text{en})]$ or the monofluoro-complex *cis*- $[\text{PtFCl}(\text{en})]$. However, in section 2.15 a complex, formed from the halide metathesis reaction of *cis*- $[\text{PtCl}_2(\text{en})]$ and AHF, was described which exhibited a singlet at δ -351 with a $^1J_{\text{PtF}}$ coupling of 617 Hz. Although, the complex reported in section 2.5 and (35) are

different there are limited data to definitively characterize either of the two species.

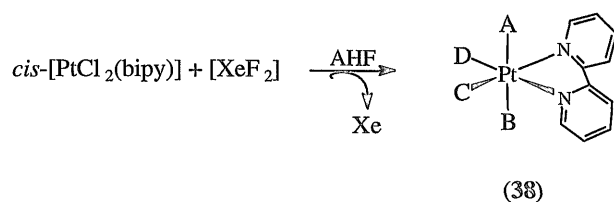
2.11 Reaction of *cis*-[PtCl₂(bipy)] with [XeF₂] in AHF

The reaction of [XeF₂] and yellow *cis*-[PtCl₂(bipy)] in AHF afforded a partially soluble orange solid. After removal of the solvent an air-stable orange solid was isolated which was subsequently dissolved in d₆-DMSO and analysed by ¹H and ¹⁹F NMR spectroscopy.

The ¹H NMR spectrum was uninformative since, several multiplets in the aromatic proton region were observed.

The ¹⁹F NMR spectrum (Figure 2.16) showed the expected resonances in chemical shift regions characteristic of *F trans F*, *F trans N* and *F trans Cl*. The ¹⁹F NMR data, are presented in Table 2.15, for the reaction shown in Scheme 2.15.

Scheme 2.15



In contrast, to the analogous reactions, discussed in sections 2.7 and 2.9, there are fewer products formed from the oxidative fluorination of *cis*-[PtCl₂(bipy)] by [XeF₂]. Notably, there are no resonances which correspond to the tetrafluoro-species *cis*-[PtF₄(bipy)].

Figure 2.16 ^{19}F NMR Spectrum of the Structural Isomers of Complex (38)

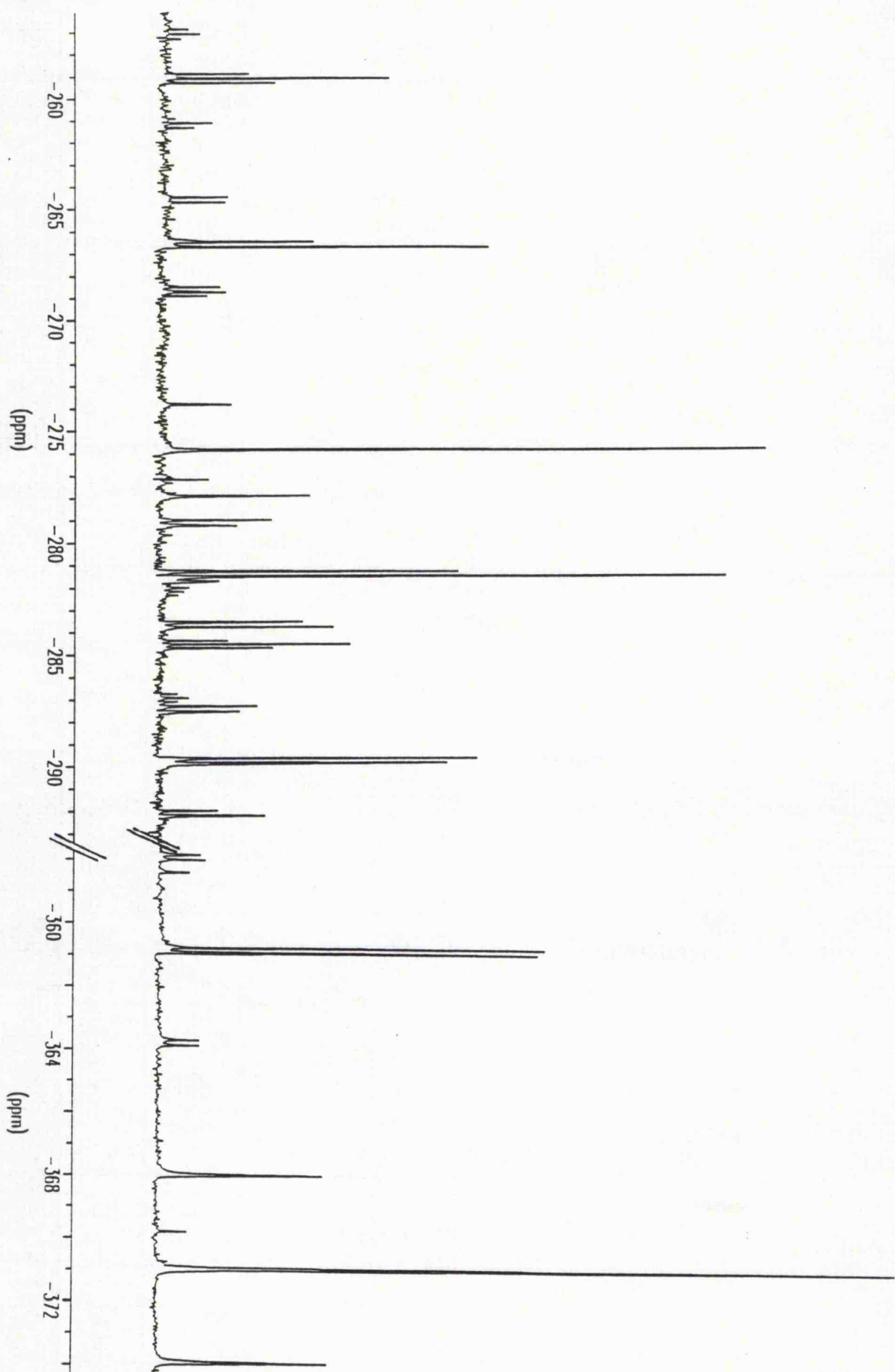


Table 2.15 ^{19}F NMR Data for the Products (38) formed from the Reaction of *cis*- $[\text{PtCl}_2(\text{bipy})]$ and $[\text{XeF}_2]$ in AHF

Structural Isomer (F or Cl)				F <i>trans</i> F (δ -360 to -371)			F <i>trans</i> N (δ -280 to -289)			F <i>trans</i> Cl (δ -258 to -275)		
A	B	C	D	$\delta(^{19}\text{F})/ppm$	$^2J(\text{FF})/Hz$	$^1J(\text{PtF})/Hz$	$\delta(^{19}\text{F})/ppm$	$^2J(\text{FF})/Hz$	$^1J(\text{PtF})/Hz$	$\delta(^{19}\text{F})/ppm$	$^2J(\text{FF})/Hz$	$^1J(\text{PtF})/Hz$
F	F	F	Cl	d -360	45	1662	t -284	45	1328	-	-	-
F	F	Cl	Cl	s -371	-	1674	-	-	-	-	-	-
F	Cl	F	F	-	-	-	d -280	61	1287	t -258	61	1144
F	Cl	Cl	F	-	-	-	d -289	66	1120	d -266	66	1137
F	Cl	Cl	Cl	-	-	-	-	-	-	s -275	-	1156

multiplicity: t = triplet, d = doublet and s = singlet

2.11.1 Reaction of *cis*-[PtCl₂(bipy)] with [XeF₂] in CH₃CN

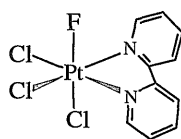
As with the previously discussed reactions the role of the solvent was investigated by performing the analogous reaction in CH₃CN.

cis-[PtCl₂(bipy)] and [XeF₂] were reacted in CH₃CN, as described in section 6.20, affording an orange solution. Removal of the solvent yielded an air-stable orange solid. The solid was analysed by ¹⁹F NMR spectroscopy and the data are presented in Table 2.16.

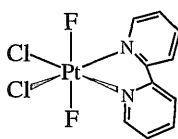
Table 2.16 ¹⁹F NMR Data of the Products from the Reaction of *cis*-[PtCl₂(bipy)] and [XeF₂] in CH₃CN

Complex	δ(¹⁹ F)/ ppm	¹ J(PtF)/ Hz
(39)	-275	1155
(40)	-284	840
(41)	-301	1318
(42)	-370	1677

The singlet resonances at δ -275 and -370 were observed in the analogous reaction in AHF and are assigned to complexes (39) and (40).



(39)



(40)

The resonances observed at δ -284 exhibits an unusually small ¹J_{PtF} coupling of 840 Hz, which is tending towards the magnitude diagnostic of a

Pt(II) species (see section 2.5). Thus, the resonance is tentatively assigned to a Pt(II) complex of the type *cis*-[PtXY(bipy)] (XY = F or X = Cl, Y = F). Furthermore, the reaction of *cis*-[PtCl₂(bipy)] with AHF, was described in section 2.5, to afford a complex which exhibited a singlet resonance at δ -331 with a $^1J_{\text{PtF}} = 834$ Hz. However, as with the *cis*-[PtCl₂(en)] reaction, as discussed in section 2.10.1, limited spectroscopic data prevents a definitive characterization and thus, the platinum(II) fluoride species remain tentatively assigned.

2.12 Reaction of *cis*-[PtCl₂(py)₂] with [XeF₂] in AHF

In contrast to the *cis*- ammonia and ethylenediamine systems the tetrafluoro-species *cis*-[PtF₄(bipy)] was not observed. Thus, in the following section we investigate the reaction of *cis*-[PtCl₂(py)₂] with [XeF₂] in AHF in order to ascertain whether the aryl nature on the N-donor ligands influences the structural isomers formed.

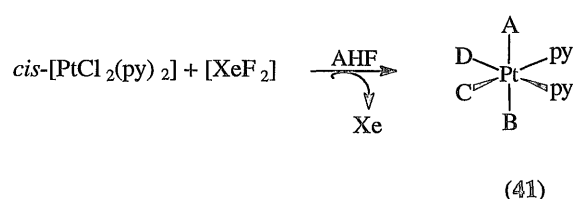
Yellow *cis*-[PtCl₂(py)₂] and [XeF₂] were reacted in AHF, in an analogous manner to that described in section 6.21, affording a sparingly soluble orange solid. The air-stable orange solid was analysed by ¹H and ¹⁹F NMR spectroscopy.

The ¹H NMR spectrum showed only broad resonances attributed to the aromatic protons on the pyridine groups and thus, was uninformative.

The ¹⁹F NMR spectrum showed the predicted two distinct chemical shift regions. In contrast to the previously reported *cis*- systems the chemical shift regions for F *trans* F and F *trans* N were comparable and the region associated with F *trans* Cl being observed at a significantly higher frequency. Since it has already been established that these reactions proceed with

retention of the arrangement of the N-donor ligands it is feasible to suggest that the products are formed according to Scheme 2.16.

Scheme 2.16



The ^{19}F NMR data for the structural isomers of complex (41) are presented in Table 2.17. It is evident from the data in Table 2.17 that the tetrafluoro-species $\text{cis-[PtF}_4(\text{py})_2]$ has been formed however, the chemical shifts for both triplets are, unlike those previously reported, comparable and this will be discussed in section 2.14. The major product formed is the *trans*, *cis*, $\text{cis-[PtF}_2\text{Cl}_2(\text{py})_2]$ (42) which exhibits a singlet resonance at δ -322 with a $^1J_{\text{PtF}} = 1755$ Hz. All attempts to obtain further evidence to help substantiate the formulations were unsuccessful. Although, in the E. I. mass spectrum the most intense peak centred at m/z 424 was attributed to $\text{cis-[PtCl}_2(\text{py})_2]$ another peak centred at m/z 442 which corresponds to $[\text{M-HF}]^+$ (where $\text{M} = [\text{PtF}_2\text{Cl}_2(\text{py})_2]$) was observed.

2.12.1 Reaction of $\text{cis-[PtCl}_2(\text{py})_2]$ with $[\text{XeF}_2]$ in CH_3CN

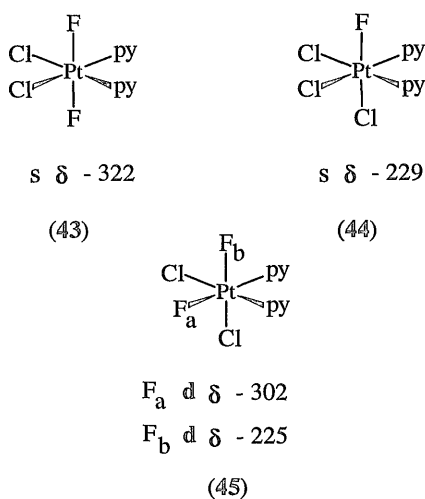
The corresponding reaction in CH_3CN was performed, as described in section 6.20, affording an orange solution. After removal of the solvent an air-stable orange solid was isolated and subsequently analysed by ^{19}F NMR spectroscopy.

Table 2.17 ^{19}F NMR Data for the Products (41) formed from the Reaction of *cis*-[PtCl₂(py)₂] and [XeF₂] in AHF

Structural Isomer (F or Cl)				<i>F trans</i> F (δ -313 to -322)			<i>F trans</i> N (δ -293 to -302)			<i>F trans</i> Cl (δ -225 to -229)		
A	B	C	D	$\delta(^{19}\text{F})$ / ppm	$^2J(\text{FF})$ / Hz	$^1J(\text{PtF})$ / / Hz	$\delta(^{19}\text{F})$ / ppm	$^2J(\text{FF})$ / Hz	$^1J(\text{PtF})$ / / Hz	$\delta(^{19}\text{F})$ / ppm	$^2J(\text{FF})$ / Hz	$^1J(\text{PtF})$ / / Hz
F	F	F	F	t -313	39	1756	t -293	39	1308	-	-	-
F	F	F	Cl	d -317	41	1750	t -301	41	1305	-	-	-
F	F	Cl	Cl	s -322	-	1755	-	-	-	-	-	-
F	Cl	Cl	F	-	-	-	d -302	61	1305	d -225	61	1206
F	Cl	Cl	Cl	-	-	-	-	-	-	s -229	-	1212

multiplicity: t = triplet, d = doublet and s = singlet

The ^{19}F NMR showed two singlets at δ -322 and -229 with $^1J_{\text{PtF}} = 1760$ and 1302 Hz respectively. Two additional doublet resonances at δ -302 and -225, $^2J_{\text{FF}} = 61$ Hz, were also observed although these only represented a minor component of the reaction mixture. All resonances had been observed previously in the analogous reaction in AHF and are attributed to the complexes (43), (44) and (45).



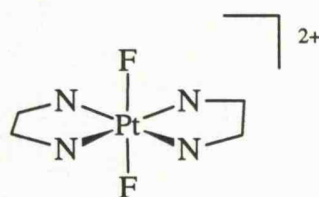
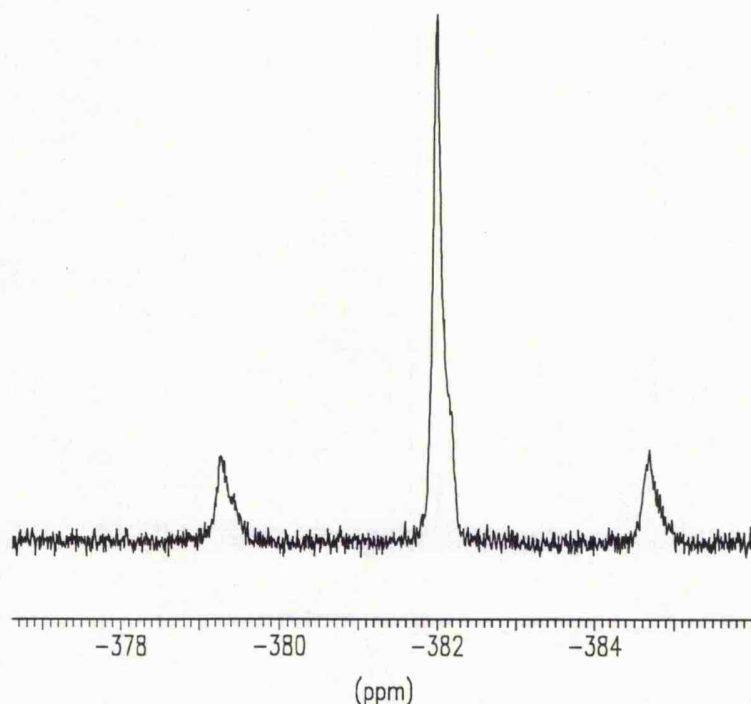
2.13 Reaction of $[\text{Pt}(\text{en})_2]\text{Cl}_2$ with $[\text{XeF}_2]$

The complex $\text{trans-}[\text{IrF}_2(\text{dppe})_2]^+$ is reported⁸⁴ to be formed from the reaction of $[\text{Ir}(\text{dppe})_2]^+$ and $[\text{XeF}_2]$ and thus, indicates that the oxidative fluorination mechanism is not concerted. Here we report the analogous reaction of $[\text{Pt}(\text{en})_2]^{2+}$ in an attempt to isolate one product and thus facilitate a comprehensive analysis.

$[\text{Pt}(\text{en})_2]\text{Cl}_2$ and $[\text{XeF}_2]$ were allowed to react in both AHF and CH_3CN yielding a partially soluble orange solid. The solid was isolated by removal of the solvent and then studied by ^{19}F NMR spectroscopy.

In both cases the ^{19}F NMR spectrum (Figure 2.17) revealed one singlet resonance at δ -382 with a $^1J_{\text{PtF}} = 1535$ Hz. Since, both the chemical shift and coupling constant are characteristic of fluorine *trans* fluorine the resonance was attributed to complex (46).

Figure 2.17 ^{19}F NMR Spectrum of Complex (46)



(46)

All attempts to obtain an interpretable mass spectrum were unsuccessful, however the infrared spectrum for complex (46) did show a band at 607 cm^{-1} which was attributed to the $\nu(\text{Pt-F})$ which compares with the reported $\nu(\text{Pt-F})$, of 587 cm^{-1} , for the complex *trans*- $[\text{PtF}_2\text{Cl}_2(\text{NH}_3)_2]$.⁷²

A sample of the material was sent for elemental analysis and the following results were achieved.

%	Element			
	C	H	N	F
Expected	11.33	3.80	13.21	8.96
Found	10.9	4.18	12.55	21.25

The analysis for fluorine is significantly higher than expected for the complex $[\text{PtF}_2(\text{en})_2]\text{Cl}_2$ thus, the compound is either impure or contains the $[\text{HF}_2]^-$ anion. The analysis figures for the complex $[\text{PtF}_2(\text{en})_2][\text{HF}_2]_2$ would be as follows.

%	Element			
	C	H	N	F
Expected	11.0	4.20	12.99	26.0

Although, the expected analysis for fluorine in the complex $[\text{PtF}_2(\text{en})_2][\text{HF}_2]_2$ is significantly higher, than that found, it is a plausible formulation.

2.14 Discussion of the Oxidative Fluorinations

All the reactions have been shown to afford platinum(IV) fluoro-species with retention of the *cis* or *trans* arrangement of the N-donor ligands.

In all the *cis* systems studied the oxidative fluorinations were found to yield several structural isomers. Precise determination of how some of these isomers were formed is beyond the realms of this thesis. However, there are precedents for both intermolecular halogen rearrangement and an initial halide metathetical reaction prior to oxidation. The reaction of *trans*-[IrCl(CO)(PEt₃)₂] and [XeF₂] was reported⁸⁴ to yield predominately [IrF₂Cl(CO)(PEt₃)₂]. However, small amounts of the two structural isomers [IrFCl₂(CO)(PEt₃)₂] and [IrF₃(CO)(PEt₃)₂] were reported to be formed as a result of intermolecular halogen rearrangement. In all cases, except *cis*- and *trans*-[PtCl₂(NH₃)₂], halide metathetical reactions have been shown to afford complexes that exhibit resonances characteristic of fluorine bound to platinum (see section 2.5). Therefore, as there is a precedent for both metathesis and intermolecular halogen rearrangement, one or the other cannot be ruled out and thus, it is likely that a combination of both results in the formation of these, otherwise unexplainable, products.

By comparing all the NMR data presented in the previous sections certain trends can be seen. In both the *cis* and *trans* systems the nature of coordinating nitrogen ligand significantly influences the ¹⁹F chemical shift of the resonances (Table 2.18).

From the data presented in Table 2.18 it can be seen that the $\delta(^{19}\text{F})$ for F *trans* F is shifted to higher frequency with a change in N-donor ligand from NH₃ to a primary amine (en) to a tertiary amine (bipy, py and NMe₃). This trend is as expected since a tertiary amine will shield the fluorine nuclei to a greater extent, as a consequence of the increased σ -donor ability, than a primary amine or NH₃ group would. This influence, exerted by the different

nature of the N-donor ligands, on the $\delta(^{19}\text{F})$ can be seen for the *F trans Cl* resonances. However, the $\delta(^{19}\text{F})$ of the *F trans N* resonances do not show the same significant dependence on the nature of the ligands.

Table 2.18 Influence of Different N-Donor ligands on the ^{19}F Chemical Shift

N-donor ligand	$\delta(^{19}\text{F})$		
	<i>F trans F</i>	<i>F trans N</i>	<i>F trans Cl</i>
NH_3	-370 to -385	-291 to -313	-282 to -294
NH_2R (en)	-365 to -379	-299 to -322	-277 to -292
NR_3			
bipy	-360 to -371	-280 to -289	-258 to -275
py	-313 to -322	-293 to -302	-225 to -229
NMe_3	-323 to -329	-	-217 to -219

A second trend, previously discussed in section 2.7, reveals that the $\delta(^{19}\text{F})$ is dependent on the number of fluorine atoms on the isomer. In other words a shift, of $\approx 5\text{-}10$ ppm, to lower frequency is observed with sequential substitution of fluorine for chlorine in all environments; *F trans F*, *F trans N* and *F trans Cl*. Although, not as apparent this trend can be seen in the data reported by Preetz and co-workers⁷⁷ for the complexes of the type $[\text{PtF}_n\text{Cl}_{6-n}]^{2-}$ ($n = 0\text{-}6$) (Table 2.19)

In the *F trans F* environment it is evident, from the data in Table 2.19, that there is almost an additive shift to lower frequency with a sequential

decrease in the number of fluorine atoms on the anion. In the *F trans* Cl environment the trend although not as obvious can still be seen.

Table 2.19 Comparison of the $\delta(^{19}\text{F})$ with the Number of Fluorine Atoms on the Complexes of the Type $[\text{PtF}_n\text{Cl}_{6-n}]^{2-}$ ($n = 0-6$)

No. of Fluorine Atoms	$\delta(^{19}\text{F})/\text{ppm}$	
	<i>F trans</i> F	<i>F trans</i> Cl
6	-357	-
5	-360	-268
4	-367	-
	-364	-267
3	-372	-273
	-	-266
2	-382	-
	-	-276
1	-	-287

A third trend, showing that the magnitude of the $^2J_{\text{FF}}$ coupling is dependent on the number of fluorine atoms in the complex, is also observed (Table 2.20). Furthermore, a larger $^2J_{\text{FF}}$ coupling is observed if the associated fluorine atoms are *trans* to chlorine and nitrogen but not fluorine (Table 2.20).

Table 2.20 Comparison of the Magnitude of the *cis* $^2J_{\text{FF}}$ Coupling with the Number of Fluorine Atoms on the Platinum-Fluoro-Amine Complexes Reported in this Chapter

No. of Fluorine atoms	$^2J(\text{FF})/\text{Hz}^{\text{a}}$	
	F <i>trans</i> F	F <i>trans</i> Cl
4	37	-
3	42	58
2	-	62

(a) average values

This trend has been observed previously, by Preetz *et al.*,⁷⁷ in the study of the ^{19}F NMR data for complexes of the type $[\text{PtF}_n\text{Cl}_{6-n}]$.

Finally, the magnitude of the $^1J_{\text{PtF}}$ coupling is found to be dependent on the *trans* ligand, this phenomenon is known as the "NMR *trans* influence"⁹⁶ (see section 2.5). Thus, the magnitude of coupling follows the order $\text{F} > \text{N} \approx \text{Cl}$ which is consistent with the increasing *trans* influence of the ligands.

References for Chapter Two

1. G. B. Kauffmann, 'Classics in Coordination Chemistry', New York, 1968.
2. F. R. Hartley, 'The Chemistry of Platinum and Palladium', Applied Science Publishers Ltd, London, 1973, chapter 7, 112.
3. G. Wilkinson, R. D. Gillard and J. A. McLverty, 'Comprehensive Coordination Chemistry', 1987, 5, 422.
4. R. B. King, 'Encyclopedia of Inorganic Chemistry', 1994, 8, 103.
5. F. Basolo and P. G. Pearson, *Prog. Inorg. Chem.*, 1962, 4, 381.
6. G. B. Kaufmann, *Inorg. Synth.*, 1963, 7, 249.
7. J. Reiset, *Compt. Rend.*, 1844, 18, 1103.
8. M. Peyrone, *Ann. Chem. Liebigs*, 1845, 51, 15.
9. G. Thiele and D. Wagner, *Chem. Ber.*, 1978, 111, 3162.
10. C. R. Kistner, J. H. Hutchinson, J. R. Doyle and J. C. Storlie, *Inorg. Chem.*, 1963, 2, 1255.
11. G. Calvin and C. E. Coats, *J. Chem. Soc.*, 1960, 2008.
12. G. B. Kaufmann, G. Slusarczuk and S. Kirschner, *Inorg. Synth.*, 1963, 17, 236.
13. G. W. Watt and D. G. Upchurch, *Inorg. Nucl. Chem.*, 1966, 2, 363.
14. K. O. Hodges and J. V. Rund, *Inorg. Chem.*, 1975, 14, 525.
15. P. K. Monaghan and R. J. Puddephatt., *J. Chem. Soc. Dalton Trans.*, 1988, 595.
16. M. Kretschmer and L. Heck, *Z. Anorg. Allg. Chem.*, 1982, 490, 205.
17. R. J. Meyer and E. H. Erich, 'GMELINS Handbuch Der Anorganischen Chemie', Verlag Chemie G. M. B. H., Berlin, 1965, 52, 32.
18. F. Eisner and O. Ruff, *Ber. Deuts. Chem. Gesellschaft*, 1905, 38, 742
19. J. A. Chandler and R. S. Drago, *Inorg. Chem.*, 1962, 356.

20. R. J. H. Clark and W. Errington, *J. Chem. Soc.(A)*, 1967, 258.
21. E. L. Muetterties, *J. Am. Chem. Soc.*, 1960, 1082.
22. R. G. Cavell and H. C. Clark, *J. Chem. Soc.*, 1962, 2962.
23. M. C. Chakravorti and A. R. Sarkar, *J. Inorg. Nucl.Chem.*, 1978, **40**, 139.
24. J. Selbin and L. H. Holmes Jr, *J. Inorg. Nucl.Chem.*, 1962, **24**, 1111.
25. R. G. Cavell and H. C. Clark, *J. Inorg. Nucl.Chem.*, 1961, **17**, 257.
26. D. L. Kepert, 'The Early Transition Metals', Academic London, 1972.
27. M. M. Ershova, M. A. Glushkova and Buslaev, *Koord. Khim.*, 1979, **5**, 532.
28. E. G. LI'in, M. M. Ershova, M. A. Glushkova and Yu. A. Buslaev, *Dokl. Akad. Nauk. SSSR*, 1978, **243**, 1459.
29. R. D. Peacock, 'Advances in Fluorine Chemistry' unpublished observation, 1961, **7**, 113.
30. C. Djordjevic and V. Katoric, *J. Chem. Soc.(A)*, 1970, 3382.
31. F. E. Dickson, R. A. Hayden and W. G. Fateley, *Spectrochimica Acta*, 1969, **25**, 1875.
32. R. D. Gillard, J. A. McCleverty and G. Wilkinson, *Comprehensive Coordination Chemistry*, 1987, **3**, 699 and references cited therein.
33. J. W. Vaugh, *Coord. Chem. Rev.*, 1981, **39**, 265 and references cited therein.
34. J. W. Vaugh, *Synth. React. Inorg. Metal-Org. Chem.*, 1979, **9**, 585 and references cited therein.
35. A. E. Ogard and H. Taube, *J. Am. Chem. Soc.*, 1958, **50**, 1004.
36. Yu. N. Shevchenko and N. K. Davidenko, *Russ. J. Inorg. Chem.* (Eng. Transl.), 1979, **24**, 1193; J. W. Vaughn, J. M. DeJorine and G. J. Seiler, *Inorg. Chem.*, 1970, **9**, 684.
37. N. Costachesscu, *J. Chem. Soc.*, 1912, **102**, 493.

38. J. Glerup, J. Josephsen, K. Michelson, E. Redersen and C. E. Schaffer, *Acta Chem. Scand.*, 1970, **24**, 247.
39. M. C. Charravorti and D. Bandyopadhyay, *J. Indian. Chem. Soc.*, 1984, **61**, 836.
40. H. C. Clark and H. J. Emeleus, *J. Chem. Soc.*, 1957, 4778.
41. O. R. Chambers, M. E. Harman, D. S. Rycroft, D. W. A. Sharp and J. M. Winfield, *J. Chem. Res.(M)*., 1977, 1846.
42. M. E. Harman, D. W. A. Sharp and J. M. Winfield, *Inorg. Nucl. Chem. Lett.*, 1974, **10**, 183.
43. V. A. Bochkareva, Yu. A. Buslaev, Yu. D. Chubar, and Yu. V. Kokunov, *Koord. Chem.*, 1975, **1(8)**, 1100.
44. G. E. Blokhina and A. A. Opalovskii, *Izv. Vyssh. Ucheb. Zaved. Khim. Khim. Technol*, 1972, **15(11)**, 1617.
45. L. Arnaudet, R. Bougon, B. Buu, M. Lance, N. Neilich, P. Thuery and J. Vigner, *J. Fluor. Chem.*, 1995, **71**, 123.
46. L. Arnaudet, R. Bougon, B. Buu, M. Lance, N. Neilich and J. Vigner, *Inorg. Chem.*, 1993, **32**, 1142.
47. L. Arnaudet, R. Bougon, B. Ban, M. Lance, A. Navaza, N. Neilich and J. Vigner, *J. Fluor. Chem.*, 1994, **67**, 17.
48. L. Arnaudet, R. Bougon, B. Ban, M. Lance, A. Navaza, N. Neilich and J. Vigner, *J. Fluor. Chem.*, 1992, **59**, 141.
49. L. Arnaudet, R. Bougon, B. Ban, M. Lance and W. C. Kaska, *J. Fluor. Chem.*, 1991, **53**, 171.
50. L. Arnaudet, R. Bougon, B. Ban, P. Charpin, J. Isabey, M. Lance, N. Neilich and J. Vigner, *Can. J. Chem.*, 1990, **68**, 507.
51. L. Arnaudet, R. Bougon, B. Ban, P. Charpin, J. Isabey, M. Lance, N. Neilich and J. Vigner, *Inorg. Chem.*, 1989, **28**, 257.
52. J. A. Connor, E. J. James, C. Oherton, J. M. A. Walshe and R. H. Head, *J. Chem. Soc. Dalton Trans.*, 1986, 511.

53. H. A. Goodwin and R. N. Sylva, *Aust. J. Chem.*, 1967, **20**, 629.
54. E. Horn and M. R. Snow, *Aust. J. Chem.*, 1984, **37**, 35.
55. S. C. Lee and R. H. Holm, *Inorg. Chem.*, 1993, **32**, 4745.
56. Y. A. Buslaev, A. S. Kanischeva, Y. V. Kokunov, Y. N. Mikhailov, G. G. Sadikov, N. M. Sinitsyn and A. A. Svetlov, *Russ. J. Inorg. Chem.*, 1989, **4**, 1599.
57. P. P. Claret and P. E. Hoggard, *Polyhedron*, 1987, **6**(7), 1621.
58. K. G. Caulton, O. Eisenstein, K. Folting, J. T. Poulton, M. P. Sigalas and W. E. Streib, *Inorg. Chem.*, 1994, **33**, 1476.
59. S. J. Eder and W. A. Herrmann, *Chem. Ber.*, 1993, **126**, 31.
60. K. S. Coleman, Personal Communications, 1995.
61. W. L. Groeneveld and S. Smit, *Inorg. Nucl. Chem. Lett.*, 1975, **11**, 277.
62. D. G. Hill and A. F. Rosenberg, *J. Chem. Phys.*, 1954, **22**, 148; 1956, **24**, 1219.
63. W. R. Matoush and F. Basolo, *J. Am. Chem. Soc.*, 1956, **78**, 3972.
64. J. Glerup, C. E. Schaffer and J. Springborg, *Acta Chem. Scand.*, 1978, **A32**, 673.
65. T. Laier, C. E. Schaffer and J. Springborg, *Acta Chem. Scand. A*, 1980, **34**, 343.
66. C. Burgess, F. R. Hartley and D. E. Rogers, *Inorg. Chim. Acta*, 1975, **13**, 35.
67. T. A. Degtyaneva, I. I. Kalinichenko and A. A. Knyazeva, *Russ. J. Inorg. Chem.*, 1967, **12**, 642.
68. S. J. Higgins and W. Levason, *Inorg. Chim. Acta*, 1986, **113**, 47.
69. M. Arif, P. A. Bates, J. Emsley and B. Hurstous, *J. Chem. Soc. Dalton Trans.*, 1989, 1273.
70. A. J. Canty, B. W. Skelton, P. R. Traill and A. H. White, *J. Organomet. Chem.*, 1991, **402**, C33.

71. S. L. Doran, A. R. Khokhar and M. P. Hacker, *Inorg. Chim. Acta*, 1985, **108**, 113.
72. L. M. Levchenko, O. G. Potapova, V. A. Shipachev, S. V. Tkachev, L. Ya Al't and S. V. Zemskov (deceased), *Russ. J. Inorg. Chem.*, 1990, **35**, 29.
73. G. M. Anderson, R. J. Puddephatt, G. Ferguson and A. J. Lough, *J. Chem. Soc., Chem. Commun.*, 1989, 1297.
74. G. M. Anderson, R. J. Puddephatt, C. Crespo, G. Ferguson and A. J. Lough, *Organometallics*, 1992, **11**, 1177.
75. R. R. Jacobson, Z. Tyekar, K. D. Karlin and J. Zubieta, *Inorg. Chem.*, 1991, **30**, 2035.
76. M. J. Shaw, H. H. Hyman and R. Filler, *J. Org. Chem.*, 1971, **36**, 2917; M. Ya. Turkina and I. P. Grageror, *J. Org. Chem.*, U. S. S. R., 1975, **11**, 335.
77. E. Pazich, G. Peters and N. Preetz, *Z. Naturforsch.*, 1993, **48b**, 1169.
78. R. D. W. Kemmitt, R. D. Peacock and J. Stocks, *J. Chem. Soc.(A)*, 1971, 846.
79. R. B. King, "Encyclopedia of Inorganic Chemistry", 1994, **8**, 224.
80. S. A. Brewer, PhD Thesis, Leicester, 1993.
81. A. V. Zelewsky, *Helv. Chim. Acta.*, 1968, **51**, 803.
82. P. S. Pregosin, *Coord. Chem. Rev.*, 1982, **44**, 247.
83. P. S. Pregosin and J. Reedijk, Unpublished results; M. Chikuma, K. C. Ott, R. J. Pollach, O. A. Gansow and B. Rosenberg, Unpublished results, 1979 from reference 82.
84. R. W. Cockman, E. A. V. Ebsworth, J. H. Holloway, H. Murdoch, N. Robertson and P. G. Watson, "Reaction of Non-metal Fluorides with some Platinum Metal Complexes," J. Thrasher and S. Strauss, ACS Symposium Series, ACS Books, 1994.

85. E. A. V. Ebsworth, N. Robertson and L. J. Yellowlees, *J. Chem. Soc., Dalton. Trans.*, 1993, 1031.
86. S. A. Brewer, K. C. Coleman, J. Fawcett, J. H. Holloway, E. G. Hope, D. R. Russell and P. G. Watson, *J. Chem. Soc., Dalton. Trans.*, 1995, 1073.
87. G. H. Milburn and M. R. Truter, *J. Chem. Soc. (A)*, 1966, 1609.
88. R. S. Osburn and D. Rogers, *J. Chem. Soc., Dalton. Trans.*, 1974, 1002.
89. S. A. Brewer, A. K. Brisdon, J. H. Holloway, E. G. Hope, L. A. Peck and P. G. Watson, *J. Chem. Soc., Dalton. Trans.*, 1995, 2945.
90. M. Atherton, K. C. Coleman, J. Fawcett, J. H. Holloway, E. G. Hope, A. Karacar, L. A. Peck and G. G. Saunders, manuscript in preparation.
91. EXCURV92, SERC Daresbury Laboratory Program, N. Binstead, S. J. Gurman and J. W. Cambell, 1992.
92. R. W. Joyner, K. J. Martin and P. Meehan, *J. Phys.C*, 1987, **20**, 4005; R. J. Price, *J. Am. Chem. Soc.*, 1987, **109**, 3667.
93. C. Bruhn, H. H. Drews, B. Meynhardt and W. Preetz, *Z. Anorg. Allg. Chem.*, 1995, **621**, 373.
94. I. I. Chernyaev, *Izbrannye Trudy (Selected Works)*, Izd. Nauka, Moscow, 1973, 56; C. Brasset, *Arkiv for Kemi Miner.*, 1948, **25(A)(19)**, 1; B. M. Craven and D. Hall, *Acta Cryst.*, 1961, **14**, 56.
95. G. K. Anderson and R. J. Cross, *Acc. Chem. Rev.*, 1984, **17**, 67.

CHAPTER

THREE

Preparation of Platinum Fluoride-

Phosphine Complexes

3.1 An Introduction to the Chemistry of Platinum Phosphine Complexes

Complexes of platinum are commonly found for oxidation states 0, II or IV. The essentially 'soft' (class b) acid character of Pt(II) is indicated by the ready formation of complexes of the type $[\text{PtX}_2(\text{PR}_3)_2]$ ($\text{X} = \text{Cl}, \text{Br}, \text{I}$ and pseudohalide; $\text{R} = \text{alkyl}, \text{aryl}$ or alkylaryl). The earliest example of a complex of this type, *cis*- $[\text{PtCl}_2(\text{PPh}_3)_2]$, was first cited in 1936 by Jensen,¹ and the literature contains an extensive selection of preparative routes to these compounds. In marked contrast, the chemistry of platinum(II) fluoro-analogues have been relatively unexplored. Outlined in the next sections is the chemistry of the platinum phosphine complexes and the analogous fluoro-species.

3.1.2 Platinum(0) Phosphine Complexes

Complexes of platinum(0) can be tetrahedral, planar three-coordinate, or linear two-coordinate. Presented in Table 3.1 are examples of platinum(0) complexes and their preparations. The tetrahedral tetrakis(triphenylphosphine)platinum(0), $[\text{Pt}(\text{PPh}_3)_4]$, readily dissociates in solution according to Scheme 3.1.

Scheme 3.1.

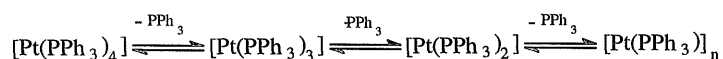


Table 3.1 A Variety of Platinum(0) Complexes and their Preparations

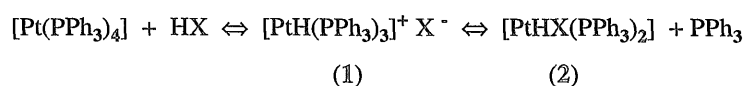
Complex	Reagents	Refs.
$[\text{Pt}(\text{PR}_3)_4]$ ($\text{PR}_3 = \text{PPh}_3, \text{PPhMe}_2$)	$\text{cis-}[\text{PtCl}_2(\text{PR}_3)_2] + \text{KOH/}$ EtOH ($\text{PR}_3 = \text{PPh}_3, \text{PPhMe}_2$)	2,3
$[\text{Pt}(\text{PR}_3)_4]$ ($\text{PR}_3 = \text{PPh}_2\text{Me}, \text{P}(\text{C}_6\text{F}_5)\text{Me}_2$)	$\text{cis-}[\text{PtCl}_2(\text{PR}_3)_2] + [\text{NaBH}_4]$ $+ 2\text{PR}_3$ ($\text{PR}_3 = \text{PPh}_2\text{Me}, \text{P}(\text{C}_6\text{F}_5)\text{Me}_2$)	4
$[\text{Pt}(\text{PR}_3)_2]$ ($\text{PR}_3 = \text{Pcy}_3, \text{PBu}^t_3, \text{PPhBu}^t_3$)	$[\text{Pt}(\text{cod})_2] + 2\text{PR}_3$ ($\text{PR}_3 = \text{Pcy}_3, \text{PBu}^t_3, \text{PPhBu}^t_3$)	5
$[\text{Pt}(\text{PEt}_3)_4]$	$[\text{Pt}(\text{PEt}_3)_2(\text{C}_2\text{O}_4)] + 2\text{PEt}_3$ $+ h\nu$	6
$[\text{Pt}(\text{PPh}_3)_2(\text{PhCCR})]$ ($\text{R} = \text{Et}, \text{Ph}$)	$[\text{Pt}(\text{PPh}_3)_2(\text{C}_2\text{O}_4)] +$ $[\text{PhCCR}] + h\nu$ ($\text{R} = \text{Et}, \text{Ph}$)	7

The tris(phosphine) complex, $[\text{Pt}(\text{PPh}_3)_3]$ is planar and the bis(phosphine) species $[\text{Pt}(\text{PPh}_3)_2]$ seems to be linear, by analogy with the isolable $[\text{Pt}(\text{PCy}_3)_2]$.⁵

The reaction chemistry of the platinum(0) complexes is dominated by oxidation reactions. Chlorine, bromine and iodine oxidatively add to $[\text{Pt}(\text{PPh}_3)_4]$ to give $\text{cis-}[\text{PtX}_2(\text{PPh}_3)_2]$ ($\text{X} = \text{Cl}, \text{Br}$ and I).^{8,9} The reaction of a protic acid, HX , with $[\text{Pt}(\text{PPh}_3)_4]$ involves initial protonation to yield a cationic hydride complex (1). However, there is no reported ^{195}Pt NMR data to confirm that initial protonation occurs rather than oxidation of the metal centre. If X is a poor ligand for platinum(II), e.g. ClO_4^- , HSO_4^- , MeCO_2^- , NO_3^- , complex (1) is the final product. When X^- coordinates strongly to

platinum(II), e.g. Cl^- , Br^- , I^- , CN^- , Ph_2PO^- , substitution occurs and the complex $[\text{PtHX}(\text{PPh}_3)_2]$ (2) is formed (Scheme 3.2).¹⁰⁻¹²

Scheme 3.2



3.1.3 The Reactions of Zerovalent Platinum Phosphine Complexes with Oxidative Fluorinating agents

Doyle reported the formation of the HF adduct, $[\text{PtHF}(\text{PPh}_3)_2]$, from the reaction of HCOF (formylfluoride) with $[\text{Pt}(\text{PPh}_3)_4]$.¹³ The reaction of anhydrous HF, which is a very strong protic acid, with $[\text{Pt}(\text{PPh}_3)_4]$ yielded the difluoride complex $[\text{PtF}_2(\text{PPh}_3)_2]$ ¹⁴ and not the HF addition product. Both formulations were mainly reliant on elemental analysis and infrared spectroscopy. For the former compound a weak band at 2240 cm^{-1} in the infrared spectrum has been attributed to a Pt-H vibration.

Further investigations by Kemmitt *et al.*¹⁵ on the action of hydrogen fluoride on $[\text{Pt}(\text{PPh}_3)_4]$ and $[\text{Pt}(\text{PMePh}_2)_4]$ enabled them to reformulate the product as the monofluorinated cation $[\text{PtF}(\text{PPh}_3)_3]^+$ and not the neutral difluoride complex. However, the formulations of this and the related species reported, $[\text{PtF}(\text{PMePh}_2)_3]^+$, were reliant on analytical data and conductance measurements. The first direct evidence for the existence, in these complexes, of a platinum-fluoride bond came from NMR studies, particularly ^{19}F NMR spectroscopy (Table 3.2), reported in 1972, by Dixon *et al.*¹⁶

Table 3.2 ^{19}F NMR Data for Complexes $[\text{PtFL}_3][\text{BF}_4]$

Complex	$\delta(^{19}\text{F})/\text{ppm}^{\text{a}}$	$^1J(\text{Pt-F})/\text{Hz}$	$^2J(\text{FP})/\text{Hz}$	
			<i>trans</i>	<i>cis</i>
$[\text{PtF}(\text{PPh}_3)_3][\text{BF}_4]^{16}$	-232	66	139	39
$[\text{PtF}(\text{PMePh}_2)_3][\text{BF}_4]^{17}$	-257	230	150	34

(a) relative to CFCl_3

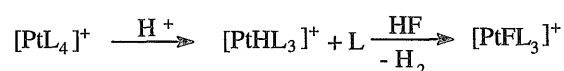
The $^1J_{\text{PtF}}$ coupling in $[\text{PtF}(\text{PPh}_3)_3][\text{BF}_4]$ is only 66 Hz, which is even smaller than the values for the other platinum(II) fluoro-complexes $[\text{PtF}(\text{PMePh}_2)_3][\text{BF}_4]$ and $[\text{PtF}(\text{PEt}_3)_3][\text{BF}_4]$ of 230 Hz (Table 3.2) and 250 Hz (section 3.1.5) respectively. According to the authors, Dixon *et al.*,¹⁷ this small value is indicative of an unusually weak Pt-F bond, a view which is supported by the facile decomposition, discussed in section 3.11, and reduced *trans* influence of fluoride in this complex. Dixon and co-workers speculated that the effect was most likely to be steric in origin, with the bulky PPh_3 groups causing a distortion of the coordination geometry around platinum, either towards a lengthening of the Pt-F bond or possibly towards a tetrahedral geometry. Mather and co-workers¹⁸ proposed that a simple relation exists between coupling constants and bond lengths in platinum phosphine complexes. However, structural data for platinum fluoride phosphine complexes are limited to only two reported examples, *cis*- $[\text{PtF}\{\text{CH}(\text{CF}_3)_2\}(\text{PPh}_3)_2]^{19}$ (Figure 3.1) and $[\text{PtF}(\text{PEt}_3)_3][\text{BF}_4]^{20}$ (section 3.1.5), in the literature. Furthermore, for the former the $^1J_{\text{PtF}}$ coupling constant has not been reported thus, any comparisons between bond lengths and coupling constants cannot be made in this area. In section 3.10 the first structural data on the complex $[\text{PtF}(\text{PPh}_3)_3][\text{SbF}_6]$ is reported, obtained by

EXAFS spectroscopy, thus allowing the first comparisons between bond lengths and coupling constants to be made.

The formation of $[\text{PtF}(\text{PPh}_3)_3]^+$ contrasts strongly with the reported¹⁰ reactions of HCl with $[\text{Pt}(\text{PPh}_3)_4]$ to form the hydride species $[\text{PtH}(\text{PPh}_3)_3]^+$ in ethanol and *trans*- $[\text{PtHCl}(\text{PPh}_3)_2]$ in benzene. Thus, the reaction of $[\text{PtL}_4]$ with AHF was adjudged to proceed *via* initial protonation (Scheme 3.3) which is analogous to that reported previously for the other protic acids HX.

According to Dixon and McFarland¹⁷ the monofluorinated cation could then be formed either by attack of protons on the coordinated hydride or by an oxidative-addition-reductive-elimination mechanism. Precedents are available for both processes in the reactions of *trans*- $[\text{PtHCl}(\text{PEt}_3)_2]$ with HBF_4 ²¹ or HCl.²² The former reacts affording the dimeric complex $[\text{Pt}_2(\mu\text{-Cl})_2(\text{PEt}_3)_4][\text{BF}_4]$ and eliminating H_2 gas. The latter oxidatively adds HCl to afford the platinum(IV) complex $[\text{PtH}_2\text{Cl}_2(\text{PEt}_3)_2]$, which has been identified by infrared and Raman spectroscopies, before irreversibly evolving H_2 to yield $[\text{PtCl}_2(\text{PEt}_3)_2]$. In the latter process HCl was used stoichiometrically, whereas AHF was used in excess and this, accompanied by its highly acidic nature, favoured the conversion of $[\text{PtHL}_3]^+$ into $[\text{PtFL}_3]^+$ by either mechanism.

Scheme 3.3

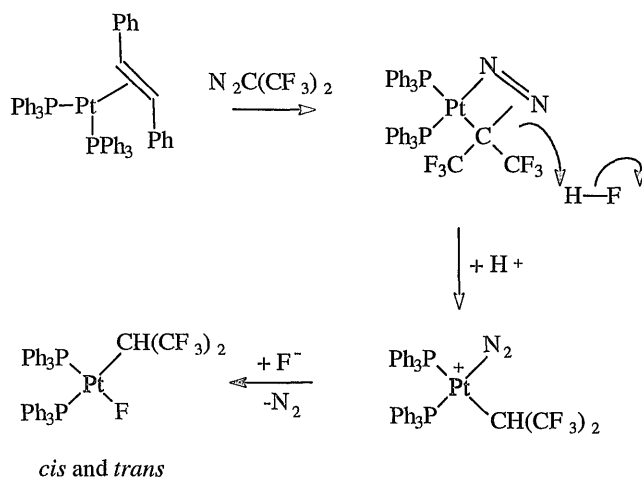


An alternative route for the oxidative introduction of fluoride into Pt(0) complexes has been reported for $[\text{Pt}(\text{PhCH}=\text{CHPh})(\text{PPh}_3)_2]$ which is

reported to react with (A) $[\text{N}_2\text{C}(\text{CF}_3)_2]$ and (B) 1,1,2-trichloro-3,3,3-trifluoropropene:-

(A) The reaction of $[\text{Pt}(\text{PhCH=CHPh})(\text{PPh}_3)_2]$ and $[\text{N}_2\text{C}(\text{CF}_3)_2]$, in the presence of a trace amount of HF, affords *cis*- and *trans*- $[\text{PtF}\{\text{CH}(\text{CF}_3)_2\}(\text{PPh}_3)_2]$ (Scheme 3.4).²³

Scheme 3.4



The reaction between $[\text{Pt}(\text{PhCH=CHPh})(\text{PPh}_3)_2]$ and $[\text{N}_2\text{C}(\text{CF}_3)_2]$, in diethyl ether, affords, *via* the addition of a second molecule of $[\text{N}_2\text{C}(\text{CF}_3)_2]$, the perfluoro-acetone azine complex $[\text{Pt}\{\text{C}(\text{CF}_3)_2\text{N=N=C}(\text{CF}_3)_2\}(\text{PPh}_3)_2]$. However, the authors propose that the reaction between the initial adduct with $[\text{N}_2\text{C}(\text{CF}_3)_2]$ and trace amounts of HF yields, over a period of days, small amounts of the two isomeric monofluoride complexes shown in Scheme 3.4.

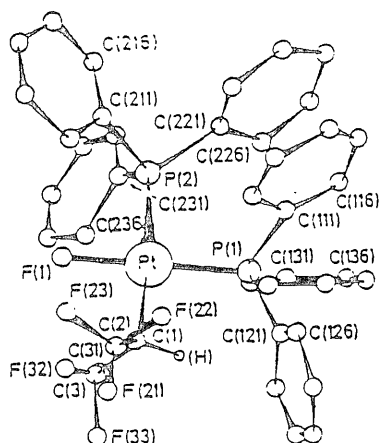
The ^{19}F NMR spectrum, recorded in CH_2Cl_2 , of the *trans* isomer showed only a quartet resonance at 50.8 ppm due to the coupling of the fluorine nuclei of the CF_3 group to the proton of the $\text{CH}(\text{CF}_3)_2$ and the two phosphine ligands. For the *cis* isomer a triplet resonance at 50.1 ppm was observed with both signals for the *trans* and *cis* isomers exhibiting platinum satellites. The multiplicity of the signals observed are not as expected, *i.e.* a doublet of triplets and a doublet of doublets of doublets (excluding coupling to the terminal fluoride) for the *cis* and *trans* isomers respectively. The correct multiplicities were probably not observed due to the magnitude of the coupling constants resulting in the overlap of resonances. The absence of the terminal fluoride resonance is a phenomenon which has previously been reported in the complexes $[\text{PtF}(\text{X})(\text{PPh}_3)_2]$ ($\text{X} = \text{Cl}$ or Br),¹⁵ however, there is little evidence for a platinum fluoride bond in these species (see section 3.1.5). The authors did not report any $^{31}\text{P}\{^1\text{H}\}$ and/or ^{195}Pt NMR data which might have shown phosphorus or platinum coupling to the terminal fluoride. Furthermore, the ^{19}F NMR spectrum was recorded in CH_2Cl_2 which has been reported to react with platinum fluoride complexes, *via* fluorine / chlorine exchange, to afford the analogous chloro-species (see section 3.11), and therefore, this would explain the absence of a terminal fluoride resonance. The existence of this fluoro-complex was formed as it was structurally characterized by a single crystal X-ray diffraction study (Figure 3.1)¹⁹ and therefore, it is plausible that the authors were not looking in the region characteristic of fluorine bound to platinum. However, it is feasible that the fluoride is, in fact, a hydroxyl group obtained from any moisture present in the solvent. Single crystal X-ray diffraction studies would be unable to distinguish between the two ligands and thus, this could explain the absence of a resonance in the ^{19}F NMR spectrum due to the terminal fluoride. Further evidence to substantiate this is that the ruthenium complex $[\text{CpRuF}(\text{PPh}_3)_2]$,²⁴ reportedly formed from the reaction of the chloride

analogue and a $[\text{NH}_4\text{F}]/[\text{Ag}_2\text{CO}_3]$ mixture in methanol, was found to exhibit no ^{19}F resonance, but more importantly was later re-formulated, by the observation of an $\nu(\text{OH})$ in the infrared spectrum, as the hydroxyl species $[\text{CpRu}(\text{OH})(\text{PPh}_3)_2]$.²⁵

(B) The reaction of $[\text{Pt}(\text{PhCH}=\text{CHPh})(\text{PPh}_3)_2]$ and 1,1,2-trichloro-3,3,3-trifluoropropene yields the platinum(IV) complex $[\text{PtCl}_2\text{F}_2(\text{PPh}_3)_2]$.²⁶

Formulation of the platinum(IV) complex was based solely on elemental analysis and thus doubt is cast on its formulation.

Figure 3.1 Crystal Structure of *cis*- $[\text{PtF}\{\text{CH}(\text{CF}_3)_2\}(\text{PPh}_3)]$

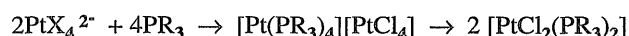


3.1.4 Platinum(II) Phosphine Complexes

Platinum(II) is a d^8 metal centre and platinum(II) complexes are almost always 16-electron and square planar, although rare five-coordinate complexes have been reported. This is the most stable oxidation state for platinum, and tertiary phosphines form a wide range of compounds of the type $[\text{PtX}_2(\text{PR}_3)_2]$ (X = halide or pseudohalide; R = alkyl, aryl or mixed alkylaryl). These complexes have been extensively studied, and consequently there is a vast literature available. Therefore, for each individual complex, the reader is directed to 'GMELINS Handbuch Der Anorganischen Chemie'²⁷ and 'Transition Metal Complexes of Phosphorus, Arsenic and Antimony'.²⁸ As a consequence of the strong coupling between the phosphorus ligand and the platinum nucleus analysis by ^{31}P and ^{195}Pt NMR spectroscopy enables, in most cases, definitive characterization of the platinum phosphine complexes.

Tertiary phosphines PR_3 react with the anionic $[\text{PtX}_4]^{2-}$ to give species of the type $[\text{PtX}_2(\text{PR}_3)_2]$ (Scheme 3.5).^{1,29} Both *cis*- and *trans*- isomers are formed which can usually be isolated *via* separation by fractional crystallization.²⁹ When R is a lower alkyl group *e.g.* PMe_3 and PEt_3 , the initially formed ionic complex, $[\text{Pt}(\text{PR}_3)_4]^{2+}$, is only slowly converted to the final product.³⁰ Thus, a more convenient method for the preparation of Pt(II) complexes of these ligands involves the reaction of *cis*- $[\text{PtCl}_2(\text{MeCN})_2]$ and two molar equivalents of the phosphine.

Scheme 3.5



Cationic complexes of the type $[\text{Pt}(\text{PR}_3)_4]^{2+}$ ($\text{PR}_3 = \text{PMe}_3$ and PEt_3)³¹ can be isolated by the addition of $[\text{KPF}_6]$ to a solution of $[\text{Pt}(\text{PR}_3)_4][\text{PtCl}_4]$

and excess PR_3 . The complex cation $[\text{Pt}(\text{PEt}_3)_4]^{2+}$ has also been reported to be formed from the reaction of *cis*- $[\text{PtCl}_2(\text{PEt}_3)_2]$ and a twofold molar equivalent of $[\text{AgClO}_4]$ in the presence of an excess of PEt_3 .³²

Another important class of platinum(II) compounds is the dinuclear halide bridging species $[(\text{PR}_3)\text{XPt}(\mu\text{-X})_2\text{PtX}(\text{PR}_3)]$, which are made from $[\text{PtX}_2(\text{PR}_3)]$ and $[\text{PtX}_2]$ ($\text{X} = \text{Cl}, \text{Br}$ and I , $\text{PR}_3 = \text{phosphine}$). The strength of the bridge bond increases in the series $\text{Cl} < \text{Br} < \text{I}$ and $\text{Cl} < \text{Et}_2\text{PO} < \text{RS} < \text{R}_2\text{P}$. The weaker bridges can be broken by phosphine ligands, PR'_3 , to give a variety of monomeric mixed phosphine complexes of platinum(II).³³⁻⁴⁰

The addition of phosphine ligands, at low temperatures, to complexes of the type $[\text{Pt}_2(\mu\text{-Cl})_2\text{Cl}_2(\text{PR}_3)_2]$ affords the ionic species $[\text{PtCl}(\text{PR}_3)_3]^+$ and $[\text{PtCl}_3(\text{PR}_3)]^-$ as the major products rather than the covalent complex $[\text{PtCl}_2(\text{PR}_3)_2]$.

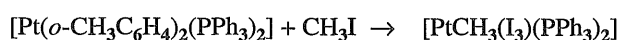
Reactions of platinum(II) phosphine complexes usually centre around halide or pseudohalide substitution. The phosphine ligands bind strongly to Pt(II) and are not readily substituted. One of the most important class of complexes that can be formed by substitution are the platinum(II) alkyls and aryls. These can be prepared by a variety of synthetic methods. The exchange of a halide ligand by an organic group is most easily accomplished using organolithium or Grignard reagents. Once formed, these Pt(II) alkyl and aryl complexes can undergo reactions to give compounds that would be difficult to synthesize by other methods. For example, compounds of the type *trans*- $[\text{PtCl}(\text{R}')(\text{PR}_3)_2]$, where R' is a methyl or an aryl, react with $[\text{NaBH}_4]$ to give the corresponding hydride complexes, *trans*- $[\text{PtH}(\text{R}')(\text{PR}_3)_2]$, through displacement of the chloride ligand.⁴¹ Alternatively, the mono-alkyl and -aryl complexes $[\text{PtX}(\text{R}')(\text{PR}_3)_2]$ can be converted into other complexes by the metathetical replacement of X . The chloride can be readily converted into the analogous bromo- or iodo-complex by an excess of lithium bromide or

sodium iodide in acetone.⁴² These reactions are greatly facilitated by the large *trans*-effect of the organic group.

Reactions at the platinum-carbon σ bond have also been extensively studied.⁴³ These reactions or chemical properties can be categorized as follows:-

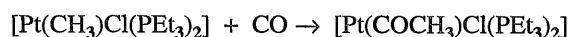
(a) Replacement reactions, whereby the organic moiety is replaced by another ligand. In the complex $[\text{Pt}(o\text{-CH}_3\text{C}_6\text{H}_4)_2(\text{PPh}_3)_2]$ the *o*-tolyl groups can be displaced by methyl groups (Scheme 3.6).⁴⁴

Scheme 3.6



(b) Insertion reactions, in which a reagent is 'inserted' into the platinum-carbon bond. Alkyl and aryl complexes of platinum(II) are converted to acyl species by treatment with carbon monoxide (Scheme 3.7).⁴⁵

Scheme 3.7

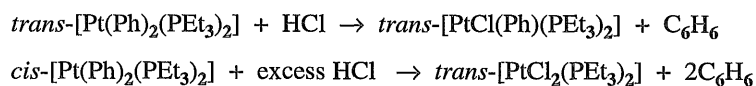


(c) Cleavage reactions, in which the platinum-carbon bond is broken. Three general methods have been outlined in the literature.

(i) Reaction with acids and protonic solvents

Although, Pt(II) complexes are not hydrolysed by water or dilute aqueous acids, they are attacked by HCl in ethanol or benzene solution (Scheme 3.8).⁴⁶

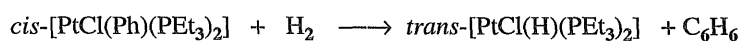
Scheme 3.8



(ii) Reaction with hydrogen

Platinum(II)-carbon bonds are readily cleaved by molecular H_2
(Scheme 3.9).⁴⁷

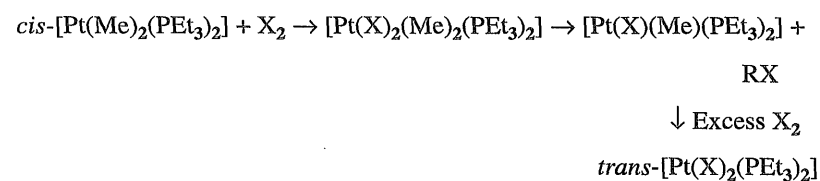
Scheme 3.9



(iii) Reaction with halogens

Cleavage of the platinum-carbon bond by halogens goes *via* the intermediate $[\text{Pt}(\text{X})_2(\text{R})_2(\text{PEt}_3)_2]$ ($\text{X} = \text{Cl}, \text{Br}, \text{I}$; $\text{R} = \text{alkyl, aryl}$). Isolation of this intermediate is possible when $\text{X} = \text{Cl}$ and $\text{R} = \text{Me}$, but when $\text{X} = \text{I}$ the intermediate, being unstable, decomposes to the platinum(II) derivative (Scheme 3.10).⁴⁸

Scheme 3.10



3.1.5 Platinum(II) Fluoride Phosphine Complexes

Zerovalent platinum phosphine complexes are reported to undergo oxidative addition with fluorine containing reagents to afford platinum(II) fluoride phosphine compounds.

Halide metathesis is well established as a convenient route to chloro-, bromo- and iodo-complexes of the type, $[\text{PtX}_2(\text{PR}_3)_2]$, $[\text{PtX}(\text{PR}_3)_3]^+$ and $[\text{PtX}(\text{R})(\text{PR}_3)_2]$ (R = alkyl, aryl and alkylaryl). The analogous fluoro-complexes, in comparison, are relatively unexplored. However, there are few reports in the literature of platinum(II) fluoride phosphine complexes prepared *via* metathetical reactions with either AHF or AgF (Table 3.3).

Table 3.3 Platinum(II) Fluoride Phosphine Complexes Prepared by Halide Metathesis

Product	Reagents	Refs.
<i>cis</i> - $[\text{PtClF}(\text{PPh}_3)_2]$	$[\text{PtCl}(\text{X})(\text{PPh}_3)_2] + \text{AHF}$ (X = Cl, H)	15
<i>cis</i> - $[\text{PtBrF}(\text{PPh}_3)_2]$	<i>cis</i> - $[\text{PtBr}_2(\text{PPh}_3)_2] + \text{AHF}$	15
$[\text{PtF}(\text{PR}_3)_3][\text{BF}_4]$	$[\text{PtCl}(\text{PR}_3)_3][\text{BF}_4] + [\text{AgF}]$ ($\text{PR}_3 = \text{PEt}_3, \text{PMe}_2\text{Ph}, \text{PPh}_3$)	17
<i>trans</i> - $[\text{PtF}(\text{R})(\text{PEt}_3)_2]$	<i>trans</i> - $[\text{PtCl}(\text{R})(\text{PEt}_3)_2] + [\text{AgF}]$ (R = Me, Ph)	49,50

As stated in chapter 1, problems are often encountered when AgF is used as a metathetical reagent. However, if conditions are optimized, then halide metathesis with AgF is a convenient route to platinum fluoride

phosphine complexes. The monofluorinated cations of the type, $[\text{PtFL}_3][\text{BF}_4]$ and the previously discussed $[\text{PtFL}_3][\text{HF}_2]$ provide the most conclusive evidence for a platinum fluoride bond from ^{19}F and $^{31}\text{P}\{^1\text{H}\}$ NMR spectroscopy. The ^{19}F NMR spectrum of $[\text{PtF}(\text{PEt}_3)_3]^+$ showed a doublet of triplets, due to the coupling of the fluoride to the *trans*- and the two *cis*-phosphine ligands, at δ -252 ppm. The associated platinum satellites were observed with a $^1J_{\text{PtF}} = 250$ Hz, the *trans* $^2J_{\text{FP}}$ coupling was 140 and the *cis* $^2J_{\text{FP}}$ was 32 Hz. This complex was also structurally characterized, by Russell *et al.*,²⁰ which confirmed the presence of the platinum-fluoride bond. The platinum-fluoride bond length, 2.043 Å, compares well with the only other reported Pt-F bond, for the complex $[\text{PtF}\{\text{CH}(\text{CF}_3)_2\}(\text{PPh}_3)_2]$,¹⁹ of 2.03 Å. Furthermore, in both cases the Pt-P bond lengths, *trans* to F, are significantly shorter (≈ 0.1 Å) than the remaining platinum phosphorus bonds.

The neutral mixed halo-complexes were characterized by infrared spectroscopy, conductivity measurements and elemental analysis. An infrared band at 302 cm^{-1} in *cis*- $[\text{PtClF}(\text{PPh}_3)_2]$ was attributed to a $\nu(\text{Pt-Cl})$ but no direct evidence for a platinum-fluoride bond was reported. This aside, the authors reported¹⁷ that it was possible that the reaction could involve oxidative addition of HF to the platinum complex followed by elimination of HCl from the platinum(IV) intermediate. The insolubility of HCl in liquid hydrogen fluoride⁵¹ would provide a driving force for this elimination. It was also suggested that AHF reacted with *trans*- $[\text{PtClH}(\text{PPh}_3)_2]$, via a platinum(IV) intermediate, to afford the same complex *cis*- $[\text{PtClF}(\text{PPh}_3)_2]$.⁵² The mono-alkyl and -aryl complexes $[\text{PtX}(\text{R}')(\text{PR}_3)_2]$ have been shown to undergo halide metathesis of chloride, for bromide and iodide (see section 3.1.4). Although, the fluoro-analogues are described when $\text{R}' = \text{Me}$ ⁴⁹ and Ph ,⁵⁰ there is no conclusive evidence for a platinum-fluoride bond.

The platinum fluoride phosphine complex, $[\text{PtClF}(\text{PEt}_3)_2]$,⁵³ has also been reported to be the product from the reaction of *trans*- $[\text{PtClH}(\text{PEt}_3)_2]$

with trifluoroethylene presumably *via* insertion into the Pt-H and then subsequent β -F elimination. No other examples of β -F elimination have been described, and since characterization was based solely on infrared spectroscopy, there is also little evidence to support this formulation.

3.1.6 Platinum(IV) Phosphine Complexes

Platinum(IV) phosphine complexes are less common than platinum(0) and platinum(II) species. Platinum(IV) phosphine complexes are conveniently prepared by the halogenation of the platinum(II) compound.⁵⁴ This route can be employed to synthesize $[\text{PtCl}_4(\text{PPr}_3)_2]$ from $[\text{PtCl}_2(\text{PPr}_3)_2]$.⁵⁵ Similarly, *trans*- $[\text{PtX}_4(\text{PEt}_3)_2]$ (X = Cl, Br, I), *cis*- $[\text{PtX}_4(\text{PEt}_3)_2]$ (X = Cl, Br) *cis*- $[\text{PtCl}_4(\text{PPhMe}_2)_2]$ and *cis*- and *trans*- $[\text{PtCl}_4(\text{PBu}_3)_2]$ can be prepared.

3.1.7 Platinum(IV) Fluoride Phosphine Complexes

In marked contrast to the platinum(II) fluoride phosphine complexes the analogous platinum(IV) compounds are limited to the poorly characterized $[\text{PtF}_2\text{Cl}_2(\text{PPh}_3)_2]$. Two routes to this complex are reported in the literature:-

(i) The previously discussed reaction of 1,1,2-trichloro-3,3,3-trifluoropropene with $[\text{Pt}(\text{PPh}_3)_4]$.²⁶

(ii) The decomposition of the platinum(II) complex, $[\text{PtCl}(\text{SF}_5)(\text{PPh}_3)_2]$, in dichloromethane or acetone.⁵² However, the formulation of the complex $[\text{PtCl}(\text{SF}_5)(\text{PPh}_3)_2]$ is itself open to debate since a recent report, by Ebsworth *et al.*,⁵⁶ found that *trans*- $[\text{MX}(\text{CO})(\text{PEt}_3)_2]$ (M = Rh, Ir) reacted with SF_5Cl in two different ways: firstly, the metal centre

extracted CIF from SF₅Cl and secondly, the compound was reported to react with the SF₄ fragment.

These platinum(IV) compounds and the ruthenium(II) complexes of the type [RuFCpL₂] (see section 3.1.3),²⁴ are the only examples of d⁶ metal fluorides containing phosphine, arsine or stibine ligands which do not contain any other strong π -acceptor ligands. Analysis by infrared spectroscopy and elemental analysis led to the formulation of these complexes. ¹⁹F NMR spectra were not recorded for the Pt(IV) complexes, and for the more recently reported complex, [RuFCpL₂], no fluoride could be detected in NMR experiments.⁵⁷

3.1.8 Summary

The majority of claimed platinum fluoride phosphine complexes have been synthesized either by oxidative addition of a fluorinating agent to a zerovalent platinum complex or by halide metathesis. These are well established as convenient routes to complexes containing the heavier halogens. However, there are instances where the methods employed to synthesize chloro, bromo and iodo complexes have not been applied in an attempt to prepare the analogous fluoro-derivatives. Thus, reactions at the platinum-carbon σ bond (as discussed in section 3.1.5), which have been shown to cleave in the presence of a protic acid (HCl) or X₂ (X = Cl or I) affording the disubstituted halide complex, were envisaged as a route into platinum fluoride phosphine complexes.

As discussed in the previous sections, many of these platinum fluoride phosphine complexes are poorly characterized with no conclusive evidence for a platinum-fluoride bond. It is also evident, that, on several occasions a terminal fluoride was formed accidentally. Thus, the work in the following chapter is concerned with a reinvestigation of some of the previously

reported systems in an attempt to elucidate the reaction products and the attempted preparation of difluoro-complexes of the type $[\text{PtF}_2(\text{PR}_3)_2]$ (R = alkyl, aryl or alkylaryl) by a variety of routes.

3.2 Reaction of *cis*- $[\text{PtMe}_2(\text{PEt}_3)_2]$ with AHF

As discussed previously platinum-carbon bonds are readily cleaved by HCl affording the mono- or dichloro-species thus, the reaction of *cis*- $[\text{PtMe}_2(\text{PEt}_3)_2]$ with AHF was anticipated to yield the difluoro-complex *cis*- $[\text{PtF}_2(\text{PEt}_3)_2]$.

White *cis*- $[\text{PtMe}_2(\text{PEt}_3)_2]$ was allowed to react with an excess of AHF, as described in section 6.15, affording a brown solution and evolving a gas (gas-phase infrared spectroscopy identified the gas as methane). The solution was then analysed by multinuclear NMR spectroscopy.

The room temperature ^{19}F NMR spectrum showed only a very intense broad singlet, at δ -180, which was attributed to the AHF solvent. All attempts to resolve any resonances characteristic of fluorine bound to platinum (δ -200 to -300) were unsuccessful.

The room temperature $^3\text{P}\{^1\text{H}\}$ NMR spectrum (Figure 3.2) revealed the following signals, each with platinum satellites a major singlet at δ 17.0, $^1J_{\text{PtP}} = 3942$ Hz; a minor singlet δ 15.2, $^1J_{\text{PtP}} = 3757$ Hz and a doublet at δ 24.5, $^1J_{\text{PtP}} = 3722$ Hz, *cis* $^2J_{\text{PP}} = 22$ Hz.

Figure 3.2 The Room Temperature $^{31}\text{P}\{^1\text{H}\}$ NMR Spectrum of the Products from the Reaction of *cis*-[PtMe₂(PEt₃)₂] and AHF

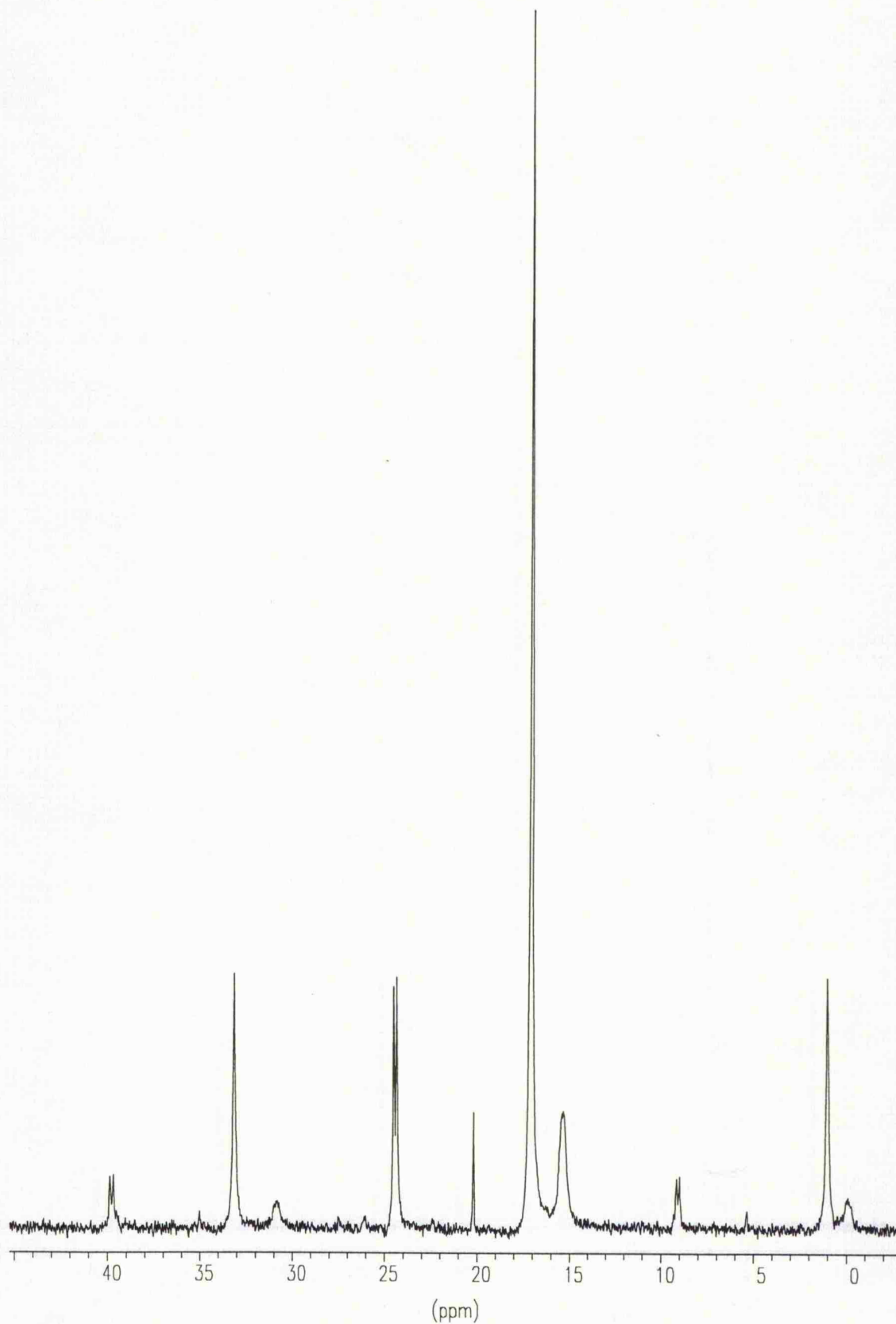
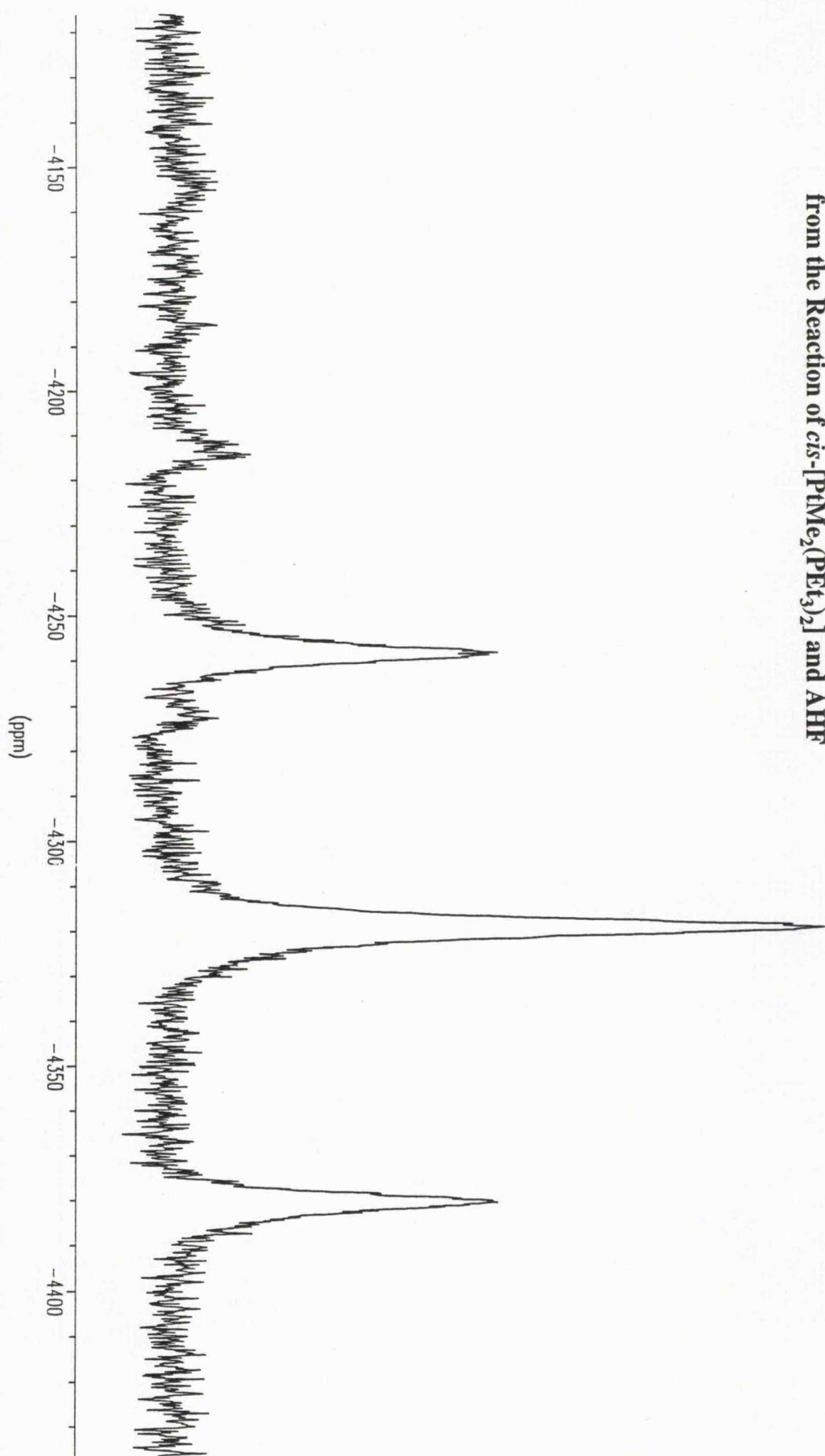


Figure 3.3 The Room Temperature $^{195}\text{Pt}\{^1\text{H}\}$ NMR Spectrum of the Products
from the Reaction of *cis*- $[\text{PtMe}_2(\text{PEt}_3)_2]$ and AHF



The corresponding ^{195}Pt NMR at 298 K (Figure 3.3) exhibited a major triplet at δ -4320, $^1J_{\text{PtP}} = 3941$ Hz and also, evidence for a second resonance at δ -4210 but, no coupling could be resolved.

Although, there is no apparent fluorine coupling to either phosphorus or platinum, both the ^{31}P and the ^{195}Pt NMR spectra revealed resonances that are shifted markedly from that of *cis*-[PtMe₂(PEt₃)₂] and *cis*-[PtCl₂(PEt₃)₂] (Table 3.4). Furthermore, the $^1J_{\text{PtP}}$ couplings are significantly larger than that observed in *cis*-[PtCl₂(PEt₃)₂].

Table 3.4 A Comparison of the $^{31}\text{P}\{^1\text{H}\}$ and $^{195}\text{Pt}\{^1\text{H}\}$ NMR Data at Room Temperature of the Products from the Reaction of *cis*-[PtMe₂(PEt₃)₂] and AHF, with *cis*-[PtMe₂(PEt₃)₂] and *cis*-[PtCl₂(PEt₃)₂]

	$\delta(^{31}\text{P})/\text{ppm}$	$\delta(^{195}\text{Pt})/\text{ppm}$	$^1J(\text{PtP})/\text{Hz}$
Reaction Products	17.0	-4320	3942
	15.2	-4210	-
<i>cis</i> -[PtMe ₂ (PEt ₃) ₂] ⁵⁸	9.0	-4653	1855
<i>cis</i> -[PtCl ₂ (PEt ₃) ₂] ⁵⁹	8.4	-4490	3507

The $^1J_{\text{PtP}}$ coupling is largely dependent on the "trans-influence"^{60, 61} of the ligands *trans* to the phosphine in the square planar Pt(II) complex as discussed in section 2.6. It is evident from the data presented in Table 3.4 that the "NMR *trans*-influence" of the methyl group is higher than that of chlorine thus, the $^1J_{\text{PtP}}$ coupling is lower in the dimethyl complex. If we consider the limited *trans*-influence series, reported by Anderson and Cross,⁶² which follows the order alkyl, aryl > PR₃ > AsPh₃ > CO > Cl⁻ and assuming that fluoride would come after chloride, it is plausible to suggest that the $^1J_{\text{PtP}}$ coupling in any difluoro-complex would be larger than that in

the analogous *cis*-dichloro-complex. However, in the cationic complexes $[\text{PtX}(\text{PR}_3)_3]^+$ ($\text{X} = \text{Cl}, \text{F}$ and $\text{PR}_3 = \text{PEt}_3, \text{PPh}_3$) the $^1J_{\text{PtP}}$, for the phosphine ligand *trans* to X, does not necessarily increase with substitution of chlorine for fluorine (Table 3.5).

Table 3.5 A Comparison of the $^1J_{\text{PtP}}$, for PR_3 *trans* to X, in the Complexes $[\text{PtX}(\text{PR}_3)_3]^+$

X	$^1J(\text{PtP})/\text{Hz}^{17}$	
	PEt_3	PPh_3
Cl	3474	3643
F	3455	3696

Furthermore, Ebsworth and Rankin⁵⁹ reported that generally the recorded δ (^{31}P) are shifted to higher frequencies by substitution of lighter for heavier halogens (Table 3.6).

It is also apparent from Table 3.6 that substituting heavier for lighter halogens results in an increase in the $^1J_{\text{PtP}}$ coupling and that the observed coupling for the products, formed from the reaction discussed in section 3.2, are not typical of P *trans* P, thus indicating that this reaction has proceeded with retention of the *cis* arrangement of phosphine ligands.

Finally, on comparing the ^{195}Pt NMR chemical shifts for a series of platinum complexes with different halide ligands; a shift to lower frequency is observed when descending the group *cf.* *trans*- $[\text{PtX}_2(\text{PMe}_3)_2]$ for $\text{X} = \text{Cl}, \text{Br}$ and I the $\delta(^{195}\text{Pt}) = -3950, -4473$ and -5539 respectively.⁵⁹

Table 3.6 $^{31}\text{P}\{^1\text{H}\}$ NMR Data for Various Platinum Phosphine Complexes

Complex	$\delta(^{31}\text{P})/\text{ppm}$	$^1J(\text{PtP})/\text{Hz}$	Refs.
<i>trans</i> -[PtCl ₂ (PEt ₃) ₂]	12.3	2457	59
<i>trans</i> -[PtBr ₂ (PEt ₃) ₂]	7.6	2368	59
<i>trans</i> -[PtI ₂ (PEt ₃) ₂]	0.2	2272	59
<i>cis</i> -[PtCl ₂ (PMe ₂ Ph) ₂]	-16.2	3548	58
<i>cis</i> -[PtBr ₂ (PMe ₂ Ph) ₂]	-16.1	3515	58
<i>cis</i> -[PtI ₂ (PMe ₂ Ph) ₂]	-18.2	3364	58
<i>trans</i> -[PtMeCl(PEt ₃) ₂]	15.4	2814	63
<i>trans</i> -[PtMeI(PEt ₃) ₂]	10.5	2728	63

The shift to higher frequency in both the $^{31}\text{P}\{^1\text{H}\}$ and $^{195}\text{Pt}\{^1\text{H}\}$ NMR and the increase in the $^1J_{\text{PtP}}$ coupling when compared to the analogous *cis*-[PtCl₂(PEt₃)₂] would suggest coordination of fluorine to platinum and the generation of *cis*-[PtF₂(PEt₃)₂].

However, in order to verify this assignment the fluorine coupling to phosphorus and platinum had to be resolved. It was plausible that the absence of any fluorine coupling was a result of a fluxional process between coordinated fluoride and 'free' fluoride in AHF. Therefore, low-temperature NMR studies were undertaken in an attempt to resolve any evidence for fluorine coordination.

The low-temperature $^{195}\text{Pt}\{^1\text{H}\}$ NMR spectra (Figure 3.4) resolved the minor resonance into a triplet of doublets, at -20°C, and the major triplet resonance into a triplet of triplets at -60°C. All the $^{195}\text{Pt}\{^1\text{H}\}$ NMR are presented in Table 3.7.

Table 3.7 $^{195}\text{Pt}\{^1\text{H}\}$ NMR Data, Recorded at -60°C , for the Reaction Products

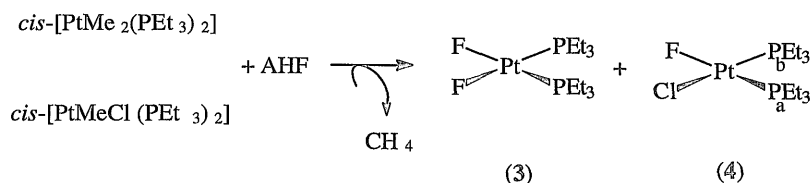
Complex	$\delta(^{195}\text{Pt})/\text{ppm}$	$^1J(\text{PtP})/\text{Hz}$	$^1J(\text{PtF})/\text{Hz}$
(3)	-4367 (tt)	3870 (3942)	600
(4)	-4252 (td)	3724 (3722)	550

multiplicity: tt = triplet of triplets, td = triplet of doublets

room temperature $^1J_{\text{PtP}}$ couplings found in parentheses

It is evident from the data, presented in Table 3.7, that the reaction between *cis*-[PtMe₂(PEt₃)₂] and AHF proceeds according to Scheme 3.11.

Scheme 3.11



The triplet of triplets arises from coupling of the platinum nucleus to two equivalent phosphorus and fluorine nuclei and is assigned to complex (3). The triplet of doublets, by analogy, is the result of the platinum nucleus coupling to two apparently equivalent phosphorus and one fluorine nucleus and is attributed to complex (4). The triplet of doublets, assigned to complex (4), is only possible if $J_{\text{PtPb}} \approx J_{\text{PtPa}}$ thus the theoretical doublet of doublets is observed as a triplet. Therefore, the triplet of doublets exhibits two couplings; $^1J_{\text{PtF}} = 550 \text{ Hz}$, which compares well with the difluoro-analogue,

Figure 3.4 Effects of Variable Temperature $^{15}\text{Pt}\{^1\text{H}\}$ on the Resonances
Shown in Figure 3.3

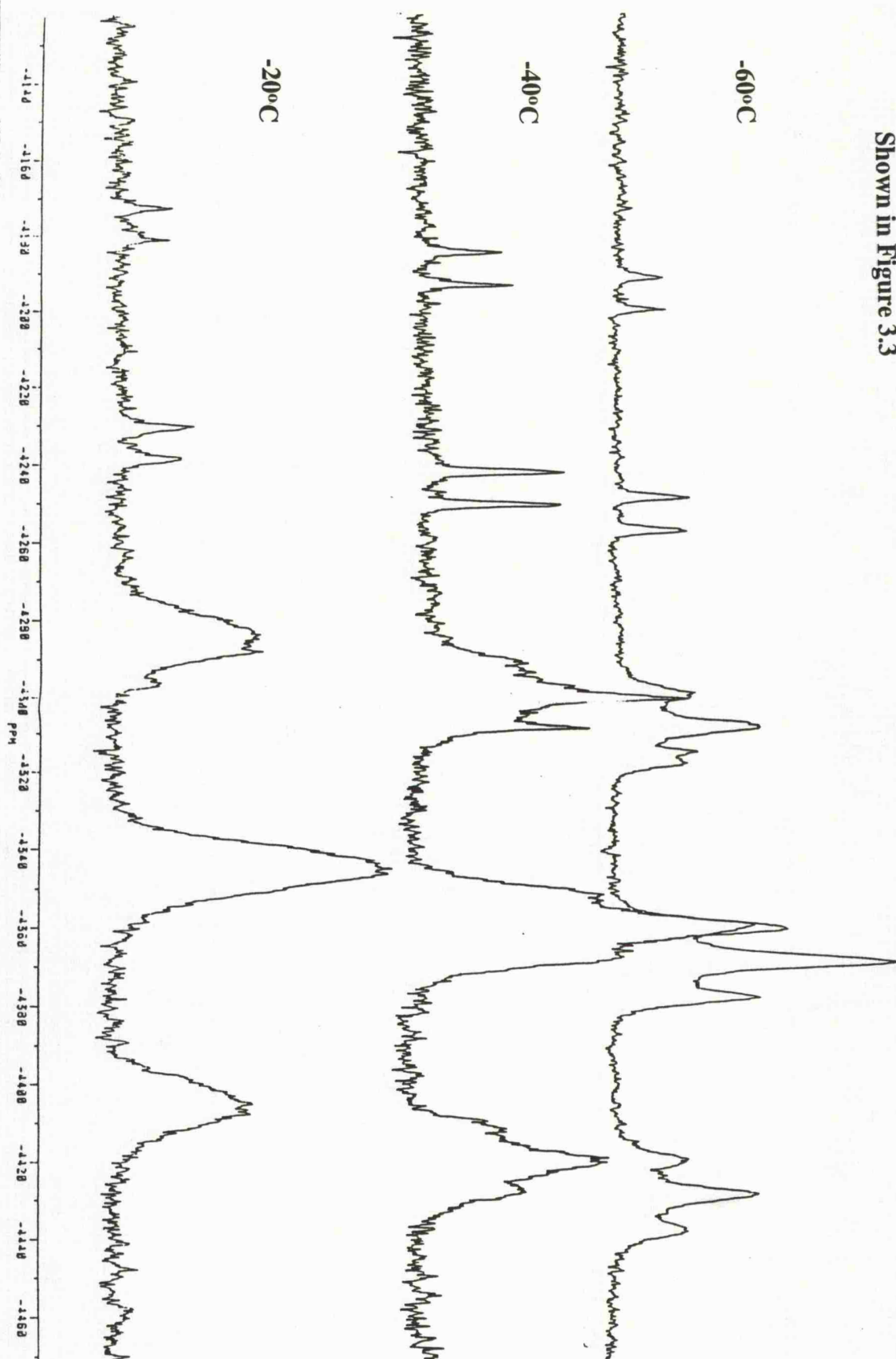


**Figure 3.5 Effects of Variable Temperature $^{31}\text{P}\{^1\text{H}\}$ on the Resonances Shown
in Figure 3.2**

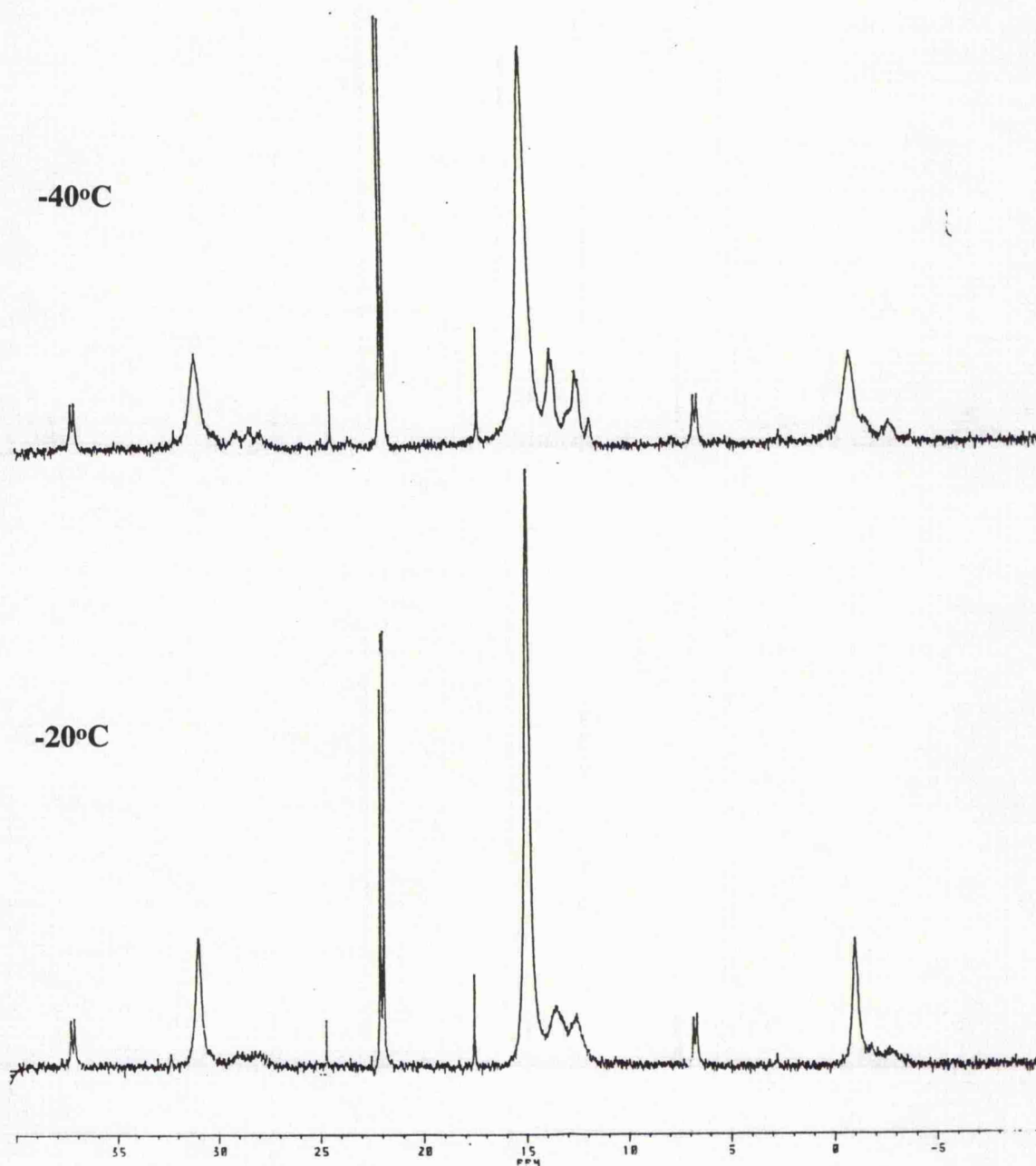
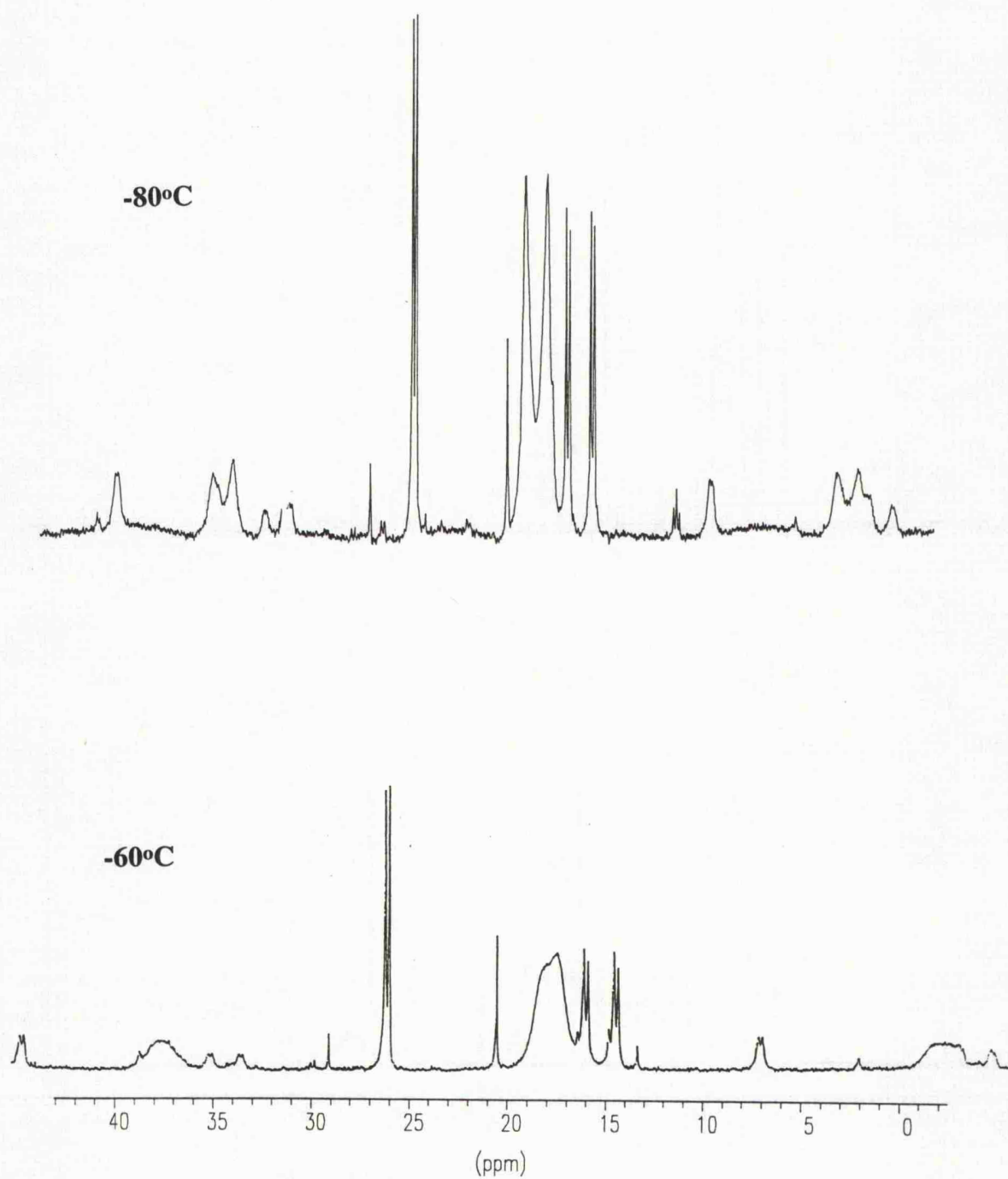


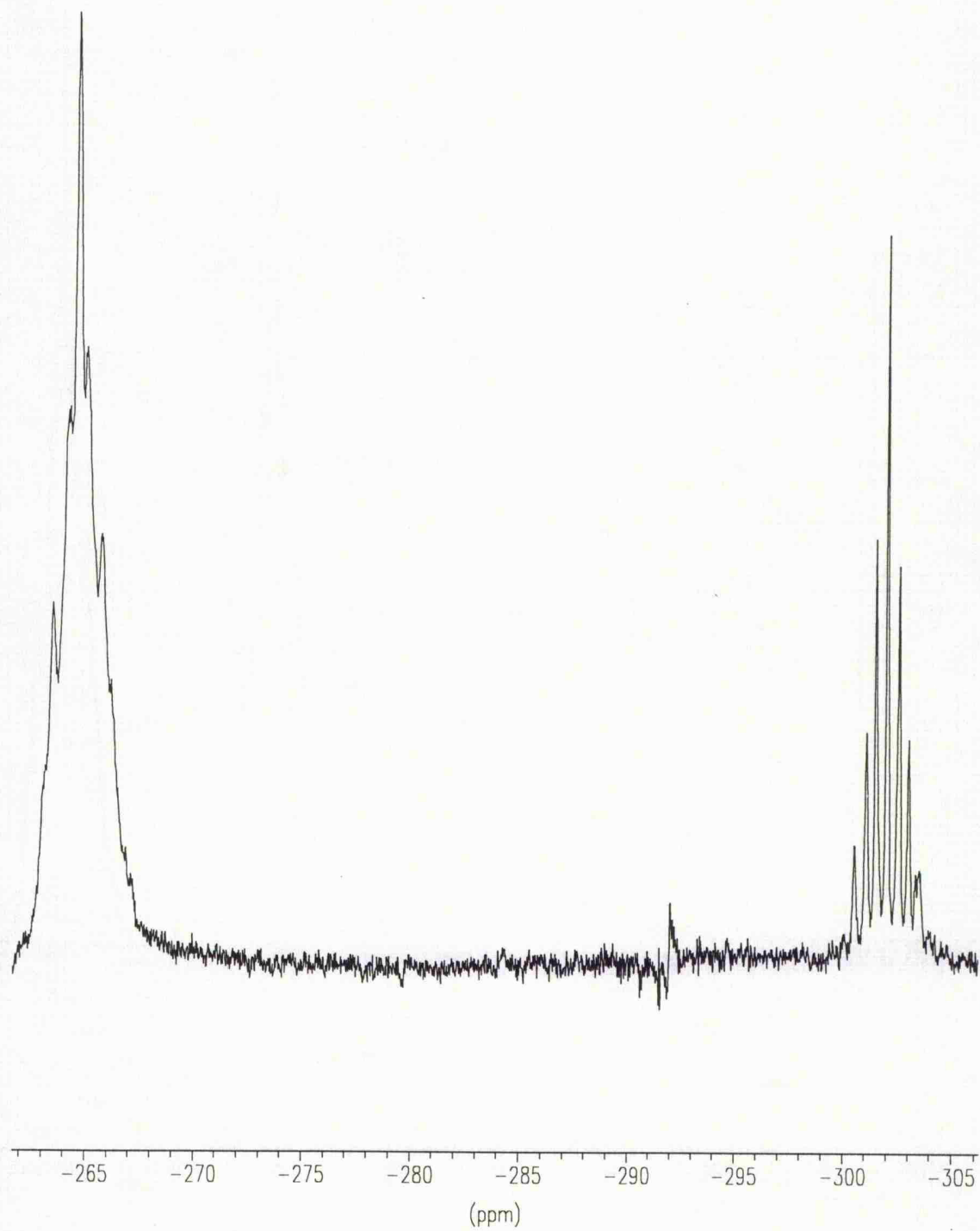
**Figure 3.6 Effects of Variable Temperature $^{31}\text{P}\{^1\text{H}\}$ on the Resonances Shown
in Figure 3.2**



and $^1J_{\text{PtP}} = 3724$ Hz. The remaining coordination site was presumed to be occupied by chlorine and not a methyl group since, the $^1J_{\text{PtP}}$ coupling constant for complex (4) is typical of a halogen *trans* to a phosphine ligand. Although, the dimethyl-complex was checked for purity by $^{31}\text{P}\{^1\text{H}\}$ NMR spectroscopy it is possible that a small amount of the complex *cis*- $[\text{PtMeCl}(\text{PEt}_3)_2]$ was formed, from the reaction between methyllithium and *cis*- $[\text{PtCl}_2(\text{PEt}_3)_2]$ and subsequently reacted with AHF thus, explaining the presence of a chloride ligand.

Low-temperature $^{195}\text{Pt}\{^1\text{H}\}$ NMR experiments showed fluorine coupling to platinum in both complexes (3) and (4) thus low-temperature $^{31}\text{P}\{^1\text{H}\}$ NMR experiments were undertaken to observe phosphorus coupling to fluorine. At -20°C the singlet at δ 15.5 broadened and collapsed and at -40°C resolved into a broad doublet (Figure 3.5). Further cooling to -60°C resulted in the broad doublet being resolved into a doublet of doublets, at δ 15.5 with a; $^1J_{\text{PtP}} = 3744$ Hz, *cis* coupling to P_b , $^2J_{\text{PP}} = 21$ Hz and *trans* coupling to F, $^2J_{\text{PF}} = 155$ Hz, and is assigned to P_a in complex (4). Both of these couplings compare well with those for the previously reported $[\text{PtF}(\text{PEt}_3)_3]^+$ of *cis* $^2J_{\text{PP}} = 19$ Hz and a *trans* $^2J_{\text{PF}} = 140$ Hz.¹⁷ The doublet observed at δ 24.1, with a $^1J_{\text{PtP}} = 3708$ Hz and *cis* $^2J_{\text{PP}} = 20$ Hz, is assigned to P_b in (4), it is only possible if the *cis* $^2J_{\text{PbF}}$ is too small to be resolved. Since there is no interaction between P_b and the fluorine nucleus, the resonance is not affected by any fluxionality exhibited by the fluorine and, thus, appears as a doublet at room temperature and remains unchanged at lower temperatures. In contrast, the major singlet at δ 17.0 assigned to *cis*- $[\text{PtF}_2(\text{PEt}_3)_2]$ (3) was unchanged at -20°C but did, however, broaden at -40°C (Figure 3.5), collapsed at -60°C , and at -80°C a broad doublet was observed, $^2J_{\text{PF}} \approx 145$ Hz with platinum satellites $^1J_{\text{PtP}} = 3785$ Hz (Figure 3.6).

Figure 3.7 The ^{19}F NMR Spectrum, Recorded at -80°C , of the Products from the Reaction of $\text{cis-}[\text{PtMe}_2(\text{PEt}_3)_2]$ and AHF



Complex (3) would undoubtedly exhibit a second order spectrum of the type AA'XX'Q which in this case gives rise to a simple doublet in the $^{31}\text{P}\{^1\text{H}\}$ NMR spectrum (Figure 3.6).

In an attempt to resolve resonances in the ^{19}F NMR spectrum that could be attributed to fluorine bound to platinum low-temperature studies were undertaken. At the low-temperature limit (-80°C) two resonances indicative of fluorine bound to platinum were resolved (Figure 3.7). The apparent triplet resonance observed at δ -302, $^2J_{\text{PF}} = 152$ Hz and $^1J_{\text{PF}} = 550$ Hz, was attributed to complex (4). It is feasible that the triplet resonance is a doublet of doublets in which the two doublet couplings are almost, if not, identical. This implies that fluorine, in complex (4), is coupling to one phosphorus nucleus (*trans* $^2J_{\text{FP}} = 152$ Hz) and one other spin active nucleus which can only be hydrogen *via* hydrogen bonding of the HF solvent. The poorly resolved multiplet at δ -265 was assigned to difluoro-complex (3), although no definitive couplings can be obtained a tentative value for the $^1J_{\text{PF}} \approx 620$ Hz is observed. In the following section the mechanism of the fluxional process observed in complexes (3) and (4) will be discussed.

Removal of the AHF *in vacuo* led to the isolation of a brown oil, unfortunately all attempts to obtain interpretable infrared and mass spectra were unsuccessful.

3.2.1 The Mechanism of the Reaction of AHF with *cis*-[PtMe₂(PEt₃)₂]

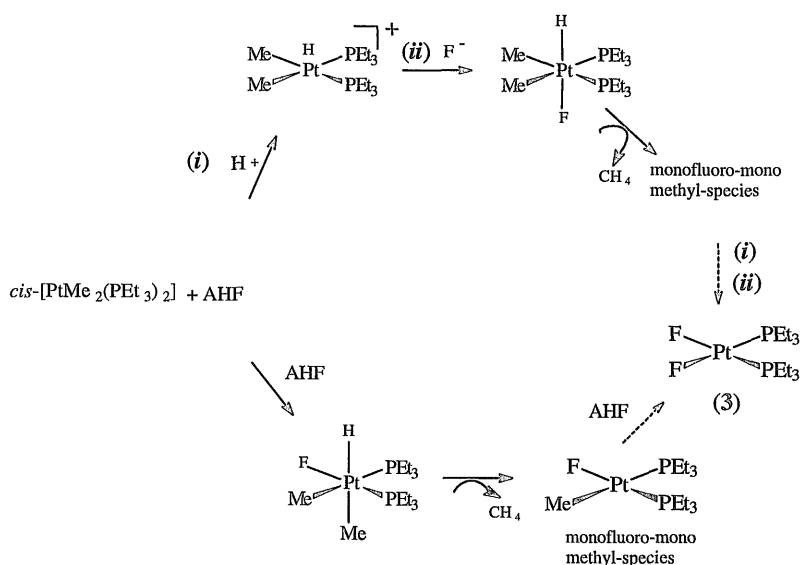
It has been shown in the previous section that AHF reacts with *cis*-[PtMe₂(PEt₃)₂] to afford predominately the difluoro-complex *cis*-[PtF₂(PEt₃)₂] with the evolution of methane. There are two plausible mechanisms for the above reaction which are outlined in Scheme 3.12:-

(i) initial protonation of the platinum centre followed by attack of the F⁻ and then subsequent, reductive elimination of methane.

(ii) oxidative addition of HF followed by reductive elimination of methane.

The reaction between *trans*-[IrCl(CO)(PPh₃)₂] and HF was reported to afford the six coordinate Ir(III) complex [Ir(H)(F)Cl(CO)(PPh₃)₂],⁶⁴ which is a product of oxidative addition. Infrared spectroscopic studies enabled Vaska to suggest that the addition of HF to the Ir(I) species was *cis* with the hydrogen entering the position *trans* to chlorine. Therefore, it is plausible that the mechanism for the reaction between the dimethyl-complex and AHF, is oxidative addition of HF and then, subsequent, reductive elimination of methane which is then repeated to give the difluoro-species.

Scheme 3.12

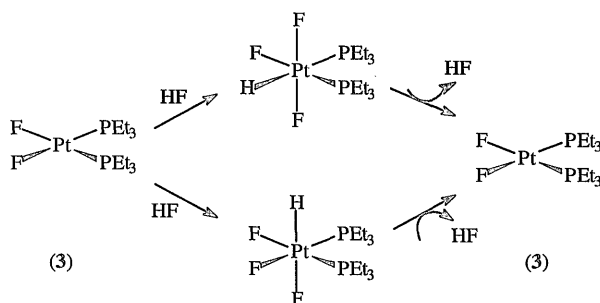


It has been shown that the difluoro-complex, $cis\text{-[PtF}_2\text{(PEt}_3\text{)}_2\text{]}$, undergoes an exchange process in AHF at room temperature in which the exchange occurs without:-

(i) cleavage of the Pt-P bond since the $^1J_{\text{PtP}}$ couplings are resolved at room temperature.

(ii) change in the stereochemistry at platinum since the magnitude of the $^1J_{\text{PtP}}$ couplings of the products are indicative of cis -phosphines. Therefore, it is plausible to suggest, considering the proposed mechanism for the formation of $cis\text{-[PtF}_2\text{(PEt}_3\text{)}_2\text{]}$, that the exchange process is due to oxidative addition of HF followed by subsequent reductive elimination of HF as depicted in Scheme 3.13.

Scheme 3.13



At room temperature this exchange process is fast and thus, only an average signal is observed in the NMR spectra. However, at low-temperatures this process is much slower and the resonances for the atoms that interact with fluorine in the difluoro-complex are resolved.

3.3 Reaction of *cis*-[PtCl₂(PEt₃)₂] with AHF

White *cis*-[PtCl₂(PEt₃)₂] was allowed to react with AHF, as described in section 6.14, yielding a pale green solution. This was anticipated to undergo halide metathesis affording the difluoro-complex observed in the reaction of the analogous dimethylplatinum complex with AHF.

The ¹⁹F NMR spectrum revealed only a broad singlet, at δ -179, which was assigned to the AHF solvent.

Analysis of this solution by ³¹P{¹H} and ¹⁹⁵Pt NMR spectroscopy showed no similarity with that observed for the difluoro-complex discussed in section 3.2. However, comparison of the NMR data of the reaction product with those of the starting material does reveal a significant difference (Table 3.8).

Table 3.8 Comparison of the NMR Data of the Reaction Product with *cis*-[PtCl₂(PEt₃)₂]^a

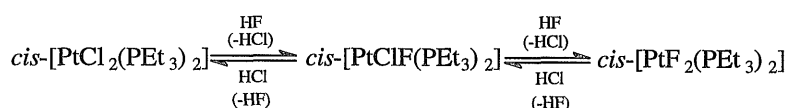
Complex	$\delta(^{31}\text{P})/\text{ppm}$	$\delta(^{195}\text{Pt})/\text{ppm}$	$^1J(\text{PtP})/\text{Hz}$
Reaction Product	17.5	-4004	3604
<i>cis</i> -[PtCl ₂ (PEt ₃) ₂]	8.4	-4469	3507

(a) all data from this work

Although all the data, when compared with the starting material, indicate a change in composition, no evidence of fluorine coupling to platinum or phosphorus was observed. The shift to higher frequency observed in both the $^{31}\text{P}\{^1\text{H}\}$ and ^{195}Pt NMR spectra are indicative of substitution of a heavier for a lighter halogen (see section 3.2). In marked contrast to the previously discussed reaction of AHF with the dimethyl-species, low temperature NMR experiments had no effect on the resonances and thus no characterizations are possible.

It was considered that any dissolved HCl, the anticipated by-product of the reaction, in the AHF solution might affect the apparent nature of the reaction product by halogen exchange. It is plausible that the exchange process, discussed in the previous section, is an important factor in the reaction between *cis*-[PtCl₂(PEt₃)₂] and AHF. In contrast to the methane gas, reductively eliminated in the reaction of the analogous dimethylplatinum complex with AHF, the evolved HCl, as well as the HF, are able to oxidatively add to the platinum(II) complex. Therefore, as a result of either HCl or HF being able to oxidatively add to the platinum(II) complex and consequently be reductively eliminated an equilibrium could exist between the starting material, a monofluoro-monochloro-analogue and the difluoro-complex (Scheme 3.14).

Scheme 3.14



In the dimethyl system, discussed in section 3.2, low-temperature NMR studies enabled the difluoro-complex to be resolved since the exchange process involved the oxidative-addition-reductive-elimination of HF to afford only this species whereas, in the analogous dichloro-system 3 products are possible (Scheme 3.14). Thus, the resonance observed at low-temperature is plausibly an average of all three compounds.

In an attempt to eliminate the possible effects of the HCl the experiment was modified by removing the AHF *in vacuo* and then subsequently re-dissolving the product in AHF. This was performed several times in an attempt to remove all HCl produced during the reaction. However, analysis of this reaction product revealed identical results to that described above thus, again, no assignments are possible.

Removal of the AHF solvent led to the isolation of a pale green oil however, all attempts to characterize the products further were unsuccessful.

3.4 Reactions of *cis*-[PtX₂(PEt₃)₂] with AHF in CD₂Cl₂ [X = Cl, Me]

As discussed in section 3.2 no fluorine coupling was resolved as a result of the fluxional behaviour of the difluoro-species in the AHF solvent. Therefore, in an attempt to resolve the fluorine coupling, CD₂Cl₂, a non-fluorine containing solvent, was employed.

Both reactions produce identical results and so are reported together. A stoichiometric amount of AHF (one molar equivalence) was condensed onto a dichloromethane solution of *cis*-[PtX₂(PEt₃)₂] at -196°C, as described in section 6.14, and allowed to warm to room temperature. In both cases effervescence was observed with the evolution of a colourless gas (gas-phase infrared spectroscopy identified the gas as methane from the reaction of the dimethyl-complex). When the reactions were complete, light brown solutions were obtained and subsequently, analysed by NMR spectroscopy. All the NMR data are presented in Table 3.9 and are compared with the values for the starting materials.

It is apparent from the data presented in Table 3.9 that the products from the reaction of *cis*-[PtX₂(PEt₃)₂] with AHF, in dichloromethane, are identical. Although, the NMR data does not show any evidence for a fluoride species (*cf.* *cis*-[PtF₂(PEt₃)₂] $\delta(^{31}\text{P})$ 17.0, $^1J_{\text{PtP}} = 3942$ Hz) it is diagnostic of a platinum(II) species with two equivalent *cis*-phosphine ligands. Furthermore, the environment of the platinum is apparently very similar to that in *cis*-[PtCl₂(PEt₃)₂] as there is only a slight change in either the platinum-phosphorus coupling constants or chemical shifts.

A plausible explanation is the formation of the dimeric chloride bridged species (5).

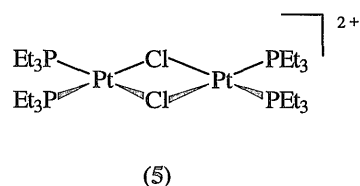


Table 3.9 Comparison of the NMR Data of the Products, from the Reaction of *cis*-[PtX₂(PEt₃)₂] with AHF in CD₂Cl₂, with *cis*-[PtCl₂(PEt₃)₂] and *cis*-[PtMe₂(PEt₃)₂]^a

Complex	$\delta(^{19}\text{F})/\text{ppm}$	$\delta(^{31}\text{P})/\text{ppm}$	$^1J(\text{PtP})/\text{Hz}$
Reaction Product (X = Cl)	-180	6.2	3451
Reaction Product (X = Me)	-179	6.0	3450
<i>cis</i> -[PtCl ₂ (PEt ₃) ₂]	-	8.4	3507
<i>cis</i> -[PtMe ₂ (PEt ₃) ₂]	-	9.0	1855

(a) all data from this work

Although, the cationic bridged complex [(PEt₃)₂Pt(μ-Cl)₂Pt(PEt₃)₂][BF₄]₂ is documented in the literature⁶⁵ there has been no reported ³¹P NMR data on this complex and any other species of this type thus making direct comparisons difficult. The counteranion is possibly [HF₂]⁻ since the observation of resonances at δ -180 in the ¹⁹F NMR spectra could be attributed to this anion.

The existence of bridging-chloride ligands in the species derived from the reaction of the dimethyl-complex would undoubtedly be a result of extraction from the dichloromethane solvent. Previous workers have advised that species of the type, [PtF(PR₃)₃]⁺ (PR₃ = PEt₃, PMe₂Ph and PPh₃),¹⁷ might undergo fluorine-chlorine exchange if exposed to chlorinated solvents. Furthermore, in section 3.11 it is shown that the complex [PtF(PPh₃)₃]⁺ does undergo fluorine-chlorine exchange, when exposed to dichloromethane, to

afford the monochloro-cation $[\text{PtCl}(\text{PPh}_3)_3]^+$. However, extraction of chlorine from dichloromethane should result in fluorination of the solvent but, in all cases no evidence to indicate the presence of fluorinated solvent was observed in the ^{19}F NMR spectra.

3.5 Reactions of *cis*- $[\text{PtCl}_2(\text{PR}_3)_2]$ ($\text{PR}_3 = \text{PMe}_3, \text{PMe}_2\text{Ph}, \text{PEtPh}_2$ and $(\text{PR}_3)_2 = \text{dppe}$) with AHF

Although characterization of the product from the reaction of *cis*- $[\text{PtCl}_2(\text{PEt}_3)_2]$ and AHF was not possible, a study was undertaken to investigate the scope of this reaction type. By varying the phosphine ligand the electronic and steric properties could be controlled.

cis- $[\text{PtCl}_2(\text{PR}_3)_2]$ and AHF were allowed to react, as described in section 6.14, affording a coloured solution which was subsequently analysed by multinuclear NMR spectroscopy.

The ^{19}F NMR spectra all showed a broad resonance (at $\approx \delta -180$) attributed to the AHF solvent.

The $^{31}\text{P}\{^1\text{H}\}$ and $^{195}\text{Pt}\{^1\text{H}\}$ NMR data for all the reaction products are presented in Table 3.10 and are compared to those of the corresponding starting materials.

In general, the reaction products show a significant change in their respective NMR data when compared to the corresponding starting material. Both the shift to higher frequencies observed in the $^{31}\text{P}\{^1\text{H}\}$ and $^{195}\text{Pt}\{^1\text{H}\}$ NMR spectra and the increased magnitude of the $^1J_{\text{PtP}}$ coupling are indicative of substitution of a heavier for a lighter halogen (see section 3.2). However, as in the *cis*- $[\text{PtCl}_2(\text{PEt}_3)_2]$ case, discussed in section 3.3, low-temperature NMR studies had no effect on the resonances and thus no fluorine coupling to either platinum or phosphorus was resolved.

Although, with the limited spectroscopic data available no characterizations are possible it is plausible to suggest that the AHF solvent is influencing the nature of the dichloro-species in some way.

Table 3.10 Comparison of the NMR Data of the Reaction products with the Starting Materials^a

Reaction Products (PR ₃)	$\delta(^{31}\text{P})$ / ppm	$\delta(^{195}\text{Pt})$ / ppm	$^1J(\text{PtP})$ / Hz
PMe ₃	-13.0(-20.7)	-4261(-4408) ^b	3678(3470)
PMe ₂ Ph	-10.0(-15.0)	-4260(-4403) ^b	3715(3547)
PEtPh ₂	12.5(9.9)	-4215(-4426) ^b	3760(3656)
dppe	47.0(47.0)	-4480(-4554) ^c	3794(3618)

(a) all data this work unless otherwise stated

(b) P. S. Pregosin, *Coord. Chem. Rev.*, 1982, **44**, 247.

(c) E. G. Hope, W. Levason and N. A. Powell, *Inorg. Chim. Acta*, 1986, **115**, 187.

starting material values found in parentheses

3.6 Reactions of *cis*-[PtMe₂(PR₃)₂] (PR₃ = PMe₂Ph, PMe₃, Pcy₃ and PEtPh₂) with AHF

The previously discussed reaction of *cis*-[PtMe₂(PEt₃)₂] with AHF (section 3.2) was shown to afford two products one of which was the difluoro-species *cis*-[PtF₂(PEt₃)₂]. Therefore, it was considered to be of

interest to investigate the scope of this reaction type. Owing to the different nature of the products all of the reactions will be discussed separately.

cis-[PtMe₂(PR₃)₂] and AHF were allowed to react, as described in section 6.15, with the evolution of a colourless gas (identified by gas-phase infrared spectroscopy as methane). All solutions were then analysed by ³¹P{¹H} and ¹⁹⁵Pt{¹H} NMR spectroscopy.

3.6.1 *cis*-[PtMe₂(PMe₃)₂]

The NMR data for the product from the reaction *cis*-[PtMe₂(PMe₃)₂] and AHF are presented in Table 3.11 along with the corresponding data for *cis*-[PtX₂(PMe₃)₂] (X = Cl and Me).

As with all the other systems studied the reaction product shows both a shift to higher frequency, in the ³¹P{¹H} and ¹⁹⁵Pt{¹H} NMR spectra, and an increase in the magnitude of the ¹J_{PtP} coupling when compared to the dimethyl-species and more importantly the dichloro-complexes. Furthermore, it is important to note the similarity in the NMR data reported for the analogous reaction with *cis*-[PtCl₂(PMe₃)₂] (Table 3.10).

Table 3.11 Comparison of the NMR Data of the Reaction Products with *cis*-[PtX₂(PMe₃)₂] (X = Cl and Me)^a

Complex	δ(³¹ P)/ ppm	δ(¹⁹⁵ Pt)/ ppm	¹ J(PtP)/ Hz
Reaction Product	-15.0	-4260	3654
X = Me ^b	-22.7	-	1745
X = Cl	-20.7	-4408 ^c	3470

(a) all data this work unless otherwise stated

(b) was prepared from the reaction of *cis*-[PtCl₂(PMe₃)₂] and MeLi (see section 6.5), difficulties were experienced in obtaining a pure sample and thus, no ¹⁹⁵Pt NMR spectrum was recorded. The reaction with AHF was performed using an impure sample.

(c) P. S. Pregosin, *Coord. Chem. Rev.*, 1982, 44, 247.

The absence of any fluorine coupling to either platinum or phosphorus, even at low-temperatures, is a phenomenon that cannot be explained. Therefore, characterization of the reaction product is not possible although, the following assumptions can be made:-

(i) The species, formed from the reaction of *cis*-[PtMe₂(PMe₃)₂] and AHF, no longer possesses a methyl group bound to platinum. Evidence to substantiate this assumption are the observation of methane gas and the absence of resonances, in the ¹H NMR spectrum, characteristic of methyl bound to platinum.

(ii) The ligand, X, in this species *trans* to the phosphines exhibits a lower "NMR *trans* influence" than that of chloride and methyl. This is borne out by the magnitude of the ¹J_{PtP} coupling.

(iii) Finally, the ligand, X, is also more electronegative than chloride since both the phosphorus and platinum nuclei are deshielded, with respect to the dichloro-species, and consequently the associated resonances are observed at a higher frequency.

Although, all the assumptions indicate the possibility of fluorine bound to platinum there is no direct evidence to support this and thus the product remains unassigned.

3.6.2 *cis*-[PtMe₂(Pcy₃)₂]

The ³¹P NMR spectrum revealed the presence of one species, a doublet at δ 35 with ¹J_{PH} = 1266 Hz. This doublet was attributed to the protonated phosphine, [HPcy₃]⁺, which is a plausible product since Pcy₃ is a very basic phosphine and thus, would be readily protonated by the strong protic acid, AHF. As a consequence the phosphine 'drops off' the platinum centre resulting in decomposition of any initial complex formed.

Unfortunately, no other species are assignable.

3.6.3 *cis*-[PtMe₂(PMe₂Ph)₂]

Preliminary experiments did reveal promising signs that a difluoro-complex could be formed. The NMR data for the reaction products and *cis*-[PtX₂(PMe₂Ph)₂] (X = Cl and Me) are presented in Table 3.12.

Table 3.12 Comparison of the NMR Data of the Reaction Products with *cis*-[PtX₂(PMe₂Ph)₂]^a

Complex	δ(³¹ P)/ ppm	δ(¹⁹⁵ Pt)/ ppm	¹ J(PtP)/ Hz
Reaction Products	-5.0 (s)	-4150 (t)	3850
	-10.5 (s)	-4275 (t)	3720
X = Me	-10.8 (s)	-4565 (t) ^b	1797
X = Cl	-15.0 (s)	-4403 (t) ^c	3547

multiplicity: s = singlet and t = triplet

(a) all data this work unless otherwise stated

(b) J. D. Kennedy, W. McFarlane, R. J. Puddephatt and P. J. Thompson, *J. Chem. Soc., Dalton Trans.*, 1976, 874.

(c) P. S. Pregosin, *Coord. Chem. Rev.*, 1982, 44, 247.

Low-temperature $^{195}\text{Pt}\{^1\text{H}\}$ NMR experiments were carried out as these were found to be the most informative in the *cis*-[PtMe₂(PEt₃)₂] system. The low-temperature NMR had no effect on the appearance of the triplet at δ -4275, but the triplet, at δ -4150, was resolved into a triplet of doublets. The following data were then extracted from the spectrum; δ -4185, $^1J_{\text{PtP}} = 3834$ Hz and $^1J_{\text{PtF}} = 566$ Hz. By analogy with the *cis*-[PtMe₂(PEt₃)₂] system, discussed in section 3.2, the doublet coupling of 566 Hz is attributed to the $^1J_{\text{PtF}}$ coupling. By analogy with the *cis*-[PtMe₂(PEt₃)₂] reaction the species formed could be the monofluoro-complex *cis*-[PtFCl(PMe₂Ph)₂]. However, the limited spectroscopic and experimental data enable only a tentative assignment.

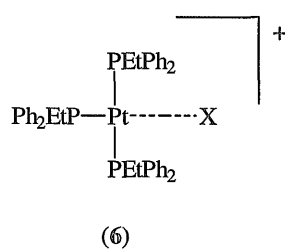
3.6.4 *cis*-[PtMe₂(PEtPh₂)₂]

Both the $^{31}\text{P}\{^1\text{H}\}$ and $^{195}\text{Pt}\{^1\text{H}\}$ NMR spectra showed some surprising results. The room temperature $^{31}\text{P}\{^1\text{H}\}$ NMR spectrum (Figure 3.8) showed a singlet at δ 6.0, $^1J_{\text{PtP}} = 4325$ Hz, and three other singlets at δ 43, 30 and 16 but, for these resonances no ^{195}Pt satellites were resolved. The $^{195}\text{Pt}\{^1\text{H}\}$ NMR spectrum (Figure 3.9), at 298 K, revealed four peaks at δ -4602, -4650, -4700 and -4745. It was not clear from this spectrum whether any of these resonances were coupled to each other.

In light of two of the previous systems exhibiting fluxional behaviour such a possibility was considered in this case.

The low-temperature $^{195}\text{Pt}\{^1\text{H}\}$ NMR experiments, at 223 K, resolved the four resonances into a doublet of triplets (Figure 3.10) implying that there are two phosphorus environments, in a ratio of 2:1, coordinated to this platinum species. The doublet of triplets was observed at δ -4735 with a $^1J_{\text{PtP}} = 4629$ and 2289 Hz.

Considering the results obtained from the low-temperature $^{195}\text{Pt}\{^1\text{H}\}$ NMR experiments there is only one possible arrangement which would account for the multiplicity and the $^1J_{\text{PtP}}$ coupling:



The $^1J_{\text{PtP}}$ coupling for the *trans* phosphines would be significantly smaller than the corresponding coupling for the phosphine *trans* to X, assuming X is a halogen or any other ligand possessing a lower "*trans* NMR influence" than the phosphine. This marked difference in the $^1J_{\text{PtP}}$ coupling can be clearly seen in the cationic monofluoro-complexes $[\text{PtF}(\text{PPh}_3)_3]^+$ and $[\text{PtF}(\text{PEt}_3)_3]^+$ (discussed in section 3.9) where the coupling constants of 3696 and 3455 Hz respectively¹⁷ for the phosphine *trans* to fluorine are significantly larger than the corresponding coupling for the mutually *trans* phosphines of 2650 and 2382 Hz respectively.

Figure 3.8 The Room Temperature $^3\text{P}\{^1\text{H}\}$ NMR Spectrum of the Products
from the Reaction of *cis*- $[\text{PtMe}_2(\text{PEtPh}_2)_2]$ and AHF

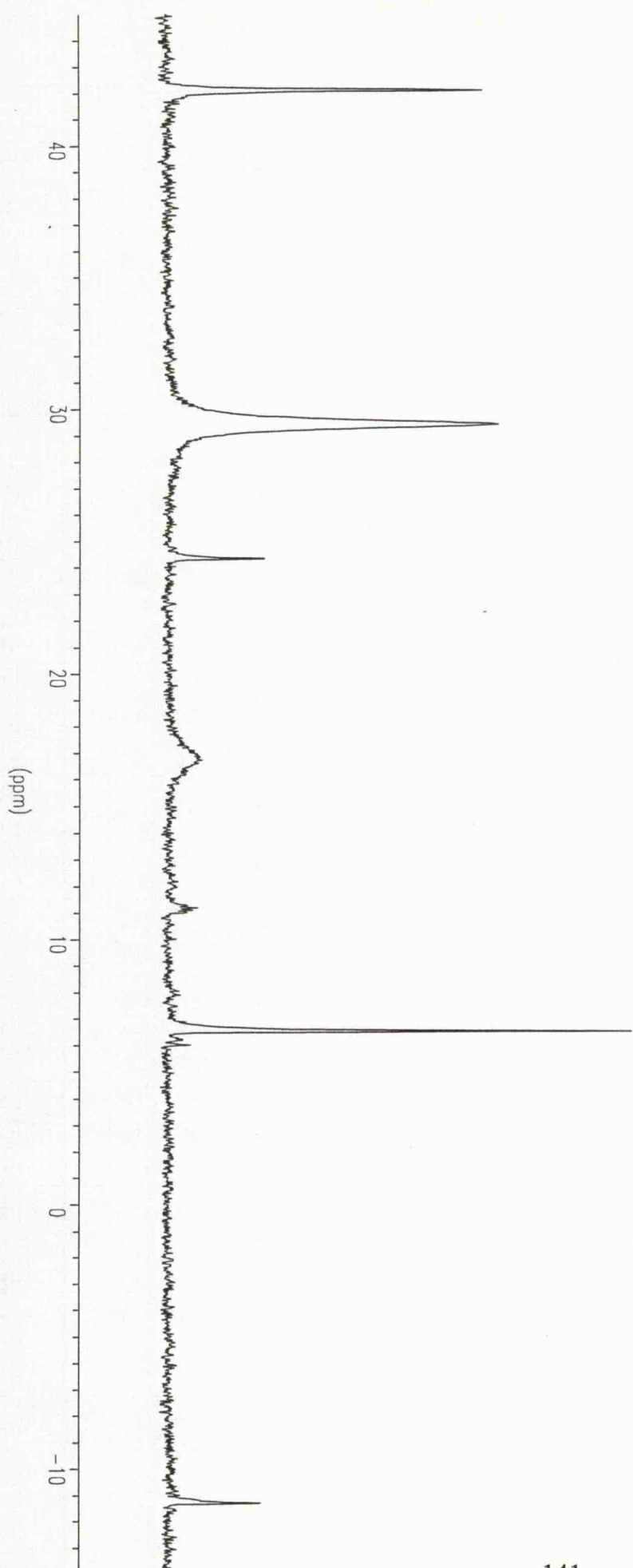


Figure 3.9 The Room Temperature $^{195}\text{Pt}\{^1\text{H}\}$ NMR Spectrum of the Products
from the Reaction of *cis*- $[\text{PtMe}_2(\text{PEtPh}_2)_2]$ and AHF

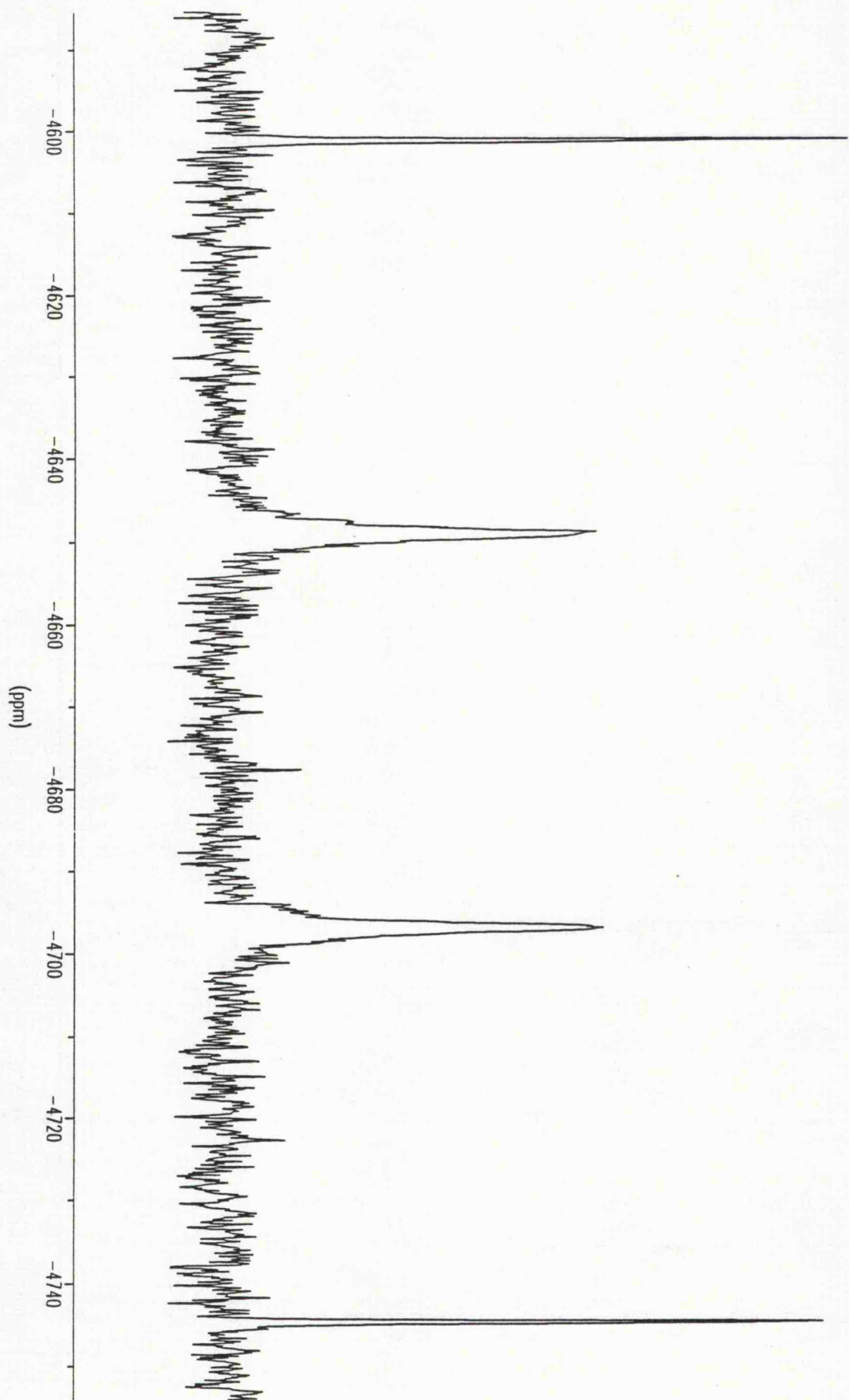
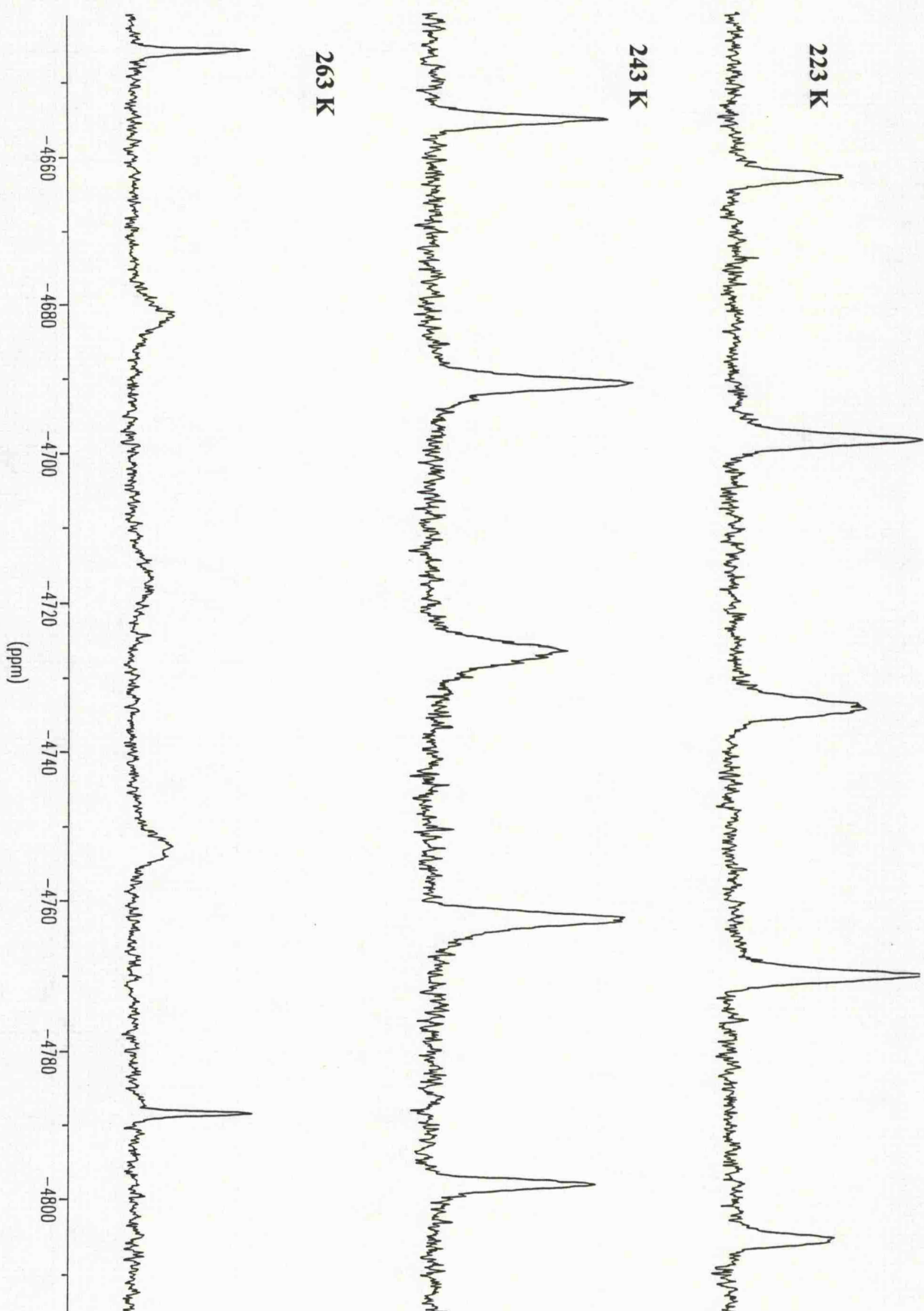


Figure 3.10 Effects of Variable Temperature $^{15}\text{Pt}\{^1\text{H}\}$ on the Resonances

Shown in Figure 3.8



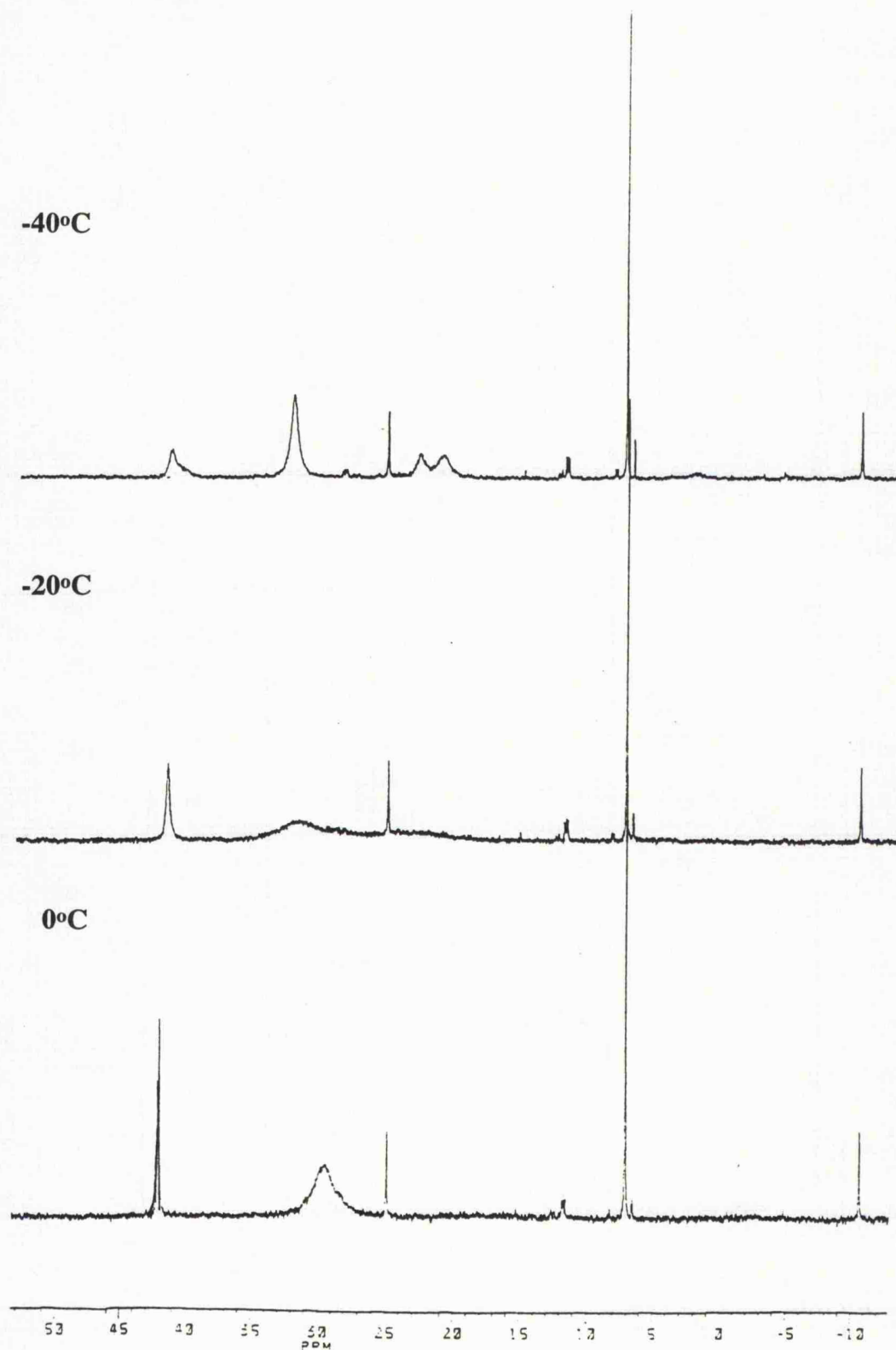
The low-temperature $^{31}\text{P}\{^1\text{H}\}$ NMR spectrum of (6), assuming X has spin $I \neq 1/2$, would be expected to show a doublet and a triplet, in a 2:1 ratio, with the associated ^{195}Pt satellites. However, the low temperature $^{31}\text{P}\{^1\text{H}\}$ NMR spectrum showed the two singlets at δ 43 and 30 collapse at -40°C and -20°C respectively (Figure 3.11) with the emergence of a new species and then with further cooling to -55°C being resolved into two singlets, in a 2:1 ratio, with the associated ^{195}Pt satellites (Figure 3.12). The singlet observed at δ 6.0, at 298 K, remained unchanged at low temperatures. The $^{31}\text{P}\{^1\text{H}\}$ NMR data, recorded at -55°C , for the reaction products are presented in Table 3.13.

Table 3.13 The $^{31}\text{P}\{^1\text{H}\}$ NMR Data, Recorded at -55°C , for the Reaction Products

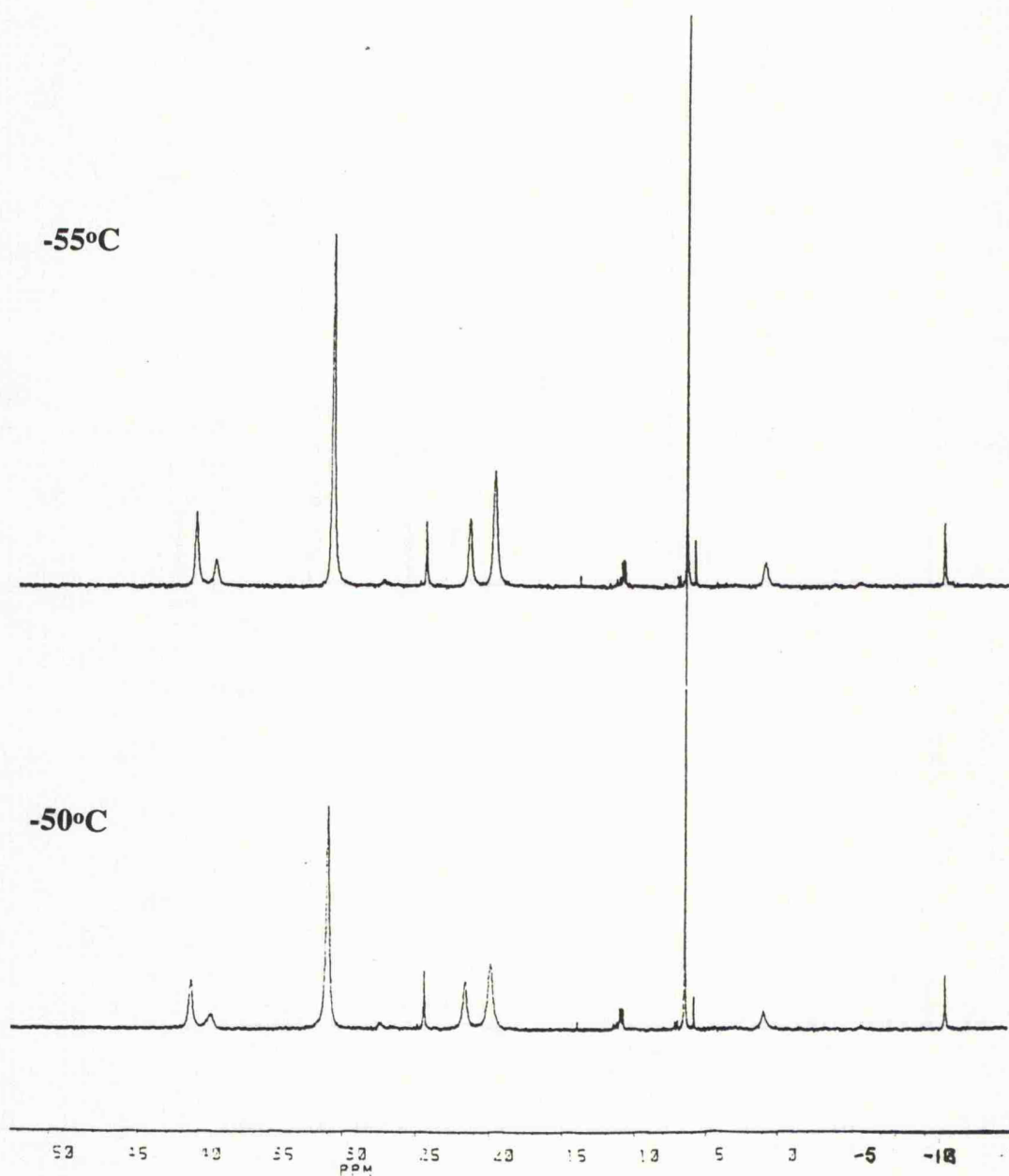
$\delta(^{31}\text{P})/\text{ppm}$	$^1J(\text{PtP})/\text{Hz}$
s 32.0	2275
s 21.0	4632
s 6.0	4350

multiplicity: s = singlet

Figure 3.11 Effects of Variable Temperature $^{31}\text{P}\{^1\text{H}\}$ on the Resonances
Shown in Figure 3.8



**Figure 3.12 Effects of Variable Temperature $^{31}\text{P}\{^1\text{H}\}$ on the Resonances
Shown in Figure 3.8**



Although, no $^2J_{\text{PP}}$ coupling was resolved at -55°C it is evident from the data, in Table 3.13, that the singlets observed at δ 32.0 and 21.0 with $^1J_{\text{PtP}}$ coupling of 2275 and 4632 Hz respectively are consistent with structure (6). The chemical shift for the P *trans* P environment occurs at a higher frequency than the corresponding P *trans* X environment. This is, again, comparable to the two cationic monofluoro-complexes $[\text{PtF}(\text{PEt}_3)_3]^+$ and $[\text{PtF}(\text{PPh}_3)_3]^+$ in which the P *trans* P chemical shifts are observed at a higher frequency than the P *trans* F (see section 3.9).

The nature of X can now be addressed by considering the unusually large $^1J_{\text{PtP}}$ coupling. The largest $^1J_{\text{PtP}}$ coupling constants have been observed for the platinum(0) complexes of the type $[\text{Pt}(\text{PR}_3)_3]$ for $\text{PR}_3 = \text{PEt}_3$, Pcy_3 and PPh_3 being of the magnitude 4220, 4236 and 4370 Hz respectively.^{66, 67} Therefore, for a platinum(II) complex the one possible explanation for such a large $^1J_{\text{PtP}}$ coupling is that X is HF solvent and thus, very weakly bound. It could be argued that solvation of the HF is stabilizing this arrangement of the phosphine ligands but, has no influence on the Pt-P bond *trans* to it. As a consequence the $^1J_{\text{PtP}}$ coupling, for P *trans* HF, is extremely large since the phosphine is effectively *trans* to no other ligand and is therefore, not affected by the "NMR *trans* influence" which lowers the magnitude of this coupling to different extents depending on the nature of the ligand *trans* to the phosphine.

3.7 Reactions of *cis*- $[\text{PtX}_2(\text{PPh}_3)_2]$ (X = Cl, Me) and AHF

The complex *cis*- $[\text{PtFCl}(\text{PPh}_3)_2]$ was reportedly formed from the reaction of *cis*- $[\text{PtCl}_2(\text{PPh}_3)_2]$ and AHF (see section 3.1.5).¹⁵ Therefore, it was thought necessary to repeat this reaction in order to confirm, or

otherwise, this formulation. The analogous reaction of the dimethylplatinum(II) complex was also performed for comparison.

White *cis*-[PtX₂(PPh₃)₂] (X = Cl, Me) and AHF were allowed to react, as described in sections 6.14 and 6.15, yielding an insoluble yellow solid. The AHF solvent was removed *in vacuo* and the resulting solid was then analysed by infrared spectroscopy and mass spectrometry.

The Nujol mull infrared spectrum of the product, from the reaction of *cis*-[PtCl₂(PPh₃)₂] and AHF, revealed 3 bands at 444 (m), 423 (m) and 302 (m) cm⁻¹ which compared well to those previously reported by Kemmitt *et al.* for the complex *cis*-[PtFCl(PPh₃)₂]¹⁵ {*cf.* *cis*-[PtCl₂(PPh₃)₂] ν (Pt-Cl) 316 (m) and 293 (m) cm⁻¹}. The two bands at \approx 400 cm⁻¹ were assigned to the Pt-P vibrations with the band at 302 cm⁻¹ being attributed to a ν (Pt-Cl). Comparison of the infrared data of the product with that of the starting material indicate that both chlorines are no longer present in the *cis*-configuration. Furthermore, it has been reported previously that it is difficult to differentiate between terminal and bridging chlorines and, therefore, the possibility of a chlorine-bridged dimer can not be ruled out.⁶⁹ The inability to observe a Pt-F vibration was reported¹⁵ to be a result of interference from the very intense modes of the triphenylphosphine ligands.

All attempts to obtain an interpretable infrared spectrum of the product, from the analogous reaction of the dimethylplatinum(II) complex, were unsuccessful. Furthermore, no interpretable mass spectra were obtained in either case.

In an attempt to elucidate the reaction products the reactions were repeated but, in this instance, the AHF was removed and the solids were subsequently re-dissolved in liquid SO₂ and analysed by ¹⁹F and ³¹P{¹H} NMR spectroscopy.

The ¹⁹F NMR spectra showed no resonances indicative of fluorine bound to platinum (δ -200 to -300).

The $^{31}\text{P}\{^1\text{H}\}$ NMR data for the reaction products are presented in Table 3.14 and are compared to the starting materials.

Table 3.14 Comparison of the $^{31}\text{P}\{^1\text{H}\}$ NMR Data of the Products with the Starting Materials^a

Reaction Product	$\delta(^{31}\text{P})$ / ppm	$^1J(\text{PtP})$ / Hz
X = Cl	15.0 (13.9)	3845 (3672)
X = Me	15.0 (28.0)	3845 (1845)

(a) all data this work
starting material values in parentheses

It is evident from the data presented in Table 3.14 that the products from the reactions of *cis*-[PtX₂(PPh₃)₂] (X = Me, Cl) and AHF, in liquid SO₂, are identical. There is no evidence for the existence of a platinum-fluoride bond in these species. However, it is possible that the coordinating SO₂ has inserted into the initially formed bond. The complex [PtF(PPh₃)₃]⁺ was reported to exhibit an unusually small $^1J_{\text{PtF}}$ coupling constant (see section 3.1.3) indicating a weak Pt-F bond.¹⁷ Therefore, it is plausible to suggest that if a platinum fluoride bond was formed, in the reactions between *cis*-[PtX₂(PPh₃)₂] (X = Cl, Me) and AHF, its strength would be comparable, and if not weaker, to that reported for [PtF(PPh₃)₃]⁺ thus, SO₂ insertion might readily occur. Further evidence to substantiate that the solvent has inserted and is weakly bound to the platinum(II) complex is that removal of the SO₂ followed by dissolution in CD₂Cl₂ led to the formation, in both cases, of *cis*-[PtCl₂(PPh₃)₂].

3.8 Discussion of the Reactions of *cis*-[PtX₂(PR₃)₂] and AHF

It is apparent from all the data, discussed in the previous sections, that the basicity of the phosphine is the important factor in determining the nature of the product formed from the reaction of the platinum-phosphine complex with AHF. The unambiguous formation of *cis*-[PtF₂(PEt₃)₂], from the reaction of the dimethyl-species with AHF, being the only real success would imply that triethylphosphine possesses the optimum basicity to stabilize the platinum-fluoride bonds. As shown, if the basicity of the phosphine is too high, in the case of Pcy₃, then the phosphine is protonated (section 3.6.2) by the AHF, if it is too low as for PPh₃, then the phosphine is unable to stabilize the initially formed Pt-F bond (section 3.7).

It has been discussed that, in both the dimethyl- and the dichloro-platinum systems studied, exchange processes are occurring in which HF, and in the case of the dichloro-complexes HCl also, are oxidatively adding to the platinum(II) complex followed by reductive elimination. Thus, it became apparent that any success in the preparation of difluorobis(phosphine)-platinum(II) complexes would ultimately come from the reaction of the analogous dimethyl-complex with AHF, rather than the dichloro-species, since the methane gas evolved cannot oxidatively add to the resulting difluoro-complex therefore eliminating the possibility of reforming the starting material or any intermediate.

3.9 Preparation of [PtF(PR₃)₃][BF₄] (PR₃ = PEt₃ and PPh₃)

Owing to the dearth of platinum fluoride phosphine complexes reported in the literature it was of interest to verify the results obtained by Dixon *et al.*¹⁷

$[\text{PtCl}(\text{PEt}_3)_3][\text{BF}_4]$ and $[\text{AgF}]$ were allowed to react in acetone, as described in section 6.17, affording a colourless solid.

$[\text{Pt}(\text{PPh}_3)_4]$ was reacted with AHF and then subsequently treated with $[\text{NaBF}_4]$, as described in section 6.16, affording a brown solid.

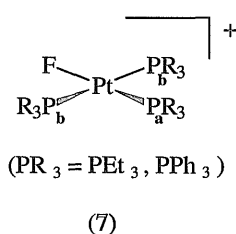
Both solids were then dissolved in d_6 -acetone and subsequently analysed by multinuclear NMR spectroscopy. All the NMR data for the complexes $[\text{PtF}(\text{PR}_3)_3][\text{BF}_4]$ ($\text{PR}_3 = \text{PEt}_3$ and PPh_3) are presented in Table 3.15.

Table 3.15 Multinuclear NMR Data for the Complexes $[\text{PtF}(\text{PEt}_3)_3][\text{BF}_4]$ and $[\text{PtF}(\text{PPh}_3)_3][\text{BF}_4]^a$

NMR Data	$[\text{PtF}(\text{PEt}_3)_3]^+$		$[\text{PtF}(\text{PPh}_3)_3]^+$	
	P <i>cis</i> F	P <i>trans</i> F	P <i>cis</i> F	P <i>trans</i> F
$\delta(^{19}\text{F})/\text{ppm}$	-251.5 (dt)		-232 (dt)	
$^2J(\text{FP})/\text{Hz}$	32	140	39	139
$\delta(^{31}\text{P})/\text{ppm}$	28.0 (dd)	3.0 (dt)	26.5 (dd)	3.0 (dt)
$^2J(\text{PP})/\text{Hz}$	19		19	
$\delta(^{195}\text{Pt})/\text{ppm}$	-4405 (dtd)		-4270 (dtd)	
$^1J(\text{PtP})/\text{Hz}$	2828	3455	2640	3701
$^1J(\text{PtF})/\text{Hz}$	250		67	

(a) all data this work

multiplicity: dt = doublet of triplets, dd = doublet of doublets, dtd = doublet of triplets of doublets



Both sets of the ^{19}F and $^{31}\text{P}\{^1\text{H}\}$ NMR, presented in Table 3.15, compare well with that reported by Dixon and Cairns.¹⁷ The ^{19}F NMR spectra for both complexes show the expected doublet of triplets with the associated ^{195}Pt satellites (Figure 3.13). This arises from the fluorine nucleus coupling to the *trans* phosphine, P_a , and the two equivalent *cis* phosphines, P_b , in complex (7). As discussed in section 3.1.3 the $^1J_{\text{PtF}}$ coupling in $[\text{PtF}(\text{PPh}_3)_3]^+$, of 67 Hz, is significantly smaller than that observed for the analogous complex $[\text{PtF}(\text{PEt}_3)_3]^+$. This smaller $^1J_{\text{PtF}}$ coupling is indicative of a weak bond and is substantiated by the facile decomposition of this complex, discussed in section 3.1.1, and the the relative Pt-F bond length which is addressed shortly.

Both the $^{31}\text{P}\{^1\text{H}\}$ NMR spectra exhibit the expected mutually coupled doublet of doublets and doublet of triplets with the associated ^{195}Pt satellites. The doublet of doublets is assigned to P_b arising from coupling *cis* to the fluorine and P_a . The doublet of triplets is attributed to P_a coupling *trans* to fluorine and *cis* to the two equivalent P_b nuclei.

The $^{195}\text{Pt}\{^1\text{H}\}$ NMR spectra, which have not been reported previously, both showed the predicted multiplicity of a doublet of triplets of doublets (Figure 3.14). By comparison of the two $^{195}\text{Pt}\{^1\text{H}\}$ NMR spectra the significant difference in the magnitude of the $^1J_{\text{PtF}}$ coupling can be clearly seen.

Figure 3.13 The ^{19}F NMR Spectrum of $[\text{PtF}(\text{PEt}_3)_3][\text{BF}_4]$

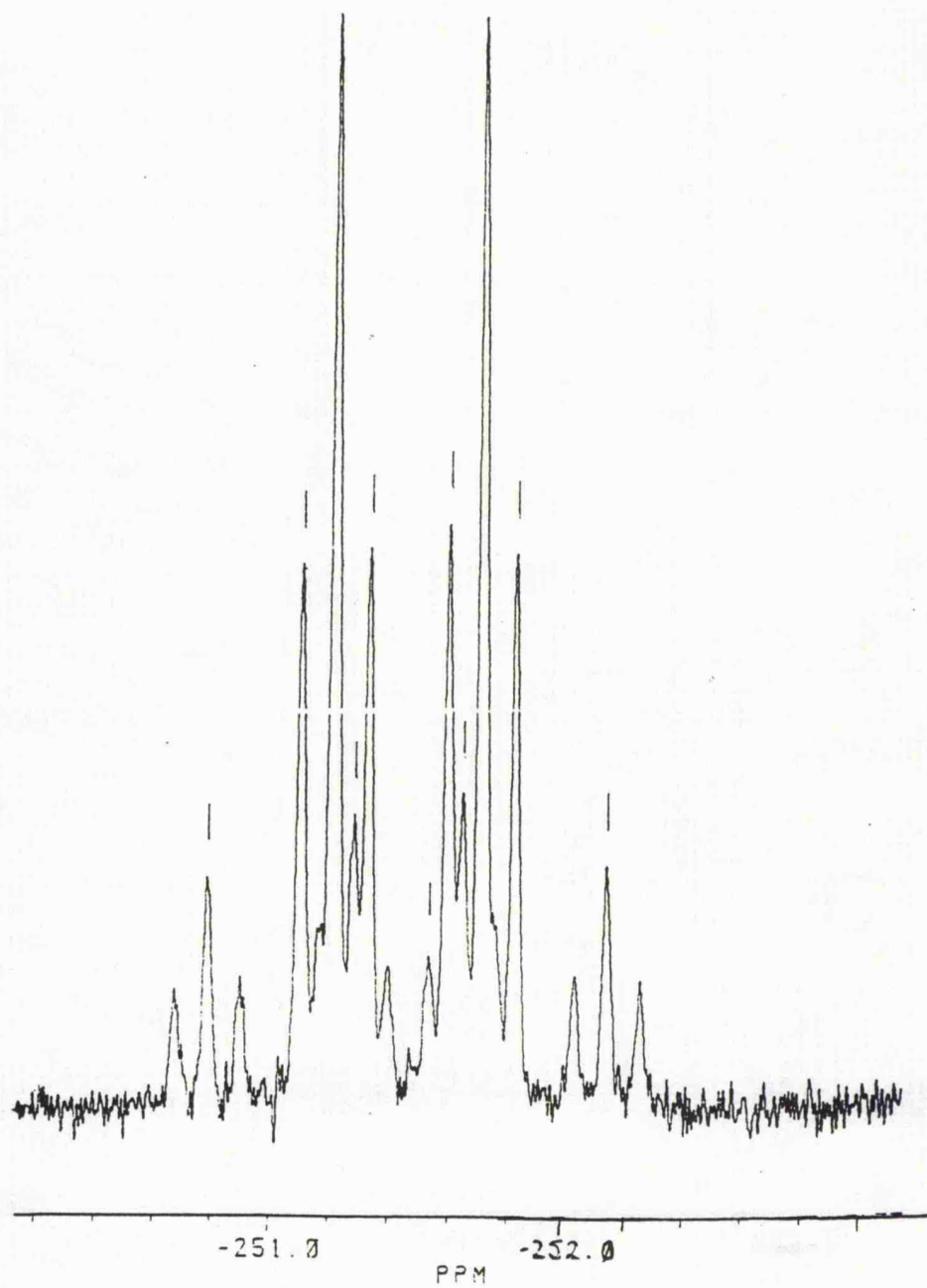
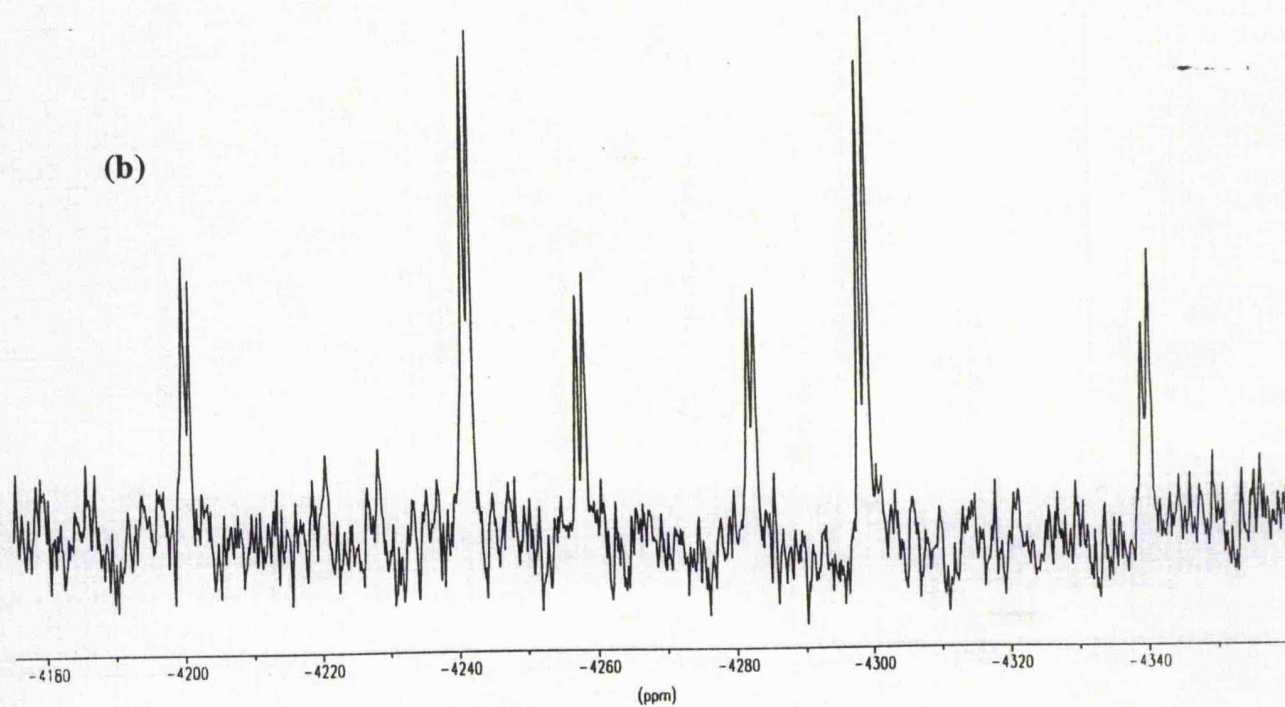
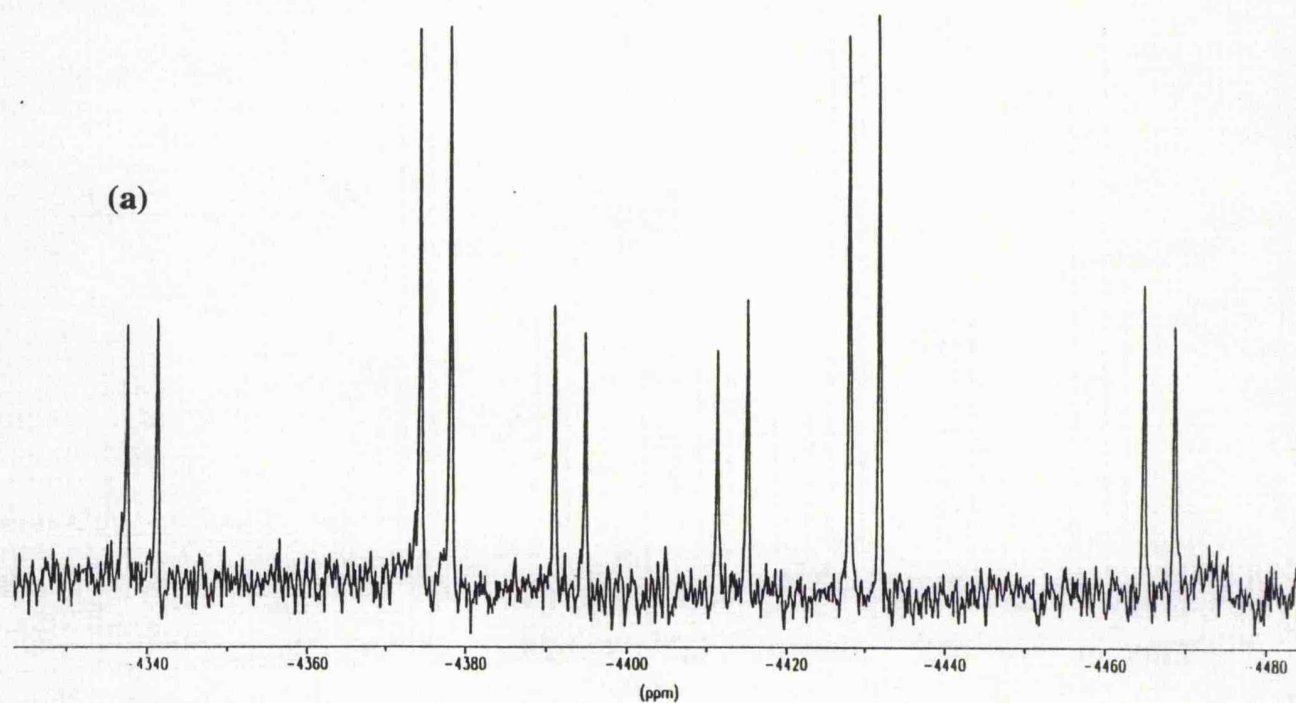


Figure 3.14 The ^{195}Pt NMR Spectrum of $[\text{PtF}(\text{PEt}_3)_3][\text{BF}_4]$ (a) and $[\text{PtF}(\text{PPh}_3)_3][\text{BF}_4]$ (b)



3.10 EXAFS Analysis of [PtF(PPh₃)₃][SbF₆]

It has been shown, in section 2.6.4, that EXAFS is a valuable technique for obtaining structural information in the absence of crystals suitable for X-ray analysis. The reliability of the data collection and treatment was confirmed by the analysis of the platinum L₁₁₁-edge EXAFS data on [PtF(PEt₃)₃][BF₄].

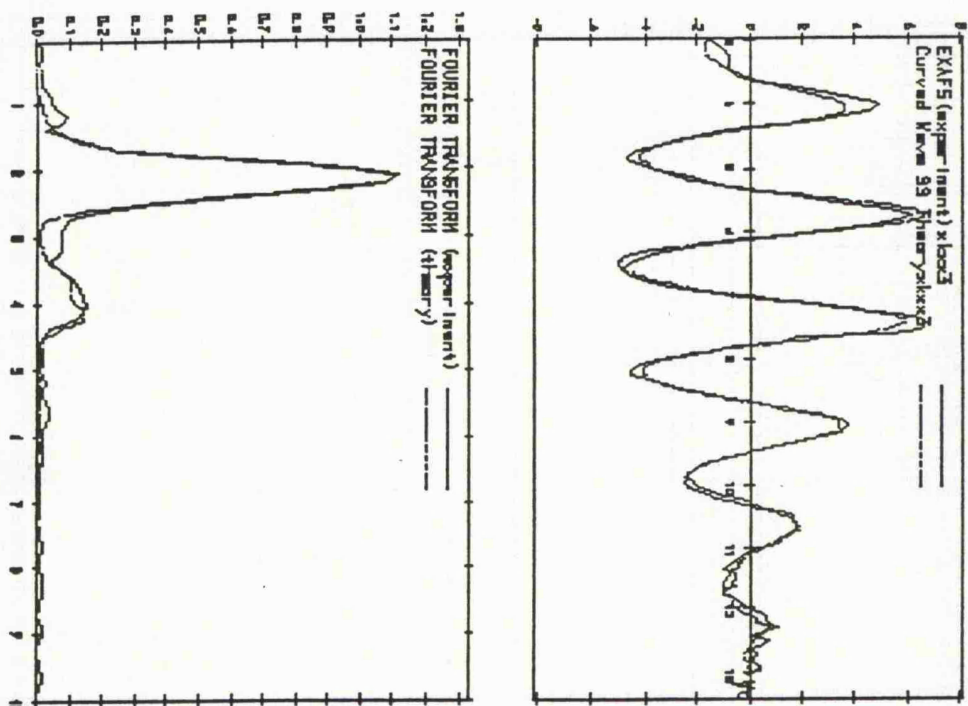
For [PtF(PEt₃)₃][BF₄] the data were modelled, utilising EXCURV92,⁷⁰ to 4 shells of 1 fluorine atom at *ca.* $r = 2.01(2)$ Å, 3 phosphorus atoms at *ca.* $r = 2.28(2)$ Å, 3 carbon atoms at a non-bonded distance of *ca.* $r = 3.73(2)$ Å and 6 carbon atoms at a non-bonded distance of *ca.* $r = 4.22(2)$ Å (Figure 3.15). The results are in satisfactory agreement, when considering the inherent accuracy of the technique, with the data obtained from the single crystal X-ray analysis (Table 3.16).

For the analogous complex [PtF(PPh₃)₃][SbF₆] the data were modelled, utilising EXCURV92,⁷⁰ to 4 shells of 1 fluorine atom at *ca.* $r = 2.03(2)$ Å, 3 phosphorus atoms at *ca.* $r = 2.27(2)$ Å, 6 carbon atoms at a non-bonded distance of *ca.* $r = 3.45$ Å and 6 further carbon atoms at a non-bonded distance of *ca.* $r = 3.72$ Å (Figure 3.16).

The bond length data obtained by EXAFS [PtF(PPh₃)₃][SbF₆] are reasonable when compared with those of the analogous complex [PtF(PEt₃)₃][BF₄] (Table 3.16).

Figure 3.15 The Background-Subtracted EXAFS (K³ weighted) and the

Fourier Transform EXAFS of [PtF(PEt₃)₃][BF₄]



```

E0      4.6D  WP1  -4.71  AFAC  0.86
EMIN    28.47  EMAX  688.76  RMIN  0.10
RMAX    10.0D  WIND  2.00  WP  0.10
FT = (1111111) FI 0.00D29 R 16.4415
N1      1.0  T1  3.0  } R1  2.012  A1  0.007
N2      3.0  T2  4.0  } R2  2.278  A2  0.014
N3      3.0  T3  4.0  } R3  3.726  A3  0.017
N4      3.0  T4  4.0  } R4  4.221  A4  0.014
EXPERIMENT Pt F03.0x
PARAMETERS Pt F03.2.par
PHASESHIFTS Pt
  
```

Figure 3.16 The Background-Subtracted EXAFS (k^3 weighted) and the

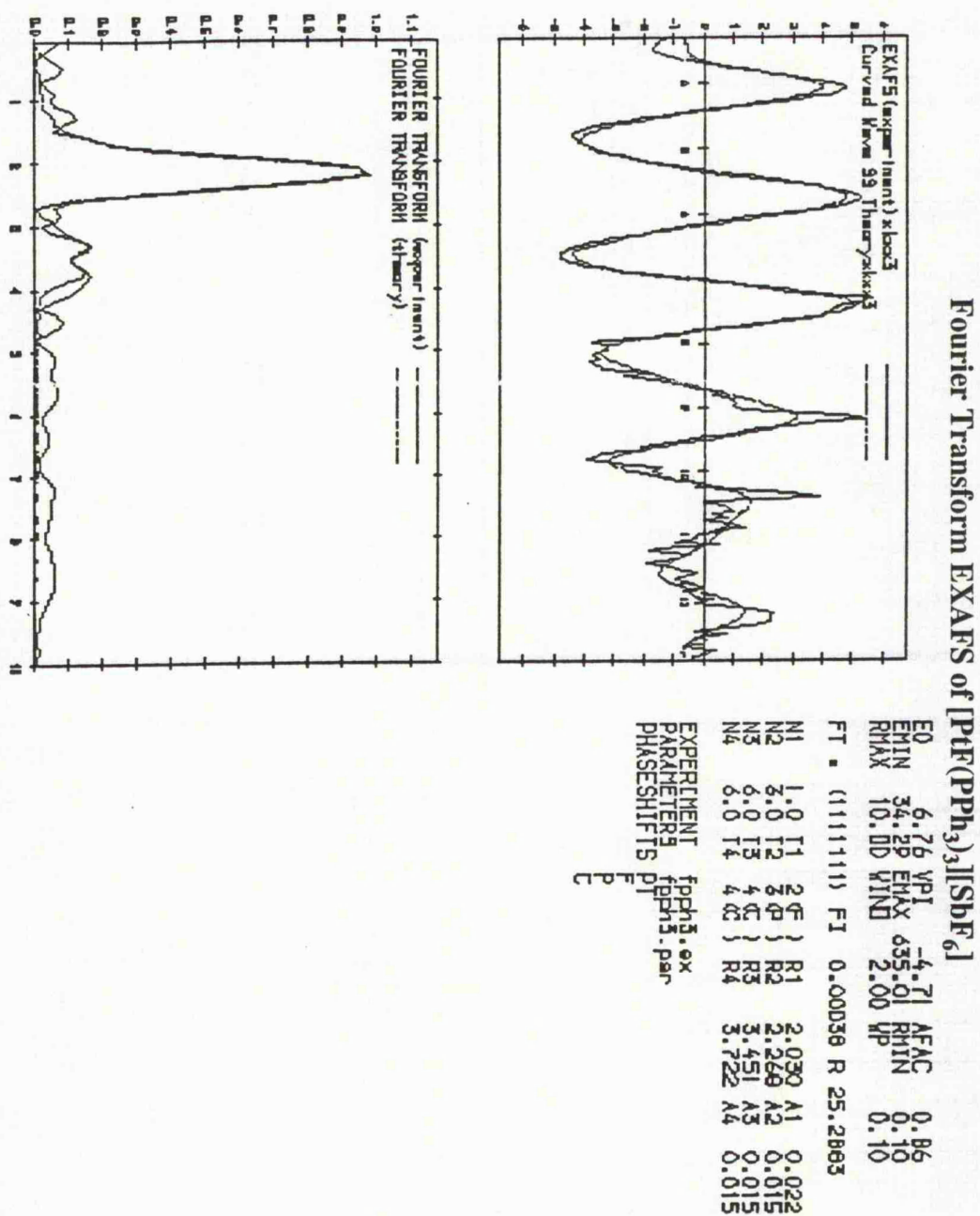


**Table 3.16 Comparison of the Bond Length (Å) Data of
[PtF(PEt₃)₃][BF₄] and [PtF(PPh₃)₃][SbF₆]**

Monocation	Pt-F	Pt-P
[PtF(PPh ₃) ₃] ⁺ ^a	2.03(2)	2.27(2)
[PtF(PEt ₃) ₃] ⁺ ^a	2.02(2)	2.28(2)
[PtF(PEt ₃) ₃] ⁺ ^b	2.043(7)	2.304(4)

(a) Data obtained from EXAFS studies

(b) Data obtained from crystal structure X-ray analysis²⁰

It is evident, from the data in Table 3.16, that the Pt-F bond length for the complex [PtF(PPh₃)₃]⁺ is the same length, within the accuracy limit of the technique (± 0.02 Å), as the analogous triethylphosphine complex. Therefore, in order to ascertain whether the Pt-F bond lengths are sufficient to explain the difference in the $^1J_{\text{PtF}}$ coupling between [PtF(PPh₃)₃]⁺ and [PtF(PEt₃)₃]⁺ a more accurate crystallographic study would have to be undertaken.

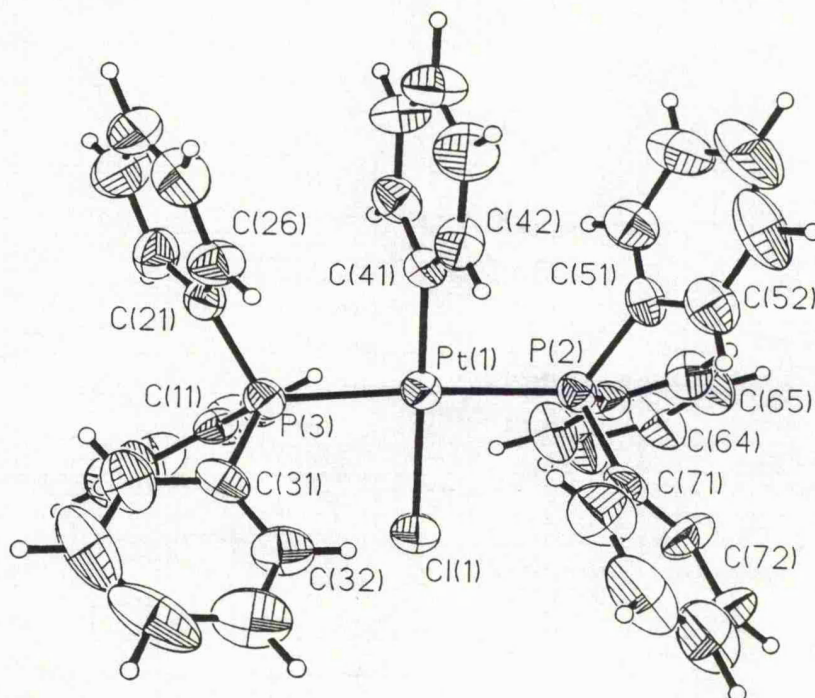
3.11 Reaction of [PtF(PPh₃)₃][X] (X = HF₂⁻ and SbF₆⁻) with CD₂Cl₂

In order to test the view held by Dixon *et al.*,¹⁷ that the weak Pt-F bond in the monocationic complex [PtF(PPh₃)₃]⁺, can be related to the anomalously low $^1J_{\text{PtF}}$ coupling, and that it had been previously reported that exposure of complexes of the type [PtF(PR₃)₃]⁺ (PR₃ = PEt₃, PMe₂Ph and PPh₃)¹⁷ to chlorinated solvents might induce fluorine-chlorine exchange it seemed of interest to investigate the reaction of [PtF(PPh₃)₃]⁺ in dichloromethane.

Initially, the complex $[\text{PtF}(\text{PPh}_3)_3][\text{HF}_2]$, formed from the reaction of $[\text{Pt}(\text{PPh}_3)_4]$ and AHF , was left in CD_2Cl_2 indefinitely. After a period of time crystals suitable for X-ray crystallographic analysis were grown. The material was found to be *trans*- $[\text{PtCl}(\text{C}_6\text{H}_5)(\text{PPh}_3)_2]$ (Figure 3.17) the structure of which had been solved previously by Conzelmann *et al.*⁷¹

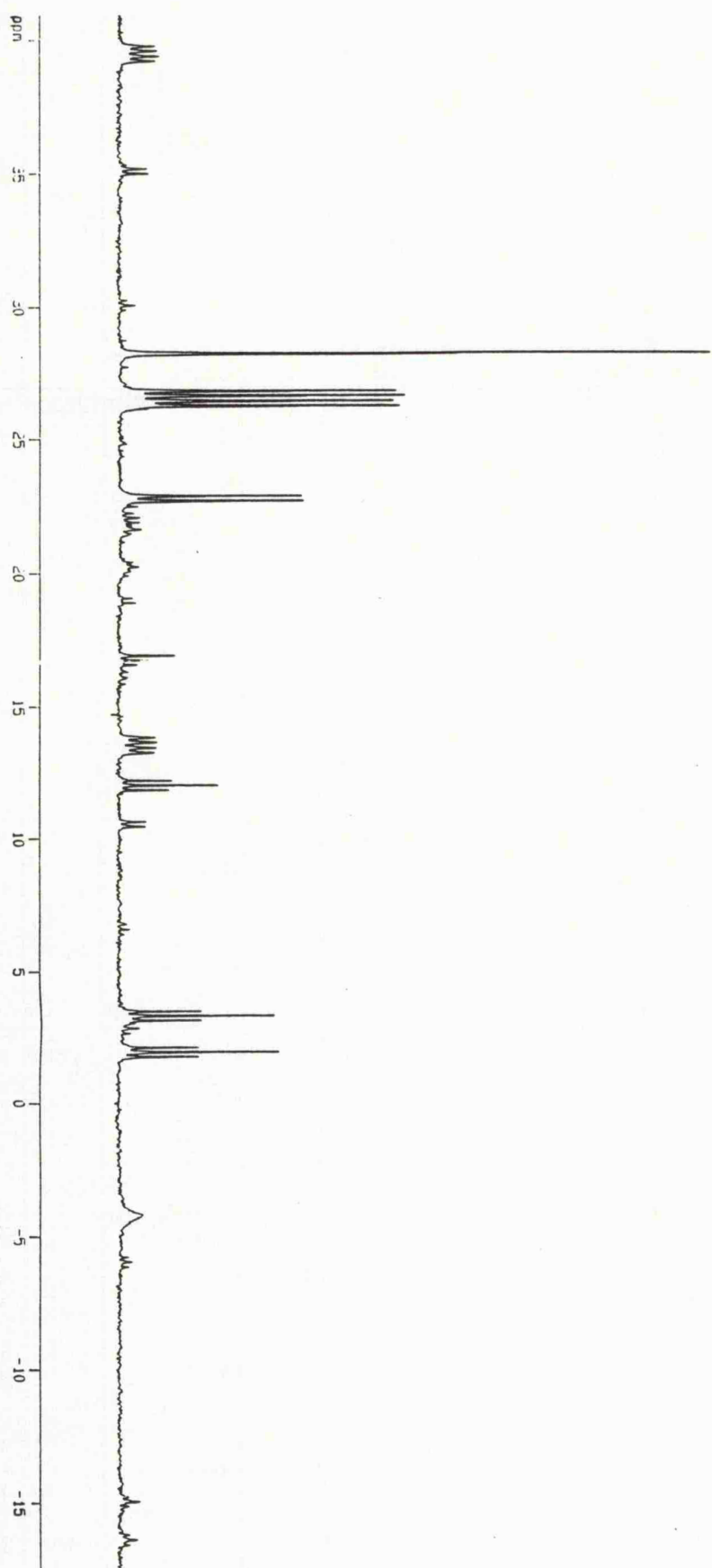
In light of this unexpected result it was thought to be of interest to investigate this decomposition process in an attempt to ascertain the intermediates.

Figure 3.17 Crystal Structure of *trans*- $[\text{PtCl}(\text{C}_6\text{H}_5)(\text{PPh}_3)_2]$



Over a period of 4 days the CD_2Cl_2 solution of $[\text{PtF}(\text{PPh}_3)_3]^+$ was monitored by $^{31}\text{P}\{^1\text{H}\}$ NMR spectroscopy. Although, no intermediates were identified decomposition ensued but, no resonance assignable to *trans*- $[\text{PtCl}(\text{C}_6\text{H}_5)(\text{PPh}_3)_2]$ was observed. It was plausible that the absence of any intermediates was a consequence of their instabilities thus, by modifying the counteranion the lifetime of any such species could be increased.

Figure 3.18 The $^{31}\text{P}\{^1\text{H}\}$ NMR Spectrum of the Products from the Reaction of $[\text{PtF}(\text{PPh}_3)_3][\text{SbF}_6]$ in CD_2Cl_2 , after 2 Hours



In an analogous study, employing the large anion $[\text{SbF}_6]^-$, the CD_2Cl_2 solution of $[\text{PtF}(\text{PPh}_3)_3][\text{SbF}_6]$ was monitored, over a period of weeks, by multinuclear NMR spectroscopy.

The $^{31}\text{P}\{^1\text{H}\}$ NMR spectrum (Figure 3.18) showed, after approximately 2 hours, the expected monofluorinated cation and suprisingly an additional platinum-containing species. The second platinum complex exhibited a mutually coupled doublet and triplet at δ 22.8 and δ 12.0 respectively with a $^2J_{\text{PP}} = 19$ Hz. The magnitude of the $^1J_{\text{PtP}}$ couplings were 2483 and 3644 Hz for the doublet and triplet resonances respectively. All the data considered there is only one explanation: the complex $[\text{PtF}(\text{PPh}_3)_3]^+$ has undergone fluorine-chlorine exchange to afford the analogous $[\text{PtCl}(\text{PPh}_3)_3]^+$. The complex $[\text{PtCl}(\text{PPh}_3)_3][\text{NO}_3]$ was reported to exhibit a doublet at δ 20.7, $^2J_{\text{PP}} = 19$ Hz, $^1J_{\text{PtP}} = 2486$ Hz and a triplet at δ 9.9, $^2J_{\text{PP}} = 19$ Hz, $^1J_{\text{PtP}} = 3645$ Hz.⁷¹ The data compares well with that for the fluorine-chlorine exchange product.

During a further two week period no other species were detected in the $^{31}\text{P}\{^1\text{H}\}$ NMR spectra however, the intensity of $[\text{PtCl}(\text{PPh}_3)_3]^+$ was found to increase relative to that of the monofluoro-complex indicating slow conversion of the latter into the former.

After another 14 days, in CD_2Cl_2 solution, 3 new mutually coupled resonances were observed in the $^{31}\text{P}\{^1\text{H}\}$ NMR spectrum all exhibiting ^{195}Pt satellites. The next $^{31}\text{P}\{^1\text{H}\}$ NMR spectrum recorded was almost 6 days later and showed that the complex $[\text{PtF}(\text{PPh}_3)_3]^+$ had completely decomposed with the monochloro-species now decreasing in intensity relative to this new platinum complex. As a consequence of the monofluoro-complex completely decomposing all the resonances and the associated ^{195}Pt satellites attributed to this new species were well resolved (Figure 3.19). The three mutually coupled resonances are two doublet of doublets at δ 21 and -68 and a triplet

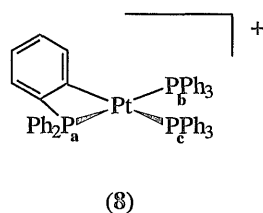
at δ 16.8, in a 1:1:1 ratio thus, indicating 3 different phosphorus environments. All the $^{31}\text{P}\{^1\text{H}\}$ NMR data for this new platinum species are presented in Table 3.17.

Table 3.17 $^{31}\text{P}\{^1\text{H}\}$ NMR Data for Complex (8)

Phosphorus atom	$\delta(^{31}\text{P})/\text{ppm}$	$^2J(\text{PP})/\text{Hz}$		$^1J(\text{PtP})/\text{Hz}$
		<i>trans</i>	<i>cis</i>	
P(a)	-68.0 (dd)	366	18	2135
P(b)	21.0 (dd)	366	18	2835
P(c)	16.8 (t)	-	18	2008

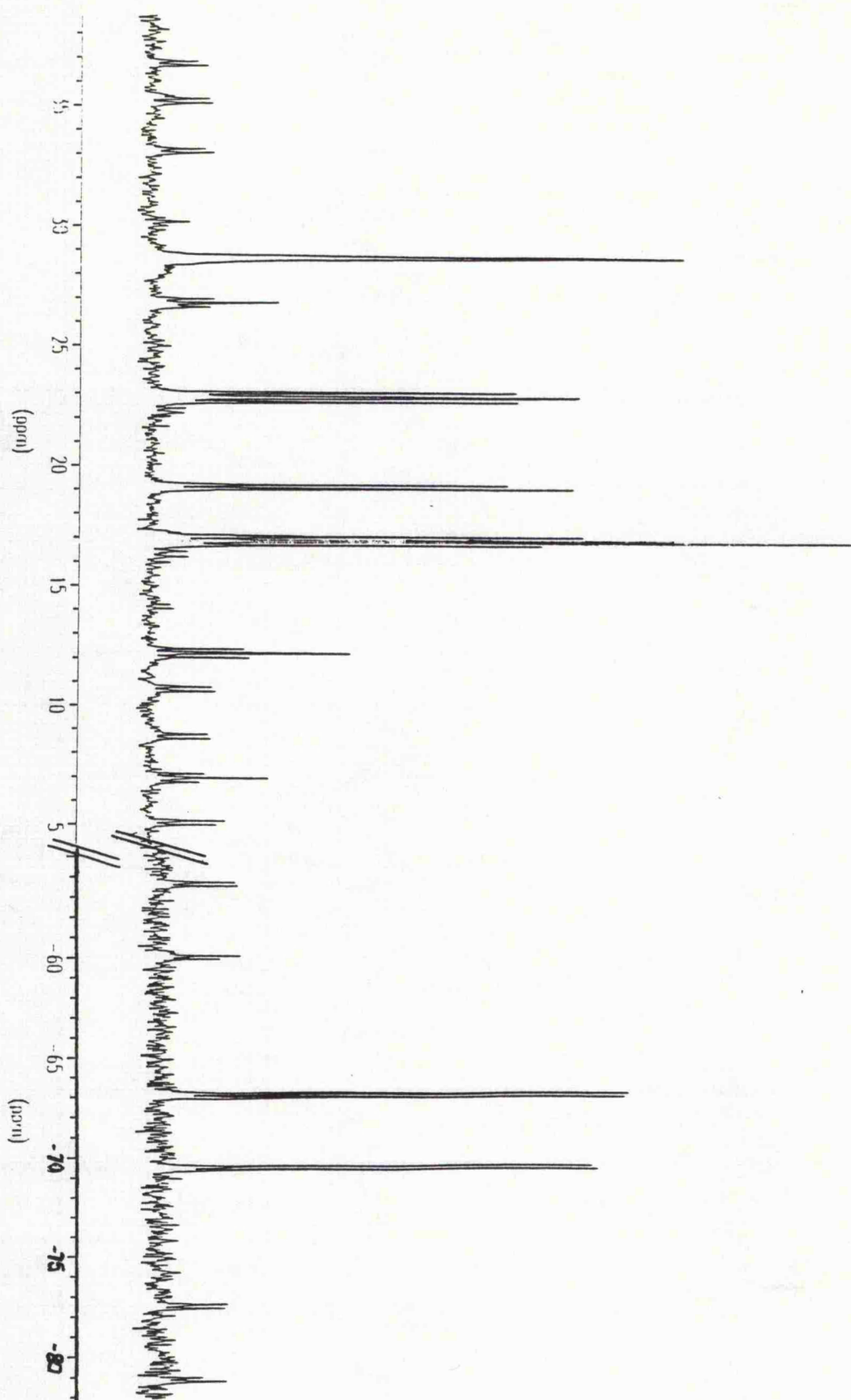
multiplicity: dd = doublet of doublets and t = triplet

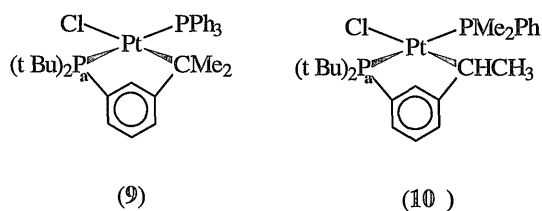
By considering all of the data, in Table 3.17, there is only one possible arrangement for three inequivalent phosphorus nuclei:-



Firstly, P_a and P_b are inequivalent by virtue of their chemical environments since P_a is bound to a phenyl ring which has orthometallated. The chemical shift of P_a is observed at an unusually low frequency but compares well with that for phosphorus atoms in the two complexes, (9) and (10), which contain phosphorus in cyclic systems.

Figure 3.19 The $^3\text{P}\{^1\text{H}\}$ NMR Spectrum of the Products from the Reaction of $[\text{PtF}(\text{PPh}_3)_3][\text{SbF}_6]$ in CD_2Cl_2 , after 14 Days





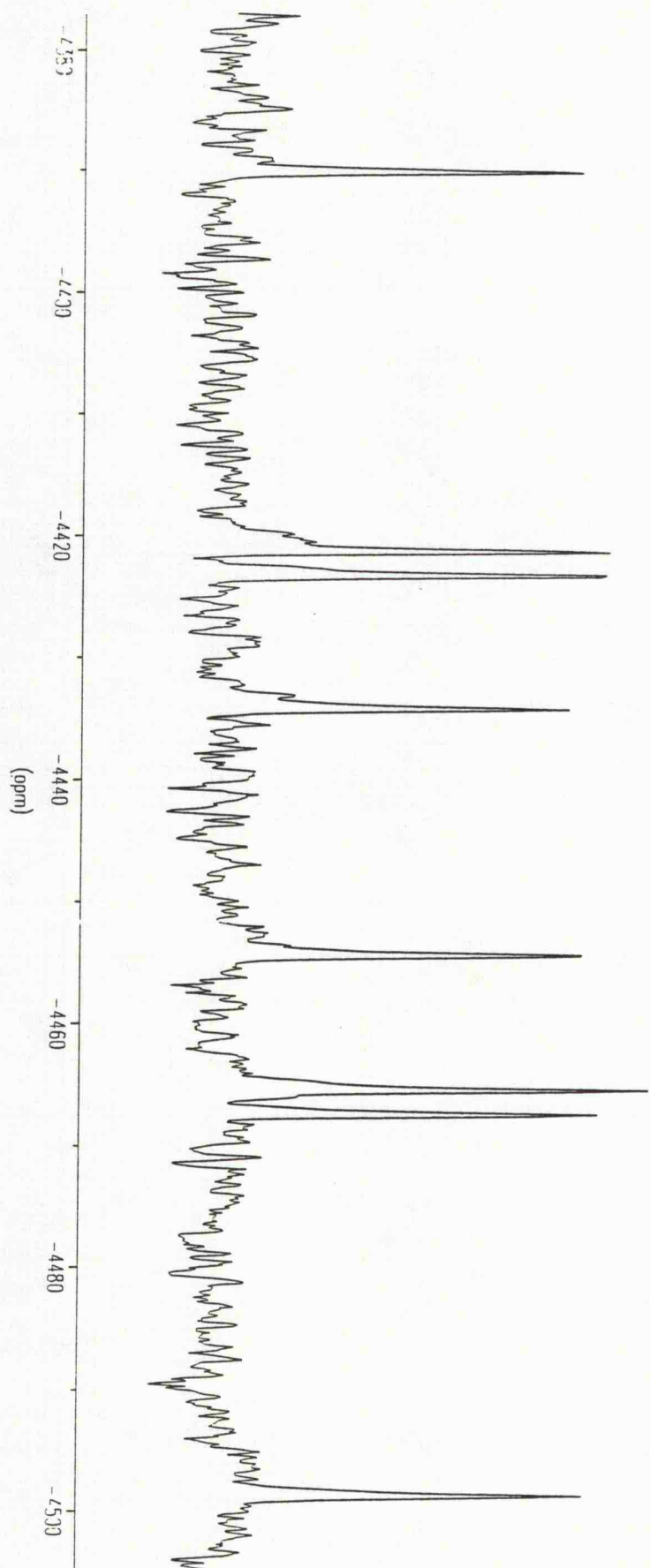
The $\delta(^{31}\text{P})$ of P_a in both complex (9) and (10) are observed at low frequencies -71.3 and -73.0 respectively.⁷³

The doublet of doublets assigned to P_a in complex (8) arises from a *trans* coupling to P_b of 366 Hz, which is characteristic of a P *trans* P coupling,⁷⁴ and a typical *cis* coupling to P_c of 18 Hz. The $^1J_{\text{PtP(a)}}$ coupling (2135 Hz) is appreciably smaller than the corresponding $^1J_{\text{PtP(b)}}$ coupling (2835 Hz). Previous reports have shown that unusually low $^1J_{\text{PtP}}$ coupling constants are a consequence of distortion of the angles at platinum and phosphorus.⁷⁵ It is evident from the bond angle data obtained from the X-ray crystal structure analysis of (8) (see section 3.12) that the internal ring angle is about 25° less than the expected value for an unconstrained Pt-P-C angle *ca.* 109° .

The doublet of doublets assigned to P_b arises from a *trans* coupling to P_a and a *cis* coupling to P_c . The chemical shift observed for P_b is in a region characteristic of P *trans* P. Furthermore, the $^1J_{\text{PtP}}$ coupling, of 2835 Hz, is of the magnitude which is typical of P *trans* P.

Finally, the triplet resonance is a consequence of P_c coupling to the apparently equivalent P_a and P_b nuclei. The $^1J_{\text{PtP}}$ coupling, of 2008 Hz, exhibited by the triplet resonance is characteristic of a phosphine ligand *trans* to an aryl group.

Figure 3.20 The $^{195}\text{Pt}\{^1\text{H}\}$ NMR Spectrum of Complex (8)



The $^{195}\text{Pt}\{^1\text{H}\}$ NMR spectrum (Figure 3.20) of (**8**) showed the expected doublet of doublets of doublets, at δ -4450, arising from platinum coupling to three inequivalent phosphorus nuclei.

A colourless solid was isolated from the CD_2Cl_2 solution which was confirmed by FAB^+ mass spectrometry to be the $[M]^+$ of (**8**) exhibiting the most intense peak centred at m/z 981.

3.12 Crystal Structure Analysis of $[\text{Pt}(\text{C}_6\text{H}_4\text{PPh}_2)(\text{PPh}_3)_2][\text{SbF}_6]$

Crystals suitable for a single crystal X-ray crystallographic study were obtained by slow evaporation of solvent from a solution of complex (**8**) in CD_2Cl_2 . The molecular structure of complex (**8**) is shown in Figure 3.21 with selected bond length and angles presented in Table 3.18.

Figure 3.21 Crystal Structure of Complex (**8**)

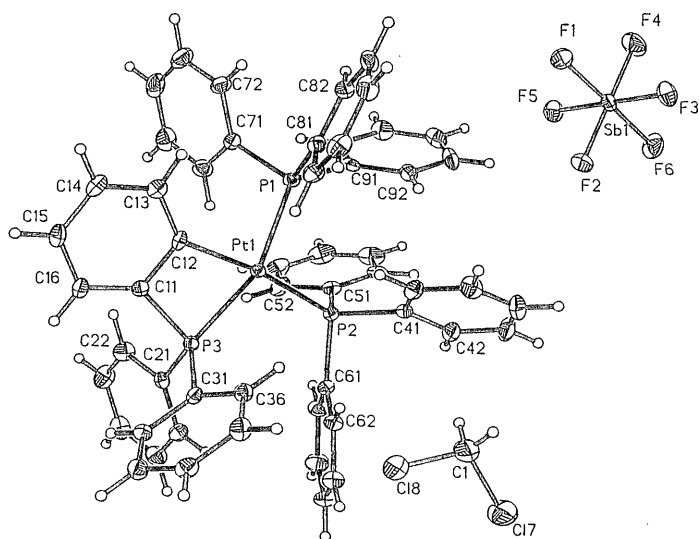


Table 3.18 Selected Bond Length (Å) and Angles (°) for Complex (8)

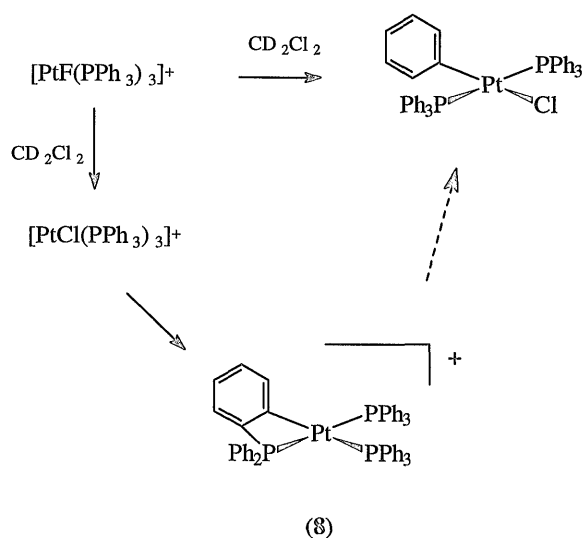
Bond Lengths	Pt-C(12) 2.090(4)	Pt-P(1) 2.3079(13)
	Pt-P(3) 2.3126(13)	Pt-P(2) 2.3229(12)
	P(3)-C(11) 1.800(5)	
Bond Angles	C(12)-Pt-P(1) 91.00(14)	C(12)-Pt-P(3) 68.4(2)
	P(1)-Pt-P(3) 158.54(4)	C(12)-Pt-P(2) 170.33(14)
	P(1)-Pt-P(2) 97.50(4)	P(3)-Pt-P(2) 102.59(4)
	C(11)-P(3)-Pt 84.7(2)	P(71)-P(1)-Pt 109.9(2)
	C(12)-C(11)-P(3) 101.1(3)	

$[\text{Pt}(\text{C}_6\text{H}_4\text{PPh}_2)(\text{PPh}_3)_2][\text{SbF}_6]$ exhibits a distorted square planar geometry with the average P-Pt-P angle being at least 10° more than unconstrained P-Pt-P angles of 90° . The C-P-Pt angle, of 84° , for the orthometallated phosphine is some 25° less than the other C-P-Pt angles which indicates a severe distortion within the complex. The Pt-P bond lengths and the Pt-C compare well with those of previously reported platinum(II) phosphine system *cf.* *trans*- $[\text{PtCl}(\text{C}_6\text{H}_5)(\text{PPh}_3)_2]$ Pt-P 2.30(3) and Pt-C 1.983(7).⁷¹

3.12 Discussion of the Decomposition of $[\text{PtF}(\text{PPh}_3)_3]^+$ in CD_2Cl_2

It is evident from the results discussed in the section 3.11 that the rate of decomposition of the monofluorinated cation is dependent on the counteranion. The decomposition rate has been shown to be faster, with the only isolated species being *trans*- $[\text{PtCl}(\text{C}_6\text{H}_5)(\text{PPh}_3)_2]$, when the anion was

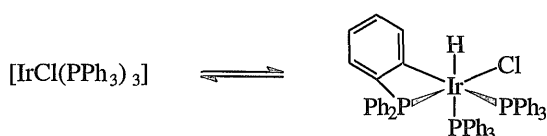
[HF₂]⁻. However, utilizing the larger anion, [SbF₆]⁻, enabled two intermediates to be isolated the monochloro-complex [PtCl(PPh₃)₃]⁺ and the novel [Pt(C₆H₄PPh₂)(PPh₃)₂]⁺. These species are the first two intermediates in the decomposition process of [PtF(PPh₃)₃]⁺ but, no evidence for the complex *trans*-[PtCl(C₆H₅)(PPh₃)₂] was found thus, the whole process is unclear. Nonetheless, these results suggest the following decomposition pathway:



As suggested by Dixon and Cairns¹⁷ the complex [PtF(PPh₃)₃]⁺ might undergo facile decomposition, indicated by the small ¹J_{PtF} coupling, in CD₂Cl₂ to afford the monochloro-analogue. The observation of the monochloro-species confirms the speculation made by Dixon and Cairns. This monochloro-complex, being sterically crowded and containing an electron rich metal centre in a low oxidation state, then subsequently undergoes orthometallation. This process undoubtedly involves intramolecular hydrogen transfer from the phosphine ligand, in which the

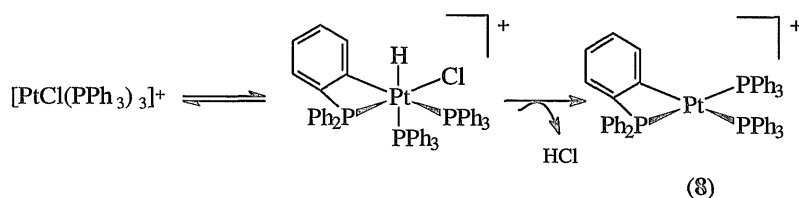
phenyl C-H bond oxidatively adds to the platinum, forming a chelate ring with the metal centre. As with the isoelectronic complex $[\text{IrCl}(\text{PPh}_3)_3]$,⁷⁶ which has been reported to undergo orthometallation (Scheme 3.16); the process involving the platinum is also feasibly reversible.

Scheme 3.16



Although, this iridium(III) complex does not reductively eliminate HCl to give the analogous Ir(I) species this is a plausible mechanistic pathway for the formation of (**8**) (Scheme 3.17).

Scheme 3.17



The driving force for the formation of (**8**) is the production of HCl which consequently forces the equilibrium over to the right.

Although, there is no direct evidence that (**8**) decomposes to give *trans*- $[\text{PtCl}(\text{C}_6\text{H}_5)(\text{PPh}_3)_2]$ it does seem a plausible route. For this decomposition pathway to occur both the Pt-P and P-C bonds, in complex

(8), must be broken. It is possible that a good proton source, such as HF or HCl produced during the orthometallation, could induce these bond cleavages yielding ultimately the complex *trans*-[PtCl(C₆H₅)(PPh₃)₂]⁷⁷ and Ph₂PCl.⁷⁶ Both species are reported to exhibit singlets in their ³¹P{¹H} NMR spectra at δ -21.4 and 78.6 for the former and the latter respectively. However, as a consequence of the nature of the counteranion, [SbF₆]⁻, the orthometallated species was stabilized to the extent whereby crystals were isolated and thus, no further decomposition ensued.

3.14 Reaction of [XeF₂] with [Pt(PEt₃)₄][PF₆]₂

In light of the success of the reactions of [XeF₂] with platinum amine complexes, discussed in chapter 2, it was thought to be of interest to investigate the potential of this reaction type in the platinum phosphine systems.

[Pt(PEt₃)₄][PF₆]₂ was allowed to react with [XeF₂] in CH₃CN, as described in section 6.18, affording a colourless solution. Analysis of this solution by ¹⁹F and ³¹P{¹H} NMR spectroscopy identified the product as [PtF(PEt₃)₃][PF₆]. The formation of this complex implies that the phosphonium ion, [Et₃PF][PF₆], has possibly been reductively eliminated from the anticipated Pt(IV) complex, [PtF₂(PEt₃)₄][PF₆]₂. However, no evidence to support the formation of this species was obtained.

The formation of this platinum(II) species indicates the apparent instability of platinum(IV) fluorides containing phosphine ligands. Furthermore, the analogous reactions with [PtF(PEt₃)₃][PF₆], *cis*-[PtCl₂(PEt₃)₂] and *cis*-[PtCl₂(dppe)] in which no assignable platinum species were observed indicates further this lack of stability of platinum(IV) fluoride-phosphine complexes. This inability to form any Pt(IV) fluoride-phosphine

complexes is further evidence to substantiate the assertion that the previously reported Pt(IV) complex, $[\text{PtF}_2\text{Cl}_2(\text{PPh}_3)_2]$ (see section 3.1.7), is incorrectly formulated.

3.15 Summary

In marked contrast to the platinum amine fluoride complexes, discussed in chapter 2, the analogous platinum phosphine systems were found to be almost incompatible with the fluoride ligand. Such a concept can be understood by considering the different donor abilities of the Lewis bases. Amines are hard σ -donors in comparison to the softer nature of phosphines. Since, the platinum centre becomes a 'harder' acid, in terms of the Pearson rules, on coordination of the fluoride ligand the amines, being harder σ -donors, are therefore more able to stabilize the platinum fluoride bond. This explains the inability to form platinum(IV) fluoride phosphine complexes.

References for Chapter Three

1. K. A. Jensen, *Zeit. Anorg. Allg. Chem.*, 1936, **229**, 225.
2. L. Malatesta and C. Cariello, *J. Chem. Soc.*, 1958, 2323.
3. B. Clarke, M. Green, R. B. L. Osborn and F. G. A. Stone, *J. Chem. Soc. (A)*, 1968, 167.
4. H. C. Clark and K. Itoh, *Inorg. Chem.*, 1971, **10**, 1707.
5. R. O. de Jongh and R. Van der Linde, *J. Chem. Soc., Chem. Commun.*, 1971, 563.
6. R. S. Paineasa and N. C. Trogler, *Organometallics*, 1982, **1**, 768.
7. D. M. Blake and C. J. Nyman, *J. Am. Chem. Soc.*, 1970, **92**, 5359.
8. N. S. Aky and H. A. Tayim, *J. Inorg. Nucl. Chem.*, 1974, **36**, 1071.
9. D. M. Roundhill, *Inorg. Chem.*, 1970, **9**, 254.
10. F. Bonati, F. Cariati and R. Ugo, *Inorg. Chem.*, 1966, **5**, 1128.
11. J. T. Dumler, K. Thomas, B. W. Renoe, C. J. Nyman and D. M. Roundhill, *Inorg. Chem.*, 1972, **11**, 1075.
12. P. Foley and G. M. Whiteside, *Inorg. Chem.*, 1980, **19**, 1402.
13. G. Doyle, *J. Organomet. Chem.*, 1982, **224**, 355.
14. J. McAvoy, K. C. Moss and D. W. A. Sharp, *J. Chem. Soc.*, 1965, 1376.
15. R. D. W. Kemmitt, R. D. Peacock and J. Stocks, *J. Chem. Soc.(A)*, 1971, 846.
16. K. R. Dixon and J. J. McFarland, *J. Chem. Soc., Chem. Commun.*, 1972, 1274.
17. M. A. Cairns, K. R. Dixon and J. J. McFarland, *J. Chem. Soc.*, 1975, 1159.
18. G. G. Mather, A. Pidcock and (the late) G. J. N. Rapsey, *J. Chem. Soc., Dalton Trans.*, 1973, 2095.
19. J. Howard and J. Woodwood, *J. Chem. Soc. Dalton Trans.*, 1973, 418.

20. D. R. Russell, M. A. Mazid and P. A. Tucker, *J. Chem. Soc. Dalton Trans.*, 1973, 1620.
21. K. R. Dixon and D. J. Hawke, *Canad. J. Chem.*, 1971, **49**, 3252.
22. D. W. W. Anderson, E. A. V. Ebsworth and D. W. H. Rankin, *J. Chem. Soc. Dalton Trans.*, 1973, 854.
23. J. Clemens, M. Green and F. G. A. Stone, *J. Chem. Soc. Dalton Trans.*, 1973, 1620.
24. M. I. Bruce, R. C. F. Gardner and F. G. A. Stone, *J. Chem. Soc. Dalton Trans.*, 1976, 81.
25. C. M. Jones and N. M. Doherty, Unpublished results; Ref. 57.
26. W. J. Bland and R. D. W. Kemmitt, *J. Chem. Soc.(A)*, 1969, 2062.
27. R. J. Meyer and E. H. Erich, 'GMELINS Handbuch Der Anorganischen Chemie', Verlag Chemie G. M. B. H., Berlin, 1957, **68**, 349.
28. C. A. McAuliffe (ed.) 'Transition Metal Complexes of Phosphorus, Arsenic and Antimony', Wiley, New York, 1973.
29. J. Chatt and R. G. Wilkins, *J. Chem. Soc.*, 1951, 2532.
30. G. B. Kauffmann and L. A. Teter, *Inorg. Synth.*, 1963, **7**, 245.
31. D. Cole-Hamilton, *J. Chem. Soc. Dalton Trans.*, 1984, 2249.
32. J. Kozelka, H. Luthi, E. Dubler and R. W. Kunz, *Inorg. Chim. Acta.*, 1984, **86**, 155.
33. R. G. Pearson and M. M. Muir, *J. Am. Chem. Soc.*, 1966, **88**, 2163.
34. F. Basolo, H. B. Gray and R. G. Pearson, *J. Am. Chem. Soc.*, 1960, **88**, 4200.
35. J. Chatt and B. T. Heaton, *J. Chem. Soc.(A)*, 1968, 2745.
36. J. Chatt and J. M. Davidson, *J. Chem. Soc.*, 1964, 2433.
37. R. G. Hayter and S. F. Humiec, *Inorg. Chem.*, 1963, **2**, 306.
38. G. W. Bushnell, K. R. Dixon, R. G. Hunter and J. J. McFarland, *Can. J. Chem.*, 1972, **50**, 2694.

39. M. M. Muir and E. M. Cancio, *Inorg. Chim. Acta*, 1970, **4**, 565.
40. M. M. Muir and E. M. Cancio, *Inorg. Chim. Acta*, 1970, **4**, 568.
41. Encyclopedia, see A. Dedieu, 'Hydride Complexes of the Transition Metals', Cambridge 1992.
42. J. D. Kennedy, W. McFarland, R. J. Puddephatt and P. J. Thompson, *J. Chem. Soc. Dalton Trans.*, 1976, 874.
43. F. R. Hartley, 'The Chemistry of Platinum and Palladium' Applied Science publishers Ltd. London, 1973, **12**, 324; and references cited therein.
44. C. R. Kistner, J. H. Hutchinson, J. R. Doyle and J. C. Storlie, *Inorg. Chem.*, 1963, **2**, 1255.
45. G. Booth and J. Chatt, *J. Chem. Soc. (A)*, 1966, 634.
46. J. Chatt and J. M. Davidson, *J. Chem. Soc.*, 1959, 4020.
47. J. Chatt and B. L. Shaw, *J. Chem. Soc.*, 1962, 5075.
48. J. Chatt and B. L. Shaw, *J. Chem. Soc.*, 1959, 705.
49. N. M. Doherty and S. C. Critchlow, *J. Am. Chem. Soc.*, 1987, **109**, 7906
50. D. R. Coulson, *J. Am. Chem. Soc.*, 1976, **98**, 3111.
51. J. H. Simons in 'Fluorine Chemistry,' ed. J. H. Simons, Academic Press, New York, 1950, **1**, 225.
52. R. D. W. Kemmitt, R. D. Peacock and J. Stocks, *J. Chem. Soc., Chem. Commun.*, 1969, 554.
53. H. C. Clark and W. S. Tsang, *J. Am. Chem. Soc.*, 1967, **89**, 529.
54. A. D. Troitskaya and Z. L. Shimakova, *Russ. J. Chem. (Engl. Transl)*, 1971, **16**, 872.
55. G. Booth, *Adv. Inorg. Chem. Radiochem.*, 1964, **6**, 1.
56. R. W. Cockman, E. A. V. Ebsworth, J. H. Holloway, H. Murdoch, N. Robertson and P. G. Watson, "Reaction of Non-metal Fluorides with

some Platinum Metal Complexes," J. Thrasher and S. Strauss, ACS Symposium Series, ACS Books, 1994.

57. K. Coleman, Personal Communications.
58. Ref. 42 and R. K. Harris, K. J. Packer and P. Reams, *J. Chem. Soc., Dalton Trans.*, 1986, 1015.
59. D. W. Anderson, E. A. V. Ebsworth and D. W. H. Rankin, *J. Chem. Soc., Dalton Trans.*, 1973, 2370; P. S. Pregosin, *Coord. Chem. Rev.*, 1982, 44, 247.
60. A. Pidcock, R. E. Richards and L. M. Venanzi, *J. Chem. Soc. (A)*, 1966, 1707.
61. F. H. Allen, A. Pidcock and C. R. Waterhouse, *J. Chem. Soc. (A)*, 1970, 2087; F. H. Allen and S. N. Sze, *J. Chem. Soc. (A)*, 1971, 2054; L. M. Venanzi, *Chem. Brit.*, 1968, 4, 162; E. R. Hammer, R. D. W. Kemmitt and M. A. R. Smith, *J. Chem. Soc., Dalton Trans.*, 1977, 261.
62. G. K. Anderson and R. J. Cross, *Acc. Chem. Rev.*, 1984, 17, 67.
63. R. S. Paonessa, A. L. Prignano and W. C. Trogler, *Organometallics*, 1985, 4, 647.
64. L. Vaska, *J. Am. Chem. Soc.*, 1966, 88, 5325.
65. H. C. Clark, K. R. Dixon and W. J. Jacobs, *J. Am. Chem. Soc.*, 1969, 91, 1346.
66. D. H. Gerloch, A. R. Kane, G. W. Parshall and E. L. Muetterties, *J. Am. Chem. Soc.*, 1971, 93, 3543.
67. D. Grove and L. M. Venanzi, Unpublished results, ETH-Zurich, 1977.
68. D. Grove and L. M. Venanzi, Unpublished results, ETH-Zurich, 1977; P. Boron and L. M. Venanzi, Unpublished results, ETH-Zurich, 1977.
69. H. C. Clark, K. R. Dixon and W. J. Jacobs, *J. Am. Chem. Soc.*, 1968, 90, 2259.

70. EXCURV92, SERC Daresbury Laboratory Program, N. Binstead, S. J. Gurman and J. W. Cambell, 1992.
71. W. Conzelmann, J. D. Koola, U. Kunze and J. Stahle, *Inorg. Chim. Acta*, 1984, **89**, 147.
72. F. Dejong, J. J. Bour and P. P. J. Schlebos, *Inorg. Chim. Acta*, 1988, **154**, 89.
73. P. S. Pregosin and R. W. Kunz, ³¹P and ¹³C NMR of Transition Metal Phosphine Complexes' Springer-Verlag, Berlin, Heidelberg, New York, 1979.
74. P. S. Braterman, R. J. Cross, L. Manojlovic-Muir, K. W. Muir and G. Young, *J. Organomet. Chem.*, 1975, **84**, C40.
75. P. Bhattacharya, PhD Thesis, Imperial College, London, 1995.
76. G. M. Parshall, *Acc. Chem. Rev.*, 1970, **3**, 139.
77. C. Eaborn, K. J. Odell and A. Pidcock, *J. Chem. Soc., Dalton Trans.*, 1978, 357.
78. R. Appel, K. Geisler and H. Scholer, *Chem. Ber.*, 1977, **110**, 376.

CHAPTER

FOUR

The Reactions of Iridium(I) Carbonyl-

Phosphine Complexes with Xenon

Difluoride

4.1 A Brief History of Vaska's Complex and its Analogues

Vaska first prepared the complex, *trans*-[IrCl(CO)(PPh₃)₂],¹ in 1961, and ever since reactions involving this complex and related species is probably one of the most extensively studied areas in organotransition-metal chemistry. A variety of analogous Vaska's complexes of the type, *trans*-[IrX(CO)(PPh₃)₂] (X = anionic ligand), have appeared in the literature.² Principle methods of preparation for the Vaska's complex are treatment of [IrCl₃·H₂O] with the phosphine, either after passage of CO or more usually by refluxing in a CO-releasing solvent, such as a high-boiling alcohol or DMF.³ Replacement of the chloride ligand by other anions, e.g. F, I and Br, can be conveniently achieved by metathesis, or by treatment with [NaBH₄].^{3,4} The variation of $\nu(\text{CO})$ values with anion has been correlated with the total electronegativity or π -donor ability of X. Ligands such as F with a high π -donor ability result in low $\nu(\text{CO})$ values³ (Table 4.1).

Table 4.1 $\nu(\text{CO})$ of Complexes of the type *trans*-[IrX(CO)(PPh₃)₂]²

X	$\nu(\text{CO})^a \text{ cm}^{-1}$
F	1957
Cl	1965
Br	1966
I	1967

(a) CHCl₃ solution

As mentioned earlier in this section, these complexes and their chemical behaviour have been extensively studied. One of the major areas investigated has been oxidative addition reactions, whereby a general

molecule AB adds to *trans*-[IrX(CO)(PPh₃)₂] such that the product [IrX(A)(B)(CO)(PPh₃)₂] now contains iridium in oxidation state +(III). The scope for AB is large, in that HX, X₂ or RX (X = Cl, Br, I, F; R = alkyl etc) or a very wide range of related molecules may be employed. The octahedral Ir(III) products formed are generally stable and readily characterized, and, on the basis of infrared and ¹H NMR spectroscopic studies, it has been concluded, many years ago, that the addition is stereospecifically *cis*, with the phosphine ligands remaining mutually *trans*.⁵

For the preparation of analogues of Vaska's complex that contain other tertiary phosphine or arsine ligands, there are several methods that appear in the literature. The five most convenient methods are described below :-

(A) Treating a boiling solution of Na₃[IrCl₆] or other halide salt of iridium(III) in alcohol with CO, followed by cooling and addition of the appropriate ligand.⁶

(B) Ligand exchange may be carried out on Vaska's complex in toluene or similar solvents.⁷

(C) Preparation of [IrCl(CO)₂(toluidine)] followed by treatment with the appropriate phosphine.⁸

(D) Reaction of the polymer, [IrCl(CO)₃]_n, with 2 molar equivalents of the appropriate phosphine in refluxing toluene.⁹

(E) Reaction of [IrX₃] (X = Cl, Br) with 2 molar equivalents of the appropriate phosphine in refluxing 2-methoxyethanol.¹⁰

A vast number of complexes of the type, *trans*-[IrX(CO)L₂] (X = halide or pseudohalide, hydride) have been prepared by these methods and a range of representative examples are presented in Table 4.2, together with their methods of preparation and their characteristic carbonyl stretching frequencies.

Table 4.2 Complexes of the type *trans*-[IrX(CO)L₂]

X	L	$\nu(\text{CO}) \text{ cm}^{-1\text{a}}$	Preparation	Refs.
Br	PEt ₃	1990	A, B, C	6, 7, 8
Cl	PEt ₂ Ph	1934	A, C	6, 8
I	PEt ₂ Ph	1945	A, C	6, 8
Cl	PMe ₂ Ph	1960	A	6
Br	PMe ₂ Ph	1961	A	6
I	PMe ₂ Ph	1957	A	6
Cl	PMe ₃	1938	A, B	6, 7
Cl	PCy ₃	1931	A, D	6, 9
Cl	P(C ₆ F ₅) ₃	1995	E	10
Br	P(C ₆ F ₅) ₃	1996	E	
Cl	AsPh ₃	1958	A, C	

(a) Nujol mulls

Although complexes of the type *trans*-[IrX(CO)L₂] (X = Cl, Br and I) are well studied and characterized, the fluoride-containing analogues are, in comparison, relatively unexplored. In the following section the chemistry of fluoride-containing species reported in the literature will be outlined.

4.2 Fluoride-Containing Vaska's complexes

Reaction of the Vaska's complex with AgF in boiling acetone affords the fluoro-analogue in low yield.¹¹ However, the modification of this synthetic route by the *in situ* formation of AgF from the reaction of [Ag₂CO₃] with [NH₄F] in methanol leads to a substantial increase in yield.^{3b}

Subsequently tri-*p*-tolylphosphine,¹² alkylidiphenyl-phosphine,¹³ AsPh₃^{14,15} and SbPh₃¹⁴ fluoro-Vaska's derivatives have been prepared by this route. The majority of the formulations reported in the literature have been reliant mainly upon infrared data, of the carbonyl stretching frequencies, and elemental analysis where frequently the authors did not analyse for fluorine. Conclusive evidence for the iridium fluoride bond in fluoro-Vaska's complex has been obtained from ³¹P{¹H} NMR studies (Table 4.3) and, to date, these are the only reported NMR data for an Ir(I) fluoro-complex.¹⁶

**Table 4.3 ³¹P{¹H} NMR Data for Complexes of the type *trans*-
[IrX(CO)(PPh₃)₂]**

X	δ(³¹ P)/ ppm	Ref.
F ^a	24.4 ^b	16
Cl	23.9 ^c	17
Br	22.4 ^c	17
I	19.5 ^b	16

(a) appears as a doublet, ²J_{PF} 19.7 Hz (b) In CD₂Cl₂

(c) In C₆D₆ solution at 40°C

As with the carbonyl stretching frequencies discussed in section 4.1 there is a definite trend, in that substitution of a lighter halogen results in a shift to higher frequency for the ³¹P{¹H} resonance. This can be attributed to the increased electronegativity of the halogen and, thus, the extent of deshielding of the phosphorus nuclei.

Forster¹⁸ has reported that halide preference in aprotic media for the d⁸ complexes *trans*-[MX(CO)(PPh₃)₂] (M = Rh, Ir) follows the order X = Cl > Br > I. Hence, contrary to the Pearson hard and soft acid and base predictions, in aprotic solvents, the fluoro-derivatives may frequently be

found to be the most stable halocarbonyl species. Thus, fluoride would be expected to be preferred over chloride in CH_2Cl_2 . This observed halide preference is consistent with a strong π -back-bonding effect related to the ability of the anion to compete with the *trans*-CO ligand in removing electron density from Rh(I) $d\pi$ -orbitals ($\text{F} < \text{Cl} < \text{Br} < \text{I}$).¹⁹ This can be directly related to the $\nu(\text{CO})$ values observed for *trans*- $[\text{IrX}(\text{CO})(\text{PPh}_3)_2]$, which follow the trend $\text{X} = \text{F} < \text{Cl} < \text{Br} < \text{I}$ (Table 4.1). However, the lability of the fluoride ligand, in protic solvents, is greatly increased by virtue of the strong hydrogen bonding of the uncomplexed fluoride ion to the protons of the solvent (see chapter 1). As a result of this phenomenon various derivatives of *trans*- $[\text{MX}(\text{CO})(\text{PPh}_3)_2]$ ($\text{M} = \text{Rh}, \text{Ir}$)²⁰ have been synthesized, by Vaska and Peone, from the metathesis reaction of *trans*- $[\text{MF}(\text{CO})(\text{PPh}_3)_2]$ in methanol.

The reaction between dioxygen and *trans*- $[\text{IrX}(\text{CO})\text{L}_2]$ are considered as acid-base reactions, with the metal complex acting as a Lewis base. Thus, factors increasing the electron density at the metal centre, in the absence of unfavourable steric effects, should enhance oxygen addition. It has been shown that the relative rates of dioxygen uptake by the complexes *trans*- $[\text{IrX}(\text{CO})(\text{PPh}_2\text{R})_2]$ ($\text{R} = \text{Ph}, \text{Me}, \text{Et}$ and $\text{X} = \text{F}, \text{Cl}, \text{Br}$ and I) follow the order $\text{R} = \text{Ph} < \text{Et} < \text{Me}$ and $\text{X} = \text{F} < \text{Cl} < \text{Br} < \text{I}$,¹³ which represent an increase in phosphine basicity and a decrease in the electronegativity of the halogen. Variation of the halide enhanced the rate of oxygen take up, by the complexes *trans*- $[\text{IrX}(\text{CO})(\text{PPh}_2\text{R})_2]$, in the order $\text{F} < \text{Cl} < \text{Br} < \text{I}$. Thus, this was used to argue the opposite trend for increased electron density at the metal centre, previously derived from the $\nu(\text{CO})$ frequencies.

Although, complexes of the type *trans*- $[\text{IrF}(\text{CO})\text{L}_2]$ ($\text{L} = \text{Lewis base}$) have been relatively well studied only for the triphenylphosphine derivative has $^{31}\text{P}\{^1\text{H}\}$ and ^{19}F NMR spectroscopic data been reported.

It has been shown that the Ir(I) chloro- and fluoro-derivatives do undergo oxidative addition reactions to the corresponding Ir(III) complexes

and throughout the following sections these reactions with other reagents will be discussed further.

4.3 Iridium(III) Fluoro-Carbonyl-Phosphine Complexes

The preparations of Ir(III) fluoro-carbonyl-phosphine complexes were, until recently, almost entirely dominated by the oxidative fluorination of a substrate A-B to *trans*-[IrX(CO)(PR₃)₂] (X = Cl, Br or I and A-B is a fluorinating agent); or alternatively by the oxidative addition reaction of A-B with *trans*-[IrF(CO)(PPh₃)₂]. Described in the following sections are the iridium(III) carbonyl-phosphine-fluoride complexes formed by these methods.

4.3.1 Oxidative Fluorination Reactions of Vaska's Complex and its Derivatives

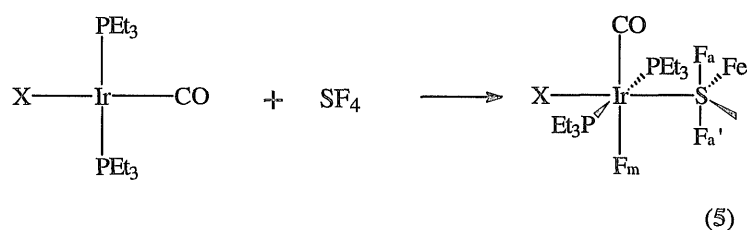
The complexes prepared by this method are listed below in Table 4.4.

The formulations of (1), (2), (3) and (4) in Table 4.4, according to their reports, depend on the $\nu(\text{CO})$ frequencies and/or their elemental analysis without fluorine being analysed and thus, there is little evidence to support such formulations. The synthesis of [IrFX(SF₃)(CO)(PEt₃)₂] (X = Cl, Br and I), formed from the reaction of *trans*-[IrX(CO)(PEt₃)₂] and [SF₄] in CH₂Cl₂ at 200 K (Scheme 4.1), was the first concerted effort to form Ir(III) complexes containing a terminal fluoride ligand.

**Table 4.4 Iridium(III) Fluoro-Carbonyl-Phosphine Complexes Formed
by the Reaction of *trans*-[IrX(CO)L₂] with a Substrate A-B**

Product	Reagent	Refs.
[IrFClH(CO)L ₂] (1) L = PMe ₃ , PPh ₃	<i>trans</i> -[IrCl(CO)L ₂] + [HCOF]	21
[IrFHX(CO)(PPh ₃) ₂] (2) X = Cl, Br, I	<i>trans</i> -[IrX(CO)(PPh ₃) ₂] + HF	5
[IrFCl(SO ₂ C ₁₀ H ₇)(CO)(PPh ₃) ₂] (3)	<i>trans</i> -[IrCl(CO)(PPh ₃) ₂] + [FSO ₂ C ₁₀ H ₇]	22
[IrFCl ₂ (CO)(PPh ₃) ₂] (4)	<i>trans</i> -[IrCl(CO)(PPh ₃) ₂] + [SF ₅ Cl]	23
[IrFX(SF ₃)(CO)L ₂] (5) X = Cl, Br, I and L = PEt ₃ , PEt ₂ Ph, PMe ₂ Ph, PEtPh ₂ and PPh ₃	<i>trans</i> -[IrX(CO)L ₂] + [SF ₄]	24,25
[IrFX(SeF ₃)(CO)L ₂] (6) X = Cl, Br, I and L = PEt ₃ , PEt ₂ Ph, PMe ₂ Ph, PEtPh ₂ and PPh ₃	<i>trans</i> -[IrX(CO)L ₂] + [SeF ₄]	25
[IrF ₂ X(CO)(PEt ₃) ₂] (7) X = Cl, Br, I	<i>trans</i> -[IrX(CO)(PEt ₃) ₂] + [XeF ₂]	25
[IrFCl(NSF ₂)(CO)(PPh ₃) ₂] (8)	<i>trans</i> -[IrCl(CO)(PPh ₃) ₂] + [NSF ₃]	26

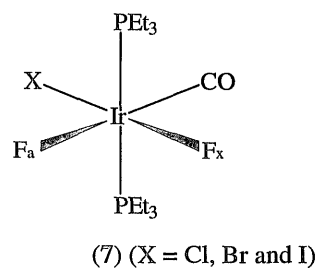
Scheme 4.1



This ultimately led Cockman *et al.* to investigate the oxidative fluorinating properties of $[\text{SF}_4]$, $[\text{SeF}_4]$ and $[\text{XeF}_2]$ with Vaska's derivatives, as these were anticipated to afford the d^6 fluoro-complexes. Low-temperature multinuclear NMR spectroscopy was applied to study these reactions. As a result, the importance of this analytical technique in elucidating reaction products within such systems was recognized. The complexes, $[\text{IrFX}(\text{SF}_3)(\text{CO})(\text{PEt}_3)_2]$ ($\text{X} = \text{Cl}, \text{Br}$ and I),²⁵ were identified by their ^{19}F and $^{31}\text{P}\{^1\text{H}\}$ NMR spectra, with the chloro-analogue being characterized by partial elemental analysis, infrared spectroscopy and the first single crystal X-ray diffraction study of an Ir(III)-F complex. In the ^{19}F NMR spectrum at 200 K resonances assignable to the metal-bound fluoride *trans* to carbonyl were observed at relatively low frequencies (δ -336 to -356), and three resonances, in the region associated with F bound to a main-group element, were attributed to the SF_3 ligand. The three resonances observed at 200 K, are a result of the inequivalence of the fluorines due to the lone pair of electrons of the S(IV). At 298 K, the resonances assigned to the three SF nuclei gave a single very broad peak. Recently, this fluxional behaviour was found to be influenced by the other ligands in the complex, and by their geometric relationship.²⁴ In the series $[\text{IrFX}(\text{SF}_3)(\text{CO})(\text{PEt}_3)_2]$ coalescence temperatures increase in the order $\text{F} < \text{Cl} < \text{Br} < \text{I}$. The authors also reported that changing the ligand, L, had a dramatic effect on the spectra. In

$[\text{IrFX}(\text{SF}_3)(\text{CO})\text{L}_2]$, where L is a tertiary phosphine, similar spectra were obtained for PEt_3 , PEt_2Ph , PMe_2Ph and PPh_3 ; when $\text{L} = \text{PEtPh}_2$, two isomers are formed, one with F *trans* to CO and the other with F *trans* to X, while the complex with $\text{L} = \text{PPh}_3$ reacts slowly with $[\text{SF}_4]$, and no reaction is observed when $\text{L} = \text{Pcy}_3$. Although, analogous SeF_3 derivatives (**6**) are formed from the reaction of *trans*- $[\text{IrCl}(\text{CO})(\text{PEt}_3)_2]$ and $[\text{SeF}_4]$, the corresponding TeF_3 complexes are found to be short lived and decomposed even at low temperatures.

The reaction of *trans*- $[\text{IrX}(\text{CO})(\text{PEt}_3)_2]$ ($\text{X} = \text{Cl}, \text{Br}$ and I) with $[\text{XeF}_2]$ is smooth at 240 K in CH_2Cl_2 . Low-temperature ^{19}F and $^{31}\text{P}\{^1\text{H}\}$ NMR spectra revealed that the reaction afforded xenon and, predominately, the anticipated Ir(III) complex $[\text{IrF}_2\text{X}(\text{CO})(\text{PEt}_3)_2]$, in which the fluorine atoms adopt a *cis* configuration and the phosphines are mutually *trans*. As a result of intermolecular halogen exchange, small amounts of the two isomeric monofluorides $[\text{IrFX}_2(\text{CO})(\text{PEt}_3)_2]$, and the trifluoride, $[\text{IrF}_3(\text{CO})(\text{PEt}_3)_2]$ are also formed. However, these products represent only 10 % of the mixture.



The ^{19}F NMR spectrum of (7) revealed two doublets of triplets of equal intensity. One was in the chemical shift region associated with F *trans* CO and the other in a region assignable to F *trans* to a halide (Table 4.5).

Table 4.5 ^{19}F and $^{31}\text{P}\{^1\text{H}\}$ NMR Data for *cis*- $[\text{IrF}_2\text{X}(\text{CO})(\text{PEt}_3)_2]^{25}$

Chemical Shifts/ ppm				Coupling Constants/ Hz		
X	$\delta(\text{P})$	$\delta(\text{F}_a)$	$\delta(\text{F}_x)$	$^2J(\text{F}_a\text{F}_x)$	$^2J(\text{PF}_a)$	$^2J(\text{PF}_x)$
F	6.9	-288.5	-470.6	96	31	18
Cl	6.1	-299.1	-488.7	115	29	18
Br	4.7	-303.2	-392.0	130	31	22
I	3.2	-313.8	-364.6	143	33	21

With reference to Table 4.5, certain trends in NMR parameters are observed. Not only are there two distinct ranges for the ^{19}F chemical shifts, but there is also a trend in the coupling constants. Notably, $^2J_{\text{PF}_a}$ is invariably larger than $^2J_{\text{PF}_x}$, with only a slight dependency on X. In contrast the magnitude of $^2J_{\text{FF}}$ shows a strong dependency on X following the order $\text{F} < \text{Cl} < \text{Br} < \text{I}$. The $\delta(\text{F}_x)$ values, with the exception of the chloride analogue, which is probably an error in the literature, are reported to shift to higher frequency on substitution of a lighter for a heavier halogen. This trend is as expected since the π -acceptor ability for the halides follows the order $\text{F} < \text{Cl} < \text{Br} < \text{I}$ therefore, the fluoride nucleus assigned to F *trans* I resonance, in the iodo-complex, will be deshielded with respect to the other halo-species. Finally, the $\delta(\text{F}_a)$ values shift to lower frequency on substitution of a lighter for a heavier halogen.

Watson *et al.*²⁶ recently reported that the relatively unreactive compound $[\text{NSF}_3]$ undergoes oxidative addition, across the $\text{S}^{\text{VI}}\text{-F}$ bond, with *trans*- $[\text{IrCl}(\text{CO})(\text{PPh}_3)_2]$ to afford $[\text{IrFCl}(\text{NSF}_2)(\text{CO})(\text{PPh}_3)_2]$ (**8**). Complex (**8**) was characterized by a combination of multinuclear NMR, infrared spectroscopy and single crystal X-ray diffraction (see section 5.6). The ^{19}F

NMR spectrum revealed two resonances a triplet at δ -338, which is in a region characteristic of *F trans* CO, with a $^2J_{\text{FP}} = 28$ Hz, and a broad singlet at δ 121 which was attributed to fluorines bound to the sulphur. The $^{31}\text{P}\{^1\text{H}\}$ NMR spectrum showed the associated doublet at δ -6.6.

4.3.2 Oxidative Addition Reactions of Fluoro-Vaska's Complexes

The oxidative addition reactions of the fluoro-Vaska's complex are, in nearly all cases, analogous to those of the extensively studied chloro-complex. The complexes listed in Table 4.6 have been prepared *via* these reactions.

Table 4.6 Oxidative Addition of a Substrate A-B to Fluoro-Vaska's Derivatives, *trans*-[IrF(CO)L₂]

Product	Reagent	Refs.
[IrFH(SiR ₃)(CO)(PPh ₃) ₂] (SiR ₃ = SiPh ₃ and SiMeCl ₂)	[HSiR ₃]	27
[IrFMe(CO)(PPh ₃) ₂]	[MeI]	28
[IrF(O ₂)(CO)L ₂] (L = PMePh ₂ , PEtPh ₂ and PPh ₃)	[O ₂]	29,13
[IrF(1,2-O ₂ C ₆ Cl ₄)(CO)(PPh ₃) ₂]	[1,2-O ₂ C ₆ Cl ₄]	30
[IrFI ₂ (CO)(PPh ₃) ₂]	[I ₂]	2b
[IrF(η^2 -NH=NC ₆ H ₃ -2-Br)(CO)(PPh ₃) ₂] ⁺	[(2-BrC ₆ H ₄ N ₂)BF ₄]	31

The formulations of the complexes in Table 4.6 were dependent on infrared spectroscopy, with no other analytical technique being employed. It

is evident that, until recently, very little ^{19}F , ^{31}P and ^{13}C NMR data were available for iridium(III) carbonyl-phosphine-fluoride systems. However, as a result of a resurgence in low-valent transition-metal fluoride chemistry, more analytical techniques have been utilized, especially multinuclear NMR spectroscopy, to identify the reaction products.

4.4 Summary

It may be apparent from the literature that, until recently, the formulations of the fluoro-complexes of iridium, oxidation state (I) and (III), were mainly reliant on infrared and elemental analysis. However, the work by Holloway *et al.*, and more recently Ebsworth *et al.*, has highlighted the importance of multinuclear NMR spectroscopic data in elucidating these reaction systems and thus definitive characterization.

Xenon difluoride is reasonably inert to organic solvents and is well established as a convenient route for the introduction of fluorine into low-valent metal centres. In the previous sections, it was shown that $[\text{XeF}_2]$ reacts with the neutral iridium(I) complex, *trans*- $[\text{IrCl}(\text{CO})(\text{PEt}_3)_2]$, to afford, predominantly, $[\text{IrClF}_2(\text{CO})(\text{PEt}_3)_2]$. However, this is the only reported reaction of its type and there are no structural data available for such species.

Halide-exchange reactions and oxidative fluorination with $[\text{XeF}_2]$ have already been shown to give routes to Ir(I)-F and Ir(III)-F derivatives in a number of cases. The general applicability of these reactions has not been established and therefore, in this chapter attempts to develop these methodologies are outlined. Although the work outlined in this chapter is not exhaustive, some new Ir-F complexes are described which indicates that further investigations in these areas are required.

The reactions of $[\text{XeF}_2]$ with the Vaska's derivatives, *trans*- $[\text{IrX}(\text{CO})(\text{PR}_3)_2]$ ($\text{X} = \text{F}, \text{Cl}$ when $\text{PR}_3 = \text{PPh}_3$ and $\text{X} = \text{Cl}$ when $\text{PR}_3 = \text{Pcy}_3$) are reported in the following sections. These particular derivatives were investigated since the literature contains convenient preparative routes to these complexes and more importantly spectroscopic data. All species have been characterized by NMR, infrared and mass spectrometry. To date, structural analysis data on the Vaska's derivatives have been limited to reports on *trans*- $[\text{IrCl}(\text{CO})(\text{PPh}_3)_2]$,³² *trans*- $[\text{IrCl}(\text{CO})\{\text{P}(\text{C}_6\text{H}_4\text{-}o\text{-CH}_3)_3\}_2]$,³³

and *trans*-[IrCl(CO){P(C₆H₄-*p*-CH₃)₃}₂].³⁴ The structural characterization of several Vaska's derivatives, including fluoro-Vaska's, employing EXAFS spectroscopy are discussed in this chapter.

4.5 Preparation of *trans*-[IrF(CO)(PPh₃)₂]

Owing to the dearth of structural information on Vaska's derivatives it was thought to be of interest to prepare *trans*-[IrF(CO)(PPh₃)₂] and, subsequently, undertake EXAFS in an attempt to obtain structural data.

Yellow *trans*-[IrCl(CO)(PPh₃)₂] (used as obtained from Aldrich Chemicals) and a mixture of [NH₄F]/[Ag₂CO₃] were reacted, as described in section 6.11, affording the yellow *trans*-[IrF(CO)(PPh₃)₂] which was analysed by a combination of ¹⁹F, ³¹P{¹H} NMR, infrared spectroscopy and mass spectrometry.

The ³¹P{¹H} NMR spectrum of *trans*-[IrF(CO)(PPh₃)₂], in CDCl₃, revealed the expected doublet at δ 25.2 with a ²J_{PF} = 29 Hz and an additional resonance at δ 24.1 which was attributed to chloro-Vaska's complex.¹⁶

The corresponding ¹⁹F NMR spectrum showed the associated triplet resonance at δ -258.6, ²J_{FP} = 29 Hz.

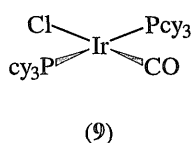
Although, the δ(³¹P) compares well with that previously reported, 24.4 ppm,¹⁷ there is a discrepancy between the magnitude of the reported ²J_{PF} coupling constant (19.7 Hz, see Table 4.3)¹⁷ with that observed. The agreement between the ¹⁹F and ³¹P{¹H} NMR data here suggests that the higher ²J_{PF} coupling constant is correct. Furthermore, by analogy with the ²J_{PF} couplings, for F *trans* CO, observed for the range of complexes of the type [IrF₃(CO)(PR₃)₂], discussed in chapter 5, the magnitude of 29 Hz appears typical.

In contrast to the $^{31}\text{P}\{^1\text{H}\}$ NMR spectrum which revealed the presence of both chloro- and fluoro-Vaska's the corresponding Nujol mull infrared spectrum showed only one $\nu(\text{CO})$ band at 1945 cm^{-1} which is attributed to *trans*- $[\text{IrF}(\text{CO})(\text{PPh}_3)_2]$ and is comparable with the reported literature value of 1942 cm^{-1} .³⁷ The FAB⁺ mass spectrum revealed the expected $[M]^+$, for *trans*- $[\text{IrF}(\text{CO})(\text{PPh}_3)_2]$, at $m/z = 763$ but no parent ion for chloro-Vaska's complex was observed. It is evident from the data presented above that the presence of chloro-Vaska's complex in the NMR spectrum is not due to unreacted starting material, since no carbonyl stretching frequency for chloro-Vaska's complex was observed in the infrared spectrum, but is a result of reaction with the CD_2Cl_2 solvent and thus inducing chlorine/fluorine exchange. Comparable halogen-exchange reactions in Ir(III) complexes have been outlined previously.

4.6 Preparation of *trans*- $[\text{IrCl}(\text{CO})(\text{Pcy}_3)_2]$

$[\text{IrCl}(\text{CO})_3]_n$ and Pcy_3 were reacted in toluene, as described in section 6.12.1, affording a yellow solution. Removal of the solvent *in vacuo* yielded a yellow solid which was dissolved in CDCl_3 and subsequently, analysed by $^{31}\text{P}\{^1\text{H}\}$ NMR spectroscopy.

The Nujol mull infrared spectrum of *trans*- $[\text{IrCl}(\text{CO})(\text{Pcy}_3)_2]$ (**9**) exhibited the expected one band at 1933 cm^{-1} which is in the region characteristic of a terminal carbonyl. This compares well with the previously³⁵ reported value of 1931 cm^{-1} . All attempts to obtain an interpretable mass spectrum were unsuccessful.



The $^{31}\text{P}\{^1\text{H}\}$ NMR spectrum of complex (9), which has not been previously reported, revealed a singlet resonance at δ 30.7. This is consistent with the expected shift, to a higher frequency, on coordination of the Pcy_3 ligand.

4.6.1 Reaction of *trans*- $[\text{IrCl}(\text{CO})(\text{Pcy}_3)_2]$ and $[\text{NH}_4\text{F}]/[\text{Ag}_2\text{CO}_3]$ in Methanol

All attempts to prepare the analogous fluoro-derivatives of the complex *trans*- $[\text{IrCl}(\text{CO})(\text{Pcy}_3)_2]$, by the route described in section 4.5, were unsuccessful.

The partial solubility of *trans*- $[\text{IrCl}(\text{CO})(\text{Pcy}_3)_2]$ in methanol, compared to that of *trans*- $[\text{IrCl}(\text{CO})(\text{PPh}_3)_2]$, is a plausible explanation for the inability to form the analogous fluoro-derivative *via* the method described in section 4.5. Furthermore, the increased basicity of the Pcy_3 , in comparison to the PPh_3 , could affect the lability of the chloride ligand, thus preventing metathetical replacement of the chloride for fluoride.

4.7 EXAFS Analysis of *trans*-[IrCl(CO)(Pcy₃)₂]

The value of EXAFS, as a technique for obtaining structural data when X-ray crystallographic studies are unavailable, has been outlined in previous chapters.

Initially, for *trans*-[IrCl(CO)(Pcy₃)₂] the data were modelled, utilizing EXCURV92,³⁶ to 4 shells of 1 chlorine atom at *ca.* $r = 2.32(2)$ Å, 2 phosphorus atoms at *ca.* $r = 2.30(2)$ Å, 1 carbon atom at *ca.* $r = 1.79(2)$ Å and 1 oxygen atom at *ca.* $r = 2.91(2)$ Å using localised C_{2v} symmetry and a fixed Ir-C-O bond angle of 180° for multiple scattering (Figure 4.1.1). An additional weak feature around 3.5 Å was observed upon examination of the Fourier transform. This feature was attributed to the 6 nearest carbon atoms, to the iridium centre, on the cyclohexyl groups. So, further modelling of the EXAFS data using 5 shells resulted in a significant reduction in the R-factor and fit index (Figure 4.1.2).

The bond length data, obtained by EXAFS studies, for *trans*-[IrCl(CO)(Pcy₃)₂] are reasonable when compared with the data obtained by X-ray crystallographic studies of *trans*-[IrCl(CO)(PPh₃)₂] (Table 4.7).³²

Table 4.7 Comparison of the Bond Length (Å) Data of *trans*-[IrCl(CO)(Pcy₃)₂] and *trans*-[IrCl(CO)(PPh₃)₂]

Complex	Ir-Cl	Ir-P	Ir-C	C-O
<i>trans</i> -[IrCl(CO)(Pcy ₃) ₂] ^a	2.32(2)	2.30(2)	1.79(2)	1.12(2)
<i>trans</i> -[IrCl(CO)(PPh ₃) ₂] ^b	2.382(3)	2.330(1)	1.791(13)	1.161(18)

(a) Data obtained by EXAFS studies

(b) Data obtained by X-ray crystallographic studies

Figure 4.1.1 The Background-Subtracted EXAFS (K^3 weighted) and the Fourier Transform EXAFS of *trans*-[IrCl(CO)(Pcy₃)₂] (modelled to 4 shells)

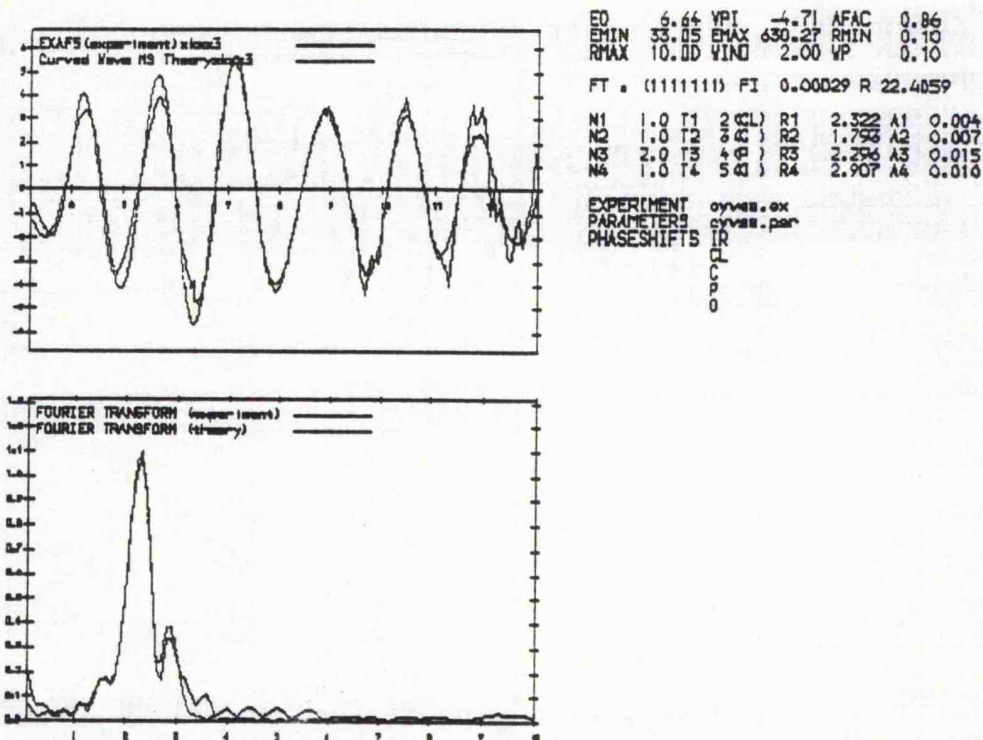
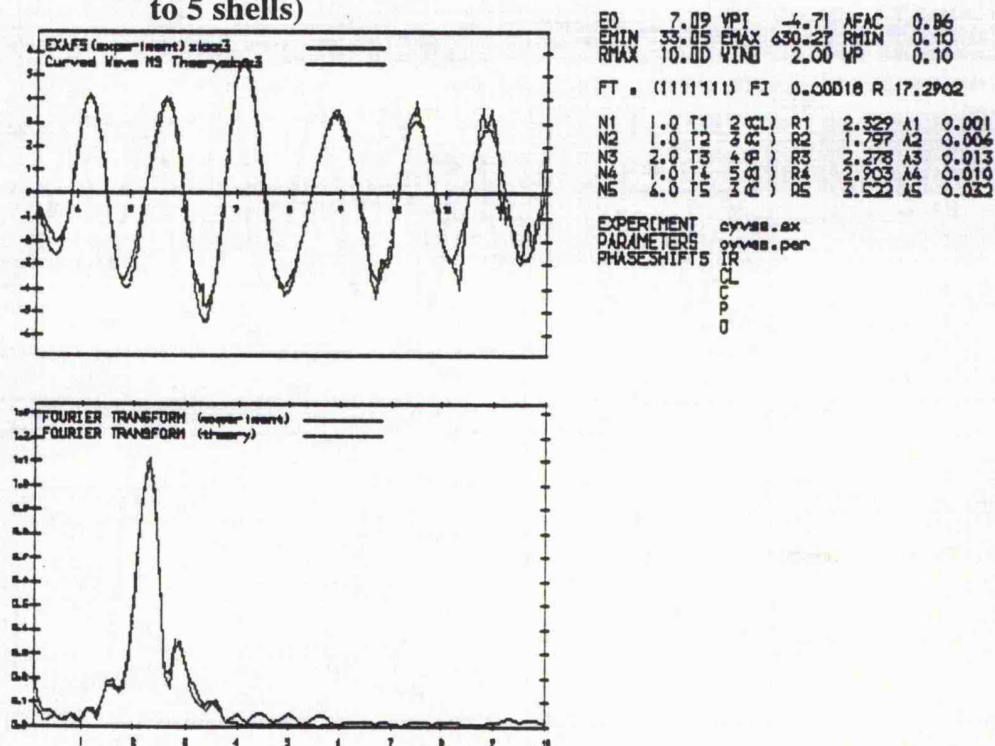


Figure 4.1.2 The Background-Subtracted EXAFS (K^3 weighted) and the Fourier Transform EXAFS of *trans*-[IrCl(CO)(Pcy₃)₂] (modelled to 5 shells)



4.8 EXAFS Analysis of *trans*-[IrF(CO)(PPh₃)₂]

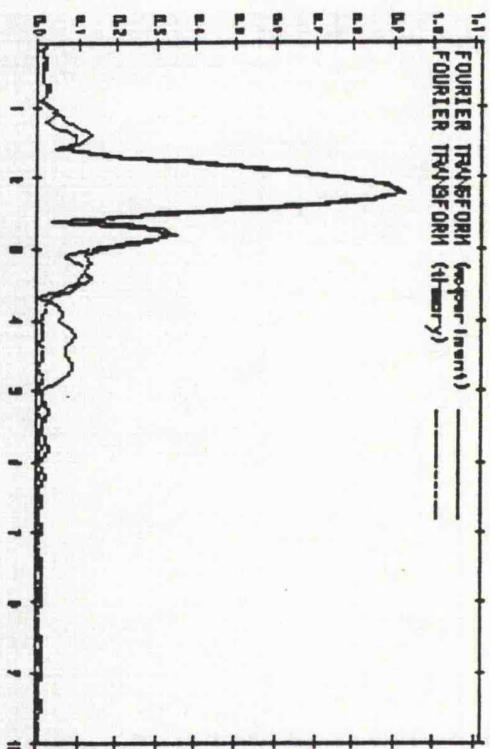
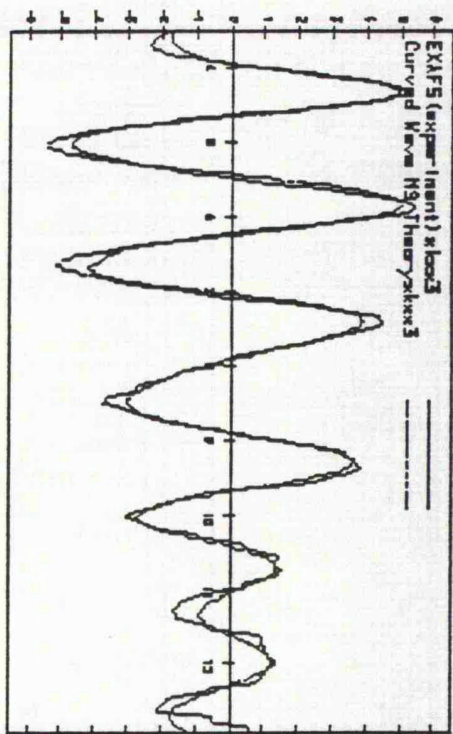
Our inability to obtain single crystals of *trans*-[IrF(CO)(PPh₃)₂] is not surprising since there have been very few crystallographic determinations for Vaska's derivatives and iridium fluorides. Therefore, EXAFS spectroscopy was utilized to obtain structural data. In the absence of structurally characterized iridium(I) fluoride complexes as model compounds, the reliability of the data collection and treatment was confirmed by the collection and analysis of iridium L₁₁₁-edge EXAFS data on *trans*-[IrCl(CO)(Pcy₃)₂] (see section 4.7).

The data were modelled to 5 shells of 1 fluorine atom at *ca.* $r = 1.95(2)$ Å, 2 phosphorus atoms at *ca.* $r = 2.28(2)$ Å, 1 carbon atom at *ca.* $r = 1.79(2)$ Å, 1 oxygen atom at *ca.* $r = 2.87(2)$ Å and 6 carbon atoms at non-bonded distance of $3.43(2)$ Å using localised C_{2v} symmetry and a fixed Ir-C-O bond angle of 180° for multiple scattering (Figure 4.2).

The Ir(I)-F bond length obtained by EXAFS for *trans*-[IrF(CO)(PPh₃)₂] of $1.95(2)$ Å is not unreasonable when compared with the previously reported Ir(III)-F bond lengths of $1.998(3)$ and $2.089(2)$ in [IrF(COF)(CO)(PEt₃)₂]⁺³⁸ and [IrClF(NSF₂)(CO)(PPh₃)₂]²⁵ respectively. The Ir-C bond length ($1.79(2)$ Å) compares well with the two lengths, reported in Table 4.7, for *trans*-[IrCl(CO)(PPh₃)₂] and *trans*-[IrCl(CO)(Pcy₃)₂]. However, the shorter C-O bond length ($1.08(2)$ Å) observed for *trans*-[IrF(CO)(PPh₃)₂] in comparison with that observed for *trans*-[IrCl(CO)(PPh₃)₂] ($1.161(18)$ Å) is not in agreement with their $\nu(\text{CO})$ of 1942 and 1950 cm⁻¹.³⁵ The lower frequency should manifest itself in the infrared spectrum, and consequently, the C-O bond length should be shorter however, due to the inaccuracy in EXAFS $1.08(2)$ is the same as $1.12(2)$ or $1.161(18)$ Å. This highlights the inaccuracy sometimes inherent in the EXAFS technique.

Figure 4.2 The Background-Subtracted EXAFS (K^3 weighted) and the

Fourier Transform EXAFS of *trans*-[IrF(CO)(PPh₃)₂]



E0	13.30	VP1	-4.71	AFAC	0.86		
EMIN	33.05	EMAX	630.27	RHIN	0.10		
RMAX	10.00	WIN	2.00	WP	0.10		
FT	(11111111)	F1	0.00025	R	16.4067		
N1	1.0	T1	3.45	R1	1.953	A1	0.002
N2	1.0	T2	3.45	R2	1.769	A2	0.010
N3	2.0	T3	4.40	R3	2.278	A3	0.008
N4	1.0	T4	5.40	R4	2.673	A4	0.013
N5	6.0	T5	3.45	R5	3.420	A5	0.028
EXPERIMENT	fysakal.aex						
PARAMETERS	fysakal.par						
PHASESHIFT5	IR						
	F L C D						

EXPERIMENT
PARAMETERS
PHASESHIFTS

fvsakal.ex
fvsakal.par
F L C P D

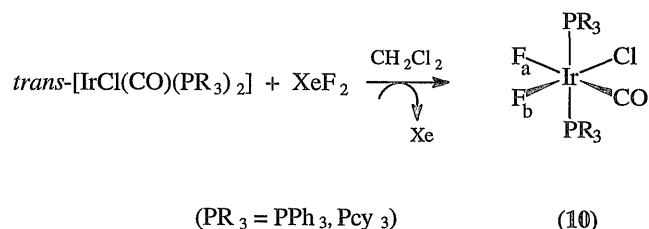
4.9 Reaction of *trans*-[IrCl(CO)(PR₃)₂] (PR₃ = PPh₃ and Pcy₃) with [XeF₂]

Ebsworth *et al.*,²⁵ reported that the reaction of *trans*-[IrX(CO)(PEt₃)₂] (X = Cl, Br, I) and [XeF₂], in CH₂Cl₂, afforded predominately the difluoride complex [IrF₂X(CO)(PEt₃)₂] as discussed in section 4.3.1. It was, therefore, of interest to investigate the analogous reactions with *trans*-[IrCl(CO)(PR₃)₂] (PR₃ = PPh₃ and Pcy₃).

trans-[IrCl(CO)(PR₃)₂] and [XeF₂] were allowed to react, as described in section 6.13 in CH₂Cl₂ affording a yellow solution. Removal of the solvent *in vacuo* yielded yellow solids which were dissolved in CDCl₃ and subsequently, analysed by multinuclear NMR spectroscopy.

The reaction between *trans*-[IrCl(CO)(PR₃)₂] and [XeF₂] proceeds according to Scheme 4.2 to give the complexes *cis*-, *cis*-, *trans*-[IrF₂Cl(CO)(PR₃)₂].

Scheme 4.2



The ¹⁹F NMR (Figure 4.3) and the ³¹P{¹H} NMR (Figure 4.4) spectra for both complexes revealed mutually coupled doublet of triplets and doublet of doublets respectively. The NMR data are presented in Table 4.8 and

compared with the previously reported complex *cis*-, *trans*-
 $[\text{IrF}_2\text{Cl}(\text{CO})(\text{PEt}_3)_2]$.²⁵

**Table 4.8 NMR Data for the Complexes of the Type, *cis*-, *trans*-
 $[\text{IrF}_2\text{Cl}(\text{CO})(\text{PR}_3)_2]$**

PR ₃	¹⁹ F					³¹ P{ ¹ H}
	δ/ ppm		² J/ Hz			δ/ ppm
	F _a /(dt)	F _b /(dt)	F _a F _b	F _a P	F _b P	P/(dd)
PPh ₃	-292	-380	132	29	19	-7.0
Pcy ₃	-297	-404	118	29	17	6.0
PEt ₃	-299	-489	115	29	18	6.0

Multiplicity: dt = doublet of triplets, dd = doublet of doublets

It is evident from the data, in Table 4.8, that there are two distinct ¹⁹F chemical shifts. The doublet of triplets, assignable to F_a, arises from coupling *cis* to F_b and *cis* to the two equivalent phosphines and is observed in a region characteristic of F *trans* CO.³⁹ By the same reasoning the resonance associated with F_b appears as a doublet of triplets, but is observed at a lower frequency indicative of F *trans* to a halide.²⁵ The doublet of doublets, observed in the ³¹P{¹H} NMR spectra, arises from the two equivalent phosphorus atoms coupling *cis* to both F_a and F_b and is therefore, consistent with the structure of (10).

Although the two chemical shift regions, observed in the ¹⁹F NMR spectra are distinct, the δ for F_b, in the PEt₃ analogue, is reported at a lower

Figure 4.3 ^{19}F NMR Spectrum of *cis*-, *trans*- $[\text{IrF}_2\text{Cl}(\text{CO})(\text{Pcy}_3)_2]$

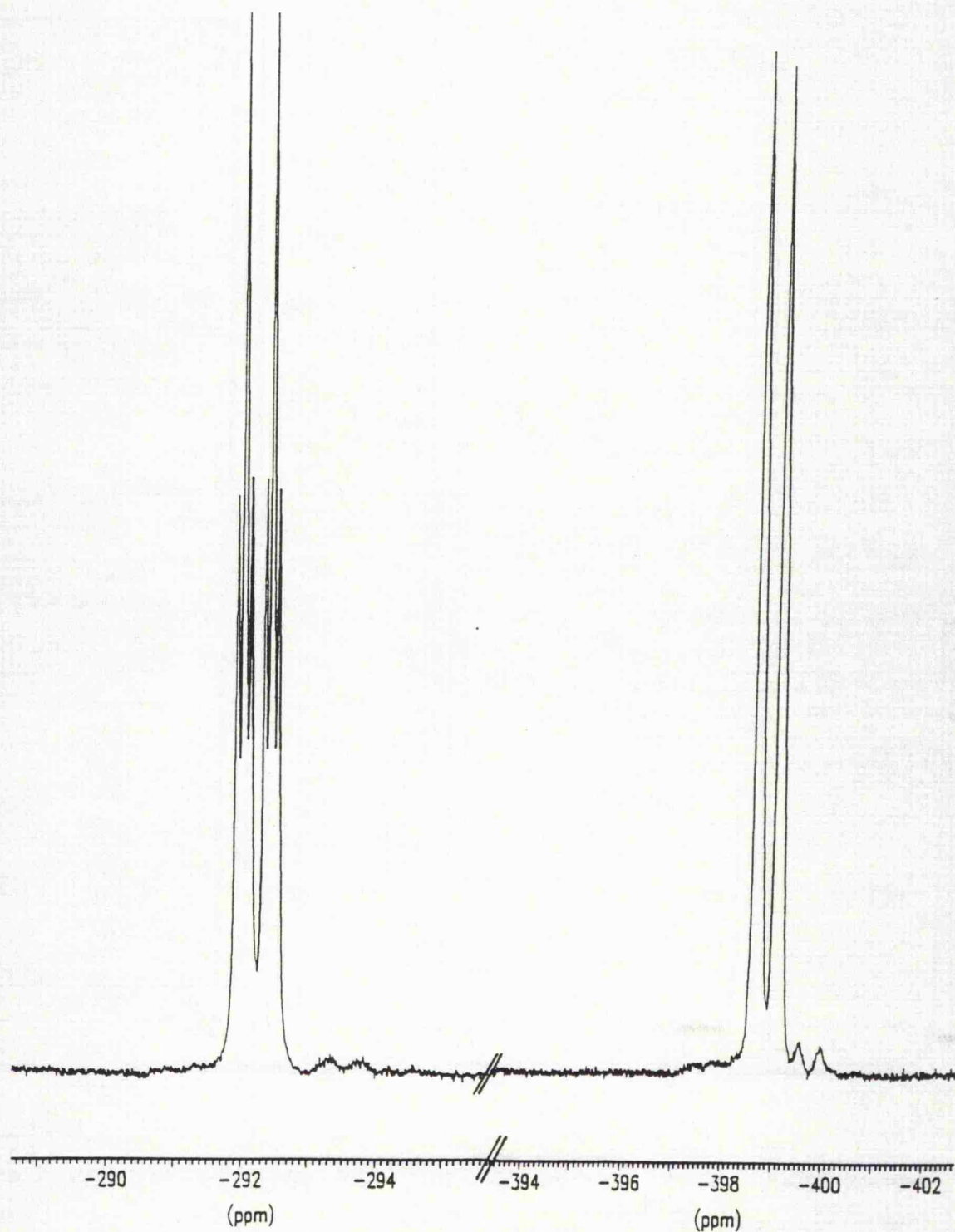
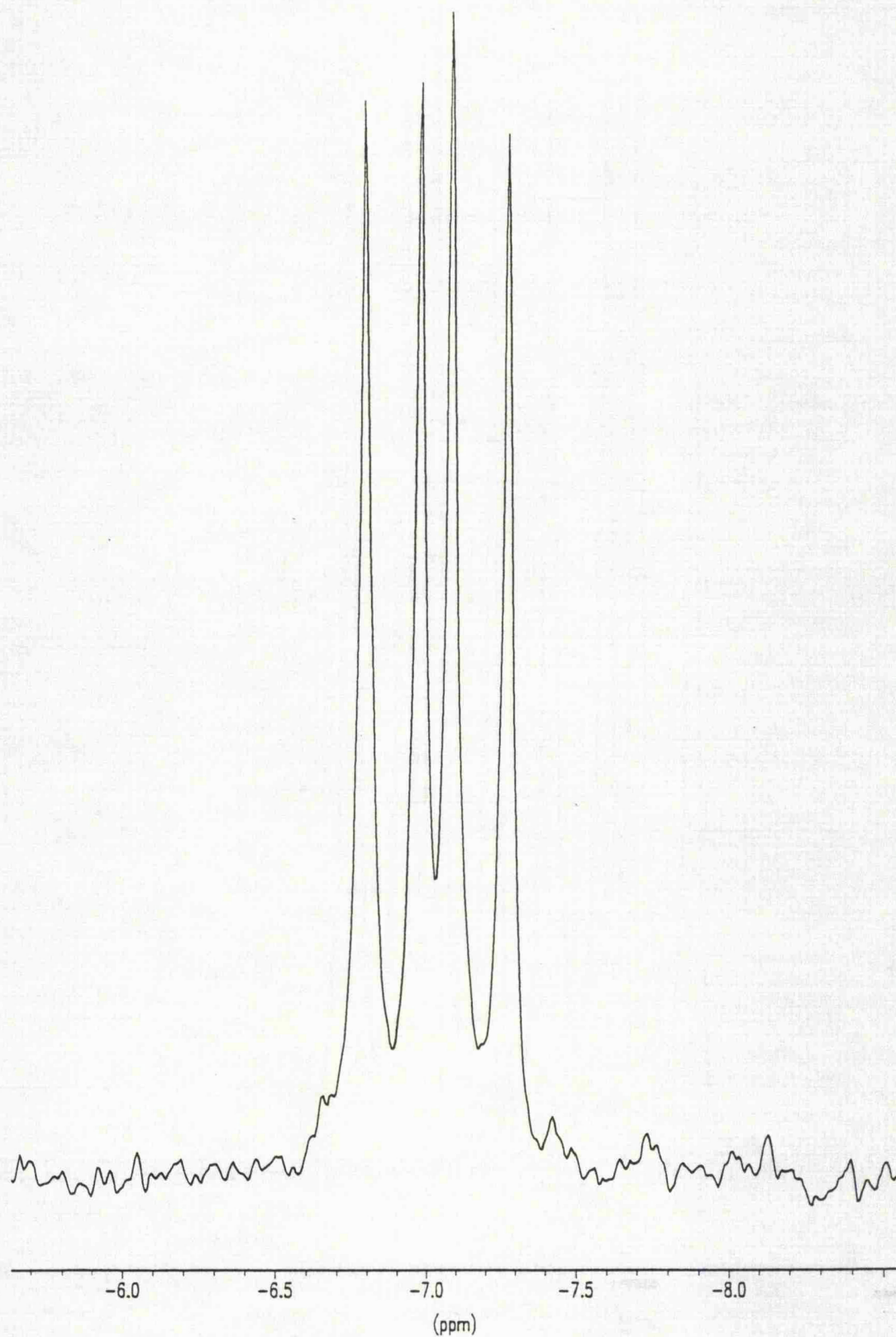
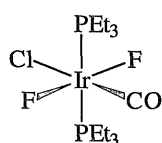


Figure 4.4 $^{31}\text{P}\{^1\text{H}\}$ NMR Spectrum of *cis*-, *trans*- $[\text{IrF}_2\text{Cl}(\text{CO})(\text{PPh}_3)_2]$



frequency than in the corresponding PPh_3 and Pcy_3 derivatives. This $\delta(^{19}\text{F})$ of -489 is plausibly in the region characteristic of F *trans* F⁴⁰ (see Chapter 5) and not F *trans* Cl as the authors suggest. Furthermore, on examination of the data presented in Table 4.5 (see section 4.3.1) the trend of a shift to lower frequency, on substitution of a heavier for a lighter halogen, for F_a, in the complexes $[\text{IrF}_2\text{X}(\text{CO})(\text{PEt}_3)_2]$,²⁵ breaks down when X = Cl. Therefore, it is plausible that the authors have reported an incorrect chemical shift, since the only other explanation would be the formation of complex (11), in which F is *trans* to F. However, complex (11) would exhibit triplets in both the ^{19}F and $^{31}\text{P}\{^1\text{H}\}$ NMR spectra.



(11)

As observed in the complexes of the type *cis*-, *trans*- $[\text{IrF}_2\text{X}(\text{CO})(\text{PEt}_3)_2]$ (X = F, Cl, Br, I), the $^2J_{\text{PFa}}$ coupling is larger than the corresponding $^2J_{\text{PFb}}$ for the analogous species *cis*-, *trans*- $[\text{IrF}_2\text{Cl}(\text{CO})(\text{PR}_3)_2]$ ($\text{PR}_3 = \text{PPh}_3, \text{Pcy}_3$). A more extensive study on the complexes *mer*-, *trans*- $[\text{IrF}_3(\text{CO})(\text{PR}_3)_2]$ ($\text{PR}_3 =$ various tertiary phosphines), in chapter 5, reveals the influence of the phosphine ligand on the magnitude of the $^2J_{\text{PF}}$ coupling.

The Nujol mull infrared spectra of complexes (10) showed the expected single band, in a region associated with a terminal carbonyl, at 2027 and 2010 cm^{-1} for the PPh_3 and Pcy_3 derivatives respectively. However, for the PPh_3 system two further bands at 1965 and 1949 cm^{-1} were also observed, in a region characteristic of terminal carbonyl ligands, indicating the presence of two other species which are discussed shortly. This increase

in $\nu(\text{CO})$, from 1950 and 1933 cm^{-1} for *trans*- $[\text{IrCl}(\text{CO})(\text{PR}_3)_2]$ ($\text{PR}_3 = \text{PPh}_3$, Pcy_3), on oxidation of the planar complexes is an effect that has been attributed to a decrease in the π -donor properties of the central atom on oxidation.^{41,42}

The FAB^+ mass spectrum of the PPh_3 derivative of complex (**10**) did not show the parent ion, but did show sequential loss of ligands from $[\text{M}-\text{F}]^+$ centred at m/z 799. Furthermore, a second fragment pattern centred at m/z 815 was also observed, and is attributed to another iridium(III) phosphine-carbonyl containing species which is discussed below. All attempts to obtain an interpretable mass spectrum of the Pcy_3 derivative of complex (**10**) were unsuccessful.

Resonances due to other species were, in addition to those attributed to *cis*-, *trans*- $[\text{IrF}_2\text{Cl}(\text{CO})(\text{PPh}_3)_2]$, also observed in the corresponding ^{19}F and $^{31}\text{P}\{^1\text{H}\}$ NMR spectra. In the ^{19}F NMR spectrum (Figure 4.5) two additional triplets were observed at δ -322 and -414 with $^2J_{\text{FP}}$ couplings of 29 and 17 Hz respectively. The $^{31}\text{P}\{^1\text{H}\}$ NMR spectrum (Figure 4.6) revealed the two associated doublets at δ -9.0 and 14.0.

All the data considered and by comparison with that reported for *cis*-, *trans*- $[\text{IrF}_2\text{Cl}(\text{CO})(\text{PPh}_3)_2]$ the most likely explanation is that the difluoro-complex has undergone fluorine-chlorine exchange to yield the two isomeric monofluoride complexes $[\text{IrFCl}_2(\text{CO})(\text{PPh}_3)_2]$ (**12**) and (**13**) (Scheme 4.3).

Figure 4.5 ^{19}F NMR Spectrum of the Products from the Reaction of *trans*- $[\text{IrCl}(\text{CO})(\text{PPh}_3)_2]$ and $[\text{XeF}_2]$

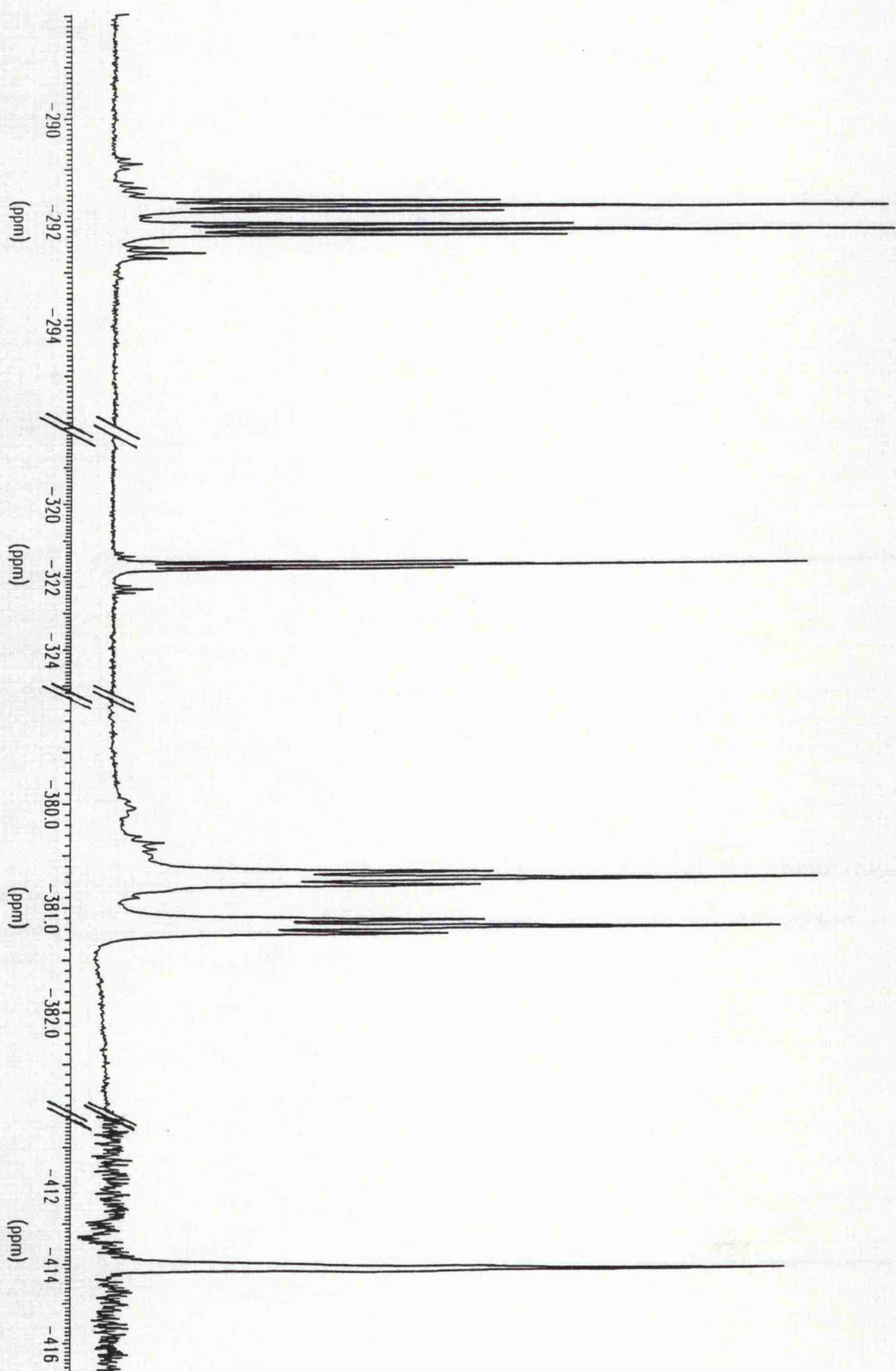
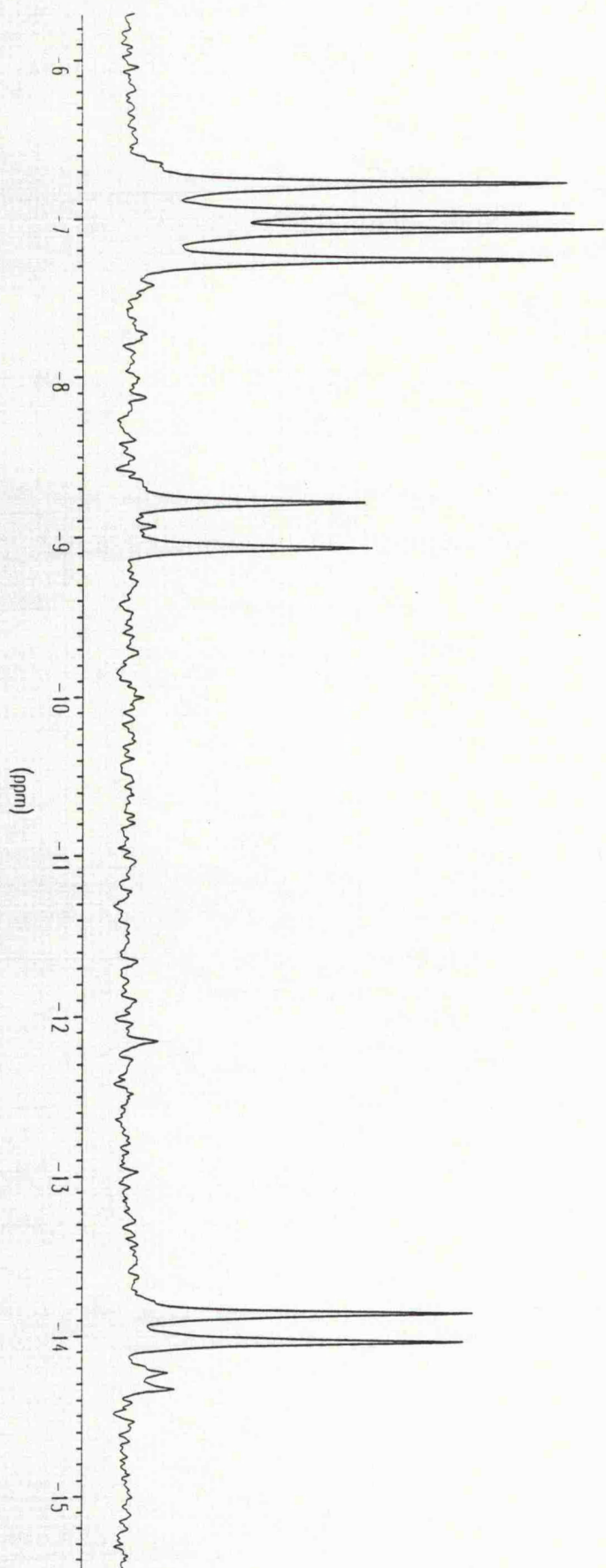
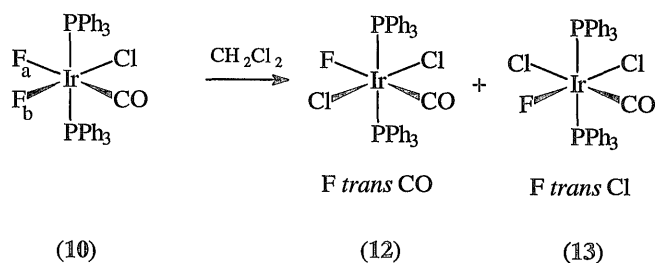


Figure 4.6 $^{31}\text{P}\{^1\text{H}\}$ NMR Spectrum of the Products from the Reaction of *trans*- $[\text{IrCl}(\text{CO})(\text{PPh}_3)_2]$ and $[\text{XeF}_2]$

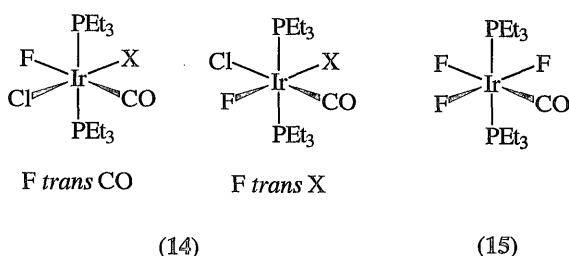


Scheme 4.3



Complex (12) would exhibit a triplet, in a chemical shift region characteristic of F *trans* CO, and a doublet in the ^{19}F and $^{31}\text{P}\{^1\text{H}\}$ NMR spectra respectively. Thus, the triplet observed at $\delta(^{19}\text{F})$ -322 and the doublet at $\delta(^{31}\text{P})$ -9, with a $^2J_{\text{FP}} = 29$ Hz, are consistent with the structure of (12). By the same reasoning the other triplet observed in the ^{19}F NMR spectrum at δ -414, which is in a region indicative of F *trans* Cl, and the associated doublet, in the $^{31}\text{P}\{^1\text{H}\}$ NMR spectrum, with a $^2J_{\text{FP}} = 17$ Hz are consistent with the structure of complex (13). Furthermore, the additional bands, at 1965 and 1949 cm^{-1} , reported in the infrared spectrum can be assigned to complexes (13) and (12). Finally, the additional fragment pattern observed at m/z 815 corresponds to loss of fluorine ($[M-\text{F}]^+$) from either complex (12) or (13).

As discussed in section 4.3.1 the reaction of *trans*- $[\text{IrX}(\text{CO})(\text{PEt}_3)_2]$ ($\text{X} = \text{Cl}, \text{Br}, \text{I}$) and $[\text{XeF}_2]$, in CH_2Cl_2 , affords predominantly the complex *cis*-, *trans*- $[\text{IrF}_2\text{X}(\text{CO})(\text{PEt}_3)_2]$, but, small amounts of the two isomeric monofluorides, when $\text{X} = \text{Cl}$, $[\text{IrFCl}_2(\text{CO})(\text{PEt}_3)_2]$ (14) and of the trifluoride, *mer*-, *trans*- $[\text{IrF}_3(\text{CO})(\text{PEt}_3)_2]$ (14), are reported to be formed as a result of intermolecular halogen exchange.²⁵



However, in the case when $X = \text{Br}$ or I reaction with the solvent, CD_2Cl_2 , resulted in the formation of mixed chloro-halo-fluoro-complexes (14).²⁵

Unfortunately, no NMR data were reported for complexes (14)²⁵ thus, no direct comparisons can be made with complexes (12) and (13). However, in section 5.10 we report that the reactions of the complexes *mer*-, *trans*- $[\text{IrF}_3(\text{CO})(\text{PR}_3)_2]$ with the solvent, CD_2Cl_2 , afford various mixed chloro-fluoro-derivatives of these species.

In marked contrast no other resonances were observed in the ^{19}F or $^{31}\text{P}\{^1\text{H}\}$ NMR spectra of *cis*-, *trans*- $[\text{IrF}_2\text{Cl}(\text{CO})(\text{Pcy}_3)_2]$, implying a greater stability compared to the PPh_3 derivative.

All attempts to form the analogous Ir(III) difluoro-complexes, from the reaction of *trans*- $[\text{IrCl}(\text{CO})(\text{PR}_3)_2]$ ($\text{PR}_3 = \text{PPh}\{\text{C}_6\text{F}_5\}_2$, $\text{P}\{\text{C}_6\text{F}_5\}_3$) and $[\text{XeF}_2]$, were unsuccessful. The reactions resulted in decomposition of the starting materials with the formation of the difluorophosphoranes, R_3PF_2 , in both cases implying that the phosphine ligands are labile in these complexes and thus, not able to stabilize an Ir-F bond.

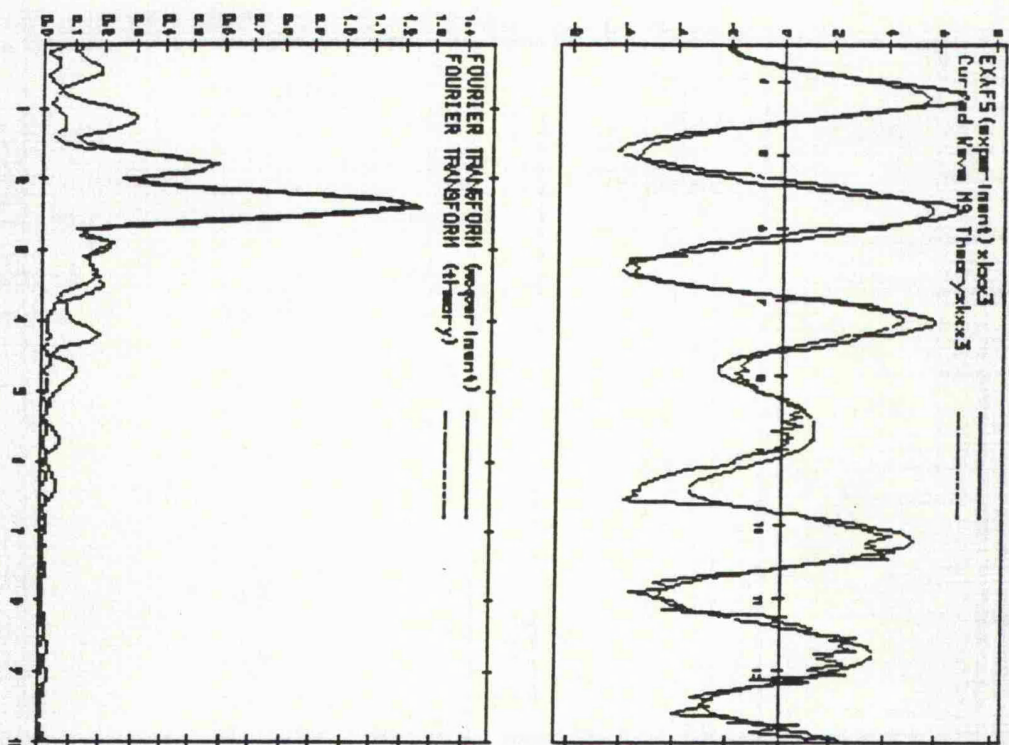
4.10 EXAFS Analysis of *cis*-, *trans*-[IrF₂Cl(CO)(Pcy₃)₂]

EXAFS spectroscopic studies were undertaken in an attempt to obtain structural data on *cis*-, *trans*-[IrF₂Cl(CO)(Pcy₃)₂] since no single crystals could be obtained. In the absence of structurally characterized iridium(III) fluoride-phosphine-carbonyl complexes as model compounds, the reliability of the data collection and treatment was confirmed by the collection and analysis of iridium L₁₁₁-edge EXAFS data on *trans*-[IrCl(CO)(Pcy₃)₂] and *trans*-[IrF(CO)(PPh₃)₂] (see sections 4.7 and 4.8 respectively).

The data were modelled to 5 shells of 2 fluorine atoms at *ca.* $r = 1.87(2)$ Å, 2 phosphorus atoms at *ca.* $r = 2.36(2)$ Å, 1 carbon atom at *ca.* $r = 1.68(2)$ Å, 1 oxygen atom at *ca.* $r = 2.89(2)$ Å and 6 carbon atoms at non-bonded distance of $3.48(2)$ Å using localised C_{2v} symmetry and a fixed Ir-C-O bond angle of 180° for multiple scattering (Figure 4.7).

The Ir(III)-F bond length obtained by EXAFS for *cis*-, *trans*-[IrF₂Cl(CO)(Pcy₃)₂] of $1.87(2)$ Å is significantly shorter than the corresponding distances previously reported for [IrF(COF)(CO)(PEt₃)₂]⁺³⁸ and [[IrClF(NSF₂)(CO)(PPh₃)₂]²⁵ of $1.998(3)$ and $2.089(2)$ Å respectively. The Ir-C bond length ($1.68(2)$ Å) is also significantly shorter than the corresponding distances, reported in Table 4.7 (see section 4.7), for *trans*-[IrCl(CO)(PPh₃)₂] and *trans*-[IrCl(CO)(Pcy₃)₂]. However, the longer C-O bond length (1.21 Å) observed for *cis*-, *trans*-[IrF₂Cl(CO)(PPh₃)₂] in comparison with that observed for *trans*-[IrCl(CO)(Pcy₃)₂] (1.12 Å) is not in agreement with their $\nu(\text{CO})$ of 2010 and 1933 cm^{-1} respectively. The shorter C-O bond length should manifest itself in the infrared spectrum consequently, the $\nu(\text{CO})$ should be observed at a higher frequency. However, it is important to consider that a change in oxidation state,

Figure 4.7 The Background-Subtracted EXAFS (K^3 weighted) and the Fourier Transform EXAFS of $[\text{IrF}_2\text{Cl}(\text{CO})(\text{PPh}_3)_2]$



```

E0      13.89 VPI      -7.00 AFAC      1.00
ENIN    33.05 ENMAX   630.27 RHIN      0.10
RMAX    10.00 WIND     2.00 WP         0.10
FT = (1111111) F1 0.00047 R 29.0047
N1      1.0 T1      2.00 R1      2.194 A1      0.002
N2      1.0 T2      3.00 R2      1.682 A2      0.006
N3      2.0 T3      4.00 R3      2.365 A3      0.009
N4      1.0 T4      5.00 R4      2.892 A4      0.016
N5      2.0 T5      6.00 R5      1.871 A5      0.011
N6      0.0 T6      3.00 R6      3.478 A6      0.013
EXPERIMENTAL PARAMETERS
PHASESHIFT5 IR
CL
C
P
O
F

```

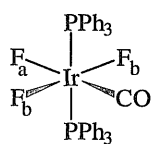
from (I) to (III), is accompanied by an increase in the carbonyl stretching frequencies (see section 4.9, page 204).

4.11 Reaction of *trans*-[IrF(CO)(PPh₃)₂] with [XeF₂]

In chapter 5 the preparations of the complexes *mer*-, *trans*-[IrF₃(CO)(PR₃)₂] (PR₃ = various tertiary phosphines), formed from the reaction of the highly reactive *fac*-[IrF₃(CO)₃] and the appropriate phosphine, are described. The reaction of *trans*-[IrF(CO)(PPh₃)₂] and [XeF₂] was anticipated to afford the trifluoro-complex *mer*-, *trans*-[IrF₃(CO)(PPh₃)₂] which would be a more convenient route to these trifluoro-species.

Yellow *trans*-[IrF(CO)(PPh₃)₂] and [XeF₂] were reacted in CH₂Cl₂, as described in section 6.13, yielding a green solution. An air-stable green solid was isolated, after removal of the solvent, which was dissolved in CD₂Cl₂ and subsequently analysed by ¹⁹F and ³¹P{¹H} NMR spectroscopy.

The ¹⁹F NMR spectrum revealed two mutually coupled resonances a triplet of triplets at δ -281.3, ²J_{FF} = 96 Hz, ²J_{FaP} = 29 Hz and a doublet of triplets at δ -451.4, ²J_{FbP} = 20 Hz, in 1:2 ratio (Figure 4.8). The corresponding ³¹P{¹H} NMR showed a doublet of triplets (Figure 4.9) at δ -6.4, which is appropriate for *trans* phosphine ligands; both coupling constants are characteristic of *cis*-²J_{PF}. By analogy with the complexes reported in chapter 5 all the NMR data are consistent with the structure of complex (16).



(16)

The full characterization of complex (16) is addressed in chapter 5 with other species of this type.

Figure 4.8 ^{19}F NMR Spectrum of Complex (16)

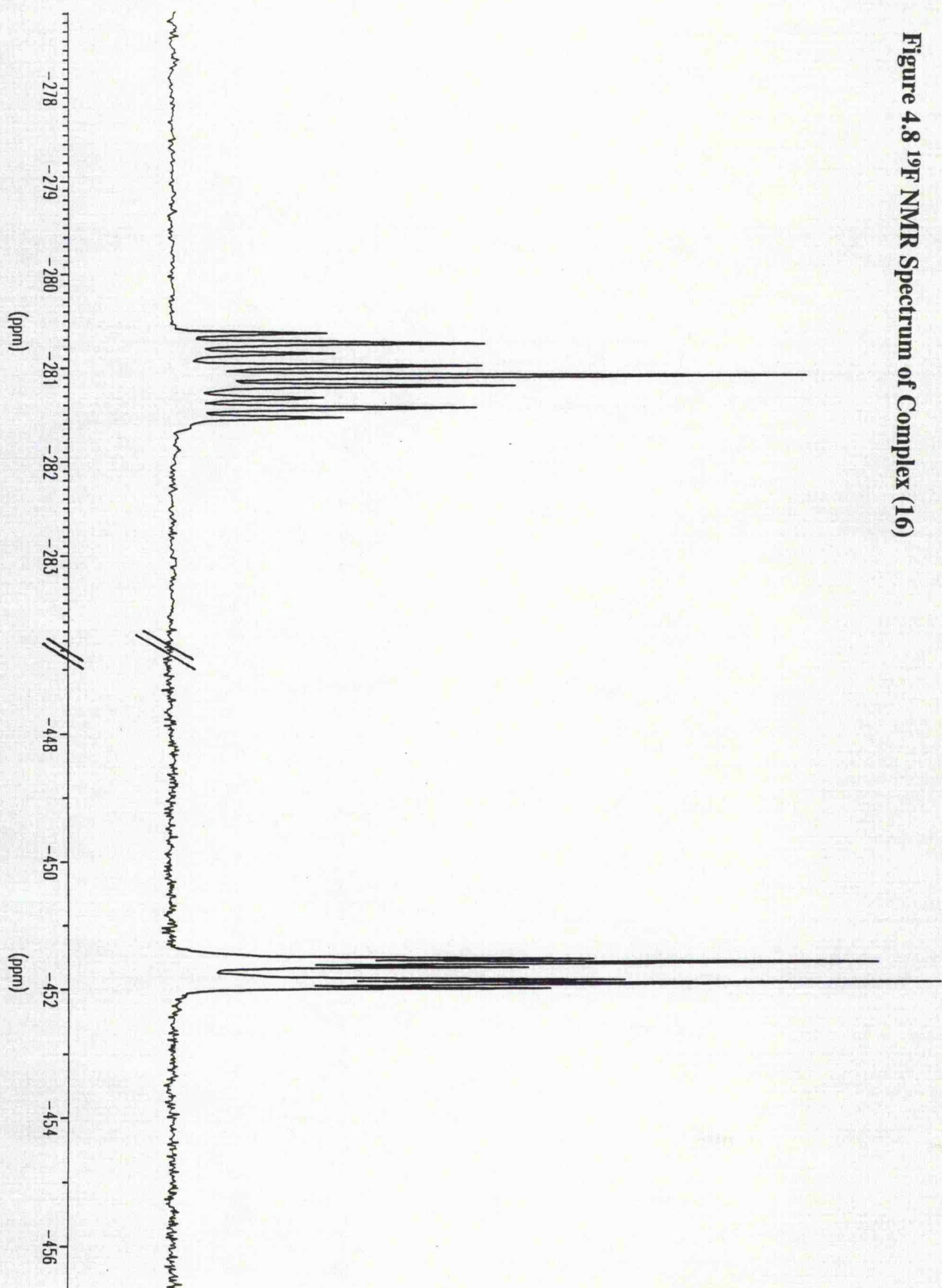
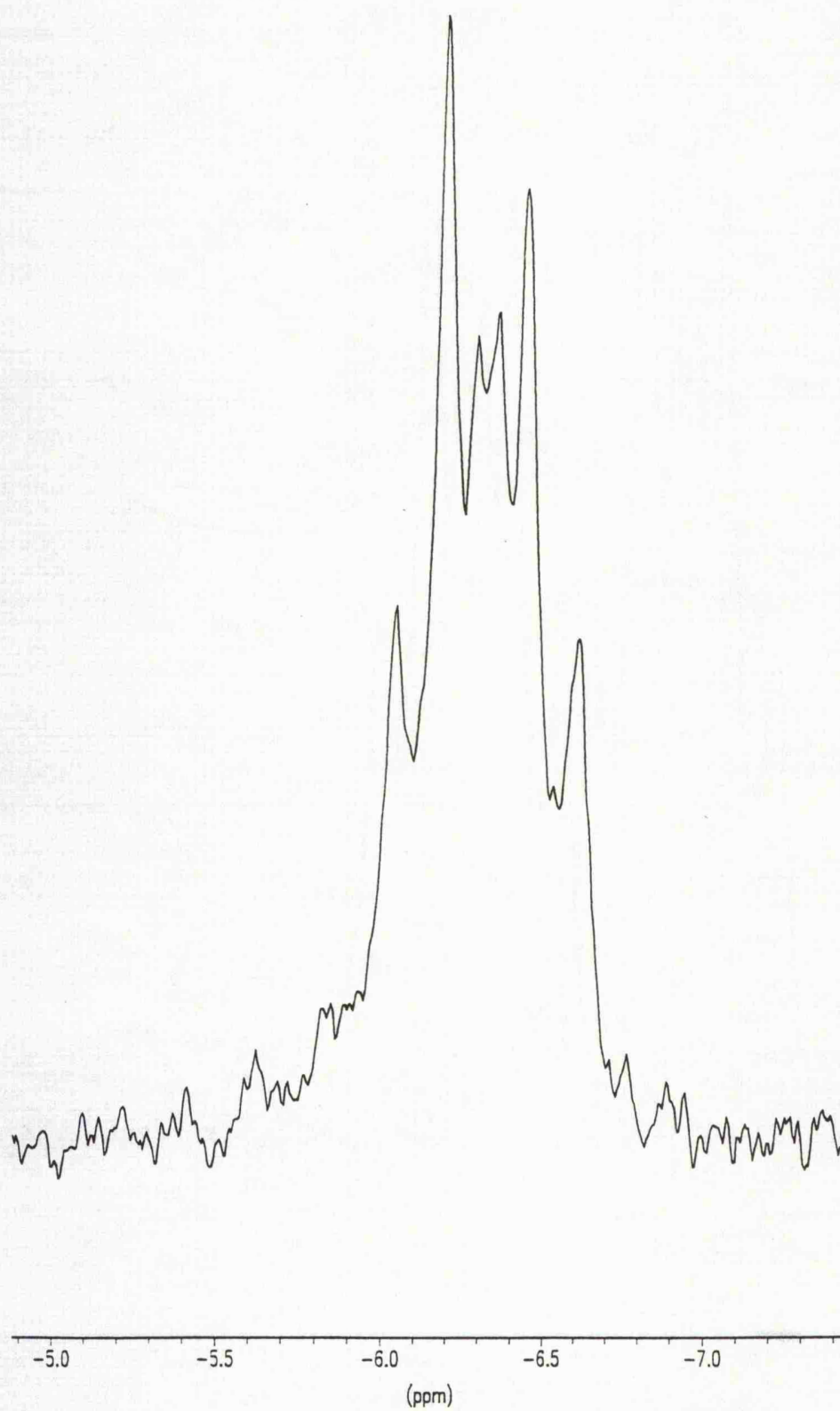


Figure 4.9 $^{31}\text{P}\{^1\text{H}\}$ NMR Spectrum of Complex (16)



References for Chapter 4

1. L. Vaska, *Inorg. Synth.*, 1968, **11**, 101.
2. (a) L. Vaska and J. Peone, *J. Chem. Soc., Chem. Commun.*, 1971, 418; (b) C. A. Reed and W. R. Roper, *J. Chem. Soc., Dalton Trans.*, 1973, 1370.
3. (a) K. Vrieze, J. P. Collman, C. T. Sears and M. Kubota, *Inorg. Synth.*, 1968, **11**, 101; (b) L. Vaska and J. Peone, *ibid.*, 1974, **15**, 64.
4. G. Wilkinson, R. A. Schunn and W. G. Peet, *Inorg. Synth.*, 1971, **13**, 126.
5. L. Vaska, *J. Am. Chem. Soc.*, 1966, **88**, 5325.
6. A. J. Deeming and B. L. Shaw, *J. Chem. Soc. (A)*, 1968, 1887 and references therein.
7. W. Strohmeier, W. Rehder-Stirnweiss and G. Reishig, *J. Organomet. Chem.*, 1971, **27**, 393.
8. U. Klabunde, *Inorg. synth.*, 1974, **15**, 83.
9. Graham Saunders, Personal Communications.
10. M. Atherton, J. H. Holloway, E. G. Hope and G. C. Saunders, *Polyhedron*, in press.
11. A. A. Grinberg, M. M. Singh and Yu. S. Varshavskii, *Russ. J. Inorg. Chem.*, 1968, **13**, 1399.
12. T. Sakakura, T. Sodeyama, K. Sasaki, K. Wada and M. Tanaka, *J. Am. Chem. Soc.*, 1990, **112**, 7221.
13. C. A. McAuliffe and R. Pollock, *J. Organomet. Chem.*, 1974, **77**, 265.
14. K. Goswami and M. M. Singh, *J. Ind. Chem. Soc.*, 1979, **56**, 477.
15. C. A. McAuliffe and R. Pollock, *J. Organomet. Chem.*, 1974, **69**, C13.
16. A. F. Williams, S. Bhaduri and A. G. Maddock, *J. Chem. Soc., Dalton Trans.*, 1975, 1958.
17. P. E. Garrou and G. E. Hartwell, *Inorg. Chem.*, 1976, **15**, 646.

18. D. Forster, *Inorg. Chem.*, 1972, **11**, 1686.
19. R. Brady, B. R. Flynn, G. L. Geoffroy, H. B. Gray, Jr. J. Peone and L. Vaska, *Inorg. Chem.*, 1976, **15**, 1485; R. G. Pearson, *Inorg. Chem.*, 1973, **12**, 712.
20. Refs 2., 11. and N. A. Buzina, M. M. Singh and S. Yu. Varshavskii, *Russ. J. Inorg. Chem.*, 1971, **16**, 1372.
21. G. Doyle, *J. Organomet. Chem.*, 1982, **224**, 355.
22. J. Blumm and G. J. Scharf, *J. Org. Chem.*, 1970, **35**, 1895.
23. R. D. W. Kemmitt, R. D. Peacock and J. Stocks, *J. Chem. Soc., Chem. Commun.*, 1969, 554.
24. R. W. Cockman, E. A. V. Ebsworth and J. H. Holloway, *J. Am. Chem. Soc.*, 1987, **109**, 2194.
25. R. W. Cockman, E. A. V. Ebsworth, J. H. Holloway, H. Murdoch, N. Robertson and P. G. Watson, "Reaction of Non-metal Fluorides with some Platinum Metal Complexes," J. Thrasher and S. Strauss, ACS Symposium Series, ACS Books, 1994.
26. P. G. Watson, E. Lork and R. Mews, *J. Chem. Soc., Chem. Commun.*, 1994, 1069.
27. S. N. Blackman, R. N. Haszeldine, R. V. Parish and J. H. Setchfield, *J. Chem. Res., Synop.*, 1980, 170.
28. M. Kubota, G. W. Keifer, R. M. Ishikawa and K. E. Bencala, *Inorg. Chim. Acta.*, 1972, **7**, 195.
29. Refs 2(b) and R. J. Fitzgerald, N. Y. Sakkab, R. S. Strange and V. Narutis, *Inorg. Chem.*, 1973, **12**, 1081; L. S. Chen, C. V. Senhoff and L. Vaska, *Science*, 1974, **174**, 587.
30. N. E. Buke, A. Singhal, M. J. Hintz, H. Hui, J. Ley, L. R. Smith and D. M. Blake, *J. Am. Chem. Soc.*, 1979, **101**, 74.
31. A. B. Gilchrist and D. Sutton, *J. Chem. Soc., Dalton Trans.*, 1977, 677.

32. M. R. Churchill, J. C. Fetting, L. A. Buttrey, M. D. Barkan and J. S. Thompson, *J. Organomet. Chem.*, 1988, **340**, 257.
33. R. Brady, W. H. Decamp, B. R. Flynn, M. L. Schneider, J. D. Scott, L. Vaska and M. F. Werneke, *Inorg. Chem.*, 1975, **14**, 2669.
34. M. R. Churchill, J. C. Fetting, B. J. Rappoli and J. D. Atwood, *Acta Cryst.*, 1987, **C43**, 1697.
35. J. Chatt, D. P. Melville and R. L. Richards, *J. Chem. Soc (A)*., 1969, 2841.
36. EXCURV92, SERC Daresbury Laboratory Program, N. Binstead, S. J. Gurman and J. W. Campbell, 1992.
37. F. A. Cotton, G. Wilkinson and P. L. Gaus, 'Basic Inorganic Chemistry,' Chapter 24, 532.
38. A. J. Blake, R. W. Cockman, E. A. V. Ebsworth and J. H. Holloway, *J. Chem. Soc., Chem. Commun.*, 1988, 529.
39. E. A. V. Ebsworth, N. Robertson and L. Y. Yellowlees, *J. Chem. Soc., Dalton Trans.*, 1993, 1031.
40. S. A. Brewer, J. H. Holloway and E. G. Hope, *J. Chem. Soc., Dalton Trans.*, 1994, 1067.
41. L. Vaska and S. S. Bath, *J. Am. Chem. Soc.*, 1966, **88**, 1333.
42. P. B. Chock and J. Halpern, *J. Am. Chem. Soc.*, 1966, **88**, 3511.

CHAPTER

FIVE

The Syntheses and Characterization

of Iridium(III)

Fluoride-Carbonyl-Phosphine Complexes

5.1 Introduction

In the previous chapter the chemistry of Vaska's complex, *trans*-[IrCl(CO)(PPh₃)₂], and its derivatives was described. As stated in section 4.3 the preparations of iridium(III) carbonyl-phosphine-fluoride complexes were almost entirely dominated by oxidative fluorination reactions of Vaska's complex and its derivatives or direct oxidative addition to fluoro-Vaska's. Subsequently, chapter 4 outlined the preparations of air-stable iridium(III) carbonyl-phosphine-fluoride complexes, formed by the oxidative fluorination of Vaska's complex and its analogous species by [XeF₂]. However, with the recent unambiguous assignment of an iridium(III) complex stabilized only by carbonyl and fluoride ligands, *fac*-[IrF₃(CO)₃],¹ a novel route was reported for the synthesis of an Ir(III) carbonyl-phosphine-fluoride complex *mer*-, *trans*-[IrF₃(CO)(PMe₃)₂].² Described below are the previously successful methods used for the incorporation of fluorine into an iridium carbonyl-phosphine complex.

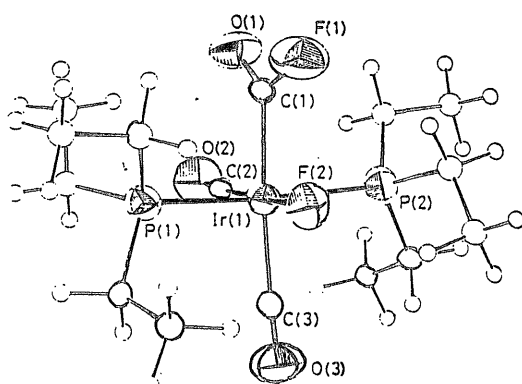
(A) The 'unusual' oxidative fluorination reactions of [XeF₂] to cationic species of the type, [Ir(CO)₃L₂]⁺ (L = PMe₃, PEt₃, PMe₂Ph, PEt₂Ph and PEtPh₂), [Ir(CO)(PMe₃)₄]⁺ and the neutral complex [Ir(CO)₂Cl(PMe₃)₂].

(B) Substitution of the carbonyl ligand in the novel, highly reactive *fac*-[Ir(CO)₃F₃], by Lewis bases.

5.2 Reactions of [XeF₂] with the Cationic Species [Ir(CO)₃L₂]⁺

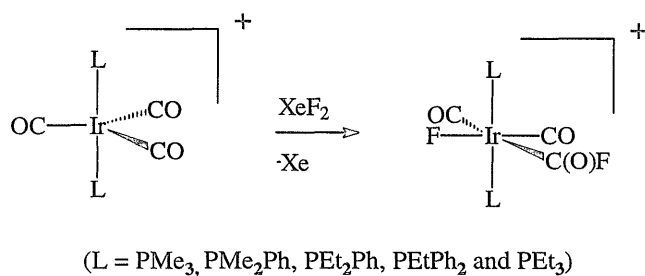
The complex [IrF(COF)(CO)₂(PEt₃)₂]⁺, characterized by X-ray crystallography (Figure 5.1),³ can be formed by the formal addition of two fluorine atoms across an iridium carbonyl bond in [Ir(CO)₃(PEt₃)₂]⁺.

Figure 5.1 Molecular Structure of $[\text{IrF}(\text{COF})(\text{CO})(\text{PEt}_3)_2]^+$



This was the first complex to contain the fluoroacetyl ligand and was reported by Blake *et al.*³ A subsequent study, by Ebsworth *et al.*,⁴ was undertaken to investigate the nature and scope of this reaction type. $[\text{XeF}_2]$ was reacted with a range of cationic five-coordinate iridium carbonyl (Scheme 5.1) containing complexes possessing different electronic and steric properties.

Scheme 5.1

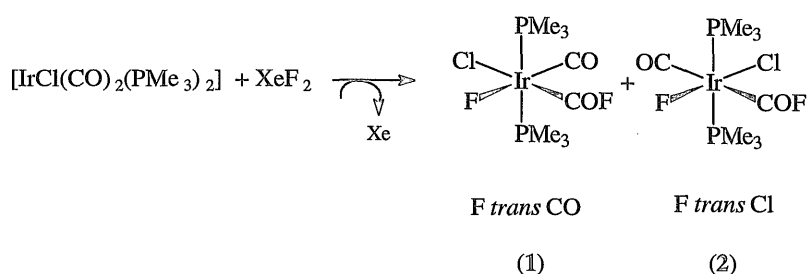


Control of steric and electronic properties are easily and conveniently achieved by varying the phosphine ligand. Reaction between $[\text{XeF}_2]$ and the complexes, $[\text{Ir}(\text{CO})_3\text{L}_2]^+$ occurs between 240 - 260 K in CH_2Cl_2 . The

fluoroacyl complexes were characterized by $^{19}\text{F}\{^1\text{H}\}$ and $^{31}\text{P}\{^1\text{H}\}$ NMR spectroscopy. In the ^{19}F NMR spectrum two resonances were observed. One was in the region associated with F bound to iridium *trans* to CO,⁵ and the other in the region associated with acyl fluorine.¹ The former showed coupling to the phosphorus atoms and the acyl fluorine. The latter showed a doublet coupling to the metal-bound fluoride. As with the complex *cis*-, *trans*- $[\text{IrF}_2\text{X}(\text{CO})(\text{PEt}_3)_2]$, discussed in the previous chapter, certain trends were observed in the NMR parameters. These will be discussed in some detail in section 5.5.1.

The analogous reaction of $[\text{IrCl}(\text{CO})_2(\text{PMe}_3)_2]$ with $[\text{XeF}_2]$ was reported to afford, at 250 K, two isomeric fluoroacyl complexes (1) and (2) in a 1:3 ratio (Scheme 5.2).⁴

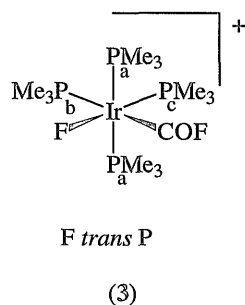
Scheme 5.2



Both complexes were characterized by $^{19}\text{F}\{^1\text{H}\}$ and $^{31}\text{P}\{^1\text{H}\}$ spectroscopy. Complex (1) showed two resonances in the $^{19}\text{F}\{^1\text{H}\}$ spectrum, a triplet of doublets, at δ -323, attributed to the fluorine *trans* to carbonyl and a doublet, at δ 135, assigned to the fluoroacyl group.³ The $^{31}\text{P}\{^1\text{H}\}$ NMR spectrum revealed the expected doublet, arising from the two equivalent phosphorus atoms coupling to the terminal fluorine, at δ -18.9.

Complex (2) exhibited $^{19}\text{F}\{^1\text{H}\}$ and $^{31}\text{P}\{^1\text{H}\}$ NMR spectra analogous to those of (1) but, the terminal fluorine was observed, at δ -452, in a chemical shift region associated with F *trans* Cl.⁶ However, this reported chemical shift for the resonance associated with F *trans* to Cl seems to be in the region characteristic of F *trans* F (δ -449 to -471, see section 5.5.1, Table 5.1).

Ebsworth *et al.*,⁴ also reported that the reaction of $[\text{Ir}(\text{CO})(\text{PMe}_3)_4]^+$ with $[\text{XeF}_2]$ gave, at 215 K, the fluoroacyl complex (3).



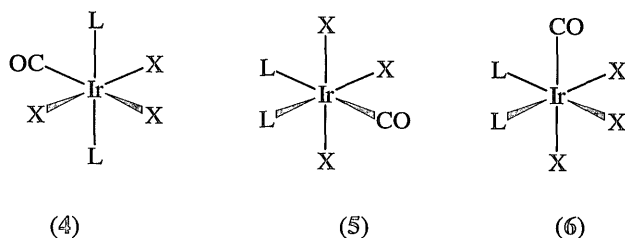
Complex (3) was characterized by $^{19}\text{F}\{^1\text{H}\}$ and $^{31}\text{P}\{^1\text{H}\}$ NMR spectroscopy. The $^{19}\text{F}\{^1\text{H}\}$ NMR spectrum revealed resonances; at δ -347, attributed to F *trans* P which showed coupling to P_a (39 Hz), P_b (40 Hz), P_c (140 Hz) and F (on COF) and one assigned to the fluorine on the fluoroacyl group which showed coupling to P_b (114 Hz) and the metal-bound fluorine (24 Hz). The $^{31}\text{P}\{^1\text{H}\}$ NMR spectrum showed three resonances attributed to P_a , P_b and P_c , in a 2:1:1 ratio, which showed coupling to the other spin $1/2$ nuclei except the fluorine on the fluoroacyl group. Complex (3) was isolated as a white solid which on exposure to the air decomposed rapidly.

5.3 The Reaction between *fac*-[IrF₃(CO)₃] and a Lewis base

Complexes of the type, [IrX₃(CO)L₂] (X = anionic ligand other than H; L = neutral donor ligand) may be prepared by the following methods:-

- (a) Carbonylation of [IrX₃L₃].
- (b) Reaction of an alcoholic solution of ligands with an iridium halido complex.
- (c) Oxidative addition of halogens, pseudohalogens and related molecules to [IrX(CO)L₂].
- (d) Action of halogens or a halogen source on compounds of the type [Ir(CO)L₃]⁺ or [IrX₂(carbon ligand)(CO)L₂].⁷

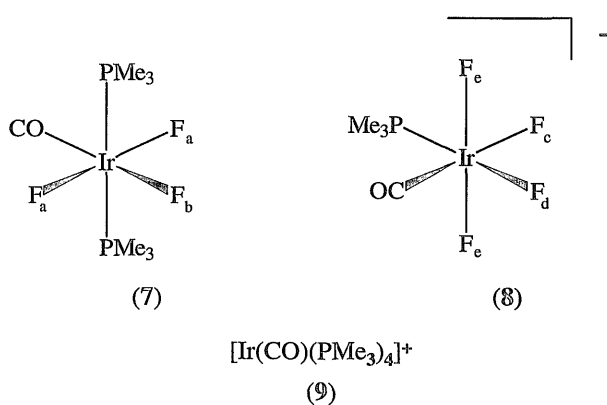
In general three octahedral arrangements are possible for this ligand array, *i.e.* (4), (5) and (6), and in many cases all three have been obtained, *e.g.* for (X = Cl and L = PPh₃). The three isomers have $\nu(\text{CO})$ values of 2073(4), 2105(5) and 2073(6).⁸



More isomers are of course possible if all the X ligands are not equivalent.

Until recently, there has been only one reported example of a fluoro-complex of the type, [IrX₃(CO)L₂]⁹ (X = F and L = PEt₃), from the reaction of *trans*-[IrCl(CO)(PEt₃)₂] with [XeF₂], discussed earlier and it only represented a minor component of the reaction mixture. However, with the recent synthesis and unambiguous characterization of *fac*-[IrF₃(CO)₃], a

novel route into such species was reported by Brewer *et al.*² The substitution of carbonyl ligands by various σ -donor ligands such as phosphines, arsines, stibines, nitrous oxide and amines are well documented in the literature.¹⁰ The Lewis base, PMe_3 , was found to react with *fac*- $[\text{IrF}_3(\text{CO})_3]$, in CD_2Cl_2 , at room temperature, with the evolution of CO. Combinations of ^{19}F , ^{31}P and ^{13}C NMR spectroscopic data revealed the presence of two major species in solution, (7) and (8), and evidence of a third complex, (9), which did not contain fluorine, was obtained through $^{13}\text{C}\{^1\text{H}\}$ and $^{31}\text{P}\{^1\text{H}\}$ NMR data.²



The ^{19}F NMR spectrum of complex (7) revealed two mutually coupled resonances, a doublet of triplets and a triplet of triplets in a 2:1 ratio. The first resonance associated with F_a is in chemical shift region typical of *trans* F,¹¹ and the second is in a region characteristic of F *trans* CO.⁵ This reaction and the associated NMR parameters are discussed in detail in section 5.5.1 (page 227).

5.4 Summary

Iridium(III) carbonyl-halogen-phosphine complexes of the type $[\text{IrXY}_2(\text{CO})(\text{PR}_3)_2]$ ($X = \text{F}, \text{Cl}, \text{Br}$; $Y = \text{Cl}, \text{Br}, \text{I}$ and $\text{PR}_3 =$ tertiary phosphine ligands) have been widely studied.⁸ The majority of the complexes of the heavier halogens have been formed by halogenation of *trans*- $[\text{IrCl}(\text{CO})(\text{PPh}_3)_2]$. Although, the fluoro-complexes obtained were formed by the reaction of Cl_2 , Br_2 , or I_2 and *trans*- $[\text{IrF}(\text{CO})(\text{PPh}_3)_2]$, there is no reported example of F_2 gas being employed, presumably for practical reasons.

However, recently Brewer *et al.* successfully identified the trifluoride complex *mer*-, *trans*- $[\text{IrF}_3(\text{CO})(\text{PMe}_3)_2]^2$ formed by the reaction of *fac*- $[\text{IrF}_3(\text{CO})_3]$ and PMe_3 . This complex represents only the second reported d^6 iridium complex of the type, *mer*-, *trans*- $[\text{IrF}_3(\text{CO})(\text{PR}_3)_2]$ (where $\text{PR}_3 = \text{PMe}_3$ and PEt_3), with the PEt_3 analogue being only a minor component of the reaction between *trans*- $[\text{IrCl}(\text{CO})(\text{PEt}_3)_2]$ and $[\text{XeF}_2]$ (see section 4.3.1).⁹ Thus, this class of organometallic fluoride complexes is an area poorly developed and so the reactions of *fac*- $[\text{IrF}_3(\text{CO})_3]$ with a variety of Lewis bases have been studied. The stability and reactivity of the products formed is addressed in this chapter.

5.5 Reactions of *fac*-[IrF₃(CO)₃] with Monodentate Phosphine Ligands

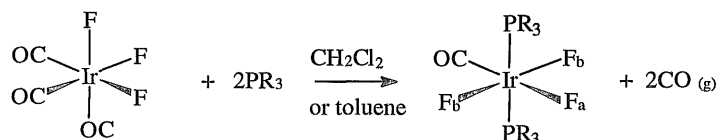
Black *fac*-[IrF₃(CO)₃] is not soluble in organic solvents (*e.g.* dichloromethane, toluene) however, on addition of the Lewis base, as described in sections 6.9 and 6.10, rapid reaction occurs, at room temperature, with the evolution of CO gas, and all the metal complex dissolves affording a yellow solution. Removal of the solvent, after approximately ten minutes, yields air-stable solids or oils.

Note: During the studies of the reactions between *fac*-[IrF₃(CO)₃] and various Lewis bases problems were encountered in attempts to obtain pure products. The main problem was trying to maintain the correct stoichiometric ratio of 2:1 for the Lewis base:*fac*-[IrF₃(CO)₃] and induce a quantitative reaction. Since, the *fac*-[IrF₃(CO)₃] was highly reactive, surface decomposition ensued immediately as it was suspended in either of the organic solvents employed. Furthermore, the time scale for completion of the reaction was found to be governed by the solubility of the Lewis base in the solvent thus, an increase in solubility resulted in a faster reaction time and therefore, the decomposition time of the starting material was shortened. The Lewis bases were found to have a better solubility in CH₂Cl₂ than in toluene, therefore the reaction time was faster. However, reaction of the final product with the CH₂Cl₂ if left suspended in solution for too long gave further species (see section 5.10.1). It became apparent that these reactions were difficult to control in terms of obtaining pure products as either additional species were formed or the product was contaminated with excess phosphine, since the correct stoichiometry was hard to maintain, which was troublesome to remove. In order to limit the amount of time the product, from the reaction of *fac*-[IrF₃(CO)₃] and the appropriate Lewis base, was exposed to the dichloromethane solution the reaction was constantly monitored by the

effervescence produced and as soon as this ceased the solvent was removed *in vacuo* (approximately 5-10 minutes).

The reaction between *fac*-[IrF₃(CO)₃] and PR₃ proceeds according to Scheme 5.3 to give complexes *mer*-, *trans*-[IrF₃(CO)(PR₃)₂] **5a** - **5j**.

Scheme 5.3



5.5.1 ¹⁹F and ³¹P{¹H} NMR Spectroscopy

The ³¹P{¹H} NMR spectra of complexes **5a** - **5j** show a doublet of triplets (Figure 5.2) at chemical shifts appropriate for *trans*- phosphine ligands; both couplings are characteristic of *cis*- ²J_{PF} interactions. The ¹⁹F NMR spectra show two mutually-coupled resonances, a triplet of triplets and a doublet of triplets (Figure 5.3), in a 1:2 ratio, assigned to F_a and F_b respectively. The doublet and triplet couplings are typical of *cis*- ²J_{FF} with the remaining triplet coupling on each resonance arising from *cis*- coupling of the fluorines to the two equivalent *trans*- phosphine ligands, which are consistent with the ³¹P{¹H} NMR spectra. The chemical shifts for the resonances assigned to F_b and F_a are in a region characteristic of fluorine *trans*- fluorine¹¹ and fluorine *trans*- carbonyl⁵ respectively. The ¹⁹F and ³¹P{¹H} NMR data for these complexes are presented in Table 5.1.

As discussed in section 5.3, Brewer² reported that the reaction between *fac*-[IrF₃(CO)₃] and PMe₃ afforded three major species in solution;

Figure 5.2 $^{31}\text{P}\{^1\text{H}\}$ NMR Spectrum of *mer-, trans*- $[\text{IrF}_3(\text{CO})(\text{PMe}_2\text{Ph})_2]$

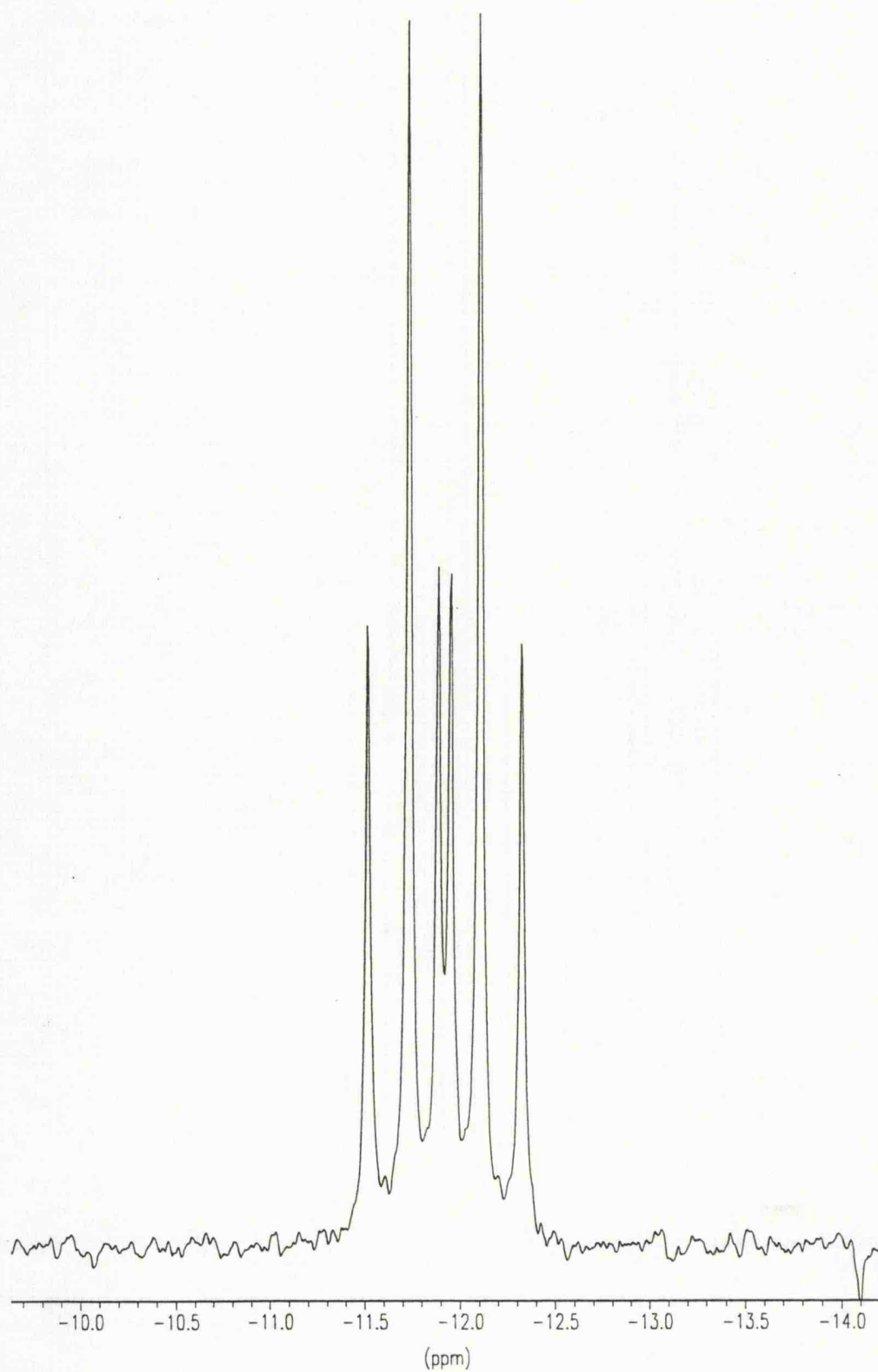
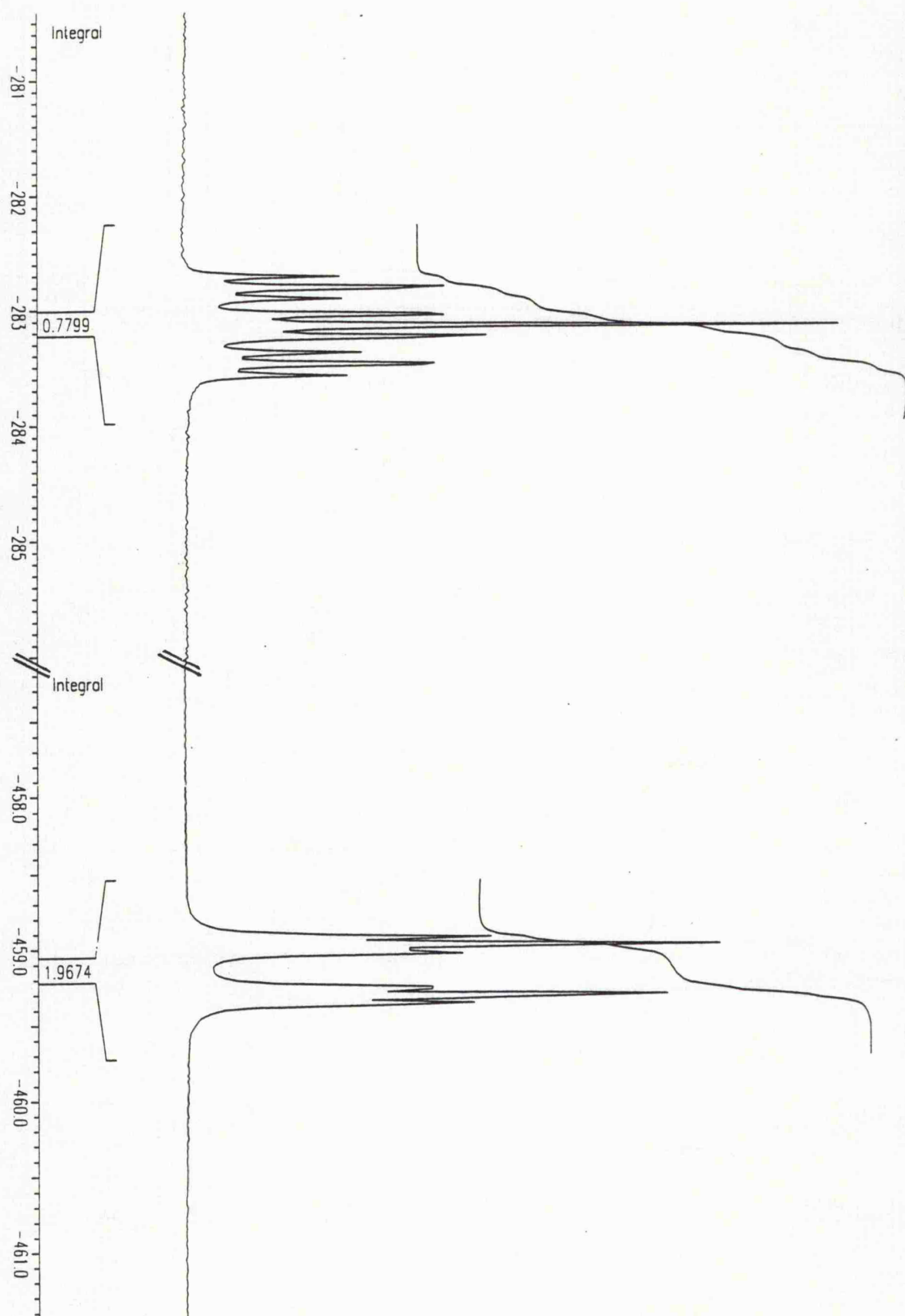
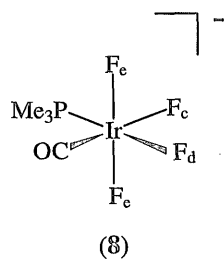


Figure 5.3 ^{19}F NMR Spectrum of *mer*-, *trans*- $[\text{IrF}_3(\text{CO})(\text{Pcy}_3)_2]$



mer, trans-[IrF₃(CO)(PMe₃)] (7), [IrF₄(CO)(PMe₃)]⁻ (8) and [Ir(CO)(PMe₃)₄]⁺ (9). The ¹⁹F NMR spectrum of complex (8) showed three resonances at δ -225, -249 and -433, associated with F_c, F_d and F_e, in a ratio of 1:1:2. The couplings were consistent with the structure of (8), which was confirmed by the observation of a doublet of doublet of triplets in the ³¹P{¹H} NMR spectrum at δ -29.2.



However, in all cases, even when repeating the PMe₃ reaction, these and the related species (8) and (9), for the range of phosphine ligands used, were not observed. One can only speculate that these complexes, (8) and (9), were formed as a result of the author using an excess of PMe₃ in the reaction with *fac*-[IrF₃(CO)₃]. The ¹⁹F and ³¹P{¹H} NMR data of complex (7) and the previously discussed [IrF₃(CO)(PEt₃)₂] (Table 5.2) are comparable with those presented in Table 5.1 with only minor discrepancies in the values.

**Table 5.1 ^{19}F and $^{31}\text{P}\{^1\text{H}\}$ Data for the Complexes *mer*-, *trans*-
 $[\text{IrF}_3(\text{CO})(\text{PR}_3)_2]$ 5a - 5j**

PR ₃	$\delta(^{19}\text{F})$ / ppm		$\delta(^{31}\text{P})$ / ppm	$^2J(\text{F}_a\text{F}_b)$ / Hz	$^2J(\text{F}_a\text{P})$ / Hz	$^2J(\text{F}_b\text{P})$ / Hz
	F _a	F _b				
5a PMe ₃ ^a	-285	-471	-12.0	97	38	23
5b PEt ₃ ^a	-287	-470	8.6	99	31	21
5c PPh ₃ ^a	-277	-449	-6.4	98	30	19
5d PPh ₂ (C ₆ F ₅) ^a	-289	-448	-11.0	96	30	19
5e Pcy ₃ ^a	-281	-458	7.4	98	27	14
5f P(<i>p</i> -MeC ₆ H ₄) ₃ ^a	-278	-451	-6.0	98	30	19
5g P ^{<i>i</i>} Pr ₃ ^b	-283	-461	17.5	96	27	15
5h PEtPh ₂ ^b	-282	-455	-1.4	101	32	19
5i PMe ₂ Ph ^b	-281	-463	-11.9	98	37	22
5j PMePh ₂ ^b	-284	-460	-9.5	99	36	20

(a) in CD₂Cl₂

(b) in C₆D₆

Table 5.2 ^{19}F and $^{31}\text{P}\{^1\text{H}\}$ NMR Data for $[\text{IrF}_3(\text{CO})(\text{PMe}_3)_2]$ and $[\text{IrF}_3(\text{CO})(\text{PEt}_3)_2]$

PR_3	$\delta(^{19}\text{F})$ / ppm		$\delta(^{31}\text{P})$ / ppm	$^2J(\text{F}_a\text{F}_b)$ / Hz	$^2J(\text{F}_a\text{P})$ / Hz	$^2J(\text{F}_b\text{P})$ / Hz	Refs.
	F_a	F_b					
PMe_3^a	-285	-471	-14.2	97	38	24	2
PEt_3^a	-289	-471	6.9	96	31	18	9

(a) CD_2Cl_2 solution

Brewer, upon comparison of the NMR data, stated that the relative ^{19}F NMR chemical shifts and coupling constants were insensitive to changes in the phosphine ligands. However, with a more extensive study, an apparent trend in the ^{19}F NMR data can be seen. The coupling constants $^2J_{\text{FP}}$ generally increase on going from the widest to the narrowest cone angle in complexes **5a - 5j** (Table 5.3).

In a previous study, by Ebsworth *et al.*,⁴ on complexes of the type $[\text{IrF}(\text{COF})(\text{CO})_2(\text{PR}_3)_2]^+$ ($\text{PR}_3 = \text{PEt}_3, \text{PMe}_3, \text{PMe}_2\text{Ph}, \text{PEt}_2\text{Ph}$ and PEtPh_2) a similar trend was also reported (Table 5.4).

Coupling constants in coordinated phosphines have been explained by considering the percentage s-orbital character in the metal-phosphorus bond which is in turn related to the angle between the substituents (Figure 5.4) on the free phosphine.¹³ The C-P-C angle for phosphines containing large substituents and thus possessing large cone angles (Figure 5.4) generally open less on coordination as a result of steric crowding.

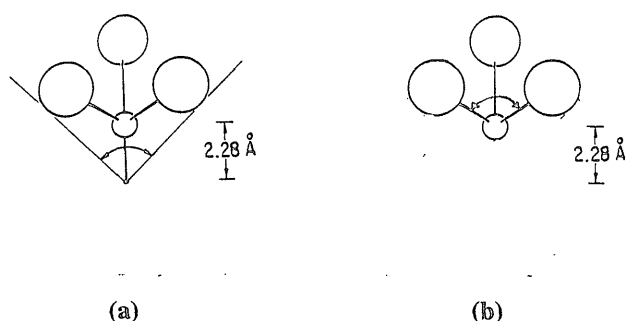
Table 5.3 Comparison of $^2J_{\text{FP}}$ Coupling Constant and Cone Angle of the phosphines in Complexes 5a - 5j

Phosphine	Cone Angle ¹²	$^2J(\text{F}_\text{a}\text{P})/\text{ Hz}$	$^2J(\text{F}_\text{b}\text{P})/\text{ Hz}$
Pcy ₃	170	27	14
P ⁱ Pr ₃	160	27	15
PPh ₂ (C ₆ F ₅)	158	30	22
P(<i>p</i> -MeC ₆ H ₄) ₃	145	30	19
PPh ₃	145	30	19
PEtPh ₂	140	32	19
PMePh ₂	136	36	20
PEt ₃	132	31	21
PMe ₂ Ph	122	37	22
PMe ₃	118	38	23

Table 5.4 Comparison of $^2J_{\text{FP}}$ Coupling Constant and Cone Angle of the phosphines in Complexes [IrF(COF)(CO)₂(PR₃)₂]⁺

Phosphine	Cone Angle ¹²	$^2J(\text{FP})/\text{ Hz}$
PEtPh ₂	140	29
PEt ₂ Ph	136	31
PEt ₃	132	31
PMe ₂ Ph	122	36
PMe ₃	118	39

Figure 5.4 Schematic Diagram of (a) Cone Angle and the (b) Angle between Substituents on Phosphines



Thus, the amount of s-orbital character in the metal phosphorus bond is less than for complexes of phosphine ligands with smaller substituents. This is reflected in the coupling constants, the larger the degree of s-character the larger the coupling constant. It is evident from Table 5.3 that other factors influence the couplings $^2J_{\text{FaP}}$ and $^2J_{\text{FbP}}$ since the variation with cone angle is not regular.

Brewer stated that the observed difference in ^{31}P chemical shifts was associated with the π -acidity of the two phosphines. However, upon comparison of their pK_a values, 8.65 and 8.69 for PMe_3 and PEt_3 respectively, it is apparent that other factors are involved in determining the ^{31}P chemical shifts on coordination of the phosphine. Coordination chemical shifts ($\Delta^{31}\text{P} = \delta_{\text{complex}} - \delta_{\text{free ligand}}$) depend on the electronegativity of the substituents on phosphorus and the change in the C-P-C angle, in the phosphine ligand, on coordination. The magnitude of Δ tends to be less for larger ligands, as seen for complexes **5a** - **5j** (Table 5.5), this is again due to the C-P-C angles of the phosphines with larger substituents opening less on coordination.

Table 5.5 Comparison of Cone Angle and Coordination Chemical Shift (Δ) of Various Phosphines in Complexes 5a - 5j

Phosphine	Cone Angle ¹²	pKa ¹²	$\delta(^{31}\text{P})/\text{ppm}^a$ (free ligand)	$\Delta(^{31}\text{P})/\text{ppm}$
Pcy ₃	170	9.70	11.3	-3.9
P(ⁱ Pr) ₃	160	-	20.0	-2.5
PPh ₂ (C ₆ F ₅)	158	-	-24.7	13.7
P(<i>p</i> -MeC ₆ H ₄) ₃	145	3.84	-2.5	-3.5
PPh ₃	145	2.73	-6.0	-0.4
PEtPh ₂	140	-	-12.3	10.9
PMePh ₂	136	4.57	-27.7	18.2
PEt ₃	132	8.69	-20.1	28.7
PMe ₂ Ph	122	6.5	-47.6	35.7
PMe ₃	118	8.65	-62.2	50.2

(a) referenced relative to 85 % H₃PO₄

It is evident from Table 5.5 that the coordination chemical shifts, $\Delta(^{31}\text{P})$, of the fluoro-complexes [IrF₃(CO)(PR₃)₂] are loosely related to the cone angle, of the phosphine ligand. This angle opening generally results in a higher frequency shift upon coordination.

Ebsworth and co-workers⁴ also reported a similar trend in the phosphine coordination chemical shifts for their fluoroacyl complexes, [IrF(COF)(CO)₂(PR₃)₂]⁺ (Table 5.6).

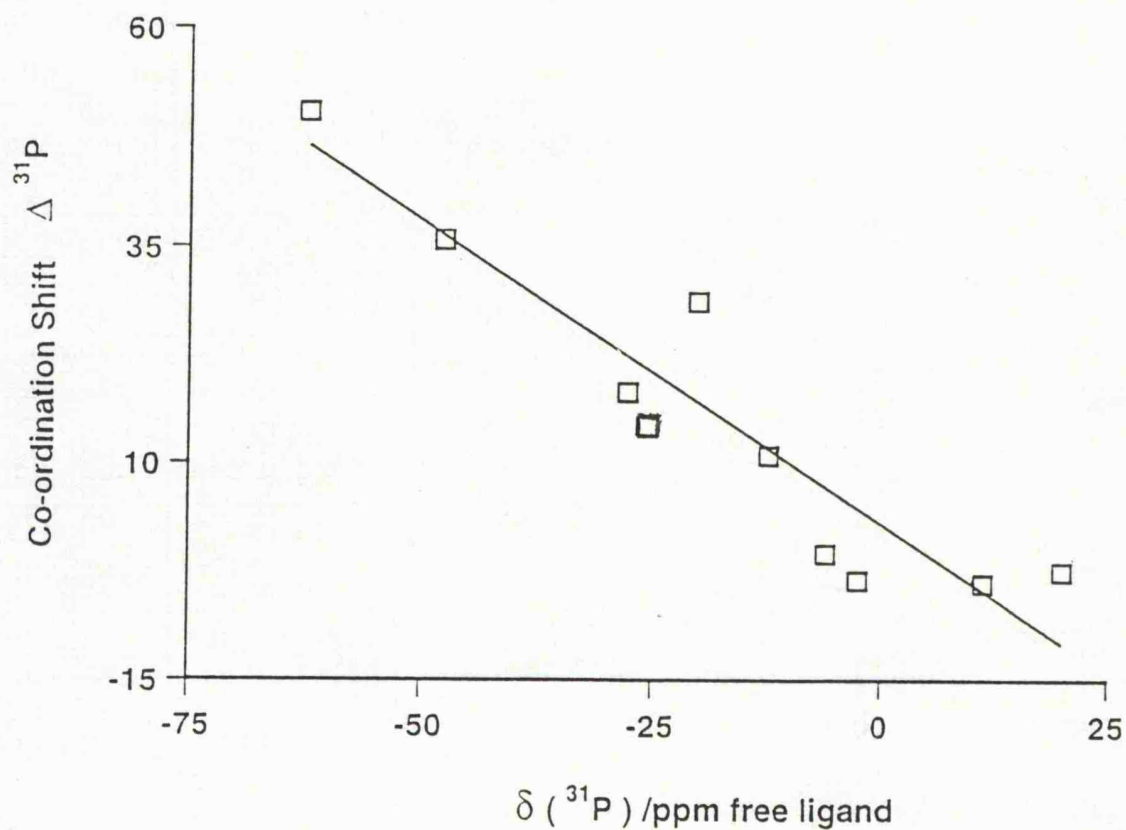
Table 5.6 Comparison of Cone Angle and Coordination Chemical Shift (Δ) for the Complexes $[\text{IrF}(\text{COF})(\text{CO})_2(\text{PR}_3)_2]^+$

Phosphine	Cone Angle ¹²	$\delta(^{31}\text{P})/\text{ppm}$ (free ligand)	$\Delta(^{31}\text{P})/\text{ppm}$
PEtPh_2	140	-12.3	4.2
PEt_2Ph	136	-5.5	12.0
PEt_3	132	-20.1	22.9
PMe_2Ph	122	-47.6	24.4
PMe_3	118	-62.2	38.4

The complex $[\text{IrF}_3(\text{CO})(\text{PPh}_2\text{C}_6\text{F}_5)_2]$ containing the phosphine $\text{PPh}_2(\text{C}_6\text{F}_5)$, which has a wider cone angle than $\text{P}(p\text{-MeC}_6\text{H}_4)_3$, PPh_3 and PEtPh_2 has an unexpectedly larger coordination shift. This implies that the electronegativity of the substituent C_6F_5 , on phosphorus, is having a major influence on the coordination chemical shift, $\Delta^{31}\text{P}$, in the complex $[\text{IrF}_3(\text{CO})(\text{PPh}_2\text{C}_6\text{F}_5)_2]$. However, recent investigations by Saunders *et al.*,¹⁴ involving complexes of the type $[\text{RhCl}(\text{CO})\{\text{PPh}_x(\text{C}_6\text{F}_5)_{3-x}\}_2]$ have shown no comparable trends in the coordination shifts, $\Delta^{31}\text{P}$, as the number of pentafluorophenyl rings are increased.

Mann and co-workers¹⁵ reported that there is a linear correlation between the chemical shift of the free phosphine, δ , and the coordination shift, $\Delta^{31}\text{P}$. This linear correlation is apparent for the complexes **5a** - **5j** (Figure 5.5).

Figure 5.5 A Graph Showing the Linear Relationship Between δ (Free Phosphine) and the Coordination Chemical Shift ($\Delta^{31}\text{P}$) for the Complexes *mer*-, *trans*-[IrF₃(CO)(PR₃)₂]



5.5.2 Infrared and Mass Spectrometry

All previously reported studies involving the preparation of iridium(III) fluoride phosphine carbonyl complexes employed multinuclear NMR spectroscopy (see sections 5.2 and 5.3) to elucidate the reaction products. In most cases, the products were either found to be, or deemed to be, air-sensitive and so problems would be encountered when attempting to obtain infrared and mass spectrometry data. Thus, to date the complexes $[\text{IrF}(\text{COF})(\text{CO})_2(\text{PR}_3)_2]^+$ ($\text{PR}_3 = \text{PEt}_3^5$ and PMe_3^4) and the more recently reported $[\text{IrFCl}(\text{NSF}_2)(\text{CO})(\text{PPh}_3)_2]^{16}$ are the only examples of iridium(III) carbonyl-phosphine-fluoride compounds for which the $\nu(\text{CO})$ frequencies have been reported. However, the d^6 iridium complexes **5a** - **5j**, were found to be air-stable thus facilitating the collection of infrared and mass spectrometry data (Table 5.7). FAB⁺ mass spectrometry confirms the mononuclearity of the complexes and that, in most cases, the parent ion was not observed but the pattern for $[M-\text{CO}]^+$ was.

The infrared spectra of complexes **5a** - **5j** gave the expected single terminal $\nu(\text{CO})$ band.

Table 5.7 Infrared and Mass Spectrometry Data for Complexes 5a - 5j

Complex	$\nu(\text{CO})/\text{cm}^{-1}$	m/z
5a	2030	402 $[\text{M-CO}]^+$
5b	2024 ^a	513 $[\text{M}]^+$
5c	2024	773 $[\text{M-CO}]^+$
5d	2062	981 $[\text{M}]^+$
5e	2008	809 $[\text{M-CO}]^+$
5f	2019	857 $[\text{M-CO}]^+$
5g ^b	2006	-
5h ^b	2036 ^a	-
5i	2030 ^a	535 $[\text{M-F}]^+$
5j	2015 ^a	649 $[\text{M-CO}]^+$

all infrared spectra were recorded as Nujol mulls unless stated otherwise

(a) recorded in benzene solution

(b) several attempts were made to obtain mass spectral data, but no characterizable spectra were produced

The infrared spectrum of the starting material, *fac*- $[\text{IrF}_3(\text{CO})_3]$, shows two $\nu(\text{CO})$ bands, at 2213 and 2165 cm^{-1} as expected for an octahedral complex of C_{3v} symmetry. Both of these resonances occur at higher frequencies than that for free carbon monoxide (2143 cm^{-1})¹⁷ and also higher than that reported for other iridium(III) carbonyl fluoride complexes (2022-2137 cm^{-1})^{4,5,16}. This phenomenon of high $\nu(\text{CO})$ infrared frequencies, has been reported previously for $\text{M}(\text{CO})^+$ complexes ($\text{M} = \text{Cu}, \text{Ag}, \text{Au}$)^{18,19} and

$\text{Hg}(\text{CO})_2^{2+}$.²⁰ A simplistic view of the bonding in carbonyl compounds will help to explain this phenomenon. The bonding between CO and a transition metal is described as involving the donation of electron density from a σ orbital on the carbon to a metal orbital, while simultaneously accepting electron density from the metal $d\pi$ -orbitals into the π^* antibonding molecular orbital on the carbonyl. This latter interaction is termed back-bonding with the overall effect being a synergic type of bonding. Thus, the CO is acting as both a σ -donor and a π -acceptor. Consequently, as the $\pi^* \leftarrow d\pi$ back-bonding increases, the M-C bond should become stronger (shorter) and the C-O bond correspondingly weaker (longer), which will be manifested in the positions of the infrared active bands of the resulting complexes. Shifts to lower frequencies relative to that of free CO are a result of an increase in back-bonding. The high $\nu(\text{CO})$ infrared frequencies in the cationic complexes have been attributed to σ -donation of the slightly antibonding σ lone pair on CO to the metal with little or no π -back donation from the metal to the carbonyl. Since this antibonding orbital is now a bonding orbital this effectively increases the bond order of CO, and thus the $\nu(\text{CO})$ increases. In comparison, the carbonyl ligands in *fac*- $[\text{IrF}_3(\text{CO})_3]$ are bonded in a similar manner to that described above, where there is little or no π -back donation. The strongly electron withdrawing fluoride ligands must therefore be effectively removing electron density from the d^6 Ir(III) metal centre, increasing the σ -acceptor ability of the metal.²¹

Lewis bases, such as phosphines, are excellent donors but relatively poor acceptor ligands and so, on coordination to a metal carbonyl complex, electron density is donated to the metal centre. Consequently, the amount of back-bonding, between the metal and the carbonyl, is increased resulting in a shift to lower frequencies for the carbonyl stretching frequencies in the complexes. Thus, the expected decrease in $\nu(\text{CO})$ frequencies of the complexes **5a** - **5j** from that of *fac*- $[\text{IrF}_3(\text{CO})_3]$ can be seen in Table 5.7. It is

evident by comparing the $\nu(\text{CO})$ frequencies, in Table 5.7, that varying the phosphine ligand has little effect, this is as expected since the phosphine ligands are *cis* to the carbonyl ligand and so electronic effects are minimal.

However, for the complexes $[\text{IrF}_3(\text{CO})(\text{PR}_3)_2]$ ($\text{PR}_3 = \text{PEt}_3, \text{PMe}_2\text{Ph}$ and PPh_3) the CO stretching frequencies are lower than those for the corresponding chloro-analogues (Table 5.8) which implies that more back-bonding is present in the fluoro-compounds.

Table 5.8 Comparison of the $\nu(\text{CO})$ Infrared Frequencies for the Complexes $[\text{IrX}_3(\text{CO})(\text{PR}_3)_2]$

PR_3	$\nu(\text{CO})/\text{cm}^{-1}$		Refs.
	$\text{X} = \text{F}^{\text{a}}$	$\text{X} = \text{Cl}$	
PEt_3	2024 ^b	2031	21
PMe_2Ph	2030 ^b	2064	22
PPh_3	2024	2078	23

Nujol mulls unless otherwise stated

(a) referenced to this work

(b) benzene solution

This trend is the opposite to that expected from the high electronegativity and inductive effects of the fluoride ligands. The increased amount of back-bonding on going from chloro- to fluoro-complexes can be explained by considering the π -acceptor and π -donor ability of the halides. The π -acceptor ability follows the trend $\text{F} < \text{Cl} < \text{Br} < \text{I}$, due to the increasing availability of low lying orbitals as the group is descended, with the opposite being observed for the π -donor ability. Therefore, as chlorine is a better π -acceptor than fluorine, more electron density will be removed from the metal

π orbitals in the chloride analogue than in the fluoride. A consequence of this is a decrease in back-bonding between the metal and the carbonyl moiety and hence a higher $\nu(\text{CO})$ infrared frequency in the chloro-complex. By considering the π -donor ability of the halides the same conclusion can be ascertained. Since fluoride is a better π -donor than chloride, more electron density will be donated to the metal π orbitals in the fluoro-complex. Thus, the amount of back-bonding will increase and consequently, a decrease in the $\nu(\text{CO})$ frequency will be observed. A similar trend has been observed previously for Vaska's complex and its derivatives, *trans*- $[\text{MX}(\text{CO})(\text{PPh}_3)_2]$ ($\text{M} = \text{Ir}, \text{Rh}$; $\text{X} = \text{F}, \text{Cl}, \text{Br}, \text{I}$), whereby the $\nu(\text{CO})$ frequencies were found to follow the order $\text{X} = \text{F} < \text{Cl} < \text{Br} < \text{I}$ consistent with the increasing π -acceptor strength of the halides along this series and decreasing π -donor strength.²⁴

5.6 EXAFS Analysis of $[\text{IrF}_3(\text{CO})(\text{PEt}_3)_2]$

An inability to obtain suitable single crystals for X-ray crystallographic studies meant that structural information had to be obtained by an alternative technique. In the absence of structurally characterized iridium(III) fluoride complexes as model compounds, the reliability of the data collection and treatment was confirmed by the collection and analysis of iridium L_{111} -edge EXAFS data on $[\text{Ir}_4(\text{CO})_{12}]$ and subsequent analysis of *fac*- $[\text{IrF}_3(\text{CO})_3]$. The results for $[\text{Ir}_4(\text{CO})_{12}]$ were in satisfactory agreement with the data from the highly disordered single crystal X-ray analysis.²⁵ The fits discussed below are all compared with the average raw (background-subtracted) EXAFS data (Figure 5.6).

Initially the data were modelled, utilising EXCURV92,²⁶ to 4 shells of 3 fluorine atoms at *ca.* $r = 1.97(2)$ Å, 2 phosphorus atoms at *ca.* $r = 2.34(2)$ Å, 1 carbon at *ca.* $r = 1.75(2)$ Å and 1 oxygen at *ca.* $r = 2.98(2)$ Å using

localised C_{2v} symmetry and a fixed Ir-C-O bond angle of 180° for multiple scattering (Figure 5.6). An additional weak broad feature around 3.5 \AA was observed upon examination of the Fourier transforms. This feature was attributed to the 6 carbon atoms, nearest the metal centre, on the phosphine ligands. So further modelling of the EXAFS data using 5 shells resulted in significant reductions in the R-factor and fit index (Figure 5.7). All shells were tested for statistical significance.²⁷

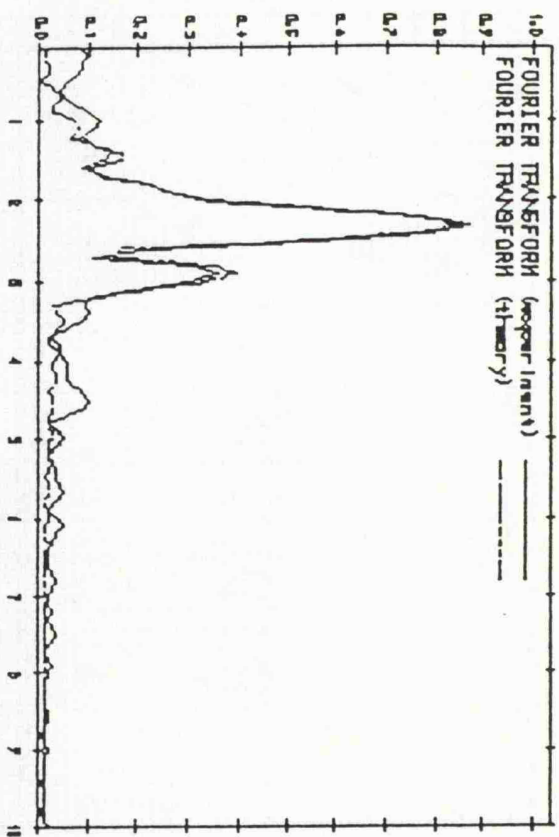
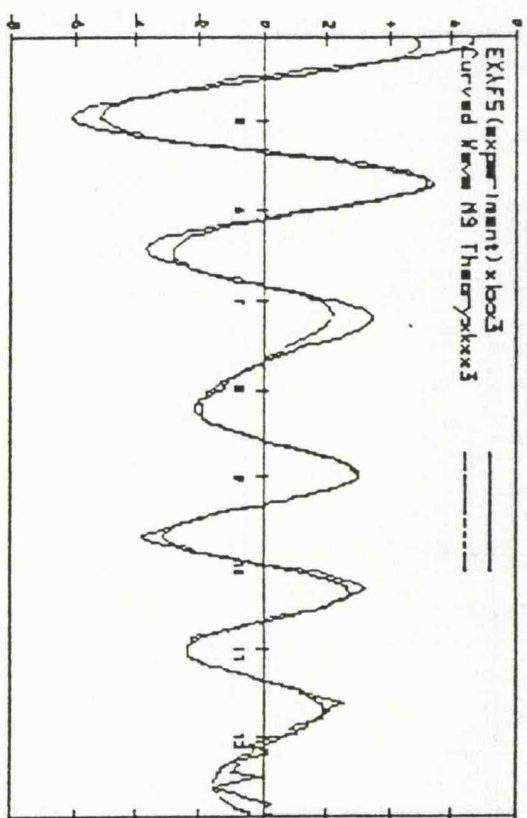
The bond length data obtained by EXAFS for *mer*-, *trans*- $[\text{IrF}_3(\text{CO})(\text{PEt}_3)_2]$ is reasonable when compared with those of other carbonyl-phosphine-fluoride complexes of low-valent metals and the previously reported *fac*- $[\text{IrF}_3(\text{CO})_3]$ (Table 5.9).

The Ir-F (terminal) bond length for $[\text{IrF}_3(\text{CO})(\text{PEt}_3)_2]$ is very similar to those previously reported (Table 5.9) all of which contain fluoride *trans*- to a carbonyl ligand, for which the M-F bond lengths fall into the range $2.089 - 1.92 \text{ \AA}$. Furthermore, the Ir-P bond lengths are also comparable to those M-P distances reported in Table 5.9. However, the Ir-C bond length when compared with those in similar iridium complexes, seems to be slightly shorter than those reported for a carbonyl *trans*- to a fluoride ligand and consequently, the C-O bond length is longer. This is expected since the $\nu(\text{CO})$ band, which is directly related to bond length, is observed at a lower frequency (2024 cm^{-1}) than that in *fac*- $[\text{IrF}_3(\text{CO})_3]$ (2213 and 2170 cm^{-1}) and $[\text{IrF}(\text{COF})(\text{CO})(\text{PEt}_3)_2]^+$ (2110 cm^{-1}).

Figure 5.6 The Background-Subtracted EXAFS (K^3 weighted) and the

Fourier Transform EXAFS of *mer*-, *trans*-[IrF₃(CO)(PEt₃)₂]

(modelled to 4 shells)



E0	9.35	VP1	-1.86	AFAC	0.57
EMIN	52.83	EMAX	630.27	RMIN	0.10
RMAX	10.00	WIND	2.00	WP	0.10
FT = (1111111) F1 0.00029 R 20.1329					
N1	1.0	T1	2.0	R1	1.967
N2	1.0	T2	3.0	R2	1.754
N3	1.0	T3	4.0	R3	2.343
N4	1.0	T4	5.0	R4	2.975
				A1	0.019
				A2	0.013
				A3	0.005
				A4	0.005

EXPERIMENT Irofpot2.9x
PARAMETERS gyvsa.par3
PHASESHIFTS IR
F C P O

Fourier Transform EXAFS of *mer*-, *trans*-[IrF₃(CO)(PEt₃)₂]

Table 5.9 Selected Bond Length Data (Å) for Various Fluoro-Complexes

Complex	M-F (<i>trans</i> -CO)	M-CO (<i>trans</i> -F)	C-O	M-P	Refs
[IrF ₃ (CO)(PEt ₃) ₂] ^b	1.97(2) ^a	1.76(2)	1.22(2)	2.35(2)	-
<i>fac</i> -[IrF ₃ (CO) ₃] ^b	1.92(2)	2.03(2)	1.01(2)	-	28
[IrF(COF)(CO) ₂ (PEt ₃) ₂] ⁺	1.998(3)	1.883(5)	-	2.401(1)	3
[IrFCl(NSF ₂)(CO)(PPh ₃) ₂]	2.089(2)	-	-	-	16
[RuF ₂ (CO) ₂ (PPh ₃) ₂]	2.011(4)	1.841(7)	1.135(9)	2.406(1)	8
[OsF ₂ (CO) ₂ (PPh ₃) ₂]	2.023(5)	1.832(10)	1.178(10)	2.418(2)	30

(a) average M-F bond length for *trans*-CO and *trans*-F

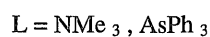
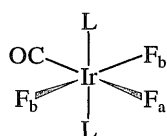
(b) Bond lengths obtained by EXAFS

5.7 The Reaction of *fac*-[IrF₃(CO)₃] with Trimethylamine and Triphenylarsine

Phosphine-fluoride complexes of the transition-metals is a relatively unexplored area (Chapters 4 and 5). However, even that particular area seems established in comparison to that of fluoride-amine (Chapter 2) and fluoride-arsine complexes of the transition-metals. To date, the only reported example of an iridium fluoro-compound containing either an amine or an arsine ligand is the triphenylarsine derivative of fluoro-Vaska's complex *trans*-[IrF(CO)(AsPh₃)₂].^{31,32}

The reaction of *fac*-[IrF₃(CO)₃] with NMe₃ and AsPh₃ gives the complexes *mer*-, *trans*-[IrF₃(CO)(L)₂] (L = NMe₃, AsPh₃) which represent the first iridium(III) fluoride-amine and arsine complexes. Although, the products have less NMR active nuclei, than those for the phosphine

complexes, assignments are made on the same basis as those for **5a** - **5j**. The ^{19}F NMR spectra show two mutually coupled resonances, a triplet and a doublet (Figure 5.8), in a 1:2 ratio, assigned to F_a and F_b respectively.



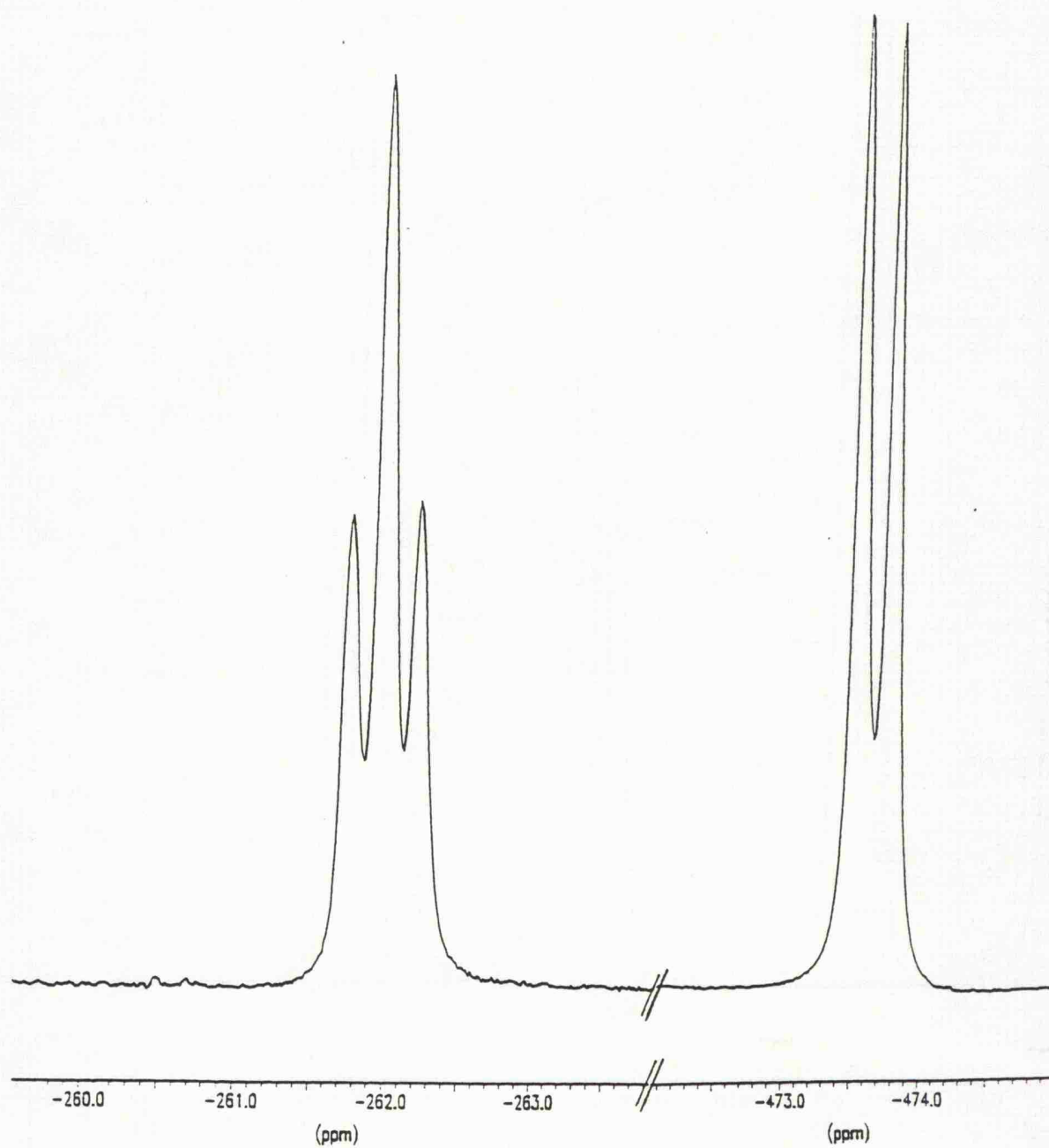
The ^{19}F NMR data of the two complexes are presented in Table 5.10

Table 5.10 ^{19}F NMR Data of the Complexes *mer*-, *trans*- $[\text{IrF}_3(\text{CO})(\text{L})_2]$
($\text{L} = \text{NMe}_3, \text{AsPh}_3$)

Complex	$\delta(^{19}\text{F})/\text{ppm}$		$^2J(\text{F}_\text{a}\text{F}_\text{b})/\text{Hz}$
	F_a	F_b	
$[\text{IrF}_3(\text{CO})(\text{AsPh}_3)_2]$	-291	-467	100
$[\text{IrF}_3(\text{CO})(\text{NMe}_3)_2]$	-225	-437	65

The chemical shifts for the resonances assigned to F_b and F_a are in regions characteristic of *F trans F*¹¹ and *F trans CO* respectively.⁵ However, the chemical shifts and more notably, the $^2J_{\text{FF}}$ coupling constants for *mer*-, *trans*- $[\text{IrF}_3(\text{CO})(\text{NMe}_3)_2]$ are significantly different to those reported for complexes **5a** - **5j** and *mer*-, *trans*- $[\text{IrF}_3(\text{CO})(\text{AsPh}_3)_2]$. Since chemical shifts and coupling constants have been explained by considering the amount of

Figure 5.8 ^{19}F NMR Spectrum of *mer*-, *trans*- $[\text{IrF}_3(\text{CO})(\text{NMe}_3)_2]$



s-orbital character in the metal-ligand bond, the differences in the $\delta(^{19}\text{F})$ and $^2J_{\text{FF}}$ of the complexes can be attributed to the π -acceptor ability of the ligands and so the NMe_3 analogue, which cannot π -accept, shows data significantly different to that for the phosphine and arsine derivatives which have ligands which can π -accept.

FAB⁺ mass spectrometry confirmed the monomeric nature of the two complexes. For both complexes the parent ions were not observed, but the pattern for $[M-\text{CO}]^+$ and $[M-\text{F}]^+$, for the triphenylarsine and trimethylamine complex respectively, were detected.

The infrared spectrum of the NMe_3 and AsPh_3 complexes showed the expected one band, in the region characteristic of a terminal carbonyl, the $\nu(\text{CO})$ infrared and mass spectrometry data are presented in Table 5.11.

Table 5.11 $\nu(\text{CO})$ Infrared and Mass spectrometry Data for the Complexes *mer*-, *trans*- $[\text{IrF}_3(\text{CO})(\text{L})_2]$ ($\text{L} = \text{NMe}_3$ and AsPh_3)

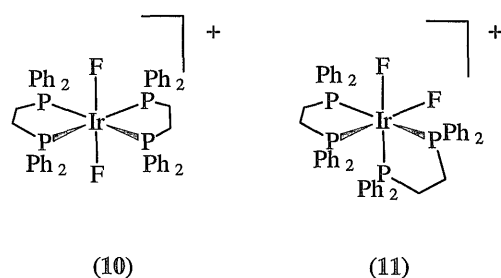
Complex	$\nu(\text{CO})^a/\text{cm}^{-1}$	m/z
$[\text{IrF}_3(\text{CO})(\text{NMe}_3)_2]$	2035	377 $[M-\text{F}]^+$
$[\text{IrF}_3(\text{CO})(\text{AsPh}_3)_2]$	2023	860 $[M-\text{CO}]^+$

(a) Nujol mulls

5.8 The Reaction of *fac*- $[\text{IrF}_3(\text{CO})_3]$ with Multidentate Phosphine Ligands

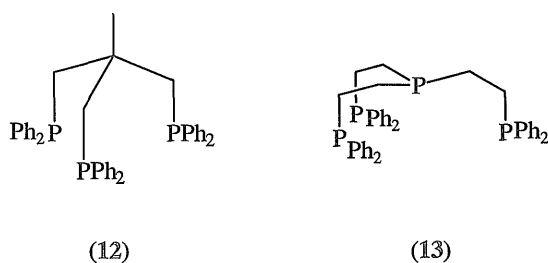
The majority of the reported iridium(III) fluoro-complexes contain monodentate phosphine ligands (Chapters 4 and 5), with the exception being the cationic $[\text{IrF}_2(\text{dppe})_2]^+$.⁹ This *trans*-complex (**10**) is formed by the

reaction of $[\text{XeF}_2]$ and $[\text{Ir}(\text{dppe})_2]^+$ whereas the analogous complex with *cis*-fluorines (**11**) is obtained by treating $[\text{Ir}(\text{dppe})_2\text{S}_2]^+$ (S = sulphur) with $[\text{XeF}_2]$, both in CH_2Cl_2 .⁹



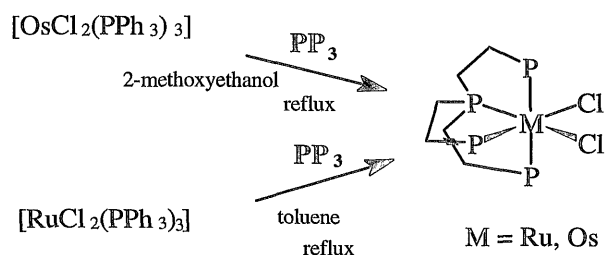
The ^{19}F NMR of complex (**10**) showed a quintet at δ -522 ppm and the $^{31}\text{P}\{^1\text{H}\}$ NMR revealed a triplet at δ 8.8 ppm with a $^2J_{\text{PF}}$ coupling of 18 Hz. In contrast the complex second-order ^{19}F and $^{31}\text{P}\{^1\text{H}\}$ NMR of (**11**) have been analysed as arising from a spin system $\text{AA}'\text{XX}'\text{YY}'$, with a ^{19}F chemical shift of δ -346.⁹

Other multidentate phosphine ligands such as the tridentate triphos (**P₃**) (**12**) and the tetradentate tetrphos (**PP₃**) (**13**) ligands have been reported to form stable metal complexes.



Siegl and co-workers reported the complex $[\text{IrCl}_3(\text{P}_3)]^{33}$ formed by the reaction of the iridium(I) compound $[\text{IrCl}(\text{CO})(\text{P}_3)]$ and Cl_2 . Recently, Bianchini *et al.*,^{34,35} reported the complexes $[\text{MCl}_2(\text{PP}_3)]$ ($\text{M} = \text{Ru}, \text{Os}$) which were formed by the reactions presented in Scheme 5.4.

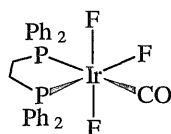
Scheme 5.4



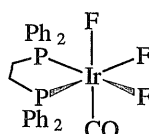
Since chloro-analogues of metal multidentate phosphine complexes are known, it was of interest to investigate the reactivity of tetraphos (PP_3) and triphos (P_3) with *fac*- $[\text{IrF}_3(\text{CO})_3]$ in an attempt to form the corresponding fluoro-derivatives of iridium. The reaction of dppe with *fac*- $[\text{IrF}_3(\text{CO})_3]$ is also outlined in an attempt to yield a bidentate phosphine complex of the type $[\text{IrF}_3(\text{CO})(\text{dppe})]$.

5.8.1 The Reaction of *fac*-[IrF₃(CO)₃] with dppe

The reaction of dppe and *fac*-[IrF₃(CO)₃], in CH₂Cl₂ at room temperature, was anticipated to afford either complex (14) or (15). Both (14) and (15) would give rise to complex multiplets, as a result of their spin systems A₂BXY and [AX]₂B respectively, in their ¹⁹F and ³¹P{¹H} NMR spectra with the latter being second-order. A mixture of two such species would complicate the spectra further and interpretation would be difficult.



(14)



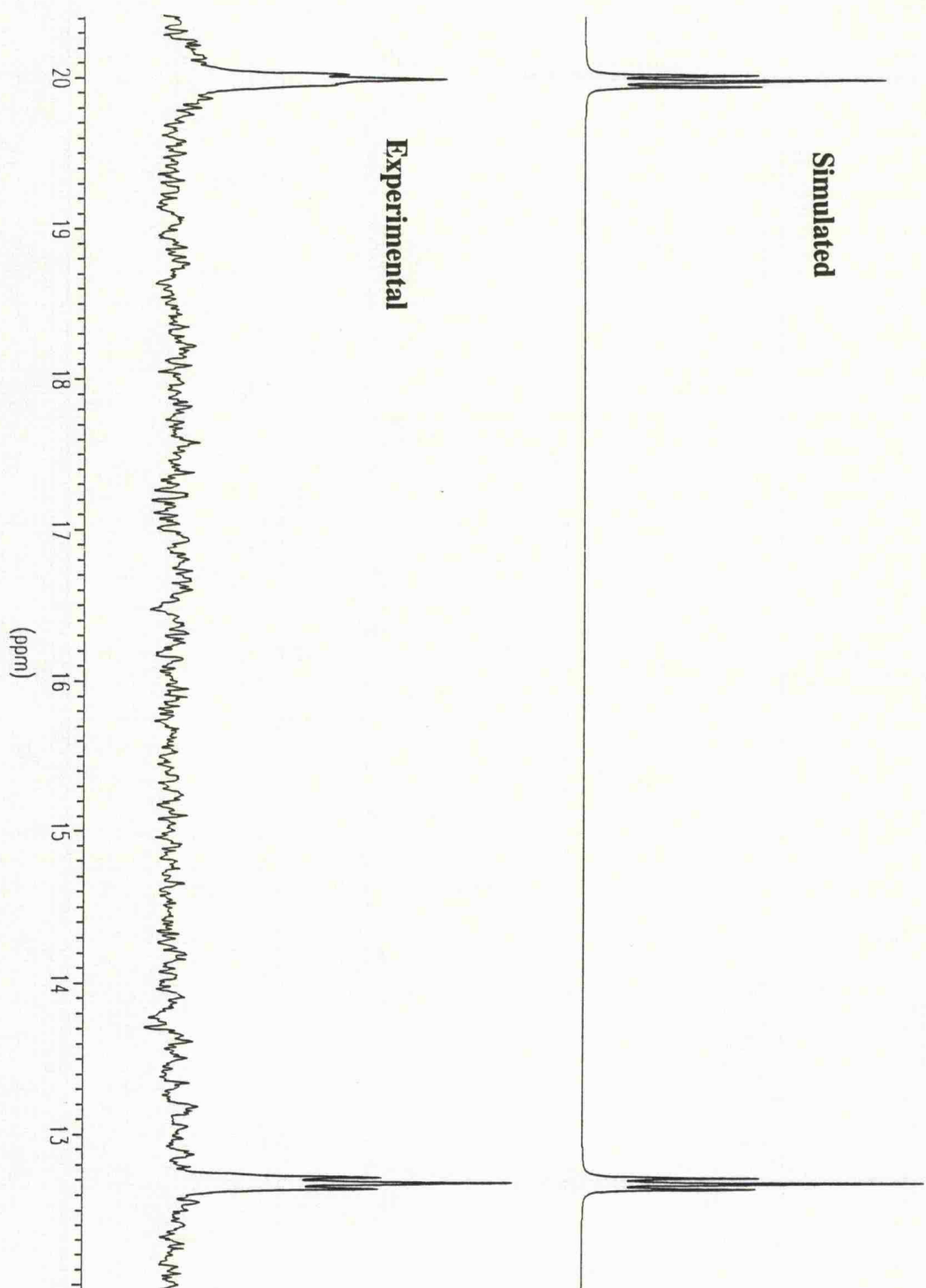
(15)

As expected the ¹⁹F and ³¹P{¹H} NMR spectra from the reaction of dppe and *fac*-[IrF₃(CO)₃], in CH₂Cl₂ at room temperature, revealed complex multiplets which could not be interpreted.

In an attempt to isolate only one of the products, (14) or (15), black *fac*-[IrF₃(CO)₃] was allowed to react with dppe in refluxing CH₂Cl₂. Removal of the solvent yielded a yellow solid, which was subsequently dissolved in CD₂Cl₂ for study by NMR spectroscopy.

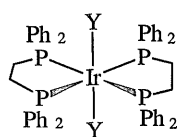
The ³¹P{¹H} NMR revealed some unexpected results (Figure 5.9) in that two triplets were observed at δ 12.7 and δ 19.8 with a coupling of 4 Hz. The ¹⁹F NMR revealed resonances at δ -138 and δ -152, with no resonances in the region indicative of fluorine bound to iridium being observed. All the resonances observed in the ¹⁹F NMR spectrum are characteristic of [SiF₆]²⁻ (δ -138) and [BF₄]⁻ (δ -152).

Figure 5.9 Experimental and Simulated $^{31}\text{P}\{^1\text{H}\}$ NMR Spectrum of Complex (16)

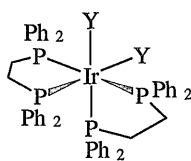


The Nujol mull infrared spectrum of the product revealed two bands, in a region associated with terminal carbonyl ligands, at 2033 and 1973 cm^{-1} . FAB⁺ mass spectrometry revealed that the product was a monomeric species and that the most intense peak, at m/z 989, corresponds to the pattern exhibited by the fragment $[\text{Ir}(\text{dppe})_2]^+$.

From the ^{19}F NMR data it is evident that there are no fluorines bound to iridium. This is consistent with the $^{31}\text{P}\{^1\text{H}\}$ NMR since the triplets show no coupling in the order of 100 Hz which is characteristic of a *cis* $^2J_{\text{PF}}$ coupling. The FAB⁺ mass spectrum revealed the presence of the fragment $[\text{Ir}(\text{dppe})_2]^+$. Thus, two dppe ligands can be arranged either *trans* (**16**) or *cis* (**17**) with respect to each other.



(16)

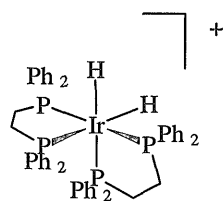


(17)

The $^{31}\text{P}\{^1\text{H}\}$ NMR spectrum of (**16**) would be a simple singlet, assuming that the Y substituent has $I \neq 1/2$, since all four phosphorus nuclei are equivalent. However, the $^{31}\text{P}\{^1\text{H}\}$ NMR spectrum of (**17**) would exhibit an AA'XX' type pattern; owing to the *trans* disposition of the A nuclei $J(\text{A}-\text{A}')$ is an order of magnitude greater than the remaining $^{31}\text{P}-^{31}\text{P}$ couplings, reducing the spectrum to 'deceptively' simple triplets for P_A and P_X from which $N[=J(\text{A}-\text{X}) + J(\text{A}-\text{X}')]^{36}$ the separation of the outer most lines of either triplet, is the only parameter which can be computed. Although, no exact couplings could be obtained from the simulated spectrum (Figure 5.9) it became evident, as predicted, that the magnitude of the *trans* phosphine is

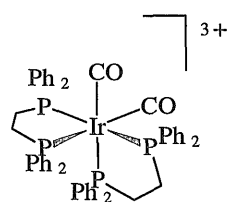
an order of magnitude larger than the other ^{31}P - ^{31}P coupling. Furthermore, the two *cis*-coupling must be of opposite signs in order to simulate the $^{31}\text{P}\{^1\text{H}\}$ NMR spectrum.

The sites Y are undoubtedly occupied by two carbonyl ligands. Although, terminal hydride ligands would also occur within the region 2000-2200 cm^{-1} in the infrared spectrum, one would expect to see evidence in the NMR studies. Furthermore, the dihydride complex $[\text{IrH}_2(\text{dppe})_2][\text{BPh}_4]$ (**18**) was reported, by Vaska *et al.*,³⁷ to exhibit two $\nu(\text{Ir-H})$ bands at 2091 and 2080 cm^{-1} . Therefore, the two bands observed at 2033 and 1973 cm^{-1} are attributed to terminal carbonyl ligands.



(18)

Thus, the product of the reaction between *fac*- $[\text{IrF}_3(\text{CO})_3]$ and dppe is tentatively assigned to the tri-cationic iridium(III) complex *cis*- $[\text{Ir}(\text{CO})_2(\text{dppe})_2][\text{X}]_3$ (**19**). There is no precedent for a six-coordinate 20 electron iridium(I) species.



(19)

This complex has C_2 symmetry and so, the irreducible representations of this symmetry, when considering the carbonyl bands is as follows:

$$\Gamma_{\text{CO}} = A + B \quad (\text{both A and B are IR active modes})$$

Thus, the expected number of carbonyl bands are observed in the infrared spectrum. Finally, the nature of the counteranion can be based on the ^{19}F NMR spectrum which revealed resonances associated with $[\text{BF}_4]^-$ and $[\text{SiF}_6]^{2-}$. These anions are the result of fluorination of the glass reaction vessel.

5.8.2 The Reaction of *fac*- $[\text{IrF}_3(\text{CO})_3]$ with Triphos (P_3)

Black *fac*- $[\text{IrF}_3(\text{CO})_3]$ was reacted with triphos (P_3) in refluxing CH_2Cl_2 . Removal of the solvent afforded a yellow solid which was subsequently dissolved in CD_2Cl_2 for analysis by NMR spectroscopy.

All attempts to obtain any interpretable spectroscopic data were unsuccessful.

5.8.3 The Reaction of *fac*-[IrF₃(CO)₃] with tetraphos (PP₃)

Black *fac*-[IrF₃(CO)₃] was reacted with tetraphos (PP₃) in refluxing CH₂Cl₂. Removal of the solvent afforded a yellow solid which was subsequently dissolved in CD₂Cl₂ for study by NMR analysis.

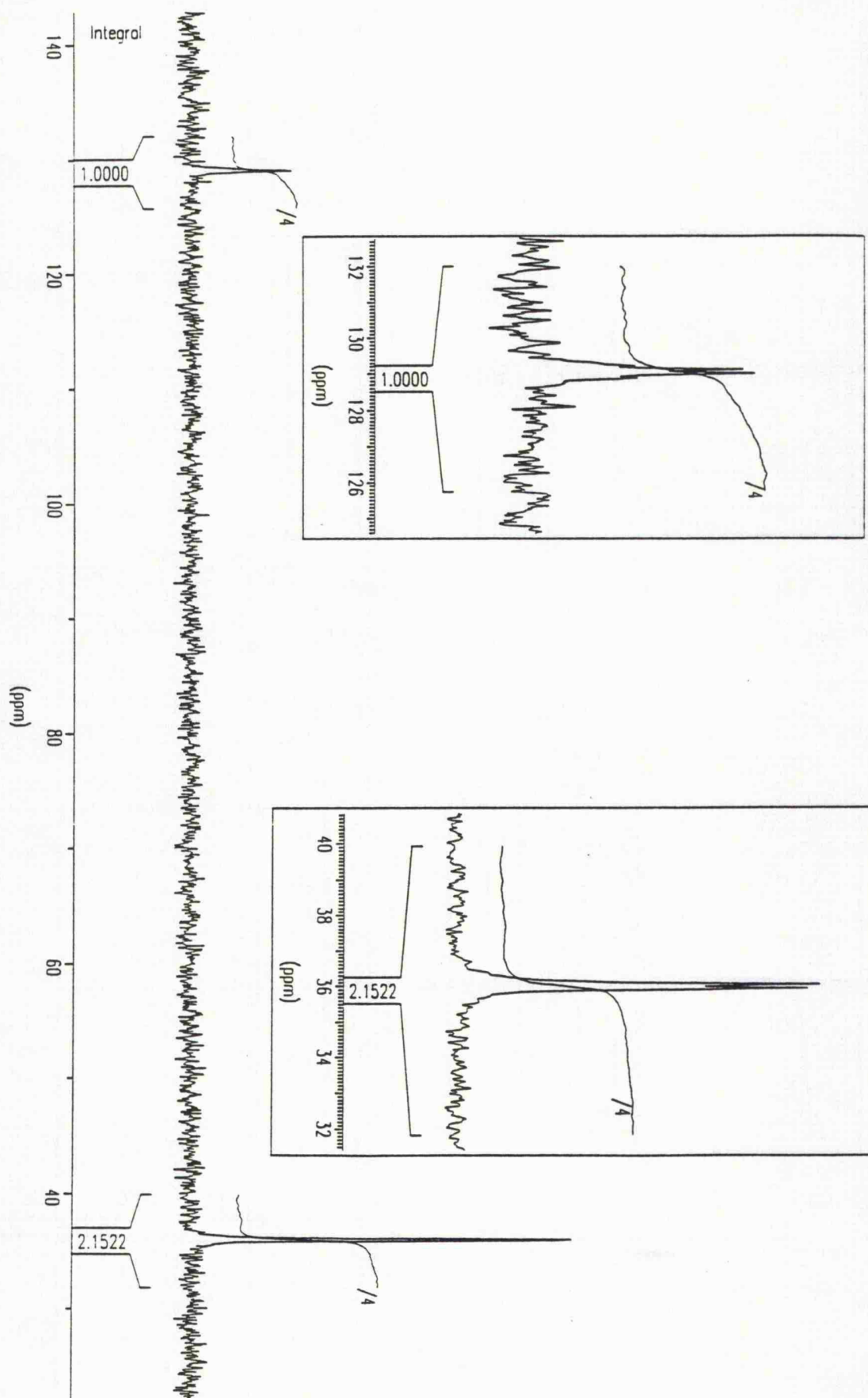
The ³¹P{¹H} NMR spectrum show two mutually coupled resonances, a quartet at δ 129 ppm and a doublet at δ 36 ppm, in a 1:3 ratio (Figure 5.10), with a ³J_{PP} coupling of 13 Hz.

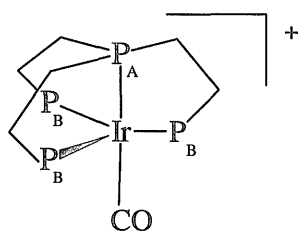
The ¹⁹F NMR spectrum revealed no resonance in a region characteristic of fluorine bound to iridium but did, however, show an intense singlet at δ -128 and 2 singlets in close proximity at δ -152. The former resonance is attributed to [SiF₆]²⁻ and the latter to [BF₄]⁻.

The infrared spectrum revealed one band, in the terminal carbonyl region, at 1960 cm⁻¹. The most intense peak in the FAB⁺ mass spectrum occurs at *m/z* 891.

From the ³¹P{¹H} it can be seen that there are two phosphorus environments, in a ratio 1:3, with one resonance appearing at a very high frequency for a coordinated phosphorus. However, this high frequency can be unambiguously attributed to the bridgehead phosphorus P_A of the PP₃ ligand.^{34,35} This resonance appears as a quartet because of coupling to three equivalent phosphorus nuclei P_B, lying in the plane of the trigonal-bipyramidal structure of complex (20). Thus, the doublet resonance, at 36 ppm, assigned to P_B arises from coupling to the bridgehead phosphorus P_A.

Figure 5.10 $^{31}\text{P}\{^1\text{H}\}$ NMR Spectrum of Complex (20)





(20)

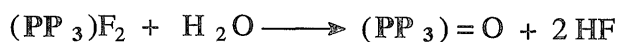
Complex (20) showed the expected one $\nu(\text{CO})$ (1960 cm^{-1}) band in the Nujol mull infrared spectrum.

The parent ion of this complex would occur at m/z 891 which is consistent with that observed in the mass spectrum of the product. In light of the data reported the indication is that the product, formed by the reaction of *fac*- $[\text{IrF}_3(\text{CO})_3]$ and tetraphos (PP_3), is a five-coordinate cationic iridium(I) complex (20). It is evident from the ^{19}F NMR spectrum that the counteranion could be either $[\text{SiF}_6]^{2-}$ or $[\text{BF}_4]^-$ (see section 5.8.1). However, there is more precedent for the latter because of its single charge and that the close proximity of the two singlets are indicative of an asymmetrical $[\text{BF}_4]^-$ environment and thus, the ion is coordinating rather than non-coordinating.

Five-coordinate cationic iridium(I) complexes of the type $[\text{Ir}(\text{CO})_3\text{L}_2][\text{AsF}_6]$ have been reported by May and co-workers,³⁸ and these also have trigonal bipyramidal geometries. May also reported the $\nu(\text{CO})$ infrared frequency, at 1958 cm^{-1} , for the complex $[\text{Ir}(\text{CO})(\text{PMePh}_2)_2\{\text{P}(\text{OPh})_3\}_2]^+$ which compares well with that observed for (20). Furthermore, the mono-hydrides $[(\text{PP}_3)\text{MH}]$ ($\text{M} = \text{Co}, \text{Rh}$)³⁹ which are also five-coordinate have been recently reported. Thus, there is evidence to support the formulation of complex (20), however, reduction of the iridium centre, from (III) to (I), must consequently lead to the oxidation of another species. Therefore, the absence of evidence to support oxidation of another

species is unexplainable, since no resonances were observed to indicate phosphine oxide, which would be formed according to Scheme 5.5.

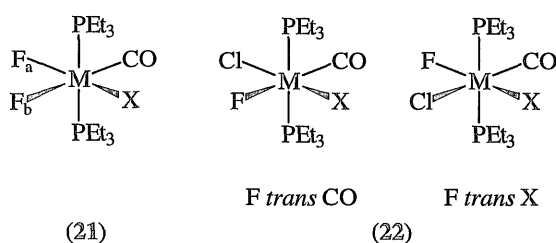
Scheme 5.5



Oxidation of excess tetraphos (PP_3) by the 'F⁺', being lost from the iridium would result in the reduction of the iridium centre from (III) to (I). Another tentative possibility is that fluorine gas was generated from the reaction producing HF on contact with moisture, which would react with the glass giving $[\text{SiF}_6]^{2-}$ and $[\text{BF}_4]^-$. The most likely explanation is that oxidation of the evolved CO has occurred.

5.9 Introduction to the Stability of the Complexes of the Type, *mer*-, *trans*- $[\text{IrF}_3(\text{CO})(\text{PR}_3)_2]$

As discussed in chapter 4, Ebsworth *et al.*⁹ reported that the reaction of *trans*- $[\text{MX}(\text{CO})(\text{PEt}_3)_2]$ (M = Rh, Ir; X = Cl, Br, I) and $[\text{XeF}_2]$, in CH_2Cl_2 , afforded predominantly the difluoride complex $[\text{MF}_2\text{X}(\text{CO})(\text{PEt}_3)_2]$ (**21**). Small amounts of the two isomeric mono- fluorides $[\text{MFX}_2(\text{CO})(\text{PEt}_3)_2]$ (**22**), and of the trifluoride, $[\text{MF}_3(\text{CO})(\text{PEt}_3)_2]$ are reported to be formed as a result of intermolecular halogen rearrangement.



However, when X = Br and I reaction with the solvent, CD_2Cl_2 , resulted in the formation of mixed chloro-halo-fluoro-complexes (22).

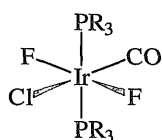
These NMR analyses enabled trends to be established for this series of related complexes. The Ir(III) products are reported to be more stable to halogen exchange than the Rh(III) analogues, with the reactivity towards halide exchange increasing in the order $\text{Cl} < \text{Br} < \text{I}$ for the rhodium system. Thus it was reported that the most stable complexes in the both the rhodium and iridium systems were the trifluorides, $[\text{MF}_3(\text{CO})(\text{PEt}_3)_2]$.

Earlier the preparation and characterization of a range of trifluoride complexes of the type, *mer*-, *trans*- $[\text{IrF}_3(\text{CO})(\text{PR}_3)_2]$ 5a - 5j were described and thus, it was thought to be of interest to investigate the reactivity towards halide exchange and the stability of these complexes.

5.10 Stability of the Complexes *mer*-, *trans*- $[\text{IrF}_3(\text{CO})(\text{PR}_3)_2]$ 5a - 5j

All of the trifluoride complexes are stable indefinitely as solids or oils, however, when kept in solution for too long decomposition occurs. The rate and extent of decomposition has been found to be governed by the solvent and the phosphine ligand. In some cases, exposure of the trifluoro-complexes to a chlorinated solvent, dichloromethane or chloroform, resulted in halide exchange (see section 5.5) and consequently the formation of the difluoro-

monochloro-complexes (23) and isomeric mono-fluoride complexes *cf* complex (22). Furthermore, decomposition has also been found to result in the reduction of the iridium(III) centre to iridium(I) affording, in some cases, the analogous iridium(I) fluoride and the analogous chloro-complex.



F *trans* F

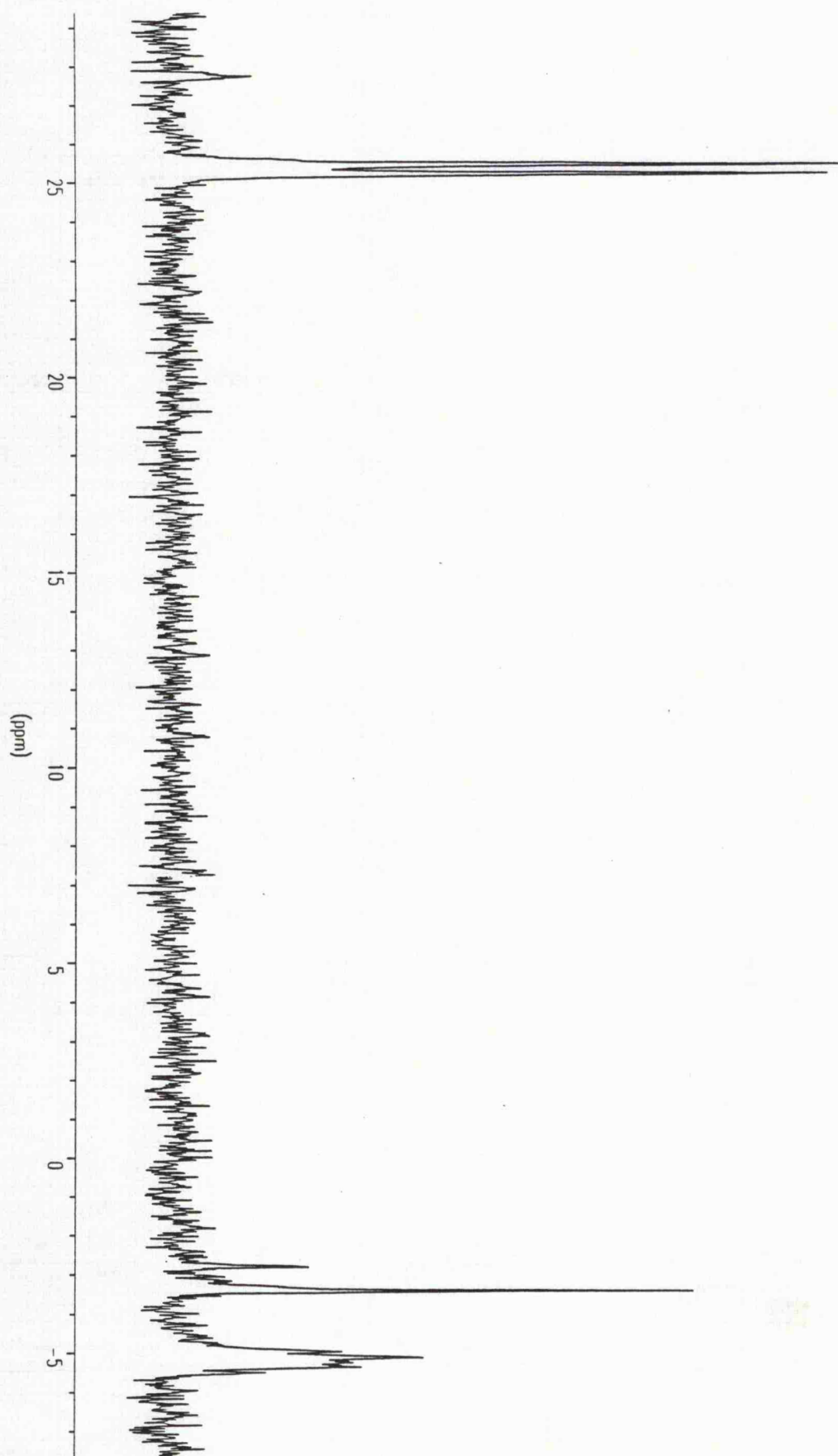
(23)

The triphenylphosphine and tricyclohexylphosphine complexes *trans*-[IrCl(CO)(PR₃)] have been shown to react with [XeF₂] affording the difluoro-species *cis*-, *trans*-[IrF₂Cl(CO)(PR₃)₂] (see Chapter 4). Thus, by comparison of the NMR data from these reactions, the decomposition products of the trifluoro- derivatives have been, in some systems, elucidated.

5.10.1 Decomposition to Iridium(I) Complexes

The decomposition of the complex *mer*-, *trans*-[IrF₃(CO)(PPh₃)₂] was monitored by NMR spectroscopy in a glass NMR tube in CD₂Cl₂ over a few hours. In addition to the resonances attributed to *mer*-, *trans*-[IrF₃(CO)(PPh₃)₂] the ³¹P{¹H} NMR spectra revealed a singlet at δ 29.6 attributed to Ph₃P=O; a doublet at δ 25.2, ²J_{PF} = 29 Hz (Figure 5.11); and a singlet at δ 24.1.

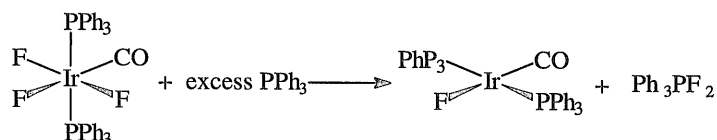
Figure 5.11 $^3\text{1P}\{\text{^1H}\}$ NMR Spectrum of the Decomposition Products of *mer*-, *trans*- $[\text{IrF}_3(\text{CO})(\text{PPh}_3)_2]$



In the ^{19}F NMR spectrum additional resonances were observed at δ -258, $^2J_{\text{FP}} = 29$ Hz (Figure 5.12); a minor triplet at δ -326, $^2J_{\text{FP}} = 24$ Hz ; and a broad singlet at δ -180 attributed to HF.

The doublet at δ 25.2 in the $^{31}\text{P}\{^1\text{H}\}$ NMR spectrum and the triplet at δ -258 in the ^{19}F NMR spectrum are assignable to the iridium(I) fluoro-complex *trans*- $[\text{IrF}(\text{CO})(\text{PPh}_3)_2]$, these values are consistent with those reported by Vaska and Peone.⁴⁰ The singlet at δ 24.1 in the $^{31}\text{P}\{^1\text{H}\}$ NMR is attributed to Vaska's complex *trans*- $[\text{IrCl}(\text{CO})(\text{PPh}_3)_2]$ and is again consistent with literature values.⁴¹ The presence of the two iridium(I) complexes indicates reduction of the iridium(III) centre which implies oxidation of another species. The presence of excess phosphine in solution would be readily oxidized to phosphorus(V). Thus, evidence from the ^{19}F and $^{31}\text{P}\{^1\text{H}\}$ NMR spectra indicates that free phosphine is oxidized to form difluorophosphorane which, consequently, leads to the reduction of the iridium(III) trifluoro-complex (Scheme 5.6).

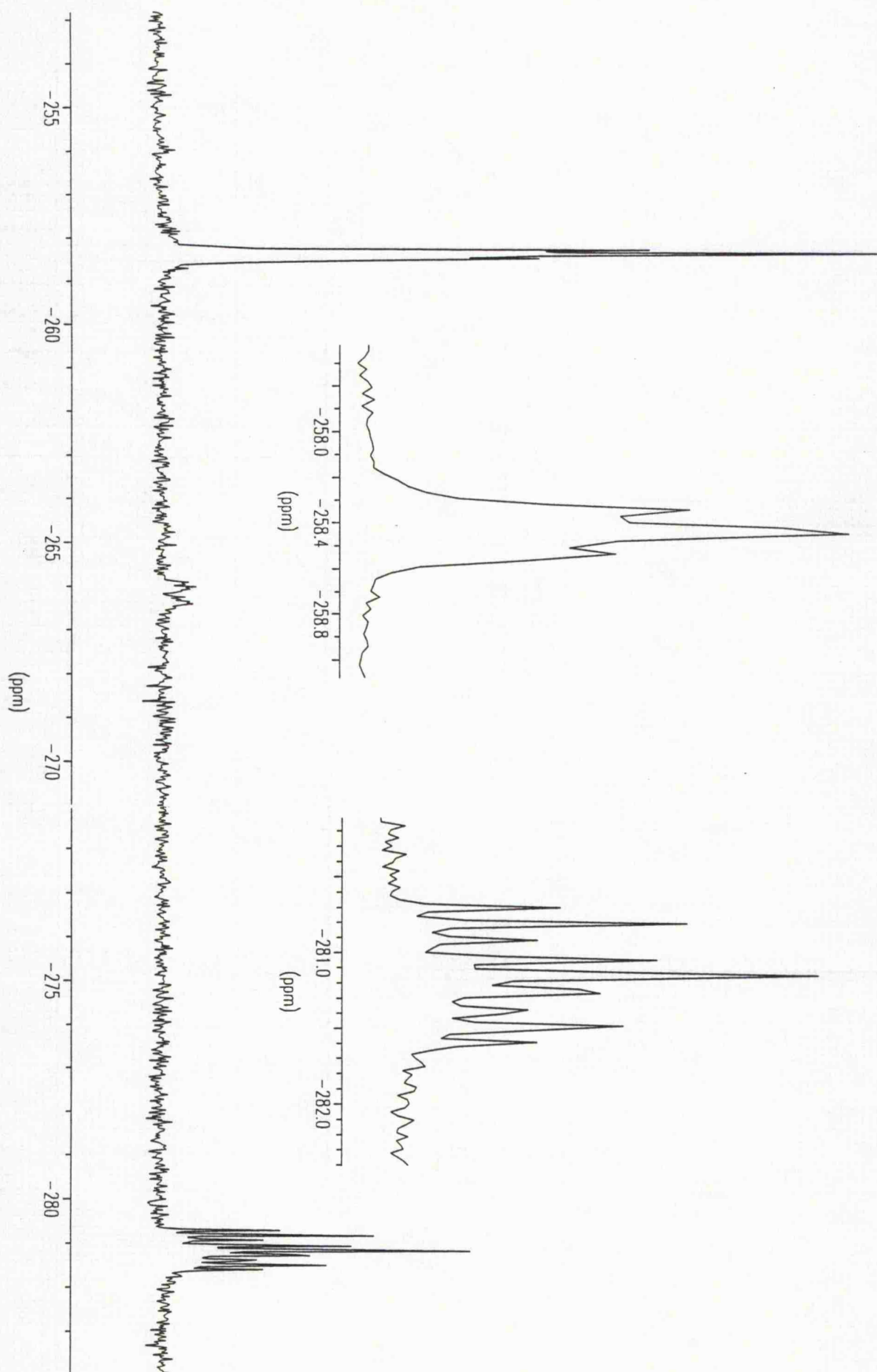
Scheme 5.6



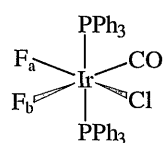
Once formed the difluorophosphorane, which is reported to readily hydrolyse,⁴² decomposes to produce $\text{Ph}_3\text{P}=\text{O}$ and HF (see Scheme 5.5) which is consistent with the NMR data.

Thus, the presence of chloro-Vaska's complex is either a result of fluorine/chlorine exchange in the iridium(I) fluoro-analogue with the

Figure 5.12 ^{19}F NMR Spectrum of the Decomposition Products of *mer*-, *trans*- $\text{IrF}_3(\text{CO})(\text{PPh}_3)_2$

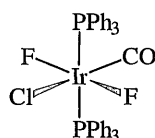


dichloromethane solvent (see Chapter 4, section 4.5) or reduction of the difluoro-mono-chloro iridium (III) species $[\text{IrF}_2\text{Cl}(\text{CO})(\text{PPh}_3)_2]$. There is no apparent evidence for the latter since there are no resonances in either the ^{19}F or $^3\text{1P}\{^1\text{H}\}$ NMR spectra which could indicate the formation of either complex (24) or (25).



F trans Cl
F trans CO

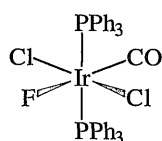
(24)



F trans F

(25)

In the ^{19}F NMR spectrum complex (24) would give rise to two mutually coupled doublet of triplets, one in the region characteristic of *F trans CO* and the other *F trans Cl* (see Chapter 4) and species (25) would show a triplet in the region typical of *F trans F*. However, the other resonance observed in the ^{19}F NMR spectrum is the minor triplet at δ -326, in a region indicative of *F trans CO*, with a $^2J_{\text{FP}} = 24$ Hz. This is tentatively assigned to the mono-fluoride complex $[\text{IrFCl}_2(\text{CO})(\text{PPh}_3)_2]$ (26), by comparison with analogous data reported in this chapter and chapter 4. The ratio of this complex to the other species formed is only a few percent and the weakness of the resonance has prevented detection of the corresponding doublet in the $^3\text{1P}\{^1\text{H}\}$ NMR spectrum.



F *trans* CO

(26)

Therefore, the reaction of *trans*-[IrF(CO)(PPh₃)₂] with the solvent (CD₂Cl₂), as described in section 4.5, most likely led to the formation of chloro-Vaska's complex.

Comparison of the complexes containing the phosphine ligands (PR₃ = Pcy₃, PPh₂(C₆F₅) and P(*p*-MeC₆H₄)₃ and P^{*i*}Pr₃) with the largest cone angles revealed a similar decomposition in that the corresponding ³¹P{¹H} NMR spectra show primarily R₃P=O and *trans*-[IrX(CO)(PR₃)₂] (X = F, Cl). Although, only the P^{*i*}Pr₃ derivative was found to exhibit a triplet, at δ -251 with a ²J_{FP} = 25 Hz, in the ¹⁹F NMR spectrum, all the systems show a doublet, in a chemical shift region diagnostic of iridium(I) species, in the ³¹P{¹H} NMR spectra (Table 5.12).

From the work presented earlier (Chapter 4, pages 192 and 211) a change in oxidation state of iridium, from (III) to (I), is accompanied by a shift to higher frequency in the ³¹P{¹H} NMR *cf.* [IrF₃(CO)(PPh₃)₂] δ -6.4 and *trans*-[IrF(CO)(PPh₃)₂] δ 25.2. Thus, for PR₃ = Pcy₃, PPh₂(C₆F₅) and P(*p*-MeC₆H₄)₃ the doublets are tentatively assigned to the iridium(I) fluoro-species (27).

Table 5.12 Comparison of $^{31}\text{P}\{^1\text{H}\}$ NMR Data of the Decomposition Products from the Complexes *mer*-, *trans*- $[\text{IrF}_3(\text{CO})(\text{PR}_3)_2]$

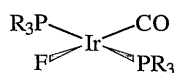
Phosphine	Iridium(I) species			$[\text{IrF}_3(\text{CO})(\text{PR}_3)_2]$	
	$\delta(^{31}\text{P})/\text{ppm}$	$^2J(\text{PF})/\text{Hz}$	$\delta(^{31}\text{P})/\text{ppm}$	$\delta(^{31}\text{P})/\text{ppm}$	$^2J(\text{PF})/\text{Hz}^a$
Pcy_3	39.2(d)	23	30.7(s)	7.4	27
P^iPr_3 ^b	48.7(d)	25	41.5(s)	17.5	27
$\text{PPh}_2(\text{C}_6\text{F}_5)^c$	17.9(d)	33	16.0(s)	-11.0	30
$\text{P}(p\text{-MeC}_6\text{H}_4)_3$	23.6(d)	29	20.9(s)	-6.0	30
PPh_3	25.2(d)	29	24.1(s)	-6.4	30

multiplicity: d = doublet and s = singlet

(a) Fluorine *trans* to carbonyl coupling

(b) In the corresponding ^{19}F NMR the associated triplet was observed at δ -251 with a $^2J_{\text{FP}} = 25$ Hz.

(c) The ^{19}F NMR spectrum showed, in addition to the resonances assigned to the pentafluorophenylphosphine groups on the Ir(III) fluoride complex, 3 multiplets at δ -124, -151 and -162 which were attributed to *ortho*-, *para*- and *meta*-F respectively on another pentafluorophenylphosphine bound to iridium. Furthermore, the $^{31}\text{P}\{^1\text{H}\}$ NMR spectrum exhibited an additional singlet resonance at δ 21 which is in a region diagnostic of an iridium(I) species (see page 273).



$\text{PR}_3 = \text{Pcy}_3, \text{PPh}_2(\text{C}_6\text{F}_5), \text{P}(p\text{-MeC}_6\text{H}_4)_3, \text{P}^i\text{Pr}_3$

(27)

The magnitude of the $^2J_{\text{PF}}$ coupling constants, for F *trans* CO, in the Ir(I) complexes, within experimental error (± 1 Hz), mirrors that observed in the analogous Ir(III) species. The smaller value (14 -22 Hz) of the $^2J_{\text{PF}}$ coupling constants observed in the Ir(III) complexes, for the fluorines *trans* to each other is further evidence to indicate the formation of these Ir(I) fluoro-complexes (27).

The absence of the corresponding triplet resonances, in a region diagnostic of Ir(I) species ($\delta \approx -250$), in the ^{19}F NMR spectra can only be explained by considering the stabilities of these iridium(I) fluoro-complexes. To date, the only reported Ir (I) fluoride-phosphine complexes are *trans*-[IrF(CO)(PPh₃)₂]⁴⁰ and the tri(*p*-tolyl)phosphine⁴³ and alkylidiphenylphosphine⁴⁴ derivatives (see Chapter 4). Of these, $^{31}\text{P}\{^1\text{H}\}$ and ^{19}F NMR data have only been reported for fluoro-Vaska's complex presumably due to the instability of the other fluoro-derivatives in solution. Further evidence to substantiate this instability is the observation of a singlet in the $^{31}\text{P}\{^1\text{H}\}$ NMR spectra which are attributed to the chloro-analogues, *trans*-[IrCl(CO)(PR₃)₂] (Table 5.12) indicating fluorine/chlorine exchange.

Although, complexes of the type *trans*-[IrCl(CO)(PR₃)₂] are well documented (see Chapter 4), there are only a few examples for which the $^{31}\text{P}\{^1\text{H}\}$ NMR data are reported.

In chapter 4 the preparation of *trans*-[IrCl(CO)(Pcy₃)₂] was described and its $^{31}\text{P}\{^1\text{H}\}$ NMR data which unambiguously identified the decomposition product of the trifluoro-complex, *mer*-, *trans*-[IrF₃(CO)(Pcy₃)₂] as the Ir(I) chloro-derivative. The presence of the trifluoro-complex *mer*-, *trans*-[IrF₃(CO)(Pcy₃)₂] { $\delta(^{31}\text{P})$ 7.4} and a significant amount of *trans*-[IrCl(CO)(Pcy₃)₂] { $\delta(^{31}\text{P})$ 30.7} (Figure 5.13) with the absence of a doublet resonance, in this particular instance, is evidence to suggest that the fluoro-analogue is unstable in solution. However, all attempts to prepare the P^{*i*}Pr₃, P(*p*-MeC₆H₄)₃ and PPh₂(C₆F₅) iridium(I) fluoro-derivatives, by

metathesis reactions like that outlined in chapter 4, were unsuccessful and, thus, assignments remain speculative.

The electronegativity of fluorine is greater than that of chlorine thus, in the complexes *trans*-[IrX(CO)(PR₃)₂] (X = F, Cl; PR₃ = tertiary phosphine), the phosphorus nuclei, in the fluoro-analogues, are significantly deshielded compared to that for the chloro-derivatives. The consequence of this is that the resonances are observed at higher frequency for the fluoro-complexes than for the analogous chloro-derivatives. This shift to a higher frequency, with fluorine/chlorine exchange, was observed in all cases (Table 5.12). Finally, the presence of phosphine oxide and HF in their respective NMR spectra is further evidence to substantiate these reductions of the Ir(III) complexes to the analogous Ir(I) species (see Scheme 5.5).

As discussed in section 5.5.1 coordination chemical shift, $\Delta^{31\text{P}}$, can be loosely related to the cone angle of the phosphine ligand. It is evident, even for the first reported ³¹P NMR data for the complexes of the type *trans*-[IrCl(CO)(PR₃)₂] {PR₃ = Pcy₃, P^tPr₃, PPh₂(C₆F₅) and P(*p*-MeC₆H₄CH₃)₃}, from Table 5.13 that the $\Delta^{31\text{P}}$ increases as the cone angle decreases. However, the PPh₂(C₆F₅) iridium(I) derivative has a larger coordination chemical shift implying that electronic factors are having a major influence on this value (see Section 5.5.1).

Figure 5.13 $^3\text{P}\{^1\text{H}\}$ NMR Spectrum of the Decomposition Products of *mer*-, *trans*- $[\text{IrF}_3(\text{CO})(\text{Pcy}_3)_2]$

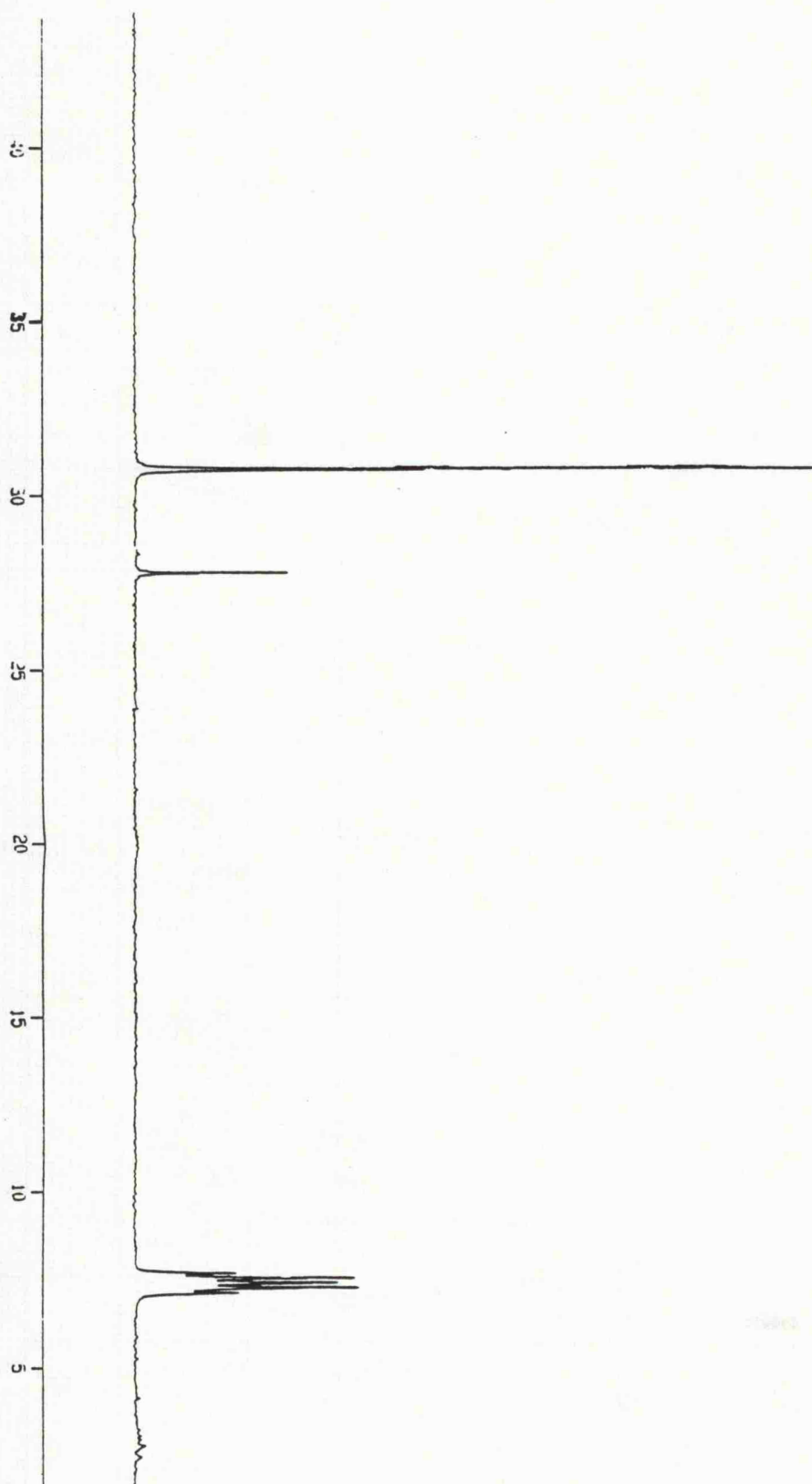
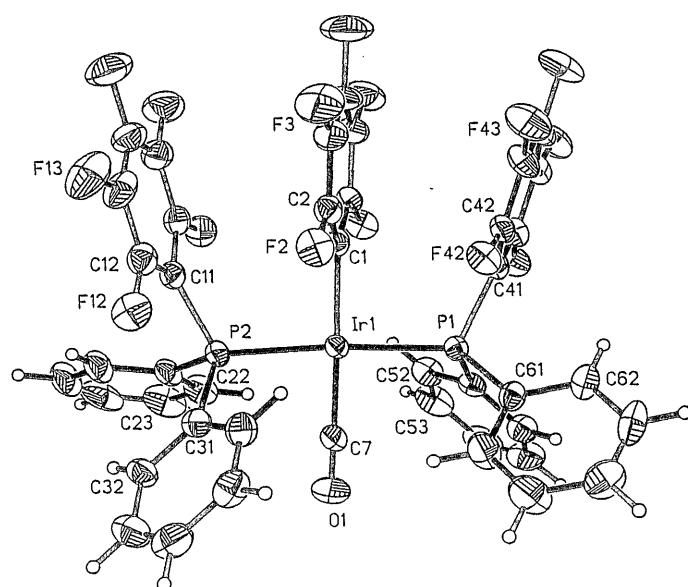


Table 5.13 Comparison of Cone Angle and Coordination Chemical Shift (Δ) for the Complexes *trans*-[IrCl(CO)(PR₃)₂]

PR ₃	$\delta(^{31}\text{P})/\text{ppm}$	Cone Angle ¹⁴	$\Delta(^{31}\text{P})/\text{ppm}$
Pcy ₃	30.7	170	19.4
P ^{<i>i</i>} Pr ₃	41.5	160	21.5
PPh ₂ (C ₆ F ₅)	16.0	158	40.7
P(<i>p</i> -MeC ₆ H ₄) ₃	20.9	145	23.4
PPh ₃	24.1	145	30.1

Figure 5.14 Molecular Structure Of Complex (28)



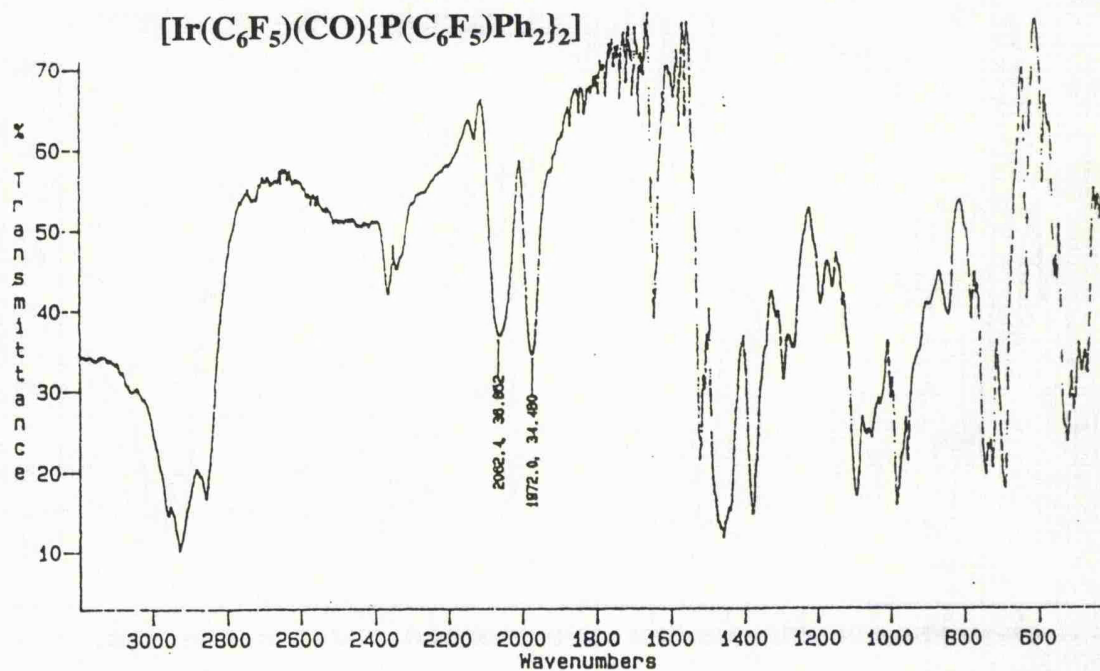
During the investigations in to the products of decomposition, crystals suitable for single-crystal X-ray structure determination were obtained from a

CD₂Cl₂ solution of [IrF₃(CO){PPh₂(C₆F₅)₂}. Analysis of the X-ray crystal structure revealed an unexpected result, the isolation of crystals of *trans*-[Ir(C₆F₅)(CO){PPh₂(C₆F₅)₂] (**28**) (Figure 5.14).

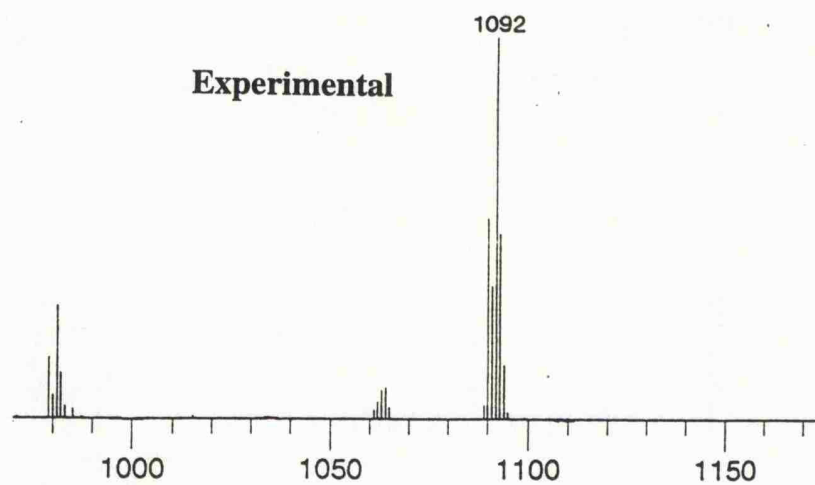
On re-examination of the NMR data obtained for the complex [IrF₃(CO){PPh₂(C₆F₅)₂] evidence for (**28**) was found. The ¹⁹F NMR spectrum show additional resonances in the *ortho*- (δ -124), *meta*- (δ -151) and *para*-fluorine (δ -162) region which can be attributed to the pentafluorophenyl ring on complex (**28**). Complex (**28**) would give rise to a singlet in the ³¹P{¹H} NMR spectrum by virtue of the two chemically equivalent phosphorus nuclei. The ³¹P{¹H} NMR spectrum of [IrF₃(CO){PPh₂(C₆F₅)₂] showed 3 singlets, in addition to the doublet of triplets assigned to the trifluoro-complex, at δ 21, 16 and 13. The singlet resonance at δ 16 has been, as previously discussed, tentatively assigned to the complex *trans*-[IrCl(CO){PPh₂(C₆F₅)₂]. Dahlenburg and Nast⁴⁵ have reported the preparation and characterization of several σ-aryl complexes of the type, *trans*-[Ir(Ar)(CO)(PPh₃)₂] where (Ar) includes C₆F₅. The reported ³¹P{¹H} NMR and infrared, ν(CO), data for the complex *trans*-[Ir(C₆F₅)(CO)(PPh₃)₂] compares well with that obtained for (**28**) (Table 5.14).

Although, the assignment of the singlet at δ 21 in the ³¹P{¹H} NMR is based on comparison with analogous data, the infrared and mass spectrometry results are more conclusive (Figure 5.15). The most intense peak in the FAB⁺ mass spectrum is observed at *m/z* 1092 which corresponds to the parent ion, [M]⁺, for (**28**). Two very strong bands, in the terminal carbonyl region, are observed in the infrared spectrum at 2062 and 1972 cm⁻¹. The former is assigned to the iridium(III) complex (see section 5.5.2) [IrF₃(CO){PPh₂(C₆F₅)₂] with the latter being attributed to (**28**).

Figure 5.15 Infrared Spectrum and the Experimental and Simulated Mass Spectra of *mer*-, *trans*-[IrF₃(CO){P(C₆F₅)Ph₂]₂ and *trans*-[Ir(C₆F₅)(CO){P(C₆F₅)Ph₂]₂



Experimental



Simulated

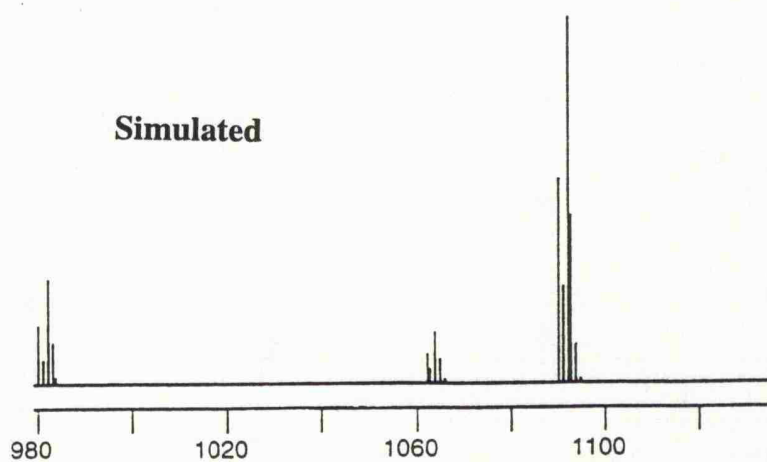


Table 5.14 Comparison of the $^{31}\text{P}\{^1\text{H}\}$ NMR Data and $\nu(\text{CO})$ Frequencies for the Complexes $\text{trans-}[\text{Ir}(\text{C}_6\text{F}_5)(\text{CO})(\text{PR}_3)_2]$

PR_3	$\delta(^{31}\text{P})/\text{ppm}$	$\nu(\text{CO})/\text{cm}^{-1}$	Refs.
PPh_3	23.62	1968 ^a	45
$\text{PPh}_2(\text{C}_6\text{F}_5)$	21.0	1972 ^a	(b)

(a) Nujol mulls

(b) this work

The mechanism for the formation of complex (**28**) is beyond the realms of this thesis. However, it is plausible to suggest that *ortho*-metallation did not occur since, this would involve both C-F bond cleavage **and** reformation. There is a precedent for the reaction of the $[\text{C}_6\text{F}_5]^-$ anion with the Ir(I) complex to yield (**28**) since, the complexes of the type *trans*- $[\text{Ir}(\text{Ar})(\text{CO})(\text{PPh}_3)_2]$ were prepared by the reaction of the analogous chloride species and the appropriate aryl anion in the form of $[\text{LiAr}]$.

5.10.2 Crystal Structure of $\text{trans-}[\text{Ir}(\text{C}_6\text{F}_5)(\text{CO})\{\text{PPh}_2(\text{C}_6\text{F}_5)\}_2]$ (**28**)

$\text{trans-}[\text{Ir}(\text{C}_6\text{F}_5)(\text{CO})\{\text{PPh}_2(\text{C}_6\text{F}_5)\}_2]$ (**28**) exhibits square planar geometry with mutually *trans* phosphine ligands (Figure 5.14). Selected bond lengths (\AA) and bond angles ($^\circ$) are presented in Table 5.15.

Table 5.15 Selected Bond Lengths (Å) and Angles (°) for Complex (28)

Bond Lengths	Ir-P(1) 2.306(1)
	Ir-P(2) 2.305(1)
	Ir-C(7) 1.871(7)
	Ir-C(1) 2.089(6)
	C(7)-O(1) 1.123(9)
	mean P-C(aryl) 1.832(4)
Bond Angles	P(1)-Ir-P(2) 175.3(1)
	P(2)-Ir-C(7) 87.7(2)
	P(2)-Ir-C(1) 92.2(2)

Although, there have been several reports on the preparation of complexes of the type $[\text{Ir}(\text{Ar})(\text{CO})(\text{PPh}_3)_2]$ there has been no structural information reported on such species. However, the metal-carbon (on the aryl ring) and the metal-phosphorus bond lengths compare well with those of the complex $[\text{Rh}(\text{C}_6\text{H}_5)\text{Cl}(\text{PPh}_3)_2]$ ⁴⁶ of 2.016(3) and 2.370(1) Å respectively. The Ir-C bond length (1.871(7) Å) is reasonable when compared with the corresponding distance of 1.791(13) Å reported for *trans*- $[\text{IrCl}(\text{CO})(\text{PPh}_3)_2]$.⁴⁷

5.10.3 Decomposition to Mixed-Halo-Iridium(III) Species

In comparison, the complexes containing the non-cyclic alkyl and mixed alkylaryl phosphine ligands decompose more readily than their cyclic analogues (Pcy_3 , Pph_3 , $\text{P}\{p\text{-MeC}_6\text{H}_4\}_3$, and $\text{PPh}_2\{\text{C}_6\text{F}_5\}$). Generally, decomposition led to very complex ^{19}F and $^{31}\text{P}\{^1\text{H}\}$ NMR spectra and so

definitive interpretation was impossible. However, in some systems the ^{19}F NMR spectra showed resonances in regions characteristic of F *trans* CO, F *trans* Cl and F *trans* F for fluorine bound to Ir(III) indicating that the decomposition products were formed from the reactions of the trifluoride species with the chlorinated solvent (see section 5.5.1) affording mixed chloro-fluoro-species.

5.11 Summary

The work presented in this chapter has shown a general route to a novel class of iridium(III) carbonyl-fluoride complexes containing a Lewis base. Furthermore, these complexes have been shown to be air-stable but, decomposition will ensue if left in a chlorinated solvent for any length of time. However, decomposition of the Ir(III) carbonyl-phosphine-fluoride complexes are proposed to afford several fluoro-Vaska's derivatives, including Pcy_3 and P^tPr_3 , which were shown to be inaccessible by direct halide metathesis with the analogous chloro-species (see Chapter 4). Finally, the novel *trans*- $[\text{Ir}(\text{C}_6\text{F}_5)(\text{CO})\{\text{PPh}_2(\text{C}_6\text{F}_5)\}_2]$ was isolated and structurally characterized as a decomposition product.

References for Chapter 5

1. S. A. Brewer, J. H. Holloway, E. G. Hope and P. G. Watson, *J. Chem. Soc., Chem. Commun.*, 1992, 1577.
2. S. A. Brewer, PhD Thesis, University of Leicester, 1993.
3. A. J. Blake, R. W. Cockman, E. A. V. Ebsworth and J. H. Holloway, *J. Chem. Soc., Chem. Commun.*, 1988, 529.
4. E. A. V. Ebsworth, N. Robertson and L. Y. Yellowlees, *J. Chem. Soc., Dalton Trans.*, 1993, 1031
5. R. W. Cockman, E. A. V. Ebsworth and J. H. Holloway, *J. Am. Chem. Soc.*, 1987, **109**, 2194.
6. R. W. Cockman, E. A. V. Ebsworth and P. G. Watson, Unpublished results.
7. S. C. Tripathi, S. C. Srivastava, R. P. Mani and A. K. Shrimel, *Inorg. Chim. Acta*, 1976, **17**, 257 and references cited therein.
8. P. R. Brookes, C. Masters and B. L. Shaw, *J. Chem. Soc.(A)*, 1971, 3756.
9. R. W. Cockman, E. A. V. Ebsworth, J. H. Holloway, H. Murdoch, N. Robertson and P. G. Watson, "Reaction of Non-metal Fluorides with some Platinum Metal Complexes," J. Thrasher and S. Strauss, ACS Symposium Series, ACS Books, 1994.
10. For example see G. Wilkinson, F. G. A. Stone and E. W. Abel "Comprehensive Organometallic Chemistry" Pergamon Press Vol 3 and 4.
11. S. A. Brewer, J. H. Holloway and E. G. Hope, *J. Chem. Soc., Dalton Trans.*, 1994, 1067.
12. M. M. Rahman, Hu-Ye. Liu, K. Eriks, A. Prock and W. P. Giering, *Organometallics*, 1989, **8**, 1 and references cited therein.
13. C. A. Tolman, *Chem. Rev.*, 1977, **77**, 3.

14. G. C. Saunders, manuscript in preparation.
15. B. E. Mann, C. Masters and B. L. Shaw, *J. Chem. Soc. (A)*, 1971, 1104.
16. P. G. Watson, E. Lork and R. Mews, *J. Chem. Soc., Chem. Commun.*, 1994, 1069.
17. K. Nakamoto, "Infrared and Raman Spectra of Inorganic and Coordination Compounds", 4th ed., Wiley- Interscience, New York, 1986, 292.
18. C. D. Desjardins, D. B. Edwards and J. Passmore, *Can. J. Chem.*, 1979, 57, 2714.
19. H. Willner and F. Aubke, *Inorg. Chem.*, 1990, 29, 2195.
20. H. Willner, M. Bodenbinder, C. Wang and F. Aubke, *J. Chem. Soc., Chem. Commun.*, 1994, 1189.
21. J. Chatt, N. P. Johnson and B. L. Shaw, *J. Chem. Soc.*, 1964, 1625.
22. B. L. Shaw and A. C. Smithies, *J. Chem. Soc.(A)*, 1968, 2784.
23. L. Vaska and S. S. Bath, *J. Am. Chem. Soc.*, 1966, 88, 1.
24. K. Vrieze, J. P. Collman, C. T. Sears and M. Kubota, *Inorg. Synth.*, 1968, 11, 101; L. Vaska and J. Peone, *ibid.*, 1974, 15, 64.
25. M. R. Churchill and J. P. Hutchinson, *Inorg. Chem.*, 1978, 17, 3528.
26. EXCURV92, SERC Daresbury Laboratory Program, N. Binstead, S. J. Gurman and J. W. Campbell, 1992.
27. R. W. Joyner, K. J. Martin and P. Meehan, *J. Phys. C*, 1987, 20, 4005; N. Binstead, S. L. Cook, J. Evans, G. N. Greaves and R. J. Price, *J. Am. Chem. Soc.*, 1987, 109, 3667.
28. S. A. Brewer, A. K. Brisdon, J. H. Holloway, E. G. Hope, L. A. Peck and P. G. Watson, *J. Chem. Soc., Dalton Trans.*, in press.
29. S. A. Brewer, K. S. Coleman, J. Fawcett, J. H. Holloway, E. G. Hope, D. R. Russell and P. G. Watson, *J. Chem. Soc., Dalton Trans.*, 1995, 1073.

30. K. S. Coleman, Personal Communications.
31. K. Goswami and M. M. Singh, *J. Ind. Chem. Soc.*, 1979, **56**, 477.
32. C. A. McAuliffe and R. Pollock, *J. Organomet. Chem.*, 1974, **69**, C13.
33. W. O. Siegl, S. J. Lapporte and J. P. Collman, *Inorg. Chem.*, 1971, **10**, 2158.
34. C. Bianchini, P. J. Perez, M. Peruzzini, F. Zanobini and A. Vacca, *Inorg. Chem.*, 1991, **30**, 279.
35. C. Bianchini, K. Hinn, D. Masi, M. Peruzzini, A. Polo, F. Zanobini and A. Vacca, *Inorg. Chem.*, 1993, **32**, 2366.
36. R. K. Harris, *Canadian J. Chem.*, 1964, 2275.
37. L. Vaska and D. L. Catone, *J. Am. Chem. Soc.*, 1966, **88**, 5324.
38. M. J. Church, M. J. Mays, R. N. F. Simpson and F. P. Stefanni, *J. Chem. Soc. (A)*, 1970, 2909.
39. C. Bianchini, P. Innocenti, A. Meli, M. Peruzzini, and F. Zanobini, *Organometallics*, 1990, **9**, 2514 and references cited therein.
40. L. Vaska and J. Peone, *Inorg. Synth.*, 1974, **15**, 64; A. F. Williams, S. Bhaduri and A. G. Maddock, *J. Chem. Soc., Dalton Trans.*, 1975, 1958.
41. A. F. Williams, S. Bhaduri and A. G. Maddock, *J. Chem. Soc., Dalton Trans.*, 1975, 1958.
42. R. Schmutzler, *Inorg. Chem.*, 1964, **3**, 421.
43. T. Sakakura, T. Sodeyama, K. Sasaki, K. Wada and M. Tanaka, *J. Am. Chem. Soc.*, 1990, **112**, 7221.
44. C. A. McAuliffe and R. Pollock, *J. Organomet. Chem.*, 1974, **77**, 265.
45. L. Dahlenberg, and R. Nast, *J. Organomet. Chem.*, 1976, **110**, 395.
46. J. Fawcett, J. H. Holloway and G. C. Saunders, *Inorg. Chim. Acta*, 1992, **202**, 111.
47. M. R. Churchill, J. C. Fetting, L. A. Buttrey, M. D. Barkan and J. S. Thompson, *J. Organomet. Chem.*, 1988, **340**, 257.

CHAPTER

SIX

Experimental

Some of the starting materials and compounds prepared and studied in this thesis are air and moisture sensitive. To prevent decomposition they were handled on either a glass vacuum line using standard Schlenk line techniques, or a metal line (Figure 6.1) with facilities to connect glass or fluoroplastic reaction vessels *via* Teflon couplings, (Figure 6.2). Preparations requiring AHF were performed using FEP reaction vessels. When handling this corrosive material extreme care must be exercised.

6.1 Metal Vacuum Line

This consisted of Monel Autoclave Engineers valves (AE-30 series) [Autoclave Engineers Inc., Erie, Pennsylvania, U. S. A.] connected *via* Autoclave Engineer connectors. Incorporated into the metal manifold were argon arc welded 'U' traps to permit separation and condensation of gases. Inlets for fluorine [Distillers MG] and argon [BOC Special Gases] were positioned as shown in Figure 6.1. Rough pump vacuum outlets were connected to a soda-lime chemical scrubber unit (volume 1 dm³) which neutralised HF and fluorine gas, thereby protecting the rotary pump [Model PSR/2, NGN Ltd.] which provided a vacuum of 10⁻² mmHg. High vacuum was achieved *via* outlets to a mercury diffusion pump coupled to a second NGN rotary pump. Typically, this provided a vacuum in the region of 10⁻⁵ mmHg. The mercury diffusion pump was protected by a glass trap, situated between the metal line and the diffusion pump, immersed in liquid nitrogen to condense any volatile products that remained after evacuation on the rough pump. A second glass trap immersed in dry ice was employed to protect the second rotary pump from mercury vapour. Pressures of 0-1500 mmHg were measured by Bourdon tube gauges [Type

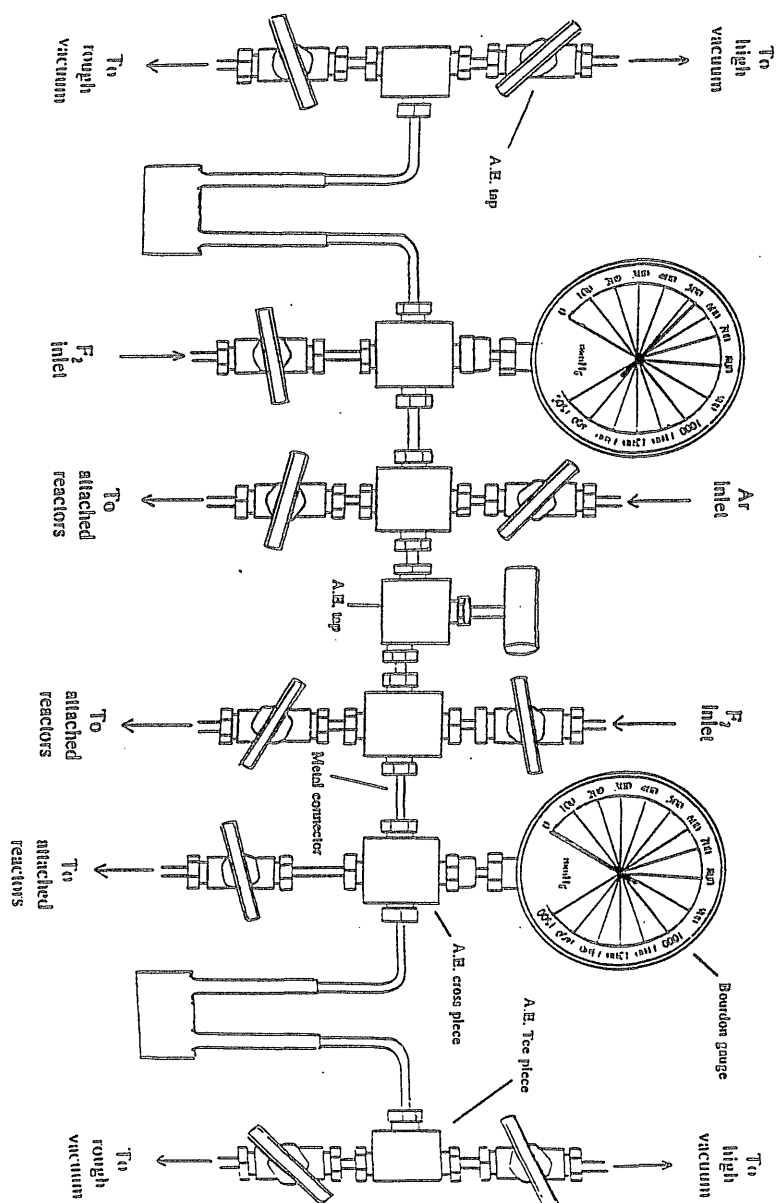
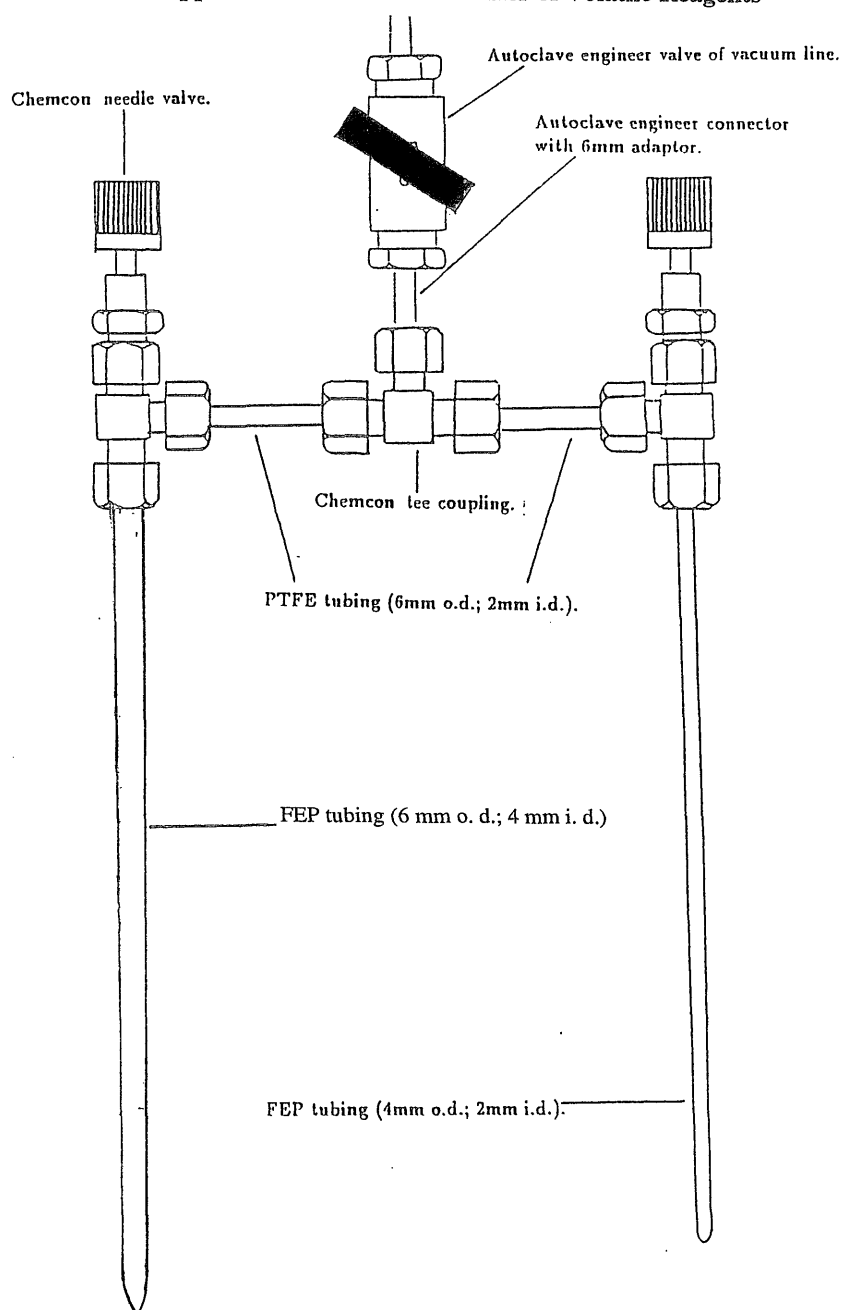


Figure 6.1 Metal Vacuum Line

Figure 6.2 Apparatus Used for the Transfer of Volatile Reagents



IF/66Z, Budenberg Gauge Co., Broadheath, Greater Manchester.] and high vacuum was measured by a Penning gauge situated between the liquid nitrogen trap and the manifold outlet.

6.2 Inert Atmosphere Dry Box

Involatile materials were manipulated in an auto-recirculating positive pressure dry box [Vacuum Atmosphere Co., VAC NE 42-2 Dri Lab.], which provided a nitrogen atmosphere with a water and oxygen content of less than 5 ppm. The quality of the atmosphere was maintained *via* circulation through columns of manganese oxide and molecular sieves which remove oxygen and water respectively. The dry box was equipped with a Sartorius balance [Model 1601 MP8]. Powdered samples were weighed in small glass boats prior to loading into the reaction vessels.

6.3 Reaction Vessels

Various glass and FEP reactors were used during the experimental work. Glass reactors were made to suit the specific reactions, and were fitted with Young's greaseless taps. For the reactions carried out in fluoroplastic, in general a straightened 6 mm o.d. FEP was first prepared by sealing at one end by heat moulding into a 7 mm i.d. glass tube. These were then connected to Chemcon coarse control needle valves [Type STD/VC-4, Production Techniques] by a PTFE 'O' compression union (see Figure 6.2). Before the introduction of the reagents, the system was evacuated to approximately 10^{-4} mmHg to ensure that a vacuum tight system had been obtained, passivated with 500 mmHg of fluorine and re-evacuated to high vacuum. Non-volatile

products were loaded into the evacuated FEP tubes in the dry box and then placed back on the vacuum line where volatile reagents and solvents could be transferred into these tubes under static vacuum (see Figure 6.3). For small scale reactions 4 mm o.d. FEP tubes were prepared (sealed at one end by heat moulding into a 5 mm NMR tube) and connected to the vacuum line in a similar manner to that described above. After reaction, the solvent was either removed to permit the analysis of the resulting product, or the tube was sealed under vacuum at the top by heating with a small ring oven, whilst the solution remained frozen at -196°C . The resulting sealed FEP tubes (Figure 6.4) could then be examined by NMR spectroscopy.

6.4 Analytical Techniques

6.4.1 Nuclear Magnetic Resonance Spectroscopy

^1H , ^{19}F , ^{31}P and ^{195}Pt NMR spectroscopies were carried out on a Bruker AM300 spectrometer at 300.13, 282.41, 121.50 and 64.52 MHz respectively and ^1H and ^{31}P on a Bruker ARX250 spectrometer at 250.13 and 101.26 MHz respectively. Spectra were recorded on air-sensitive samples in 4 mm and 6 mm o.d. FEP tubes held coaxially in 5 mm and 10 mm precision glass NMR tubes respectively containing a small amount of D_2O as the external lock substance. ^1H spectra were referenced to external TMS, ^{19}F NMR spectra to external CFCl_3 , ^{31}P to 85% H_3PO_4 and ^{195}Pt to $[\text{Na}_2\text{PtCl}_6]$, using the high frequency positive convention. All coupling constants are quoted with an experimental error of ± 1 , ± 3 and ± 3 Hz for ^{31}P , ^{19}F and ^{195}Pt NMR studies respectively.

Figure 6.3 Apparatus Used for the Transfer of Solvents

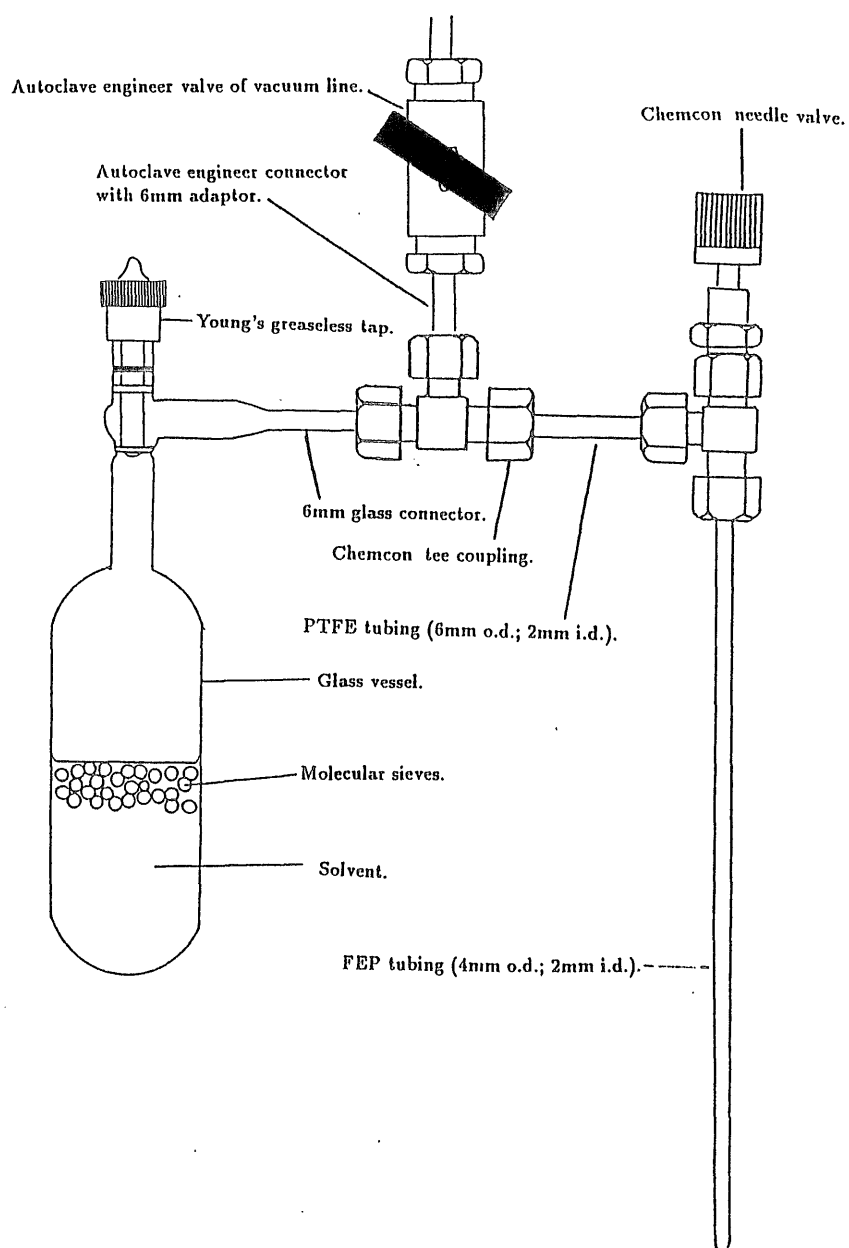
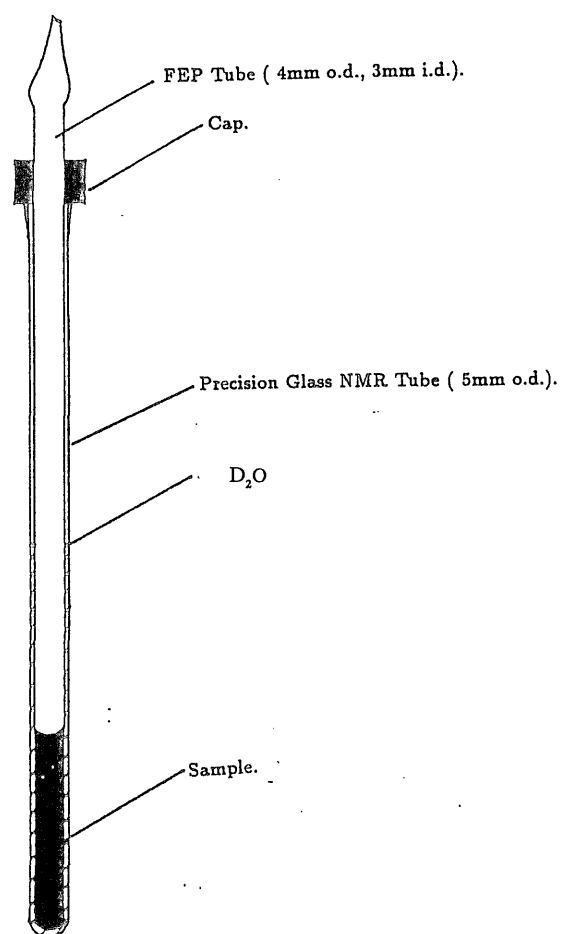


Figure 6.4 NMR Sample in 4 mm FEP Tubing



6.4.2 Infrared Spectroscopy

IR spectra were recorded as Nujol mulls compressed between KBr discs on a Digilab FTS40 FTIR spectrometer using an internal detector. Gas-phase spectra were recorded in a copper cell of length 10 cm fitted with AgCl windows. A seal was achieved between the windows and the cell of the body by means of two PTFE gaskets.

6.4.3 Mass Spectrometry

Electron impact and fast atom bombardment (FAB) mass spectra were recorded on a Kratos Concept 1H double focussing, forward geometry mass spectrometer. The samples being introduced directly into the ionising chamber.

6.4.4 EXAFS Spectroscopy

Metal L(III)-edge EXAFS data were collected at the Daresbury Synchrotron Radiation Source operating at 2 GeV (ca. 3.2×10^{-10} J) with an average current of 180 mA in transmission mode, at room temperature, on station 7.1. An order sorting Si (111) monochromator was used, offset to 50 % of the rocking curve for harmonic rejection. Typically, 4-6 data sets were collected in k space (k = photoelectron wave vector/ \AA^{-1}), and to improve the signal-to-noise ratio they were averaged using EX¹. Removal of the pre-edge background was achieved by fitting the spectrum to a quadratic or cubic polynomial and subtracting this from the whole spectrum. The atomic contribution to the oscillatory part of the absorption spectrum was approximated using polynomials and the optimum function judged by minimizing the intensity of the chemically insignificant shells at low r (r = radial distance from primary absorbing atom) in the Fourier transform. To

compensate for the decreased intensity at higher k the data was multiplied by k^3 . Modelling and analyses were performed using EXCURV92,² utilising curved-wave theory with phase shifts and back-scattering factors calculated using the normal *ab initio* methods.³

6.4.5 Preparation of EXAFS samples

60-100 mg of the sample was finely ground and diluted with boron nitride and placed in 1mm Al spacers between Sellotape strips.

6.4.6 X-ray Crystal Structure Analysis

Crystals of *trans*-[PtCl₂(NMe₃)₂] (**1**), [Pt(C₆H₄PPh₂)(PPh₃)₂][SbF₆] (**2**) and *trans*-[Ir(C₆F₅)(CO){PPh₂(C₆F₅)₂}] (**3**) suitable for single crystal X-ray crystallographic studies were obtained by slow evaporation of the solvent at room temperature in all cases. All crystals were glued to the end of a thin glass fibre using epoxy resin. Unit cell parameters were determined by least squares refinement of omega angles from approximately 40 centred reflections with $10.0 < 2\theta < 25.0^\circ$. The crystallographic data for complexes (**1**), (**2**) and (**3**) are presented in Table 6.1.

The structures were solved by Patterson methods and refinements were carried out using the SHELXTL-PC program package.⁴ For all the complexes (**1**), (**2**) and (**3**) H atoms to C atoms were included in calculated positions (C-H 0.96 Å) with a common fixed isotropic displacement parameter.

Table 6.1 Crystallographic Data for Complexes (1), (2) and (3)

	Complex (1)	Complex (2)	Complex (3)
<i>Crystal data</i>			
Empirical Formula	[C ₆ H ₁₈ Cl ₂ N ₂ Pt]	[C ₅₅ H ₄₆ Cl ₂ P ₃ PtSb]	[C ₄₃ H ₂₀ F ₁₅ OPIr]
Formula Weight	384.2	1301.57	1091.7
Temperature (K)	293	190	293
$\lambda(\text{Mo-K}\alpha)$ Å	0.71073	0.71073	0.71073
Crystal system	monoclinic	triclinic	triclinic
Space group	$P2_1/n$	$P1$	$P1$
Unit cell dimensions (Å and °)	$a = 5.987(1)$ $b = 15.192(2)$ $c = 6.411(1)$ $\alpha = 90.0(0)$ $\beta = 98.2(1)$ $\gamma = 90.0(0)$	$a = 12.4960(10)$ $b = 13.045(2)$ $c = 17.469(2)$ $\alpha = 89.61$ $\beta = 74.43$ $\gamma = 68.16$	$a = 11.695(2)$ $b = 11.910(3)$ $c = 15.535(2)$ $\alpha = 72.61(1)$ $\beta = 79.83(1)$ $\gamma = 77.16(1)$
Volume (Å ³)	577.1(2)	2532.4(5)	1999.0(1)
Z	2	2	2
Density (calc.)	2.11 gcm ⁻³	1.689 Mgm ⁻³	1.814 gcm ⁻³
Absorption coefficient (μ mm ⁻¹)	12.57	3.551	3.52
$F(000)$	360	1260	1056
Crystal size (mm)	0.6 x 0.31 x 0.22	0.71 x 0.22 x 0.14	0.76 x 0.41 x 0.26
Colour / type	yellow / block	colourless / block	yellow / block
<i>Data collection</i>			

Diffractometer	Siemens P4	Siemens P4	Siemens P4
Scan	ω	ω	ω
Index ranges	$-1 \leq h \leq 7$ $-1 \leq k \leq 18$ $-7 \leq l \leq 7$	$-1 \leq h \leq 14$ $-14 \leq k \leq 15$ $-20 \leq l \leq 20$	$-1 \leq h \leq 12$ $-13 \leq k \leq 14$ $-19 \leq l \leq 19$
Reflections collected	1574	10035	8709
Independent reflections	1131($R_{\text{int}} = 0.038$)	8606($R_{\text{int}} = 0.026$)	7531($R_{\text{int}} = 0.023$)
Observed reflections	767 [$I > 2\sigma(I)$]	7369 [$F > 4\sigma(F)$]	6428 [$I > 2\sigma(I)$]
Crystal decay	No	No	< 1 %
Absorption Correction method (max. and min.)	Semi Empirical (0.78 and 0.23)	Semi Empirical (0.99 and 0.51)	Semi Empirical (0.90 and 0.52)
Refinement			
Refinement method	Full matrix least squares on F	Full-matrix least squares on F^2	Full matrix least squares on F
Data / restraints/ parameters	767 / 0 / 57	8605 / 0 / 613	6428 / 0 / 559
Goodness-of-fit on F^2	1.20	1.026	0.5863
Final R indices	R = 0.0457 $R_w = 0.0645$	R1 = 0.0325, wR2 = 0.0711	R = 0.033 $R_w = 0.038$
R indices (all data)	-	R1 = 0.044, wR2 = 0.0758	-
Largest diff. peak and hole ($e\text{\AA}^{-3}$)	2.4, -3.1	1.622, -0.599	1.32, -0.70

6.5 Sources of Chemicals and Methods of Purification

Fluorine, F₂.

Distillers MG. This was used as supplied after being transferred into a 1 dm³ nickel can for convenience.

Hydrofluoric acid, HF.

ICI plc. After first removing any hydrogen, this was vacuum transferred into Kel-F vessels, dried with fluorine at room temperature overnight and stored over dry [BiF₅].

cis- Bis(triethylphosphine) platinumchloride, *cis*-[PtCl₂(PEt₃)₂].

Aldrich. Used as supplied.

Tetrakis(triphenylphosphine)platinum(0), [Pt(PPh₃)₄].

Aldrich. Used as supplied.

Dichloroplatinum(II), [PtCl₂].

Aldrich. Used as supplied.

cis- Dichlorodiamineplatinum(II), *cis*-[PtCl₂(NH₃)₂].

Johnson Matthey. Used as supplied.

trans- Dichlorodiamineplatinum(II), *trans*-[PtCl₂(NH₃)₂].

Johnson Matthey. Used as supplied.

cis- Dichloroethylenediamineplatinum(II), *cis*-[PtCl₂(en)].

Johnson Matthey. Used as supplied.

cis- Dichlorodi(pyridine)platinum(II), *cis*-[PtCl₂(py)₂].

Johnson Matthey. Used as supplied.

Platinum(II)bis(ethylenediamine)chloride, [Pt(en)₂]Cl₂.

Aldrich. Used as supplied.

Dodecacarbonyl tetrairidium, [Ir₄(CO)₁₂].

Aldrich. Used as supplied.

Carbonylbis(triphenylphosphine)iridium(I)chloride, *trans*-
[IrCl(CO)(PPh₃)₂].

Aldrich. Used as supplied.

Chlorotricarbonyliridium(I), [IrCl(CO)₃]_n.

Strem. Used as supplied.

Trimethylphosphine, PMe₃.

Aldrich. Stored in a glass ampoule connected to Young's Greaseless tap to allow easy manipulation on the vacuum line.

Triethylphosphine, PEt₃.

Aldrich. Stored in a glass ampoule connected to Young's Greaseless tap to allow easy manipulation on the vacuum line.

Dimethylphenylphosphine, PMe₂Ph.

Aldrich. Stored in a glass ampoule connected to Young's Greaseless tap.

Diphenylmethylphosphine, PMePh₂.

Aldrich. Stored in a glass ampoule connected to Young's Greaseless tap.

Diphenylethylphosphine, PEtPh₂.

Aldrich. Stored in a glass ampoule connected to Young's Greaseless tap.

Triphenylphosphine, PPh₃.

Aldrich. Used as supplied.

Tri-*p*-tolylphosphine, P(*p*-MeC₆H₄)₃.

Aldrich. Used as supplied.

Tricyclohexylphosphine, Pcy₃.

Aldrich. Used as supplied.

Tri-isopropylphosphine, P(C₃H₇)₃.

Aldrich. Used as supplied.

Diphenylpentafluorophenylphosphine, P(C₆F₅)Ph₂.

Fluorochem. Used as supplied.

Bis(pentafluorophenyl)phenylphosphine, $P(C_6F_5)_2Ph$.

Fluorochem. Used as supplied.

Bis(diphenylphosphino)ethane, dppe.

Aldrich. Used as supplied.

1,1,1-Tris(diphenylphosphinomethyl)ethane, triphos.

Aldrich. Used as supplied.

Tris[2-(diphenylphosphinoethyl)]phosphino, tetraphos.

Aldrich. Used as supplied.

Trimethylamine (ethanol), NMe_3 .

Fluka. Used as supplied.

Triethylamine, NEt_3 .

Lancaster synthesis. Used as supplied.

Pyridine, py.

FSA laboratory supplies. Used as supplied.

2, 2'-Bipyridyl, bipy.

Aldrich. Used as supplied.

Triphenylarsine, $AsPh_3$.

Aldrich. Used as supplied.

Silver fluoride, AgF .

Aldrich. Used as supplied.

d_2 -Dichloromethane, CD_2Cl_2 .

Aldrich. Stored in a glass ampoule connected to Young's Greaseless tap to allow easy manipulation on the vacuum line.

d_6 -Dimethylsulphoxide, dmsO.

Aldrich. Used as supplied

***cis*-Dichloro(cyclooctadiene)platinum(II), *cis*-[PtCl₂(cod)].**

Prepared according to the literature method, by the reaction of [K₂PtCl₄] and 1,5 cod in glacial acetic acid.⁵

***cis*-Bis(acetonitrile)dichloroplatinum(II), *cis*-[PtCl₂(MeCN)₂].**

Prepared according to the literature method, by the reaction of [PtCl₂] and refluxing MeCN.⁶

***cis*-Bis(triphenylphosphine)dichloroplatinum(II), *cis*-[PtCl₂(PPh₃)₂].**

Prepared according to the literature method, by the reaction of [K₂PtCl₄] and PPh₃ in ethanol.⁷

Dichloro{bis(diphenylphosphino)ethane}platinum(II), *cis*-[PtCl₂(dppe)].

Prepared according to the literature method, by the reaction of *cis*-[PtCl₂(cod)] and dppe in dichloromethane.⁸

***cis*-Bis(trimethylphosphine)dichloroplatinum(II), *cis*-[PtCl₂(PMe₃)₂].**

Prepared by the reaction of *cis*-[PtCl₂(MeCN)₂] and PMe₃ in THF.^{8a}

***cis*-Bis(dimethylphenylphosphine)dichloroplatinum(II), *cis*-[PtCl₂(PMe₂Ph)₂].**

Prepared by the reaction of *cis*-[PtCl₂(MeCN)₂] and PMe₂Ph in THF.^{8a}

***cis*-Bis(diphenylethylphosphine)dichloroplatinum(II), *cis*-[PtCl₂(PEtPh₂)₂].**

Prepared by the reaction of *cis*-[PtCl₂(MeCN)₂] and PEtPh₂ in THF.^{8a}

***cis*-Bis(triphenylphosphine)dimethylplatinum(II), *cis*-[PtMe₂(PPh₃)₂].**

Prepared by the reaction of *cis*-[PtCl₂(PPh₃)₂] and a stoichiometric amount of methyllithium in toluene.^{8a}

***cis*-Bis(triethylphosphine)dimethylplatinum(II), *cis*-[PtMe₂(PEt₃)₂].**

Prepared by the reaction of *cis*-[PtCl₂(PEt₃)₂] and a stoichiometric amount of methyllithium in toluene.^{8a}

***cis*-Bis(dimethylphenylphosphine)dimethylplatinum(II), *cis*-[PtMe₂(PMe₂Ph)₂].**

Prepared by the reaction of *cis*-[PtCl₂(PMe₂Ph)₂] and a stoichiometric amount of methyllithium in toluene.^{8a}

***cis*-Bis(diphenylethylphosphine)dimethylplatinum(II), *cis*-[PtMe₂(PEtPh₂)₂].**

Prepared by the reaction of *cis*-[PtCl₂(PEtPh₂)₂] and a stoichiometric amount of methyllithium in toluene.^{8a}

***cis*-Bis(trimethylphosphine)dimethylplatinum(II), *cis*-[PtMe₂(PMe₃)₂].**

Prepared by the reaction of *cis*-[PtCl₂(PMe₃)₂] and a stoichiometric amount of methyllithium in toluene. The white solid was analysed by ³¹P{¹H} NMR; s δ -22.7, ¹J_{PP} = 1745 Hz and ¹H NMR spectroscopy; t δ 0.4 ³J_{HP} = 7 Hz (the expected ¹⁹⁵Pt satellites were not resolved). The sample of *cis*-[PtMe₂(PMe₃)₂] was found to contain impurities.^{8a}

Dimethyl{bis(diphenylphosphino)ethane}platinum(II), *cis*-[PtMe₂(Pcy₃)₂].

Prepared by the reaction of *cis*-[PtCl₂(Pcy₃)₂] and a stoichiometric amount of methyllithium in toluene. The white solid was analysed by ³¹P{¹H}; s δ 21.4, ¹J_{PP} = 1842 Hz and ¹H; t δ 0.5 ³J_{HP} = 7 Hz (the expected ¹⁹⁵Pt satellites were not resolved). The sample of *cis*-[PtMe₂(Pcy₃)₂] was found to contain impurities.^{8a}

Tetrakis(triethylphosphine)platinum(II)hexafluorophosphate, [Pt(PEt₃)₄][PF₆]₂.

Prepared according to literature method, by the reaction of [K₂PtCl₄], PEt₃ and [KPF₆] in water.⁹

Chlorotris(triethylphosphine)platinum(II)hexafluorophosphate, [PtCl(PEt₃)₃][PF₆].

Prepared according to literature method, by the reaction of [Pt(PEt₃)₄][PtCl₄] and PEt₃ in water, followed by treatment with conc. HCl and addition of [KPF₆].⁹

***trans*-Bis(trimethylamine)dichloroplatinum(II), *trans*-[PtCl₂(NMe₃)₂].**

Prepared according to the literature method, by the reaction of [PtCl₂] and NMe₃ (ethanol solution) in acetone.¹⁰

***cis*-Dichloro(2,2'-bipyridyl)platinum(II), *cis*-[PtCl₂(bipy)].**

Prepared according to the literature method, by the reaction of $[\text{K}_2\text{PtCl}_4]$ and bipy in water.¹¹

All materials, unless otherwise stated, were checked by infrared or NMR spectroscopy, with the reported literature values, for authenticity and purity.

6.6 Solvents

Dichloromethane, CH_2Cl_2 : (B.D.H. Ltd., Spectroscopic Grade); preliminary purification by shaking with portions of $[\text{H}_2\text{SO}_4]$, water, aqueous 5 % $[\text{Na}_2\text{CO}_3]$, $[\text{NaHCO}_3]$ and then water again. Subsequently predried over $[\text{CaCl}_2]$ and then refluxed over $[\text{P}_2\text{O}_5]$ and distilled into a 2-necked round bottom flask, where it was transferred under a N_2 atmosphere into glass ampoules (connected to Young's taps) and stored over molecular sieves.

Acetonitrile, CH_3CN : (B.D.H. Ltd., Spectroscopic Grade); preliminary drying treatment was achieved by storing the solvent over 3 Å molecular sieves which had been activated by baking in an oven for 18 hours at 200 °C. Subsequently, it was refluxed over $[\text{CaH}_2]$ under a nitrogen atmosphere. After the distillation was complete, the drying agent was replaced with $[\text{P}_2\text{O}_5]$, refluxed and distilled into a double necked round bottom flask. Final drying was effected by vacuum distillation into glass ampoules (connected to a Young's tap) containing activated 3 Å molecular sieves.

Sulphur dioxide, SO_2 : (B.D.H. Ltd., Spectroscopic Grade); liquid SO_2 was directly condensed under vacuum onto $[\text{P}_2\text{O}_5]$ which was dried by baking in an oven at 200°C for 1 day and pumping under vacuum ($\sim 10^{-5}$ mmHg) overnight.

Toluene, $C_6H_5CH_3$: (B.D.H. Ltd., Spectroscopic Grade); dried over $[P_2O_5]$ for 24 hours and distilled into a 2-necked round bottom flask. Stored in glass ampoules over activated molecular sieves.

6.7 Preparation of Xenon Difluoride

This was prepared as described by Holloway.¹² Xenon gas was mixed with a 10 % excess of fluorine in a passivated one litre glass bulb (connected to a Young's tap). The reaction mixture was UV photolysed, and once adjudged to be finished (approximately 72 hours) the unreacted fluorine and xenon were removed *via* the rough pump. Purification of the xenon difluoride was achieved by sublimation under dynamic vacuum into a glass trap held at -78°C , and stored in the dry box at room temperature.

6.8 Preparation of *fac*- $[\text{IrF}_3(\text{CO})_3]$

This was prepared as described by Hope *et al.*¹³ Typically, $[\text{Ir}_4(\text{CO})_{12}]$ (0.3 g, 0.27 mmol) and a 6 molar equivalent of $[\text{XeF}_2]$ (0.28 g, 1.6 mmol) were loaded *via* the dry box into a 6 mm o.d. pre-seasoned FEP tube. The tube was then reconnected to the metal line (*c.f.* Figure 6.2), and the satellite links were passivated. Care was taken to keep the two solids separated. The reactor was then evacuated and AHF solvent was distilled into the reaction vessel at -196°C under static vacuum. Upon warming the reaction mixture to -50°C a vigorous reaction was observed accompanied by evolution of a colourless gas. Infrared spectroscopy studies of this gas showed no absorption bands and thus, was assumed to be xenon. Judicious cooling and venting of the system was implemented over 2-3 hours. After dissolution of

all the starting material the reaction mixture was warmed to room temperature and further effervescence was observed, necessitating continual temperature quenching and venting of the system. Once the reaction was complete, the resulting yellow solution was left at room temperature overnight. Removal of the AHF solvent *via* the rough pump led to the isolation of *fac*-[IrF₃(CO)₃], the resulting yellow solid was then held under dynamic vacuum until an approximate pressure reading of 0.3×10^{-4} mmHg was obtained. The compound was stored in the dry box.

The authenticity and purity of the material was checked by infrared and ¹⁹F NMR spectroscopy with the reported literature values.¹³

6.9 Reactions of *fac*-[IrF₃(CO)₃] with Lewis Bases on the Metal Vacuum Line

Initially, reactions were carried out in an analogous manner to that of *fac*-[IrF₃(CO)₃] and PMe₃ as described by Brewer.¹⁴ [IrF₃(CO)₃] (0.05 g, 0.15 mmol) was loaded into a pre-seasoned 4 mm o.d. FEP tube and connected along with ampoules of the appropriate Lewis base and CH₂Cl₂ to the metal vacuum line. Before the addition of these chemicals to *fac*-[IrF₃(CO)₃], the connectors were passivated with fluorine gas. After re-evacuation of the whole system, CH₂Cl₂ was distilled onto the *fac*-[IrF₃(CO)₃] followed by the Lewis base. Upon warming the system to room temperature effervescence was observed with the evolution of a colourless gas, which was shown by gas-phase infrared spectroscopy to be carbon monoxide, yielding a yellow solution. When the reaction had ceased removal of the volatiles yielded a solid which was re-dissolved in CD₂Cl₂ and studied by multinuclear NMR spectroscopy.

Reactions with involatile Lewis bases were performed as described above, except that the appropriate solid was loaded into the 4 mm o.d. FEP tube along with *fac*-[IrF₃(CO)₃].

6.10 Reactions of *fac*-[IrF₃(CO)₃] with Lewis Bases on a Schlenk line

Typically, *fac*-[IrF₃(CO)₃] (0.05 g, 0.15 mmol) was loaded into a Schlenk with a one molar equivalent of the solid Lewis base in a dry box. The Schlenk was then evacuated and then filled with an atmosphere of dry nitrogen before injecting freshly distilled CH₂Cl₂ or toluene (30 ml) into the reaction vessel and then the whole reaction mixture was stirred for approximately 5-10 minutes. Immediate effervescence was observed along with the formation of a yellow solution. Once the reaction was complete the mixture was filtered, in air, to remove any unreacted starting materials followed by removal of the solvent to yield an air-stable yellow solid.

Reactions employing liquid Lewis bases were carried out in an analogous manner to that described above. Introduction of the appropriate Lewis base was achieved by injecting into a suspension of *fac*-[IrF₃(CO)₃] in CH₂Cl₂ or toluene.

Reactions requiring refluxing were performed in a 2-necked round bottom flask fitted with a reflux condenser. Materials were loaded in the manner described above and then the reaction mixture was refluxed for approximately 5 hours.

Table 6.2 ^1H NMR Data and the Fragmentation Patterns for the Complexes *mer*-, *trans*- $[\text{IrF}_3(\text{CO})(\text{L})_2]$ 5a - 5j

L	δ (^1H)/ ppm	Mass Spectra Fragmentation Pattern
5a PMe_3	1.8 (t)	$[\text{M-CO}]^+$, $[\text{M-3F}]^+$, $[\text{M-3F-CO}]^+$
5b PEt_3	1.4 (m) ^a , 2.2 (m) ^b	$[\text{M-CO}]^+$, $[\text{M-3F}]^+$, $[\text{M-3F-CO}]^+$
5c PPh_3	7.5 (m)	$[\text{M-CO}]^+$, $[\text{M-3F}]^+$, $[\text{M-3F-CO}]^+$
5d $\text{PPh}_2(\text{C}_6\text{F}_5)^c$	9.5 (m)	$[\text{M-CO}]^+$, $[\text{M-3F}]^+$, $[\text{M-3F-CO}]^+$
5e Pcy_3	2.0 (m)	$[\text{M-CO}]^+$, $[\text{M-3F}]^+$
5f $\text{P}(p\text{-MeC}_6\text{H}_4)_3$	7.2 (m) ^d , 2.3 (s)	$[\text{M-CO}]^+$, $[\text{M-3F}]^+$, $[\text{M-3F-CO}]^+$
5g P^iPr_3	1.0 (m) ^a , 1.4 (m) ^b , 2.3 (m) ^b	-
5h PEtPh_2	7.2 (m) ^d , 2.0 (m) ^b , 1.0(m) ^a	-
5i PMe_2Ph	7.5 (m) ^d , 1.5 (m)	$[\text{M-CO}]^+$, $[\text{M-3F}]^+$
5j PMePh_2	7.5 (m) ^d , 2.0 (m)	$[\text{M-CO}]^+$, $[\text{M-3F}]^+$, $[\text{M-3F-CO}]^+$
NMe_3	2.7 (m)	-
AsPh_3	7.5 (m)	$[\text{M-CO}]^+$, $[\text{M-3F}]^+$, $[\text{M-3F-CO}]^+$

m = multiplet, t = triplet and s = singlet

(a) $-\text{CH}_3$, (b) $-\text{CH}_2$ and (d) aryl protons

(c) ^{19}F NMR data for the C_6F_5 ring: *ortho*-F (δ -122.8), *para*-F (δ -146.8) and *meta*-F (δ -161.0).

Presented in Table 6.2 are the ^1H NMR data and the fragmentation patterns, observed in the mass spectra, for the complexes *mer*-, *trans*- $[\text{IrF}_3(\text{CO})(\text{L})_2]$ described in section 5.5.1.

6.11 Preparation of *trans*-[IrF(CO)(PPh₃)₂]

This was prepared according to the literature method.¹⁵ *trans*-[IrCl(CO)(PPh₃)₂] (0.1 g, 0.13 mmol) was reacted in a 1:1 molar ratio with [Ag₂CO₃] in [NH₄F] solution yielding a yellow solid.

The spectroscopic data for *trans*-[IrF(CO)(PPh₃)₂] are presented in section 4.5.

6.12.1 Preparation of *trans*-[Ir(CO)Cl(PR₃)₂], for PR₃ = Pcy₃ or PPh(C₆F₅)₂

Typically, [IrCl(CO)₃]_n (0.05 g, 0.17 mmol) and a 2 molar equivalent of the phosphine were refluxed in toluene, under a nitrogen atmosphere, for approximately 5 hours. After this time the reaction mixture was filtered, to remove any unreacted [IrCl(CO)₃]_n, and then the solvent was removed *in vacuo* yielding a yellow solid.

The spectroscopic data for *trans*-[IrCl(CO)(Pcy₃)₂] are presented in section 4.6.

The complex *trans*-[IrCl(CO){PPh(C₆F₅)₂}]₂ was kindly donated by Saunders and Merrill.¹⁶

6.12.2 Preparation of *trans*-[IrCl(CO){P(C₆F₅)₃}]₂

Kindly donated and prepared as described by Saunders and Merrill.¹⁶ [IrCl₃·3H₂O] (0.2 g, 0.7 mmol) and P(C₆F₅)₃ (1.07 g, 2.0 mmol) were refluxed, under a nitrogen atmosphere, in 2-methoxyethanol for 2 hours. After this time the solvent was removed and the excess phosphine was sublimed out yielding a yellow solid.

6.13 Reactions of *trans*-[IrCl(CO)(PR₃)₂] (PR₃ = PPh₃, cy₃, P(C₆F₅)₃ and PPh(C₆F₅)₂) and *trans*-[IrF(CO)(PPh₃)₂] with [XeF₂]

These reactions were performed in a 6 mm o.d. FEP tube. *trans*-[IrCl(CO)(PR₃)₂] (0.1 g) and a one molar equivalent of [XeF₂] were loaded in a dry box. Care was taken to keep the two solids separated. The usual procedure was followed of passivating the satellite connectors. After re-evacuation of the whole system, CH₂Cl₂ was then condensed onto the reaction mixture at -196°C. Upon warming the system to room temperature effervescence was observed with the evolution of a colourless gas. Infrared studies of this gas showed no absorption bands and thus, it was assumed to be xenon. When the reaction had ceased removal of the volatiles afforded a solid, which was exposed to the air and analysed by mass spectrometry, infrared and NMR spectroscopy (as discussed in section 4.9).

6.14 Reactions of *cis*-[PtCl₂(PR₃)₂] (PR₃ = PPh₃, PMe₃, PEt₃, PMe₂Ph, PPh₂Et and (PR₃)₂ = dppe) with AHF

Typically, *cis*-[PtCl₂(PR₃)₂] (0.1 g) was loaded into a pre-seasoned 6 mm o.d. FEP tube and then re-connected to the metal line. The satellite connectors were then passivated and re-evacuated, when a vacuum in the region of 0.3×10^{-4} mmHg had been obtained AHF was condensed onto the solid at -196°C. Upon warming the reaction mixture to room temperature effervescence was observed, no gases were isolated. When the reaction was complete the AHF was either removed and the resulting solid re-dissolved in another solvent and heat sealed, or the 6 mm o.d. FEP tubes were heat sealed without removing the AHF. The vacuum sealed FEP tubes were then analysed by NMR spectroscopy.

6.15 Reactions of *cis*-[PtMe₂(PR₃)₂] (PR₃= PPh₃, PMe₃, PEt₃, PMe₂Ph, PPh₂Et and Pcy₃) with AHF

These reactions were carried out on a 100 mg scale of the appropriate platinum(II) compound, in a similar manner to that described above except that upon warming the reaction mixture to -80°C (after condensing AHF onto the solids) a vigorous reaction was observed with the evolution of a colourless gas. Gas-phase infrared studies on this gas unambiguously identified it as methane. The reaction mixture was warmed to room temperature where further effervescence was observed necessitating continual quenching and venting of the system. Upon completion of the reaction, the AHF was either removed and the resulting product re-dissolved in another solvent or retained. The 6 mm o.d. FEP tubes were then heat sealed for analysis by NMR spectroscopy.

6.16 Preparation of [PtF(PPh₃)₃][X] (X = SbF₆, BF₄)

This was prepared as described by Dixon *et al.*¹⁷ Tetrakis(triphenylphosphine)platinum(0), [Pt(PPh₃)₄] (0.3 g, 0.25 mmol) was loaded into a passivated 6 mm o.d. FEP tube and into a second tube was loaded [NaSbF₆] (0.028 g, 0.25 mmol) or [NaBF₄] (0.026 g, 0.25 mmol). After passivation and re-evacuation of the satellite connectors AHF was condensed onto the platinum(0) complex at liquid nitrogen temperature. Upon warming effervescence was observed, necessitating quenching and venting of the hydrogen produced during the reaction. When the reaction was complete the AHF solution was reacted with the [NaSbF₆] or [NaBF₄] and after 1 hour the solvent was removed *via* the rough pump to yield an air-stable brown solid.

The spectroscopic data for $[\text{PtF}(\text{PPh}_3)_3][\text{BF}_4]$ are presented and discussed in section 3.9.

6.17 Preparation of Fluoro(triethylphosphine)platinum(II) - hexafluorophosphate

This reaction was carried out according to the method of Dixon *et al.*¹⁷ Silver(I) fluoride (0.04 g, 0.3 mmol) was suspended in a solution of $[\text{PtCl}(\text{PEt}_3)_3][\text{PF}_6]$ (0.1 g, 0.14 mmol) in acetone (15 ml) and the reaction mixture was protected from intense light. After stirring for 20 hours at 25°C the black solid residue was removed by filtration and the colourless filtrate concentrated to *ca.* 2 ml by evaporation *in vacuo*. Dropwise addition of diethylether afforded the complex (0.07 g, 0.1 mmol) as a colourless solid.

The spectroscopic data for $[\text{PtF}(\text{PEt}_3)_3][\text{BF}_4]$ are presented and discussed in section 3.9.

6.18 The Reaction of $[\text{Pt}(\text{PEt}_3)_4][\text{PF}_6]_2$ with $[\text{XeF}_2]$

$[\text{Pt}(\text{PEt}_3)_4][\text{PF}_6]$ (0.05 g, 0.05 mmol) and $[\text{XeF}_2]$ (0.09 g, 0.05 mmol) were loaded into a pre-seasoned 4 mm o.d. FEP. Care was taken to keep the two solids separated. The tube was then re-connected to the metal vacuum line with an ampoule of CH_3CN and the satellite links were then passivated. After evacuation of the whole system CH_3CN was then distilled onto the platinum complex at -196°C. The reaction mixture was warmed to -10°C and effervescence was observed accompanied by the evolution of a colourless gas, presumed to be xenon. When the reaction had ceased the FEP tube was sealed as previously described for analysis by NMR.

The reactions of $[\text{PtF}(\text{PEt}_3)_3][\text{PF}_6]$ and *cis*- $[\text{PtCl}_2(\text{PR}_3)_2]$ ($\text{PR}_3 = \text{PEt}_3$ and $(\text{PR}_3)_2 = \text{dppe}$) with $[\text{XeF}_2]$ were carried out in an identical manner to that described above.

6.19 Reactions of $[\text{PtCl}_2(\text{L})_2]$ ($\text{L} = \text{NH}_3, \text{NMe}_3, \text{Py}$ and $\text{L}_2 = \text{bipy}, \text{en}$) complexes with AHF

These reactions were carried out in analogous manner to that described in 6.14. Typically, $[\text{PtCl}_2(\text{L})_2]$ ($\text{L} = \text{NH}_3, \text{NMe}_3, \text{Py}$ and $\text{L}_2 = \text{bipy}, \text{en}$) (0.1 g) were allowed to react with AHF over a period 2-24 hours. When the reaction had ceased the AHF was removed affording an air-stable orange solid. The solids were analysed by mass spectrometry, ^1H and ^{19}F NMR spectroscopy as previously described in section 2.5.

6.20 Reactions of $[\text{PtCl}_2(\text{L})_2]$ ($\text{L} = \text{NH}_3, \text{NMe}_3, \text{Py}$ and $\text{L}_2 = \text{bipy}, \text{en}$) Complexes with $[\text{XeF}_2]$ in CH_3CN

These reactions were performed as described in 6.18. $[\text{PtCl}_2(\text{L})_2]$ ($\text{L} = \text{NH}_3, \text{NMe}_3, \text{Py}$ and $\text{L}_2 = \text{bipy}, \text{en}$) (0.1 g) and a one molar equivalent of $[\text{XeF}_2]$ were loaded into a 6 mm o.d. FEP tube (connected to a Chemcon tap). Care was taken to keep the two solids separated. CH_3CN was distilled into the reaction vessel at -196°C , from a glass ampoule. The system was then warmed to room temperature and effervescence was observed with the evolution of xenon. When the reaction was complete the CH_3CN was removed *via* the rough pump and the resulting orange solid was held under dynamic vacuum until an approximate reading of 0.3×10^{-4} mmHg was obtained. Although, the solids were air-stable they were stored in the dry

box. The solids were analysed by mass spectrometry, ^1H and ^{19}F NMR spectroscopy as previously described in chapter 2.

6.21 Reactions of $[\text{PtCl}_2(\text{L})_2]$ ($\text{L} = \text{NH}_3$, NMe_3 , Py and $\text{L}_2 = \text{bipy}$, en) Complexes with $[\text{XeF}_2]$ in AHF

These reactions were carried out in analogous manner to that described above. As a result of the vigour of these reactions all were initially controlled at temperatures in the region -80 to -20°C . When the vigorous reaction had subsided the system was warmed to room temperature and further effervescence was observed. Removal of the AHF afforded air-stable orange solids. The solids were analysed by mass spectrometry, ^1H and ^{19}F NMR spectroscopy as previously described in chapter 2.

6.22 The Reaction of *trans*- $[\text{PtCl}_2(\text{NMe}_3)_2]$ with Ag^{I}

This reaction was carried out in a similar manner to that described in 6.18. Silver(I) fluoride (0.1 g, 8.0 mmol) and *trans*- $[\text{PtCl}_2(\text{NMe}_3)_2]$ (0.15 g, 4.0 mmol) were reacted in a 2:1 molar ratio in acetone (40 ml). Removal of the acetone yielded an air-stable brown solid which was analysed by ^{19}F NMR spectroscopy and mass spectrometry (see section 2.5.1).

6.23 Preparation of *trans*- $[\text{PtCl}_2(\text{NEt}_3)_2]$

$[\text{PtCl}_2]$ (0.3 g, 1.1 mmol) and NEt_3 (2.2 g, 2.2 mmol) were reacted, under an atmosphere of nitrogen, in acetone, at 0°C , affording a yellow

solution. The solvent was removed *in vacuo* yielding a brown solid which was dissolved in d_6 -acetone and subsequently analysed by ^1H NMR spectroscopy; 3H t δ 2.4, 2H q δ 3.2, $^3J_{\text{HH}} = 4$ Hz. The E. I. mass spectrum showed the most intense peak centred at m/z 468 which was attributed to the parent ion, $[M]^+$.

References for Chapter 6

1. EX, A. K. Brisdon, University of Leicester, 1992.
2. EXCURV92, SERC Daresbury Laboratory program, N. Binstead, S. J. Gurman and J. W. Campbell, 1992.
3. EXCURVE, S. J. Gurman, N. Binstead and I. Ross, *J. Phys. C.*, 1984, **17**, 143; 1986, **19**, 1845.
4. G. M. Sheldrick, SHELXTL-PC RELEASE 4.1, Program for crystal structure determination and refinement. Siemens Analytical X-ray Instruments Inc., Madison, Wisconsin, U.S.A. (1990).
5. J. X. McDermott, J. F. White and G. M. Whitesides, *J. Am. Chem. Soc.*, 1976, **98**, 6521.
6. F. R. Hartley, S. G. Murray and C. A. McAuliffe, *Inorg. Chem.*, 1979, **18**, 1394.
7. J. C. Bailar and H. Itanani, *Inorg. Chem.*, 1965, **4**, 1618.
8. M. J. Hudson, R. S. Nyholm and M. H. B. Stiddard, *J. Chem. Soc. (A)*, 1968, 40.
9. D. J. Cole-Hamilton, *J. Chem. Soc., Dalton Trans.*, 1984, 2249.
10. P. L. Goggin, R. J. Goodfellow and E. J. S. Reed, *J. Chem. Soc., Dalton Trans.*, 1972, 1298; 1976, 459.
11. G. Morgan and F. Burstall, *J. Chem. Soc.*, 1934, 965.
12. J. H. Holloway, *J. Chem. Soc., Chem. Commun.*, 1966, 22.
13. S. A. Brewer, J. H. Holloway, E. G. Hope and P. G. Watson, *J. Chem. Soc., Chem. Commun.*, 1992, 1577.
14. S. A. Brewer, PhD Thesis, University of Leicester, 1993.
15. L. Vaska and J. Peone, *Inorg. Synth.*, 1974, **15**, 64.
16. N. J. Merrill and G. C. Saunders, Personal Communications.
17. M. A. Cairns, K. R. Dixon and J. J. McFarland, *J. Chem. Soc., Dalton Trans.*, 1975, 1159.

Appendix

Appendix. Discussion of the Crystal Structure for [HNEt₃][PtCl₃(NEt₃)]

Crystals of [HNEt₃][PtCl₃(NEt₃)] (1), suitable for X-ray crystal determination, were grown from an acetone solution of *trans*-[PtCl₂(NEt₃)₂] at 0°C. A yellow crystal of (1) with dimensions 0.52 x 0.13 x 0.11 mm was glued to the end of a thin glass fibre using epoxy resin. Unit cell parameters were determined by least squares refinement of omega angles from 22 centred reflections with $9.8 < 2\theta < 24.9^\circ$. Intensities of 3518 reflections with $5 < 2\theta < 50^\circ$ and $-1 \leq h \leq 16$, $-1 \leq k \leq 14$, $-25 \leq l \leq 1$ were measured on a Siemens P4 Diffractometer using a ω technique and graphite monochromated Mo-K α radiation. No crystal decay was detected from periodically measured check reflections. The data were corrected for Lorentz and polarization effects. The reflections merged to a unique data set of 3017 reflections ($R_{\text{int}} = 2.79\%$) with 1717 having $I \geq 2\sigma(I)$ regarded as observed. An absorption correction was applied to the data set, maximum and minimum transmission factors 0.9826 and 0.5691 respectively. Crystal data for (1): [C₁₂H₃₁Cl₃N₂Pt], $M_r = 504.8$, orthorhombic, *Pbca*, $a = 12.796(4)$ Å, $b = 13.6640(10)$ Å, $c = 20.937(2)$ Å, $U = 3660.9(12)$ Å³, $Z = 8$, $D_{\text{calc}} = 1.832$ Mg m⁻³, $\lambda(\text{Mo-K}\alpha) = 0.71073$ Å, $\mu = 8.092$ mm⁻¹, $F(000) = 1968$, $T = 293$ K. Structure solution by Patterson methods and refinement were carried out using the SHELXTL-PC programme package.¹ All hydrogen atoms were included in calculated positions (C-H = 0.96 Å) with a common fixed isotropic thermal parameter (0.08 Å²). Final $R = 0.05$, $R_w = 0.414$ [$w^{-1} = [\sigma^2(F) + 0.002F^2]$], for 164 parameters. Maximum and minimum peak heights in the difference Fourier map were 1.12 and -1.36 e Å⁻³. An analysis of the weighting scheme over $|F_o|$ and $\sin \theta/\lambda$ was satisfactory.

The molecular structure of complex (1) is shown in Figure A1 with selected bond lengths and angles being presented in Table A1.

Figure A1 Crystal Structure of Complex (1)

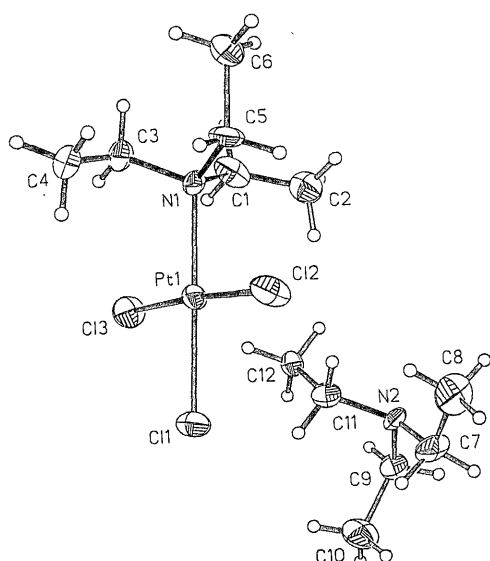


Table A1 Selected Bond Lengths (Å) and Angles (°)

Bond Lengths	Pt(1)-Cl(1) 2.311(4) Pt(1)-Cl(2) 2.228(4)
	Pt(1)-Cl(3) 2.240(4) Pt(1)-N(1) 2.128(11)
	mean N(1)-C 1.49
Bond Angles	Cl(1)-Pt(1)-Cl(2) 86.9(1) Cl(1)-Pt(1)-Cl(3) 88.8(1)
	Cl(2)-Pt(1)-Cl(3) 175.4(2) Cl(1)-Pt(1)-N(1) 178.6(3)
	Cl(2)-Pt(1)-N(1) 94.5(3) Cl(3)-Pt(1)-N(1) 89.8(3)

Complex (1) exhibits a slightly distorted square planar geometry about the platinum atom. The bond lengths and angles presented in Table A1 compare well with those reported for the complex $\text{K}[\text{PtCl}_3(\text{NH}_3)] \cdot \text{H}_2\text{O}$.² In the structure of $\text{K}[\text{PtCl}_3(\text{NH}_3)] \cdot \text{H}_2\text{O}$ it was found that the Pt-Cl bond length of 2.317(7) Å, for Cl *trans* to N, was significantly longer than the corresponding distances of 2.288(27) and 2.280(14) Å for Cl *trans* to Cl.

This difference in the Pt-Cl bond lengths is also evident from the data presented in Table A1 with the distance for the Cl *trans* to N being significantly longer.

Calculations have also revealed that there is an expected strong electronic interaction between the Cl(2) atom on [PtCl₃(NEt₃)]⁻ and the N(2) atom on [HNEt₃]⁺. The non-bonded distance has been calculated to be 3.253(11) Å.

References for Appendix

1. G. M. Sheldrick, SHELXTL-PC RELEASE 4.1, Program for crystal structure determination and refinement. Siemens Analytical X-ray Instruments Inc., Madison, Wisconsin, U. S. A. (1990).
2. Y. P. Jeannin and D. R. Russell, *Inorg. Chem.*, 1970, 9, 778.